DESIGN AND SIMULATION OF SEAWATER THERMAL DESALINATION PLANTS

Submitted in accordance with the requirements
for the degree of Doctor of Philosophy

by

Ahmed Safwat M.T. Nafey

B.Sc.& M.Sc. (Mech. Eng., Mansoura University, Egypt)

Under the supervision of
J.R. Flower, M.A., Ph.D., C.Eng., F.I.Chem.E.

Department of Chemical Engineering
The University of Leeds

November 1988

IMAGING SERVICES NORTH
Boston Spa, Wetherby
West Yorkshire, LS23 7BQ
www.bl.uk

CONTAINS PULLOUTS

To

My parents & My wife

and

Everyone who helped and encouraged me.

ABSTRACT

Water is the most important chemical component on Earth. Seawater distillation processes have a considerable promise as a technique suitable for producing large scale quantities of potable water from the seawater.

Distillation process flowsheets consist of a number of interconnected units. The development of the mathematical model describing the behaviour of these units, and the subsequent solution of this model are fundamental steps in process flowsheeting.

The first objective of this work is to develop a specialized flowsheeting program for performing design and simulation calculations for different types and configurations of seawater distillation processes.

Many numerical methods have been used for solving linear and nonlinear sets of equations representing distillation processes. Most of these methods involve the direct manipulation of the mathematical model equations without exploiting the special properties, such as the sparsity and the weak nonlinearities, of these equations. The second aim of this study is to develop a new approach taking advantages of these properties. Hence, the model equations can be linearized, and grouped according to the variable type. These groups can then be solved by linear matrix technique.

The performance of the developed program is investigated by solving many distillation process problems. The results from design and simulation calculations for large practical desalination plants are discussed. In addition to that the convergence characteristics of the new approach (such as stability, number of iterations, computing time, sensitivity to starting values, and general ease of use) are presented. Also, the validity of the approximation assumptions proposed to develop the new approach is examined.

ACKNOWLEDGEMENTS

I wish to express my deep gratitude to Dr. J. R. Flower for his invaluable advice and guidance throughout this research and the compiling of this thesis.

I would also like to express my deep gratitude and thanks to the **EGYPTIAN GOVERNMENT** who made this scholarship available and financially supported me throughout the period of this study.

Finally, I offer my deepest personal thanks to my wife, my children Heba, Belal, and Yasser, and to my family for their patience, support, and understanding.

CONTENTS

CHAPTER 1

INTRODUCTION

1.1. THE WATER PROBLEM.

Water is the most important chemical component on Earth. Arid and semi-arid zones, (less than 10 in. of rainfall per year), cover about 60% of the emerged lands. These zones have many rich soil areas for producing food, minerals, and oil. However, because of the water shortage, it only supports about 5% of the earth's population, Gaunt [1965]. Therefore, if this problem is practically solved, these areas could provide food and accommodation for a substantial proportion of the increasing world population.

On the other hand, non-arid areas, even with a wet climate, will soon face water problems, Silver [1962]. This is because of rising standards of living, increases of population, waste of water, and pollution of natural water resources by industrial waste and sewage.

On the average, demand for water increases at the rate of about 50 % (± 20 %) every ten years in industrialized countries. In arid zones it may reach several hundred per cent during the same period, D'orival [1967].

Desalting of seawater, brackish water, and/or polluted water is one of the most promising techniques to overcome local water problems in a considerable number of places. In arid regions desalting water might be the only possible solution for water supply.

1.2. DESALINATION PROCESSES.

Many techniques have been proposed for water desalination. However, only a few techniques have been developed to be used as commercial processes. Desalting processes may be classified into two general categories: (i) processes that eliminate salts from solution, such as ionic processes, (e.g. ion exchange, electrodialysis, etc), and (ii) processes that isolate pure water from solution, such as distillation, reverse osmosis, and crystallization, see Howe [1974] for

more details. The applicability of each of these processes depends on the amount of salts in the available saline water and/or on the economics of the process.

Distillation is the most developed technique for desalting water, Homig [1978]. In this process pure water is evaporated from saline solution by supplied heat. Then by condensing the released vapour the desired water is obtained.

Distillation process is applied up to very large capacities with various types of evaporators. Figure (1.1), shows schematically various types of available distillation processes. Operating principles and configurations of some of these types will be illustrated in the next chapter.

1.3. DESIGN AND SIMULATION OF DISTILLATION PROCESSES.

To design the units constructing the previous distillation processes for sizing and cost estimation, and/or for computing the performance calculations, repetitive and tedious material and energy balance calculations are usually needed. These calculations may become even more complicated because of the existence of one or more recycle streams in the process. This leads inevitably to the use of computers for performing these calculations.

1.3.1. Special Purpose Programs.

The traditional approach to the problem is to regard each new process as a new problem which may be solved by a special purpose program, (or one-off program as defined by Flower and Whitehead [1973]). Almost all the published programs, for design and simulation of distillation processes are of this type, see chapter 4. Because of the inflexibility of this type of programs, no minor flowsheet changes in the normal configuration can be made. The return on investment for this type of programs is quite attractive only if the number of plants to be designed with exactly the same configuration is large, otherwise it tends to be expensive. To write and debug a program of this type, for a large problem several months may be required. Quite often, the time scale of the process development and design will not permit this. Also, in many cases, a cost comparison between different process alternatives

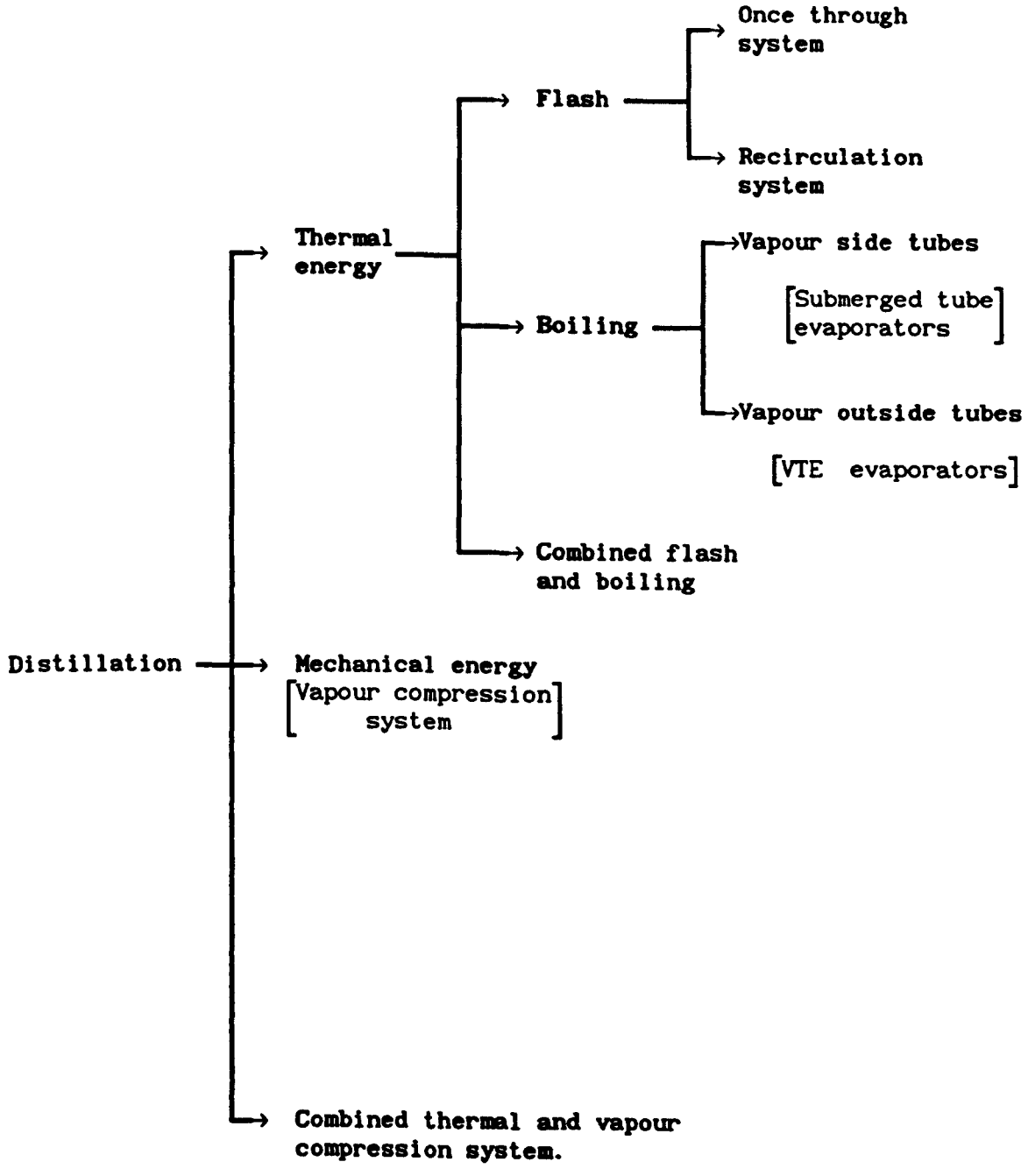

Figure (1.1), Thermal distillation processes.

may be required. This comparison has to be evaluated on the basis of the same criterion. In this case, the cost results obtained for various alternatives are more suitable for the comparison than comparing one of them with other results quoted in the literature, whose calculation basis is not known sufficiently.

To overcome these problems and limitations, it is a logical next step to develop generalized programs which can be used to calculate heat and material balances for various physically feasible configurations for a process, under different operating conditions. In fact many general flowsheeting programs are available for chemical and petroleum industries (e.g. CHESS [1968] and FLOWPACK (Berger [1979])). However, a specialized flowsheeting program for thermal desalination processes is still needed, because:

- Most general flowsheeting programs are oriented towards organic vapour - liquid systems. Therefore, significant problems may arise when inorganic solid-liquid-vapour systems are investigated, Flower et al [1982].
- Most general flowsheeting programs cannot satisfy the need for detailed models of evaporator units. On the contrary, the specialized flowsheeting program makes it much easier to develop mathematical models of adequate flexibility and realism.

One of the purposes of the present work is to develop a specialized flowsheeting program to perform design and simulation calculations for thermal desalination processes.

1.3.2. Flowsheeting Programs.

By using a flowsheeting program, the process engineer may be able to perform four different types of calculations: (i) simulation calculation, (ii) design calculation, (iii) optimization calculation and (iv) dynamic simulation calculation. The simplest type of these calculations is the *simulation calculation,* in which feed stream variables, unit parameters (such as heat transfer area), are specified. However, the internal and output stream variables are calculated.

Simulation calculations have many aspects of applications. By using a simulator, the process engineer, may be able to answer the question of "How the process will behave in a given situation", i.e. what will be its output variables if the input variables (i.e. operating

conditions) are changed. The simulation calculation may also be used to investigate the process in off-design operation, e.g. partial load or over load calculations, to be sure that pressure, temperature, and flowrate variables of the process will not be too high or too low. Also, the sensitivity of process performance to various parameters can be studied. In addition, various modifications may be tried, and the sensitivity of the process economics to key parameters and data can be determined. Simulation calculation may be considered as an experiment carried out on a mathematical model representing a process. So, the results of this calculation can be conveyed to the real process. Therefore, this sort of experimentation, (simulation study), can be used to guide the experimental program. Many runs can be performed by the simulation process and only the most promising trial in the pilot plant is used for verification. This should increase the reliability of the results and decrease the required time to obtain them.

In the *design calculation* some output stream variables are specified and some input stream variables and/or equipment parameters are calculated. Equality constraints for some variables are imposed in the process. The number of these constraints is equal to that of the variables left unspecified. The main objective of this type of calculation is to determine the equipment sizes. Also, *partial design calculations* may be performed by the flowsheeting program. Here a combination of simulation and design specifications takes place. By this type of calculation the effect of changing an existing plant topology by removing and/or replacing one or more of its units, may be examined in order to be sure about the reliability and economy of the new plant topology before the actual change. In this calculation the unit parameters of the existing units and some output stream variables are specified, and some input stream variables as well as some new unit parameters are calculated.

In the third type of calculation, the *optimization calculation*, "optimal" values for some of the flowsheet variables are determined. This may be achieved by leaving a number of design variables unspecified, and equality and/or unequality constraints for some variables are imposed in the process. The unspecified variables are then determined so as to minimize (or maximize) an objective function. In this case the number of constraints is smaller than that of the variables left unspecified.

The fourth type of calculation using a flowsheeting program is the *dynamic simulation calculation.* In this case some of the model equations are of differential form, because some variables in the flowsheet are changing with time. This type of calculation is useful in devising a control scheme for a process.

The present version of the developed program in this work is concerned with performing both design and simulation calculations for thermal desalination processes.

Many numerical methods have been used for solving the simultaneous linear and non-linear equations representing thermal desalination processes, see chapter 4. Most of these methods involve the direct manipulation of the mathematical model equations without attempting to recognize whether the model equations have any special properties that could make the solution more efficient. In fact, the second major objective of this work is to develop a new approach that takes into account the characteristics of mathematical models of thermal desalination processes . This may improve the computation efficiency, reliability, flexibility, and may reduce storage space requirement.

1.4. THE ORGANIZATION OF THE THESIS

- Chapter 2 introduces various types and configurations of saline water distillation processes.
- A rigorous mathematical model describing different units in the main thermal desalination processes is developed in chapter 3.
- The available techniques and numerical methods to design and simulate different thermal desalination flowsheets are reviewed in chapter 4. This leads to the required characteristics in the developed program, which is also outlined. Then, the proposed technique for achieving these characteristics is introduced.
- Chapter 5 demonstrates the step by step formulation of the proposed technique.
- Chapter 6 considers the transformation of the developed unit mathematical models into a specialized flowsheeting program. The program structure and operation are outlined. Chapters 7, 8, and 9 consider the developed program and the proposed technique validation and practice implementation.

- Different problem types of MSF process are examined in chapter 7. The convergence characteristics of the proposed technique during the calculations are also illustrated.
- Chapter 8 illustrates the capability of the developed program using the proposed technique to perform design and simulation calculations for different MEE process configurations. The accuracy, the efficiency, and the validity of the developed program using the proposed technique are also examined.
- Chapter 9 demonstrates the capability of the developed package to deal with problems related to hybrid systems (i.e. a system combining different desalination process types in one flowsheet).
- The material presented in this thesis is summarized and the main conclusions are presented in chapter 10. Some suggestions for further work are also given.

CHAPTER 2

TYPES AND CONFIGURATIONS OF SALINE WATER DISTILLATION PROCESSES.

2.1. INTRODUCTION.

According to the present state of technology, the only desalting technique feasible for commercial plants of medium and large size is the distillation of seawater. This technique has been practiced by Man for centuries, see Silver [1962] for the distillation process history. Distillation and other dominant desalination processes have been discussed in texts by Howe [1974], Porteous [1975], Homig [1978], and Spiegler et al [1980]. Section 2.2 gives principles and configurations of the main types of distillation processes. Each of these types has its advantages and disadvantages, as will be seen in section 2.3. Combining the advantages of individual systems into a single desalting system can improve the final performance of the combined process. This will be illustrated in section 2.4. The combination of desalination processes with power cycles will be introduced in section 2.5. Finally, the main points of this chapter will be concluded in section 2.6.

2.2. DISTILLATION PROCESS TECHNIQUES.

Saline solution can be made to boil successively many times without adding additional heat by successively reducing its pressure. This statement is true to one degree or another for almost all commercial distillation processes, since reducing the pressure is less costly than adding heat.

There are three major distillation processes being used in industry today;

- * Multi-Stage Flash (MSF).
- ** Multiple Effect Evaporation (MEE).
- *** Vapour Compression (VC) Evaporation.

In addition, there are many hybrid processes which combine two or more of the above processes.

2.2.1. Multi-Stage Flash (MSF) process.

2.2.1.a. *Recirculation MSF process:*

Flash evaporation systems have been in operation since 1957. Their economics have been clearly proven through continued use of this system to convert brackish or seawater into potable water. In the survey of the national water supply [1981] the MSF process was estimated to account for nearly 91% of cumulative distillation plant capacity. So far, this process is still the world's largest desalination system of any type, (national water supply [1981]).

Process Description:

Figure (2.1), shows a simplified flowsheet for an MSF process. This process consists of four sections:

1- Heat input section. 2- Heat recovery section.

3- Heat rejection section 4- Water treatment section.

In normal applications, the first three sections are combined into one package forming an efficient integral flash evaporator system. However, it could be separated into four separate pieces of apparatus connected by pipes. The process can be divided into the following four streams:

- Seawater stream.
- Recycle brine stream.
- Product water stream.
- Vapour streams.

(a) Seawater stream:

Seawater is pumped to the inlet of the condensing tubes in the heat rejection section, where an increased portion of seawater is provided for cooling purposes. The seawater is heated as it flows through the condenser tubes. After the seawater leaves the heat rejection section a portion of it (the cooling water) is returned to the sea. The rest of the seawater is chemically treated to prevent a build-up of scale on the surfaces of the heat recovery section tubes. This water is then discharged into carbon dioxide release tanks (decarbonator). Then the treated seawater flows into a vacuum deaerator to take off the air from the seawater. The deaerator prevents oxygen corrosion and eliminates noncondensable blanketing of the condenser tubes.

(b) Recycle Brine Stream:

On leaving the deaerator, the make-up seawater mixes with a portion of the concentrated brine stream leaving the last stage of the rejection section. The remainder of the concentrated brine stream is blown down to the sea to maintain the proper brine concentration. The recycle brine (mixture of concentrated brine and freshly treated make-up

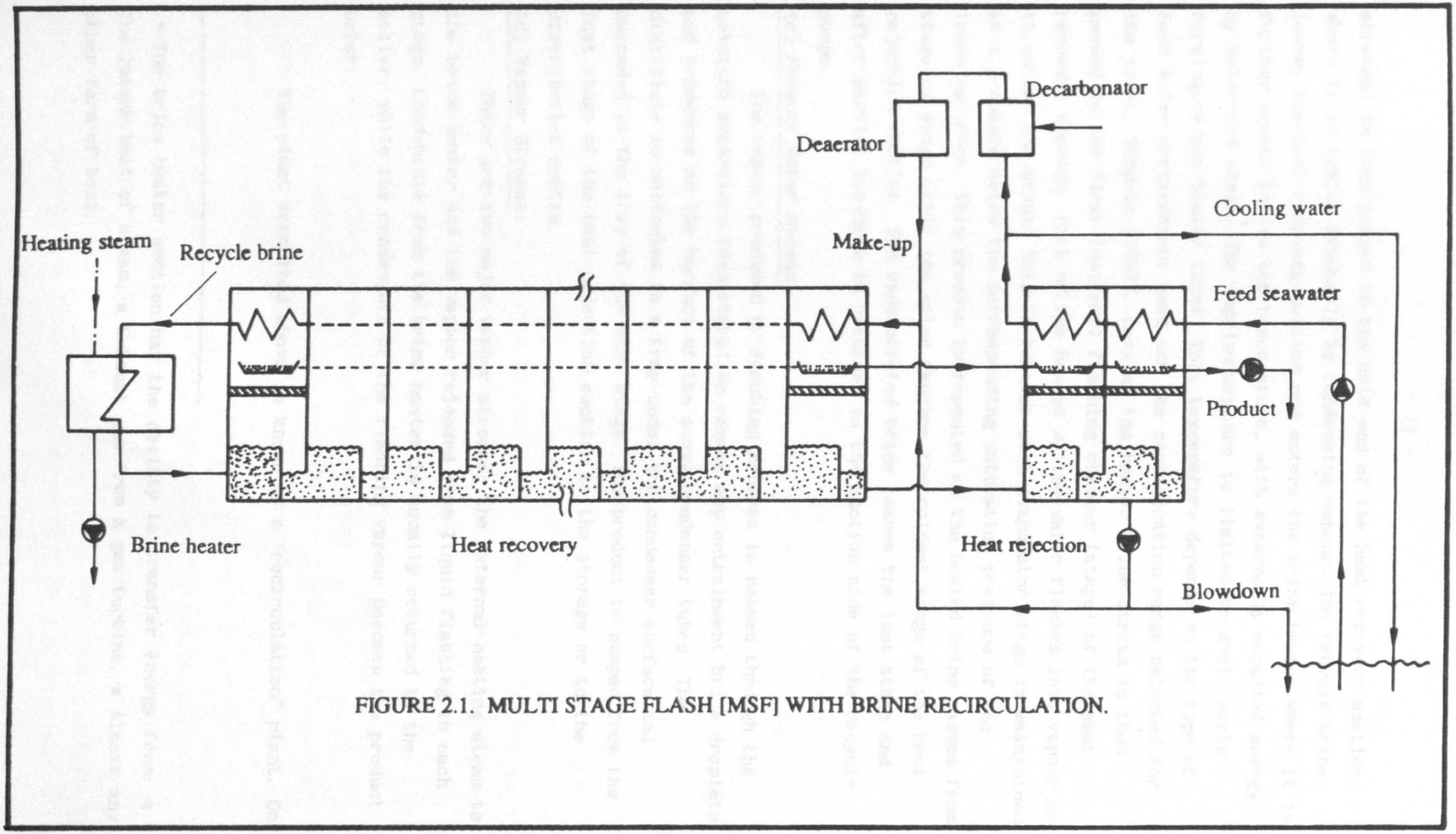

FIGURE 2.1. MULTI STAGE FLASH [MSF] WITH BRINE RECIRCULATION.

streams) is then pumped to the cold end of the heat recovery section, where it is heated gradually by condensing vapour. The recycle brine leaves the heat recovery section and enters the brine heater where it is further heated to its top temperature, with externally supplied energy by saturated steam.* The top temperature is limited to avoid scale forming on the heater tubes. This temperature depends on the type of feed water pretreatment used and the concentration range selected for the plant, Simpson [1967]. Leaving the heater brine stream is then passed to the first (hottest) flashing chamber (stage) of the heat recovery section. Part of the heated saline water flashes into vapour as it enters the stage. This is because each evaporator stage is maintained at a pressure below the corresponding saturation pressure of the incoming brine. This process is repeated as the heated brine passes from stage to stage until the brine reaches the coldest stage of the heat rejection section. The concentrated brine leaves the last stage and after partial blowdown is returned to the suction side of the recycle pumps.

(c) Product Water Stream:

The vapour produced by flashing process is passed through the moisture separators (demisters) to remove any entrainment brine droplets and condenses on the surface of the stage condenser tubes. The distillate is collected in a tray under the condenser surface and cascaded to the tray of the next stage. The product is pumped from the last stage of the heat rejection section to the storage or to the distribution system.

(d) Vapour Streams:

There are two major vapour streams; the external heating steam to the brine heater and the vapour released from liquid flashing in each stage. Condensate from the brine heater is usually returned to the boiler, while the condensate of the flashing vapour becomes the product water.

The plant described above is known as a "recirculation" plant. On

---

* The brine heater section has the ability to transfer energy from: ▪ The latent heat of steam, ▪ Exhaust gas from a gas turbine, ▪ Almost any other form of heat.

one hand this model of operation reduces the amount of chemicals needed for the water treatment, which can significantly affect the operation costs. On the other hand, the salinity of the brine at the hot end of the plant increases. Therefore, problems of corrosion and scaling increase, and the boiling point rise of the brine increases, so the thermodynamic efficiency of the whole process is reduced.

2.2.1.*b.Once-Through Process:*

A plant which does not recirculate a portion of the concentrated brine is referred to as a "Once Through" plant. In this type there is no rejection section as is the case in the recirculation type. This model of operation requires a greater quantity of chemicals for water treatment than the recirculating plants. However, the operation of the once-through system, is considerably easier, especially in the start-up, because balancing the flows through the stages is not as difficult as it can be with a recirculation plant. In addition, since the salinity is lower, there are potentially fewer problems with scaling. Due to its operational stability and simplicity, this process has a considerable merit for use in areas where operation and maintenance may be a problem. A flowsheet of a once-through plant is shown in Figure (2.2).

2.2.1.*c.Flash Stage Tube Bundle Arrangements:*

The arrangement of the condensing tube bundles in the flash evaporator shell may be parallel (long tube design) or perpendicular (cross tube design) to the brine flow in the chambers. These configurations are illustrated in Figure (2.3). Each configuration has its advantages and disadvantages (see Howe [1974] and Helal [1985]), and both are currently in use. The selection depends on the performance and/or experience of the manufacturer or the owner.

2.2.2. Multiple Effect Evaporation (MEE) Process.

This process comprises less than 7% of the total world capacity of all desalination plants in 1980, i.e. some 377000 m^3/d, (national water supply, [1981]).

Single effect or multiple effect arrangements may be used. The arrangements affect steam economy and evaporator capacity. In single effect operation, the heat supplied by steam is used only once, hence the economy, (kg of vapour/ kg of steam), is very poor, (about 0.8 for a cold feed). However, the capacity, (vapour weight per unit time for a

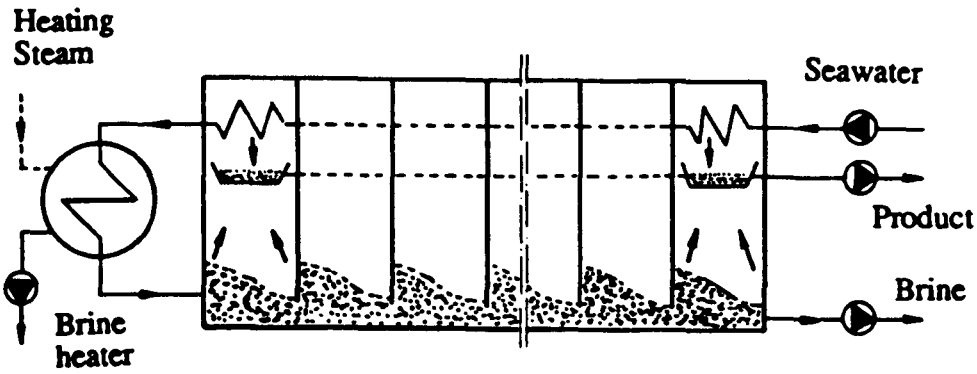

FIGURE 2.2. SIMPLIFIED MODEL OF ONCE THROUGH MSF PROCESS.

1 = Condenser tube
2 = Demister
3 = Brine
4 = Water chamber

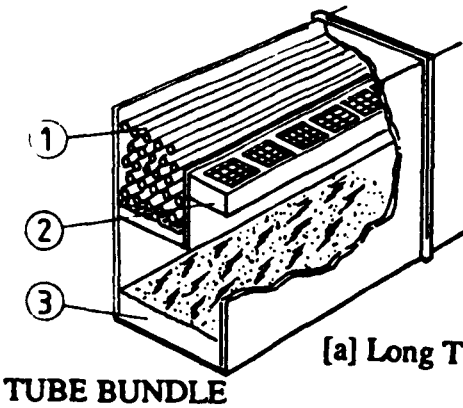

[a] Long Tube Type.

FIGURE 2.3. MSF PROCESS TUBE BUNDLE ARRANGEMENTS.

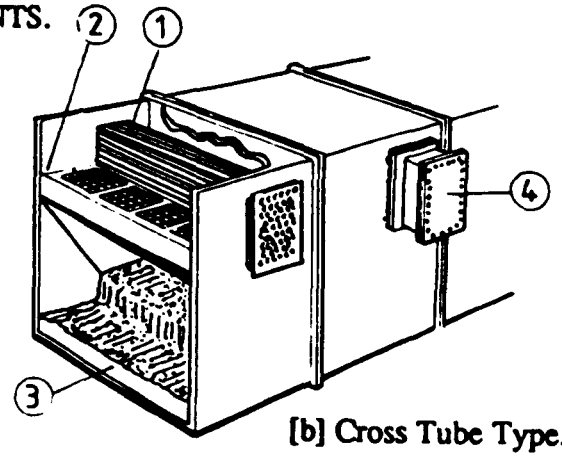

[b] Cross Tube Type.

unit heat transfer area), is usually higher than the multiple effect evaporation.

Process Description:

In multiple effect evaporation, Figure (2.4), a series of evaporators are connected together. The vapour generated in one effect is used for heating in the subsequent effect. Each effect has a lower pressure than the former, which permits the solution to boil at lower temperatures. Hence, the heat supplied to the first effect creates vapour at the pressure of the first effect. This vapour flows to the next effect and condenses, forming more vapour. The process continues until finally, the vapour generated in the last effect is condensed by external cooling water. The advantage result of this arrangement is the multiple reuse of energy which increases the system economy. A rough approximation of the economy can be obtained by multiplying the number of effects by 0.8. In addition to the saving in steam, there is also a saving in cooling water required to operate the last effect condenser, because the amount of cooling water is proportional to the steam consumption. The evaporation units (or effects) in a MEE system can be arranged in several ways. The three basic arrangements are: forward feed (the liquid feed flows in the same direction as the vapour); backward feed (the liquid and vapour flow in the reverse direction); and parallel liquid feed (the feed seawater enters each effect independently of the other). The advantages and disadvantages of these arrangements are explained by Azbel [1984]. Almost all the MEE potable water distillation plants have the forward feed configuration, Buros [1980].

Although many types of evaporator construction have been used in industry, see Standiford [1963], only three types have been used in the desalination process, Howe [1974]. They are; submerged tube evaporator, horizontal tube evaporator, and vertical tube evaporator (VTE). The configuration and characteristics of these types are illustrated in some detail by Howe [1974] and Azbel [1984].

Ojima et al [1973], has illustrated that the desalination plant of a vertical multi-effect evaporator of falling film type has the following advantages over the multi-stage flashing type, as well as the conventional multi-effect evaporator:

[1] Fewer stages (or effects) are normally required for the same process requirements.

[2] The hottest brine is generally more dilute, this gives an

FIGURE 2.4. SCHEMATIC OF A MULTIPLE EFFECT EVAPORATION [MEE] PROCESS.

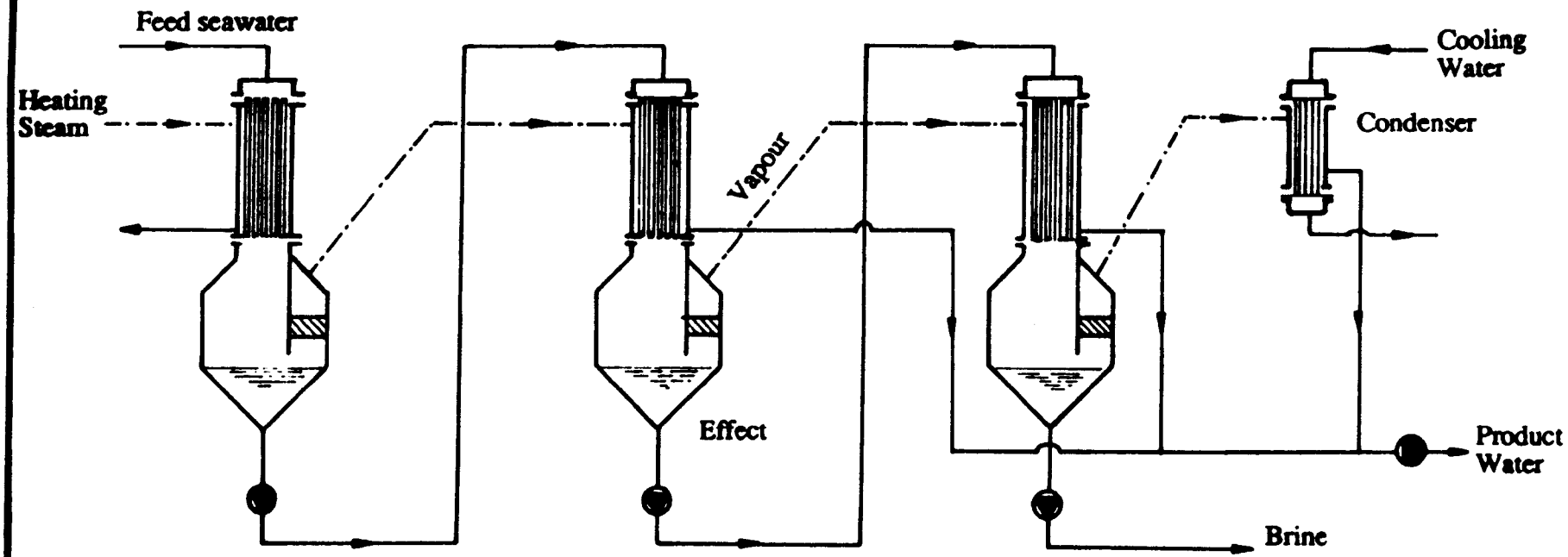

advantage in scale control.

[3] A small volume of seawater is handled, so the pumps requirements are reduced.

[4] The heat transfer coefficient is large and the required heat transfer area for unit performance is small.

2.2.3. Vapour Compression (VC) Evaporation.

Vapour compression evaporation plants contributed 1.6 % of world-wide rated desalination capacity in 1980, equivalent to a total production capacity of about 11000 m^3/d (national water supply, [1981]). This process consumes power instead of thermal energy, whether via mechanical compressor or momentum exchange (as in thermocompression by steam jet). Therefore, plants employing this process are especially attractive for applications where steam is not readily available for other distillation processes. Figure (2.5), shows a schematic flowsheet for this process.

Process Description:

In this process, vapour released from the boiling seawater in one side of the evaporator tubes is compressed by either a mechanical compressor or a steam jet (the characteristics of both methods of compression have been explained in detail by Buros [1980]). Compression rises the pressure and the saturation temperature of the vapour which is returned to the other side of the evaporator tubes to be used as a heating steam for producing additional vapour, and thus continuing the evaporation process.

The latent heats of evaporating and condensing fluids are very nearly equal. Therefore, the energy required by the compressor is merely supplied to compensate for losses, boiling point elevation, and to provide a sufficient driving force for the heat transfer operation.

The seawater feed is preheated by the condensed vapour (product) and the rejected brine streams. For start-up purposes, and for maintaining normal operating conditions in some plants, externally supplied heat is provided.

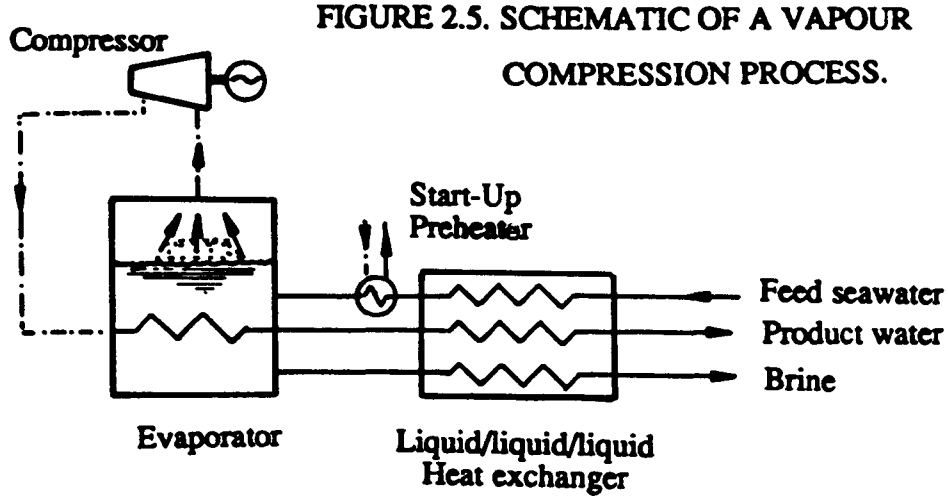

FIGURE 2.5. SCHEMATIC OF A VAPOUR COMPRESSION PROCESS.

Low thermodynamic efficiency, because of the nonisentropic compression, is inherent to the process. However, it has several advantages such as:

- High performance ratio per unit of installed heat transfer surface.
- No cooling water requirements.
- VC can be automated, so it needs only a minimum of operation attention.
- The process can be made extremely compact for minimum area requirements.

Several constraints have to be considered to make the most economic use of the inherent advantages of the process. Elsayed [1986] has introduced the rational basis for the design of VC process, and examined the effect of the different design parameters on the capital and operating costs of the system.

2.3. COMPARING THE CHARACTERISTICS OF THE MAJOR DISTILLATION PROCESSES

The average boiling point elevation, which is a function of brine concentration, in the MEE process is lower than those of the MSF (recirculation type) and the VC process. This is because the brine concentration in the first effect of the MEE process is approximately the same as the seawater feed stream, while the brine in the other two processes is much more concentrated than is the seawater stream.

In the MSF process the recirculated stream is heated without

evaporation and the flashing evaporation takes place without heat transfer. Therefore the tendency for scale formation on the heat transfer surface is reduced. On the other hand, in both MEE and VC processes, the evaporation takes place during the transfer of heat, so that the saline water is concentrated locally at points where vapour is produced. Thus scale formation tendency in these two processes is much higher than the MSF process.

In the VC process energy is utilized very efficiently, since the heat required for vapour formation is recirculated around the plant. The wasted heat from the process is much less than the latent heat of vapour formation. In contrast, both MEE and MSF processes reject amounts of heat equivalent to that given to the system. This rejected energy by cooling water is much more than that required for the vapour compressor.

2.4. DISTILLATION PROCESSES ECONOMY IMPROVEMENT.

Improving the performance ratio (kg of product/ kg of heating steam) is one of the main important means which can provide a sizable reduction in the desalting water cost. The process performance ratio may be improved by combining the advantages of two or more of the above individual distillation systems in one hybrid system. Several configurations of hybrid systems have been built or proposed, such as;

- MEE/MSF
- MEE/VC
- MSF/VC
- MEE/VC/MSF

2.4.1. Combination of Multiple Effect And Multi Stage Flash (MEE/MSF) Processes.

In this process, Figure (2.6), the MSF stages serve as the brine heating system. Potable water is mainly produced by the MEE (VTE type) component. Each effect is combined with two or three flash stages Process Description:

The seawater feed is pumped through the final condenser and the MSF unit tubes, where it is heated by the condensed vapour from the last effect and the flashed vapour respectively. After the chemical treatment the feed seawater is further heated using steam condensing in a brine heater.

The seawater flows through the flash evaporator stages at successively lower pressure and temperature in the stages. A portion of

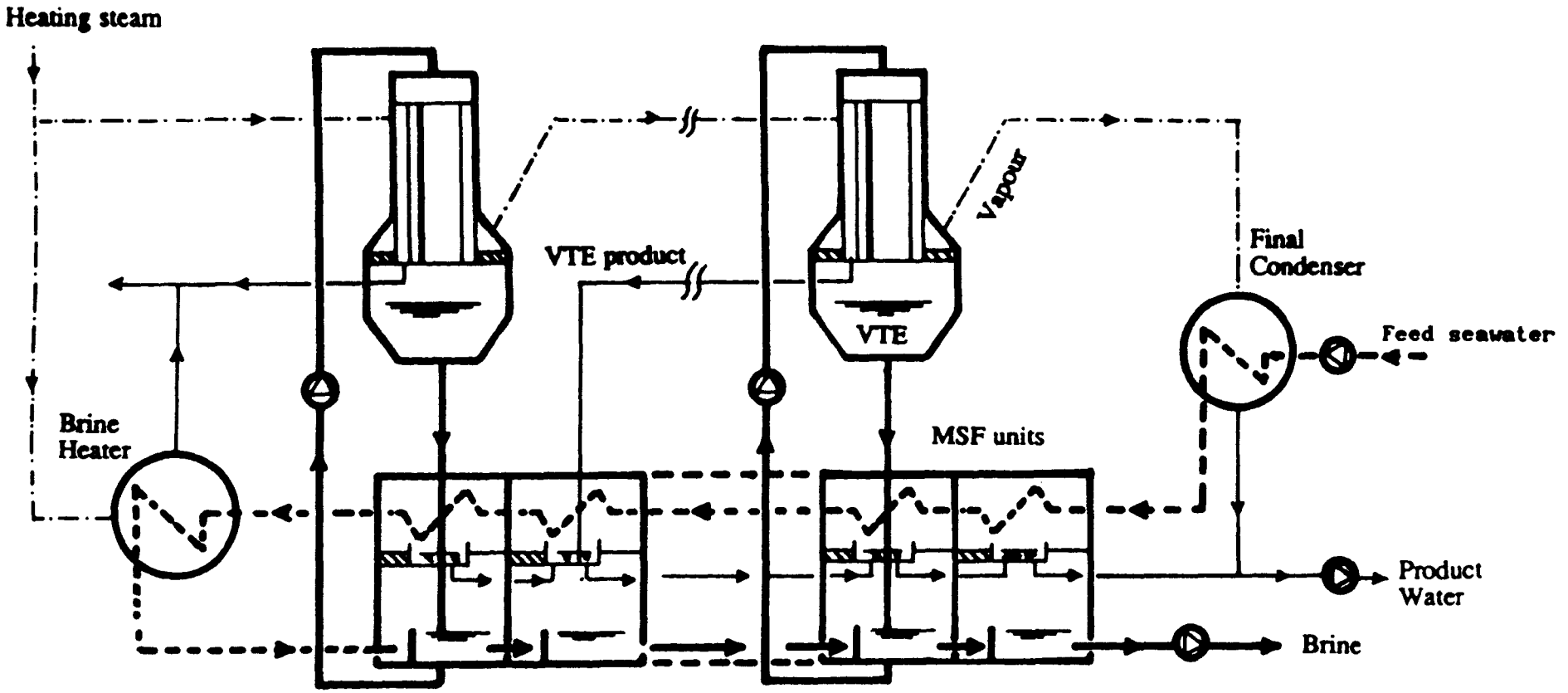

FIGURE 2.6. FLOW DIAGRAM OF A COMBINED MEE/MSF PROCESS.

the brine flowing through the flash evaporator is pumped from selected stages up into the brine chest, which feeds the vertical tube bundles of the VTE evaporator. Brine is pumped only from stages which have an equivalent pressure to the evaporation side of the desired effect. Brine discharges again from the bottom of the effect back into the flash stage from which it was pumped.

A portion of the brine evaporates in the first effect as heat is added from the condensation of the heating steam. The vapour produced in the first effect is condensed in the steam chest of the second effect to form product water and to vaporize a portion of the brine in the tube side. This process is repeated until the last effect. Vapour produced in the last effect is condensed in the final condenser. Product from each VTE flows by gravity to a cooler MSF stage product tray where it too flashes, cools down, and releases some of its heat to the feed seawater. External heating steam is condensed on the steam chest of the first effect and the brine heater.

Such configuration improves the performance ratio and hence, reduces the water production cost. The advantages of the combined MEE/MSF process over MSF alone are more evident when plant size is sufficient to justify the additional complexity of piping, instrumentation, and equipment. Hammond [1968], concluded that the combined MEE/MSF process saves 30% of the capital cost and 15% of the water cost relative to the multi-stage flash process for large plants. Both the multiple effect evaporation processes, such as VTE, and the combined processes such as MEE/MSF are capable of producing 15 and perhaps 24 kg of product water for each kg of input steam, Hapke et al [1981] and Hughes et al [1981]. In comparison, multistage flash plants usually have a considerable difficulty in operational stability at such high performance ratios. Therefore, this process is designed usually for no more than 12 as a performance ratio. The main advantage of the combined MEE/MSF process over a plant using MEE alone is the utilization of the flash stages to preheat the seawater.

Different configurations of this process can be obtained. A computer program has been written by Hapke et al [1981] for the calculation of mass and energy balances as well as the heat transfer area for the evaporators of the MEE/MSF process shown in Figure (2.6).

2.4.2. Combination of Multiple Effect And Vapour Compressor, (MEE/VC) Processes.

Large capacity, single effect evaporator plant, Figure (2.5), needs a very large and expensive compressor. This capacity can be reduced in direct proportion to the number of effects served by the compressor. However, the compression ratio also increases in direct proportion to the number of effects, and this increases the compressor cost somewhat.

Figure (2.7), exemplifies the combinations of MEE and VC processes. Similar to the previously explained VC process, in section 2.2.3. Vapour from the last effect is compressed and passed to the first effect where it is condensed on the outside of the tubes.

The advantages of this combination is that only about one third of the vapour produced in the plant passes through the compressor. Therefore, only a small size compressor is required. Thereby, a substantial saving in the capital cost is achieved.

Different forms of the MEE/VC arrangements may be obtained. Tleimat [1969] has proposed an approach in which centrifugal fans are used instead of multistage axial flow compressor. Different configurations of MEE and VC systems have been simulated by Aly [1983]. In this study the number of effects was varied from 6 to 21, and the effect of the compressor location was investigated.

2.4.3. Combination Of Multi-Stage Flash And Vapour Compressor, (MSF/VC) processes.

In this process, Figure (2.8), a number of flash stages replace the liquid/liquid heat exchanger used in the ordinary vapour compression process configuration, Figure (2.5). These flash stages would function as a heat recovery process more efficiently than the liquid to liquid heat exchanger. Also, the MSF section would produce additional distillate rather than being used only to preheat the incoming seawater feed.

Using a computer code for evaluating the material and energy balances, various configurations of integrated MSF/VC process have been investigated by Wood et al [1968], who found that the greatest advantage in terms of heat transfer surface per unit of supplied fuel is obtained

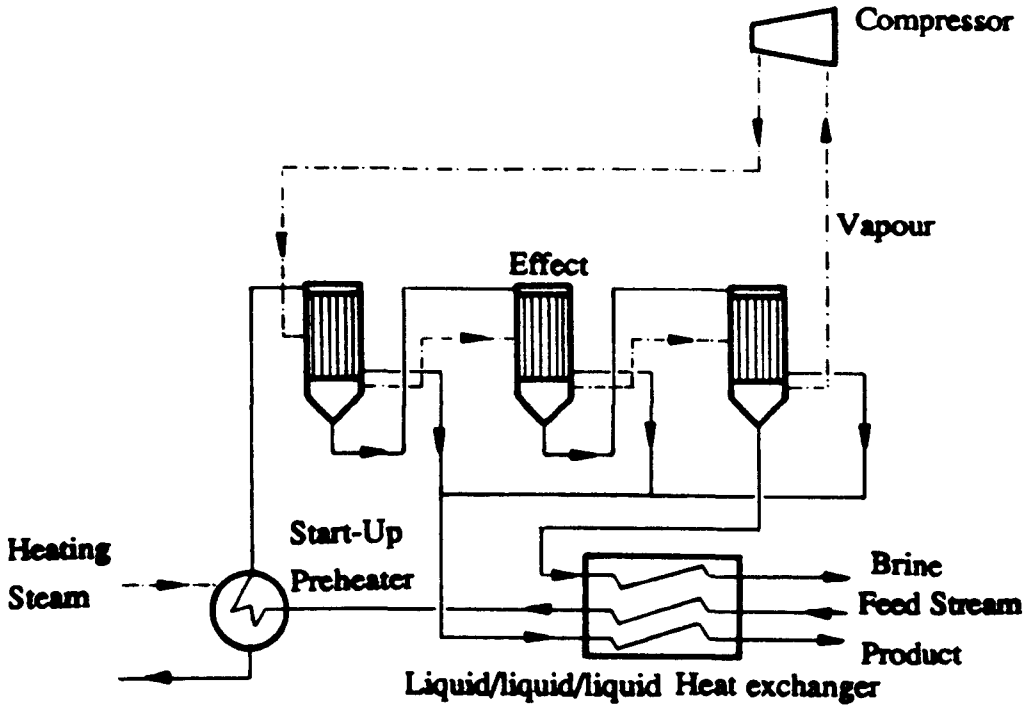

FIGURE 2.7. FLOW DIAGRAM OF A COMBINED MEE/VC PROCESS.

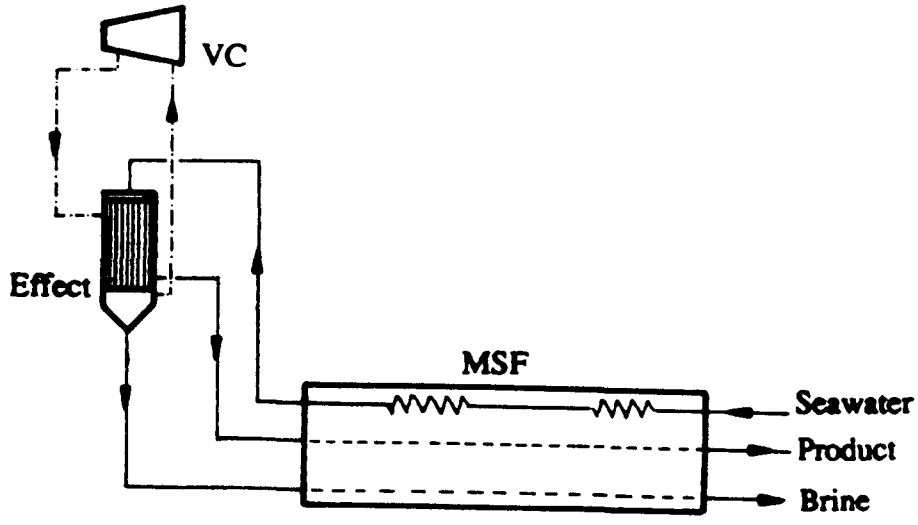

FIGURE 2.8. FLOW DIAGRAM OF A COMBINED MSF/VC PROCESS.

for the hybrid process, when the VC evaporator is coupled to the top of the MSF plant.

2.4.4. Combination of Multiple Effect, Multi-Stage Flash, and Vapour Compression Processes, (MEE/MSF/VC).

A hybrid system combining the MEE, MSF and VC processes is illustrated in Figure (2.9). In this process after the seawater feed is preheated in several MSF stages, it is chemically treated, decarbonated, and deaerated. It is then further heated through the remaining stages of MSF train and four feed preheaters (one between each two effects). The heated seawater is then sprayed inside the first effect vertical tubes, where it is evaporated using external steam supply. Vapour generated in the first effect is used as a heating steam in the next effect, and the rejected brine from the first effect is used as a feed for the second effect. This process is repeated until the fourth effect. The blowdown brine from the fourth effect then enters into the MSF section, where a portion of it is flashed.

Using the gas turbine exhaust in a waste heat boiler, steam at two levels is generated. The first level is saturated steam, and the second is superheated steam. The latter is used to drive a back pressure steam turbine, which is coupled to an electric generator. The exhaust of the back pressure turbine is mixed with the saturated steam from the low pressure boiler. This mixture is used as a heat input to the first effect. The vapour from the fourth effect is compressed to a superheated condition, which is then desuperheated before entering to the first effect.

The product water from each effect is flashed in a flash tank to the temperature of the next evaporator, giving some extra steam which is used in the next effect. Leaving the last flash tank, the product water is further flashed down in the MSF train, releasing its latent heat to heat the incoming seawater feed.

Figure (2.9) represents only one configuration for MEE/MSF/VC process. Since a number of different processes are combined in this flowsheet, it should be expected that more than one method of formulating the process exist. Newkirk et al [1970], studied the feasibility of a combined MEE/MSF/VC flowsheet similar to that of Figure

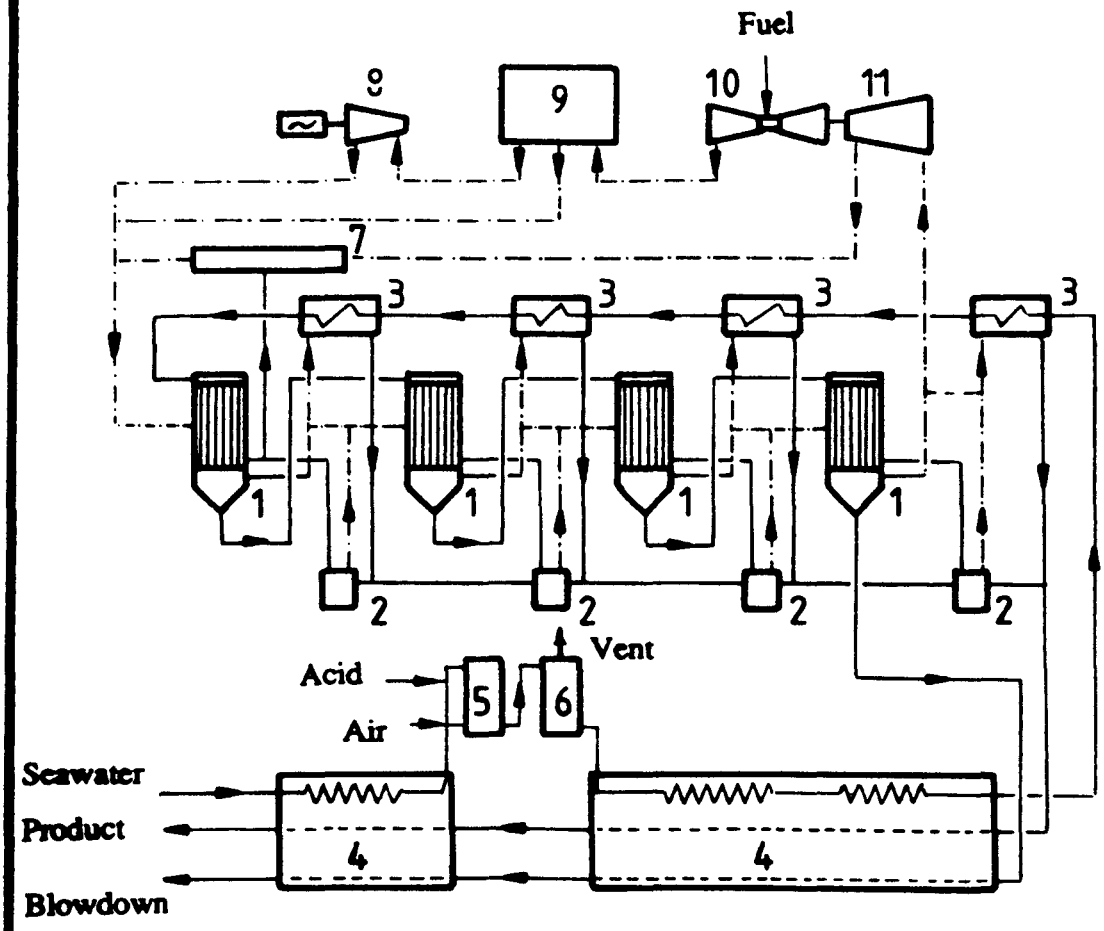

FIGURE 2.9. FLOW DIAGRAM OF A COMBINED MEE/MSF/VC PROCESS.

1 = VTE unit
2 = Flash tank
3 = Brine heater
4 = MSF units
5 = Decarbonator
6 = Deaerator
7 = Desuperheater
8 = Steam Turbine
9 = waste heat boiler
10 = Gas turbine
11 = Vapour Compressor

(2.9). Also, Senatore et al [1969] investigated the effect of the compression ratio of the compressor on the plant performance ratio for different number of effects.

2.5. DUAL PURPOSE PLANTS.

One of the most effective ways of saving energy is by using dual purpose plants, in which a power station producing electricity is combined with one of the previous illustrated distillation processes.

In general, distillation plants have a top operating temperature between 90 C and 120 C depending on the type of the additive used to prevent scale formation (polyphosphate, or sulphuric acid). However, steam can be economically produced at much higher temperatures. Therefore, by using a dual purpose plant, the high temperature steam can be used for power production, and low pressure steam for the desalting process. Steam is taken from the power cycle via, either an extraction or a back pressure turbine, depending on the desired water/power ratio.

Utilization of the waste heat from the water jackets and oil coolers of the diesel power plants is also common, particularly if the cooling water for the steam cycle is either not available or very limited.

Various combinations of power cycles and distillation processes are feasible, both water and electricity production may be obtained by one of the following configurations:

[a] Steam boiler, back pressure turbine, and desalination plant.
[b] Steam boiler, condensing turbine with steam extraction for the desalination plant.
[c] Gas turbine, waste heat boiler, and desalination plant.
[d] Diesel engines, waste heat boiler, and desalination plant.

The main dual purpose plants configurations were reviewed by D'orival [1967]. Their main features, application limits and operating characteristics are given in the light of the thermodynamic and economic nature of the various plant types.

2.6. CONCLUSION.

In this chapter, it is shown that there are many available desalination techniques to tackle the problem of water shortage. However, distillation is the most practical and economical available technique. There is a wide range of types and configurations for the distillation processes. Better understanding of the process performance and the interaction of the various operating and design variables may be achieved by performing a flowsheeting calculation for these processes. In conclusion, to enable the process engineer to deal with various types and configurations of the distillation processes, an efficient specialized flowsheeting program for performing the simulation and design calculations for these processes is required.

CHAPTER 3

MATHEMATICAL MODELS OF THERMAL DESALINATION PROCESS UNITS

3.1 INTRODUCTION.

Thermal desalination process flowsheets usually consist of a number of interconnected unit operations. One of the most important parts of the required thermal desalination flowsheeting program is the set of mathematical models for these unit operations.

The unit mathematical model provides a set of equations which can be expressed as:

output stream variables = Φ (input stream variables, unit parameters)

These equations are developed from the fundamental material and energy balances which govern the interactions of various process streams entering and leaving each unit.

The objective of this chapter is to develop mathematical models of thermal desalination process units.

The physical and thermodynamic properties of the process streams are an essential part of the mathematical model, Shacham (1982). The physical and thermodynamic correlations used in this study are shown in Appendix {A}.

3.2. MATHEMATICAL MODELS OF THERMAL DESALINATION PROCESS UNITS

A steady state simulation (or design) model of a thermal desalination process plant (as any other chemical plant) can be expressed by a system of linear and nonlinear algebraic equations, in the form:

$$F(X) = 0 \qquad (3.1)$$

where,

F = the vector of functions.

X = the vector of variables.

Here, the functions are obtained using the basic laws of

conservation of mass and energy. The variables are the components (water, salt), temperatures and pressures, of the streams into and out of a specific unit (as boiling evaporator, flash evaporator, compressor, condenser, heat exchanger, ...etc)

Equation (3.1), can represent the mathematical model of a plant. In order to develop such a mathematical model, the plant is considered as a combination of interacting elements. Each of these elements can be described by appropriate mathematical relationships. So, the system (3.1) takes the following form:

$$F_i(X) = 0 \qquad , i = 1,2,\ldots,U_N \tag{3.2}$$

where:

F_i = the subvector of functions identifying unit i.

U_N = the number of units in the plant.

3.2.1. Equations Modelling a Boiling Evaporator Effect:

The mathematical model of the Multiple Effect Evaporator (MEE) flowsheet, Figure (2.4), is essentially an appropriate combination of single effect evaporator models. A simplified diagram of a single effect is shown in Figure (3.1)

3.2.1.a. *Simplifying Assumptions:*

The MEE process mathematical model is based on the following assumptions:

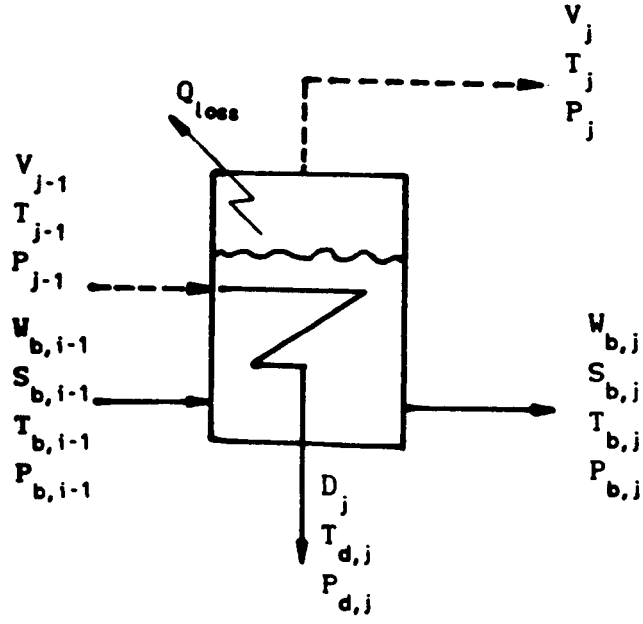

Figure 3.1 Effect unit number j

[1] The vapour in the evaporator is thermally in equilibrium with the liquid.

[2] The steam always condenses completely.

[3] No leaking of vapour or entrainment of air out or in the system.

[4] The flow of noncondensables is negligible.

[5] The condensate is withdrawn at its saturated temperature.

[6] The boiling point rise is a chemical property of the solution and not due to the static hydraulic head.

[7] The pressures of the brine and vapour streams out of an effect are equal.

[8] The product vapour is salt free.

3.2.1.b. *Energy Balance:*

Referring to Figure (3.1) the energy balance equation can be written in the following functional form (to demonstrate the sources of nonlinearity.):

$$(W_{b,j-1} + S_{b,j-1}) \times h_{b,j-1}\{T_{b,j-1}, X_{b,j-1}\} + V_{j-1} \times H_{j-1}\{T_{j-1}, P_{j-1}\} =$$

$$D_j \times h_d\{T_{d,j}, P_{j-1}\} + V_j \times H_j\{T_j, P_j\} + (W_{b,j} + S_{b,j})$$

$$\times h_{b,j}\{T_{b,j}, X_{b,j}\} + Q_{loss} \qquad (3.3)$$

where:

W	= Flowrate of water in the brine.	kg/hr
S	= Flowrate of salt in the brine.	kg/hr
X	= Salt concentration in the brine	gm/kg
V	= Vapour (or steam) flowrate to and from the effect.	
D	= Condensate flowrate	kg/hr
T	= Temperature	K
P	= Pressure	kPa
h	= liquid specific enthalpy	kJ/kg
H	= Vapour (or steam) specific enthalpy	kJ/kg
Q_{loss}	= heat losses	kJ/hr

subscripts:

j-1 = previous effect as seen from the point of view of flowing brine.

j = present effect.

b = brine into and out of the effect.

d = condensate from effect.

Equality of heating steam and condensate water temperatures:

$$T_{j-1} = T_{d,j} \tag{3.4}$$

3.2.1.c. *Heat Transfer Equation:*

The enthalpy balance on the steam chest is given by:

$$V_{j-1} \times H_{j-1} - D_j \times h_{d,j} = Q \tag{3.5}$$

The rate of heat transfer Q can be approximated by using the following relationship.

$$U_j \times A_j \times (T_{j-1} - T_{b,j}) = Q \tag{3.6}$$

where:

A_j : Heat transfer area, (m^2)

U_j : Overall heat transfer coefficient, ($kJ/hr.m^2.K$)

So, equation (3.5) takes the next form:

$$V_{j-1} \times H_{j-1} - D_j \times h_{d,j} = U_j \times A_j \times (T_{j-1} - T_{b,j}) \tag{3.7}$$

3.2.1.d. *Material balance:*

Material balance of the fresh water entering and leaving the effect gives:

$$W_{b,j-1} = W_{b,j} + V_j \tag{3.8}$$

A similar material balance equation for the salt and vapour components will be:

$$S_{j-1} = S_j \tag{3.9}$$

$$V_{j-1} = D_j \tag{3.10}$$

3.2.1.e. *Equilibrium Equation:*

At a given salt concentration ($X_{b,j}$) and temperature ($T_{b,j}$) and (T_j) for evaporator effect (j), the equilibrium correlation may be represented by the following equation:

$$BPR\ \{T_{b,j},\ X_{b,j}\} = T_{b,j} - T_j \tag{3.11}$$

where:

BPR : a function representing the boiling point rise due to the salt concentration.

3.2.1.f. *Pressure Equations:*

The following three equations relate the stream pressures in and out of the evaporator.

$$P_{j-1} = \Delta P_j + P_{d,j} \tag{3.12}$$

Assuming that steam entering and condensed leaving the evaporator chest at the same saturated temperature and pressure, so, pressure losses ΔP_j can be neglected.

$$P_j = P_{b,j} \tag{3.13}$$

Assuming the static pressure head is neglected.

$$P_j = f(T_j) \tag{3.14}$$

3.2.2. Equations Modelling a Flashing Evaporator Stage:

Although the configuration of MSF desalination plants might vary widely from plant to another, as illustrated in chapter 2, the process module usually takes the same configuration shown in Figure (3.2). This section is oriented towards developing a mathematical model for this module.

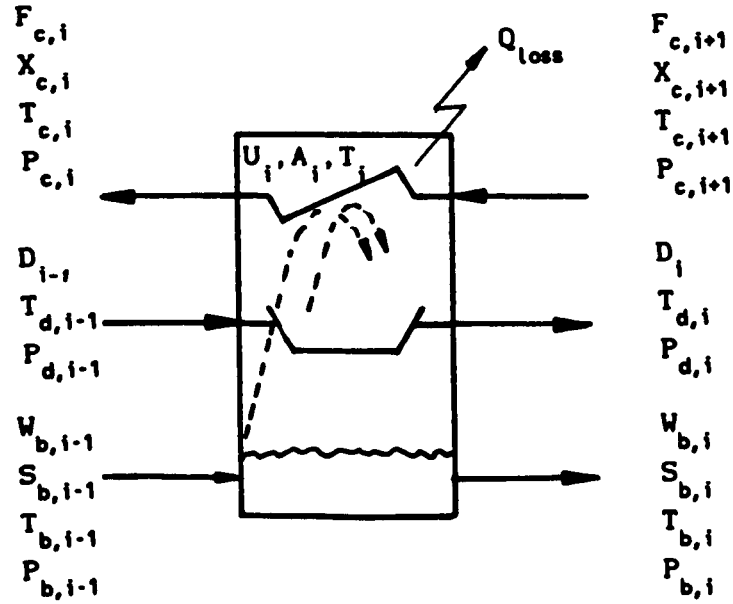

Figure 3.2 a Flash stage unit

3.2.2.a. *Simplifying Assumptions:*

The mathematical model is based on the following assumptions:

[1] The distillate product is salt free (the maximum salt concentration in the final product is usually between 5 and 50 ppm).

[2] The flash vapour is in equilibrium with the brine leaving the stage.

[3] The steam always condenses completely.

[4] The flow of noncondensables is negligible.

3.2.2.b. *Energy balance for the flashing brine:*

$$B_{i-1} \times h_{b,i-1}\{T_{b,i-1},X_{b,i-1}\} = B_i \times h_{b,i}\{T_{b,i},X_{b,i}\} + (B_{i-1} - B_i) \times H_{v,i}\{T_{b,i},P(T_i)\} \quad (3.15)$$

where:

B : Brine mass flow rate, (= W + S), (kg/hr)

i : The present stage number.

i-1 : The previous stage.

v : Flashing vapour.

3.2.2.c. *Overall material balance:*

Water balance:

$$W_{b,i-1} + D_{i-1} = W_{b,i} + D_i \quad (3.16)$$

Salt balance:

$$S_{b,i-1} = S_{b,i} \quad (3.17)$$

Water and salt balances of the cooling stream

$$W_{c,i+1} = W_{c,i} \quad (3.18)$$

$$S_{c,i+1} = S_{c,i} \quad (3.19)$$

Subscripts:

c = Cooling brine.

i+1 = The next stage number.

3.2.2.d. *Overall enthalpy balance:*

$$F_{c,i+1} \times h_{c,i+1} + D_{i-1} \times h_{d,i-1} + B_{i-1} \times h_{b,i-1} = F_{c,i} \times h_{c,i} + D_i \times h_i + B_i \times h_{b,i} + Q_{loss} \quad (3.20)$$

where:

h_c : $f(T_c, X_c)$

h_d : $f(T_d)$

Q_{loss}: Stage heat losss

3.2.2.e. *Heat transfer equation:*

The amount of heat exchanged Q_i across the condenser heat transfer surface is defined as:

$$Q_i = F_{c,i} \times Cp_{m,i} \times (T_{c,i} - T_{c,i+1})$$

$$= U_i \times A_i \times \frac{(T_{c,i} - T_{c,i+1})}{ln.((T_{d,i} - T_{c,i+1})/(T_{d,i} - T_{c,i}))} \qquad (3.21)$$

where:

LMTD : The logarithmic mean temperature difference.

A : Condenser heat transfer area.

U : Overall heat transfer coefficient.

U = Φ (ϕ_i, $T_{c,i}$, $T_{c,i+1}$, $T_{d,i}$, ID_i, OD_i, FF_i, R_f)

ϕ : Tube side brine velocity.

ID : Tube inside diameter.

OD : Tube outside diameter.

FF : Flooding factor

R_f : Fouling factor

from the above equation the following equation is obtained:

$$\frac{U \times A}{F_{c,i} \times Cp_{m,i}} = ln \frac{T_{d,i} - T_{c,i+1}}{T_{d,i} - T_{c,i}} - ln \frac{T_{d,i} - T_{c,i}}{T_{d,i} - T_{c,i+1}} \qquad (3.22)$$

After a few steps of simplification for equation (3.22) the following equation is obtained:

$$T_{c,i} - T_{c,i+1} - (T_{d,i} - T_{c,i+1})(1 - e^{-UA/F_c \times Cp_m}) = 0$$

$$(1 - E) \times T_{c,i+1} + E \times T_{d,i} - T_{c,i} = 0 \qquad (3.23)$$

where:

$$E = 1 - e^{-UA/F_c \times Cp_m}$$

Cp_m = Mean heat capacity of the cooling brine, function of temperature range and the salt concentration.

3.2.2.f. *Equilibrium correlation:*

The relation between the outlet brine temperature $T_{b,i}$ and the superheated vapour temperature $\hat{T}_i$ adjacent to the brine surface can be represented by the following equation:

$$\hat{T}_i = T_{b,i} - NEA \qquad (3.24)$$

where:

$\hat{T}_i$ = Superheated vapour temperature, K

$T_{b,i}$ = Outlet brine temperature, K

NEA = Non equilibrium allowance , K

$= \Phi (T_{b,i})$

Due to the boiling point elevation , the superheated vapour temperature $\hat{T}_i$ is subcooled to the condensation temperature at the top $T_{d,i}$, so:

$$T_{d,i} = \hat{T}_i - NEA - BPR \qquad (3.25)$$

combining equations (3.24) and (3.25),

$$T_{d,i} = T_{b,i} - BPR \qquad (3.26)$$

A. Nonequilibrium Allowance (NEA)

This temperature loss in the total flashing temperature range has been given by Homig [1978] as a plotted range which is function of the stage brine temperature. This range is approximated by a single curve which is then fitted to the following third degree polynomial, which is sufficiently accurate for application in the developed program:

$$NEA = A + B\,T_b + C\,T_b^2 + D\,T_b^3 \qquad (3.26,a)$$

where: $A = 2.556$ $B = -0.203E-1$

$C = -0.129\ E-3$ $D = 0.1123\ E-5$

T_b = stage brine temperature, C

3.3.3.g. *Pressure equations:*

The flash stage pressure is governed by the following equations:

- The relation between the pressure of the cooling water entering and leaving the condenser tube bundle is:

$$P_{c,i+1} = P_{c,i} + \Delta P_i \qquad (3.27)$$

where :

ΔP_i ≡ Pressure loss due to the friction in the tube side of the condenser. The value of ΔP_i is either given to the program as an input parameter or calculated as shown in the Appendix {A}.

- The second equation relates output brine and distillate pressures.

$$P_{d,i} = P_{b,i} \tag{3.28}$$

- In the third equation, the pressure of the distillate liquid leaving the stage is determined as a function of stage temperature T_i i.e:

$$P_{d,i} = \Phi\ (T_i) \tag{3.29}$$

3.2.3 Equations Modelling a Vapor Compressor:

A simplified diagram of the compressor unit is shown in figure (3.3). Assuming adiabatic compression, the equations representing the mass and energy balances are:

$$V_1 = V_2 = V \tag{3.30}$$

$$\omega = V \times (H_2 \{T_2, P_2\} - H_1 \{T_1, P_1\}) \tag{3.31}$$

Adiabatic Compression:

$$T_2 = T_1 \times [P2/P1]^{(\gamma-1)/\gamma} \tag{3.32}$$

where:

ω : input work to the compressor, W

γ : polytropic index, ≈ 1.327

subscripts 1 and 2 refer to inlet and outlet of the compressor respectively.

3.2.4. Equations Modelling a Mixer Unit:

The mixer unit can be thought of as the union of two pipes or a mixing tank with two inputs, and only one output stream as shown in figure (3.4). (

3.2.4.a. *Assumptions;*

[1] Ideal mixing (with no heat effect other than sensible heat)

[2] Two input streams only.

[3] Pressures in and out of the unit are equal.

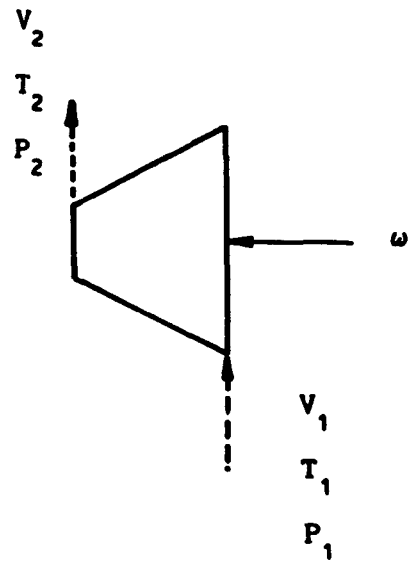

Figure 3.3 a Compressor Unit

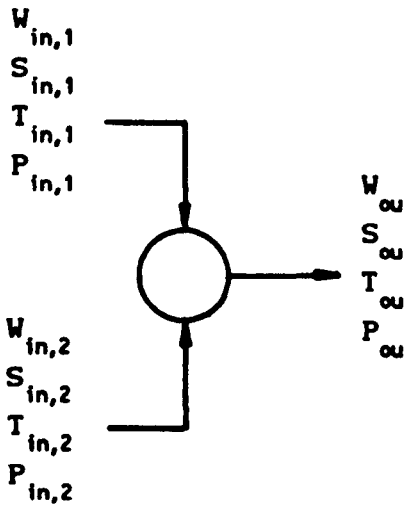

Figure 3.4. a Mixer Unit

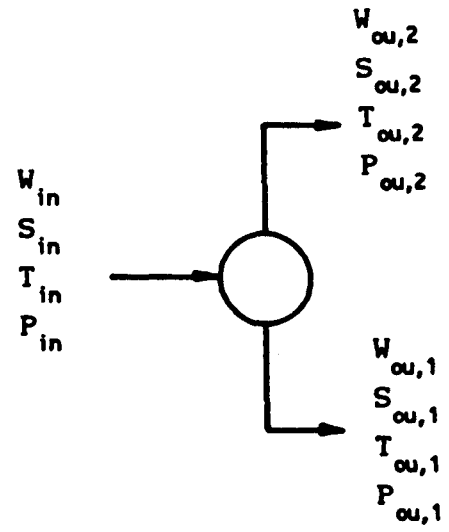

Figure 3.5. a Splitter Unit

3.2.4.b. *Energy balance:*

$$(W_{in,1} + S_{in,1}) \times h_{in,1} + (W_{in,2} + S_{in,2}) \times h_{in.2} = (W_{ou} + S_{ou}) \times h_{ou} \qquad (3.33)$$

where:

in,1 ≡ first input stream.

in,2 ≡ second input stream.

ou ≡ output stream.

3.2.4.c. *Material balance:*

Water balance:

$$W_{in,1} + W_{in,2} = W_{ou} \tag{3.34}$$

Salt balance:

$$S_{in,1} + S_{in,2} = S_{ou} \tag{3.35}$$

3.2.4.d. *Pressure equations:*

Pressures in and out of the mixer unit are assumed equal.

$$P_{in,1} = P_{ou} \tag{3.36}$$

$$P_{in,2} = P_{ou} \tag{3.37}$$

3.2.5. Equations Modelling a Splitter Unit:

The splitter is like a single pipe dividing into two smaller pipes. It is depicted in Figure (3.5).

3.2.5.a. *Assumption:*

The output streams have the same properties as the input stream, only the mass flowrates are different.

3.2.5.b. *Equalities of temperature and pressure into and out of the unit*

$$\left.\begin{aligned} T_{in} &= T_{ou,1} \\ T_{in} &= T_{ou,2} \end{aligned}\right\} \tag{3.38}$$

$$\left.\begin{aligned} P_{in} &= P_{ou,1} \\ P_{in} &= P_{ou,2} \end{aligned}\right\} \tag{3.39}$$

3.2.5.c. *Material balance:*

$$W_{in} = W_{ou,1} + W_{ou,2} \tag{3.40}$$

$$S_{in} = S_{ou,1} + S_{ou,2} \tag{3.41}$$

$$W_{ou,1} = W_{in} \times \alpha \tag{3.42}$$

$$S_{ou,1} = S_{in} \times \alpha \tag{3.43}$$

where $\alpha \equiv$ Splitting ratio.

3.2.6 Equations Modelling a Flash Unit:

In the flash unit the feed stream is separated into a liquid and a vapour stream in equilibrium, Figure (3.6).

3.2.6.a. *Assumption;*

The output streams are in equilibrium.

3.2.6.b. *Energy balance;*

$$(W + S)_{in} \times h_{in} = V_{ou,2} \times H_{ou,2} + (W + S)_{ou,1} \times h_{ou,1}$$

then:

$$W_{in} \times h_{in} + S_{in} \times h_{in} - S_{ou,1} \times h_{ou,1} - V_{ou,2} \times H_{ou,2} - W_{ou,1} \times h_{ou,1} = 0 \tag{3.44}$$

where:

$$h_{in} \equiv f(T_{in}, X_{in})$$

$$h_{ou,1} \equiv f(T_{ou,1}, X_{ou,1})$$

$$H_{ou,2} \equiv f(T_{ou,2}, P_{ou,2})$$

And the output stream temperatures are equal:

$$T_{ou,1} = T_{ou,2} \tag{3.45}$$

3.2.6.c. *Material balance:*

$$W_{in} = W_{ou,1} + V_{ou,2} \tag{3.46}$$

$$S_{in} = S_{ou,1} \tag{3.47}$$

3.2.6.d. *Pressure equation:*

$$P_{ou,1} = P_{ou,2} \tag{3.48}$$

3.2.7. Equations Modelling a Condenser Unit:

Figure (3.7) illustrates the condenser, which is a simple shell and tube heat exchanger. In the shell side, a saturated vapour or steam is condensed, without subcooling, giving its latent heat to the second

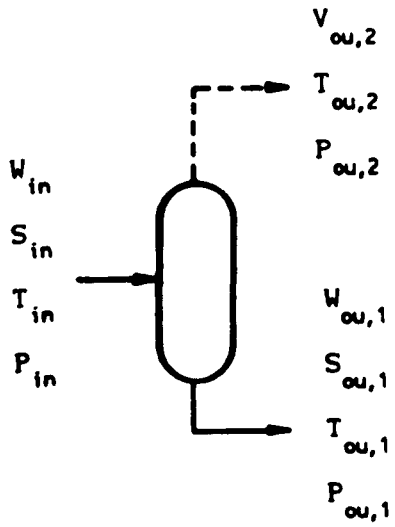

Fig. 3.6. a Flash Unit

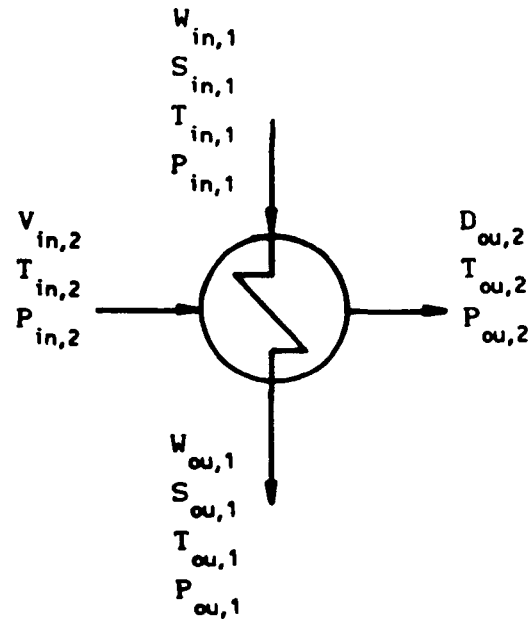

Fig. 3.7. a brine heater unit.

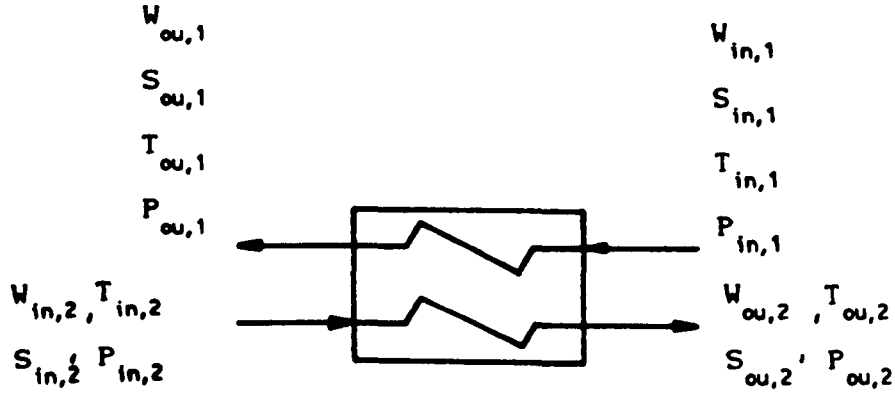

Fig. 3.8. a Concentric L/L heat exchanger unit

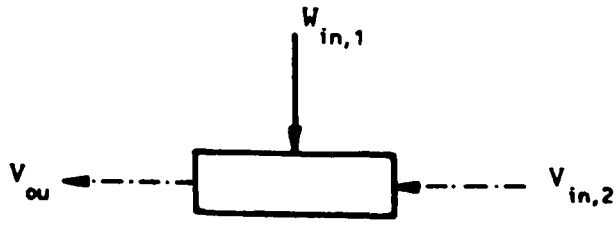

Fig. 3.9. a desuperheater unit

stream in the tube side to raise its temperature from $T_{in,1}$ to $T_{ou,1}$

3.2.7.a. *Assumption:*

Vapour or steam in the shell-side is condensed without subcooling.

3.2.7.b. *Energy balance:*

$$V_{in,2} \times (H_{in,2} - h_{d,ou,2}) + W_{in,1} \times (h_{in,1} - h_{ou,1}) + S_{in,1} \times (h_{in,1} - h_{ou,1}) = 0 \qquad (3.49)$$

where:

$$H = \Phi (T_{v,in,2}, P_{v,in,2})$$

$$h_d = \Phi (T_{d,ou,2})$$

$$h_{in} = \Phi (T_{in}, X_{in})$$

3.2.7.c. *Heat transfer:*

$$Q = (W + S)_{in,1} \times Cp_m \times (T_{ou,1} - T_{in,1}) \qquad (3.50)$$

$$= U \times A \times \left\{ \frac{T_{ou,1} - T_{in,1}}{\ln \left\{ \frac{T_{v,in,2} - T_{ou,1}}{T_{v,in,2} - T_{in,1}} \right\}} \right\} \qquad (3.51)$$

from equations (3.50), (3.51) and after some simplification we have:

$$(1 - E) \times T_{in,1} + E \times T_{v,in,2} - T_{ou,1} = 0 \qquad (3.52)$$

where:

$$E = 1 - e^{-UA/[(W + S)_{in,1} \times Cp_m]}$$

Subscripts:

in,1 : inlet cooling stream.

ou,1 : outlet cooling stream.

v,in,2 : inlet vapour (or steam) stream.

Cp_m : Mean heat capacity of cooling stream.

3.2.7.a. *Material Balance;*

$$V_{in,2} = D_{ou,2} \tag{3.53}$$

$$W_{in,1} = W_{ou,1} \tag{3.54}$$

$$S_{in,1} = S_{ou,1} \tag{3.55}$$

Temperature equality of the vapour and condensate stream

$$T_{v,in,2} = T_{d,ou,2} \tag{3.56}$$

3.2.7.e. *Pressure Equation:*

$$P_{in,1} - P_{ou,1} = \Delta P \tag{3.57}$$

where ΔP = The pressure loss due to the friction in the tube side.

3.2.8. Equations Modelling a Liquid/Liquid Heat Exchanger Unit;

Figure (3.8) shows the schematic diagram of a concentric tube countercurrent exchanger:

3.2.8.a. *Energy balance;*

$$F_{in,1} \times Cp_{m,1} \times (T_{in,1} - T_{ou,1}) = F_{in,2} \times Cp_{m,2} \times (T_{ou,2} - T_{in,2}) \tag{3.58}$$

where:

$F_{in,1}$: heating stream flowrate.
$F_{in,2}$: cooling stream flowrate.

3.2.8.b *Heat Transfer:*

Heat transfer process is governed by the following equation:

$$\frac{T_{in,1} - T_{ou,2}}{T_{ou,1} - T_{in,1}} = e^{UA \cdot \left[\frac{1}{F_{in,1} \times Cp_{m,1}} - \frac{1}{F_{in,2} \times Cp_{m,2}} \right]} \tag{3.59}$$

3.2.8.c. *Material Balance;*

$$W_{in,1} = W_{ou,1} \tag{3.60}$$

$$S_{in,1} = S_{ou,1} \tag{3.61}$$

$$W_{in,2} = W_{ou,2} \tag{3.62}$$

$$S_{in,2} = S_{ou,2} \tag{3.63}$$

3.2.8.d. *Pressure Equations:*

$$P_{in,1} - P_{ou,1} = \Delta P_1 \qquad (3.64,a)$$

$$P_{in,2} - P_{ou,2} = \Delta P_2 \qquad (3.64,b)$$

where, ΔP_1 & ΔP_2 are the pressure drop due the friction in the tube side.

3.2.9. Equation Modelling a Desuperheater Unit

Referring to Figure 3.9 the desuperheater unit may be represented by the following equations:

3.2.9.a. *Material Balance:*

$$V_{in,2} + W_{in,1} = V_{ou} \qquad (3.65)$$

3.2.9.b. *Energy Balance:*

$$H_{in,2} \cdot V_{in,2} + h_{in,1} \cdot W_{in,1} = V_{ou} \cdot H_{ou} \qquad (3\ 66)$$

where H : enthalpy of superheated vapour

3.2.9.c *Pressure Equation:*

$$P_{ou} = P_{in,2} \qquad (3.67)$$

3.3. CONCLUSION

In this chapter, the mathematical models describing the steady state behaviour of the basic units in thermal desalination processes assemblies, are presented. These models are based on the material and energy balances.

Inspection of the unit models shows that they include a number of nonlinear algebraic relationships, therefore, some form of linearization must be employed and hence iteration is necessary. Also, it will be seen that the equations are highly interlinked and sparse in nature.

CHAPTER 4

DESIGN AND SIMULATION CALCULATION APPROACHES FOR EVAPORATION PROCESSES

4.1 INTRODUCTION.

In the previous chapter, the mathematical models for the units constructing the thermal desalination process were described. The thermal distillation flowsheet usually consists of several of these units interconnected by process streams. During the last three decades, a number of techniques and numerical methods have been developed to design and simulate these flowsheets. In fact, it might be said that the history of the thermal desalination processes modelling and programming is the history of the traditional modelling and programming of chemical plants.

Several reviews of the flowsheeting of separation processes (e.g. distillation columns) are available (e.g. Sargent [1983]). However, no review has appeared in the literature that addresses the techniques and methods which have been used in solving thermal desalination processes and the evaporation processes in general. One of the main goals of this chapter is to fill in this gap in the literature. This will be achieved by classifying, and analysing the available works which have been done in the evaporation processes according to the experience gained from chemical plant flowsheeting and numerical methods.

The physical problems of simulating and designing thermal desalination processes are illustrated in section 4.2. Techniques for solving these problems are classified in section 4.3. The numerical statement of the problem is defined in section 4.4, and the numerical methods and techniques for solving this problem are reviewed in section 4.5. Also in this chapter, techniques which have been used for exploiting the mathematical model structure for a process are briefly explained in section 4.6. The required characteristics in the developed program are pointed out in section 4.7, and the proposed technique for achieving these characteristics is introduced in section 4.8. Finally,

the main points of this chapter are outlined in section 4.9.

4.2 THE PROBLEM IN BRIEF.

The most straightforward form of the simulation problem is achieved by giving the unit model equations, the value of the parameters involved, and the process feed stream specifications, to calculate all the other stream variables in the process. So, if the process units are ordered in sequence, as shown in Figure (4.1, A), the problem would be straightforward and simple. By knowing the feed stream S_1 and the required design parameters P_1 for the unit U_1, the output stream S_2 can be simply calculated. Similarly, streams S_3 and S_4 would be calculated. However, in thermal distillation process, this is not the case, because of:

i. Countercurrent flow of information and/or material in these processes, for instance:

   [1] To simulate the performance of the forward feed double effect evaporation process, Figure (4.1, B), the feed state, steam temperature and pressure, are specified. Furthermore, the vacuum level in the system is fixed at the exit of the second effect. Therefore, information of the absolute pressure level in the first effect has to be fed backward from the final effect, Stewart et. al. [1977]. In brief, a piece of information, (such as total flowrate composition, temperature, or pressure), associated with a certain process stream may travel in the opposite direction to the stream itself.

   [2] In every part of the backward feed configuration, Figure (4.1,C), and the MSF process Figure (4.1,D), countercurrent flows of material and information (because some of the variables that appear in both ends of the plant are fixed) exist, Glueck et al [1970].

ii. The existence of recycle streams. where outputs from some down stream units are fed as inputs to units early in the sequence) see Figure (4.1,E).

Therefore, the simulation and design (or controlled simulation) of seawater desalination processes are neither simple nor straightforward.

Fig. 4.1.

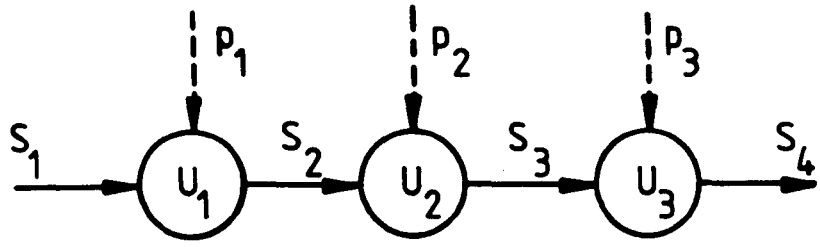

A

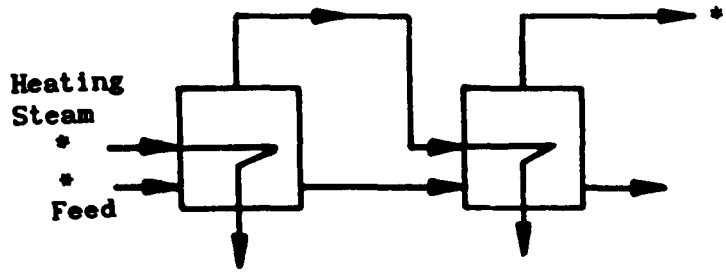

B

Forward Feed

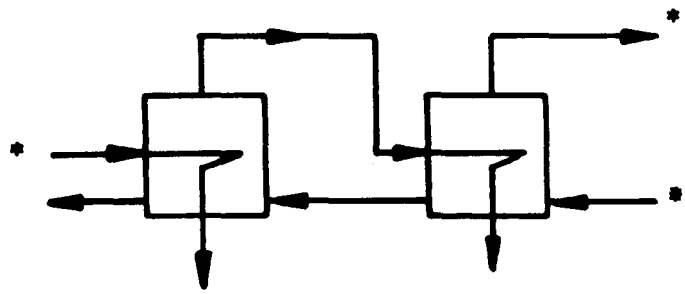

C

Feed

Backward Feed

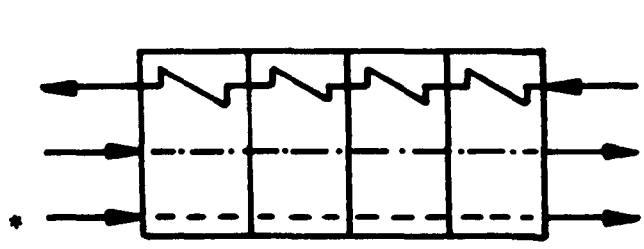

D

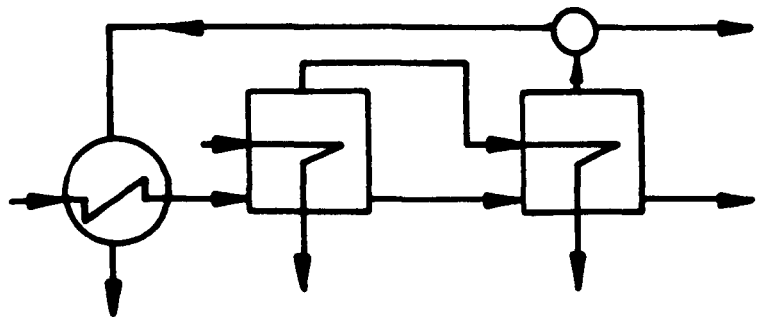

E

* Some of the Stream Variables are specified.

4.3. COMPUTATION TECHNIQUES ARCHITECTURE.

Several techniques are used to solve the equations describing a plant process. These techniques are:

- Procedure Oriented Approach.
- Simultaneous Modular Approach.
- Equation Oriented Approach.

4.3.1. Procedure Oriented (PO) Approach.

In this approach each process unit is modelled by a separate subroutine (or module). Each unit module calculates the output stream variables by knowing the input stream and the unit design parameters, i.e. the process unit modules are typically simulation oriented, Chen et al [1985]. Different unit modules of the process are called by an executive program in a suitable calculation sequence determined by the flowsheet topology.

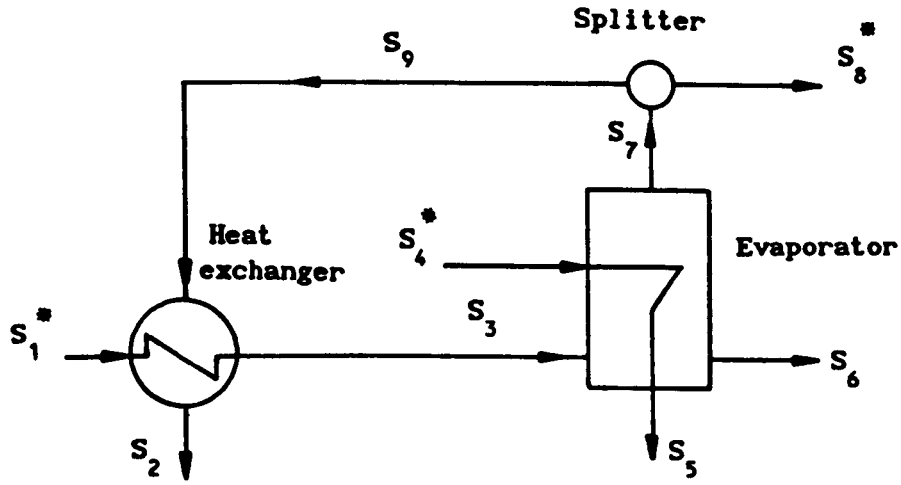

* Some of the stream variables are specified.

figure (4.2)

For example the above simple flowsheet in Figure (4.2), has the following:

[1] A fixed design specification (vapour temperature T_v, or pressure), of the stream S_8.

[2] A recycle stream, S_9

[3] A number of unit operations which are represented by nonlinear mathematical models.

Therefore, three levels of iterations are needed to perform the

required calculations. By knowing the process topology, the unit parameters, the feed streams data, and the design specifications, a program using the procedure oriented approach would perform the computation as follows:

[1] Guess the temperature T_v, (specified), of the stream S_8.

[2] Given S_1, guess stream S_9 (tear stream).

[3] Since all input streams are known, sequentially all the output streams, i.e. S_2, S_3, S_5, S_6, S_7, S_8, and S_9, can be calculated. In fact, the mathematical equations for the given flowsheet are not well suited to direct solution, because of the nonlinearities and the implicit dependence of physical properties on temperature, pressure, and salt content. Therefore, each unit is handled by an iterative process. So, the first iterative level for solving this process would be the module level.

[4] If the calculated and the guessed stream values of S_9 are within a specified small tolerance, the second iterative level (flowsheet level) converges. Otherwise, a new value for the stream S_9 is estimated and steps [2], [3], and [4] are repeated.

[5] If the final calculated value of T_v and the specified (fixed) value are within a specified small tolerance, the calculation of the third outermost iterative loop (control loop) converges. Otherwise, the mismatch between the calculated and specified values of T_v is used to update the guess of the stream S_8, and steps [1], [2], [3], [4], and [5] are repeated.

Many numerical methods have been used to obtain successive estimates for streams S_9 and S_8. For detailed description of these methods see Westerberg et al [1979] or Motard et al [1975].

For simulating an MSF process, Glueck and Bradshaw [1970] have used the Newton Raphson method to update the guessed values for the iteration variable (vapour space temperature). Helal [1985] used Broyden and bisection methods to update the successive guessing of some MSF process parameters. Helal has found that the number of flowsheet evaluations using the bisection method is much higher than that required using the Broyden method.

4.3.1.a. Advantages of The Procedure Oriented Approach.

Procedure Oriented (PO) approach has the following advantages:

i- *Efficient Numerical Solution.*

Each unit module is solved individually. So, according to the module mathematical model structure, one or more specialized numerical methods can be used. Thus, the module calculations can be very efficient.

ii- *Easy to Understand and to Implement.*

Because of the modular structure of the PO programs, new units can be easily added to an existing program. The testing of unit modules can be done separately. Also, because the information flow in the program is similar to the material flow in the process, PO programs are easily understood.

4.3.1.b. Utilization of PO Approach in Evaporation Processes.

Using the idea of the procedure oriented approach, a number of programs were developed in the early sixties by a number of companies for their own plant designers. The "FLASH" program was developed by Easterday [1965]. It is written in FORTRAN II, and performs heat and material balance calculations for an MSF process. In this program feed seawater temperature and concentration are fixed at 65 F and 3.5 per cent respectively. The condenser tubes for both heat recovery and rejection sections have the same length.

To overcome the severe limitations in the "FLASH" program, the "SALINE" program was developed by Griffith et al [1965]. It is a modified version of the "FLASH" program, written in FORTRAN IV. The performance ratio and feed seawater temperature are specified in the input data. The number of the heat rejection stages can be automatically varied during optimization computation. An option to adjust the stage length rather than the brine velocity has been provided. However, some restrictions are still inherent in the program. For instance, heat and material balances are based on equal heat transfer area in all heat recovery stages, and the salt concentration of the feed seawater is fixed at 3.5 per cent.

" ORSEF" program was written by Mothershed [1966] in FORTRAN II language. The program determines the operating characteristics, geometry, and costs of MSF process. Also, the program can calculate the optimum balance between energy consumption and heat transfer area.

The above three programs were tailored to perform calculations for specific fixed arrangement configuration, (brine recirculation type), using stage to stage technique.

Easterday et al [1966], observed some differences in the above programs results. They referred these differences to the differences in engineering approaches (e.g. determination of heat transfer coefficients, pump head, and cost), numerical procedure, and the physical properties.

" MSF21 " which was written by Fort (1972), is another FORTRAN IV code, for performing design, cost, or optimization calculation for an MSF plant. The program was written for a fixed flowsheet of the process. The computations are based on the first, and last stages of each section (recovery, and rejection) and a typical middle recovery stage. Therefore, the program runs rapidly, however, it does not give the stage by stage parameters.

Many design features have been built into the program, such as: the temperature of both the heat rejection stream and the blowdown streams are equal. The flowrate of the recycle stream is always greater than zero. So, the once through type can not be designed. These features added limitations to the use of the program.

" VTE21" is another subprogram of the overall system " ECON21" which consists of six parts. VTE21 was written by Fort et al [1976] in FORTRAN IV language. Design, costing, or optimisation calculations are performed by the program for a vertical tube evaporation plant. The code is specifically written for a fixed flowsheet that consists of vertical tube effects, multi stage preheater condensers, and a brine heater, Figure (2.6). The computations are performed for each vertical tube effect, and the first, last, and the middle stage of the preheater stages.

The above two programs were not developed for performing detailed design computations. Therefore, many approximations have been applied for a rapid calculation and overall design optimization.

Glueckstern et al [1976], have modified, and updated the cost functions of the MSF21 and VTE21 programs to perform the evaluation and design optimization for small size plants.

The application of "NETWORK 67" general flowsheeting program to design and simulate an MEE system was described by Andrew [1968]. The program was written in ALGOL. The flexibility of the program has been achieved at the expense of simplicity. The user should have a good programing knowledge before the program can be effectively applied.

Jernqvist et al [1966] have published a description of a computer program denoted 'EVAPOCHALM', for computing performance and design calculations for almost arbitrary black liquor MEE plants. The program is based on a so-called "unit cell" which comprises an evaporator vessel, three heat exchangers, one liquor, one condensate flash tank, and a liquor mixing vessel. Mass and energy balances of the unit cell components are performed by a separate subroutine for each unit, and repeated from a unit cell to another. Data is given to the program via a connection matrix. The program is written in ALGOL 60.

'INDAK' program, published by Schalien et al [1970], approximately has the same components as 'EVAPOCHALM' program, i.e. connection matrix, and unit cell. However, no information about these components are given. The authors have claimed that INDAK has been shown to be valid for all evaporator systems of pulping industries, but this has not been illustrated.

The principles of modularity by the unit cell and flowsheet description by the connecting matrix, presented by Jernqvist et al [1966], have been used by Bolmstedt et al [1974] in developing 'INDUNS' program. This program was written in FORTRAN IV. The program was developed for the evaluation and design calculations of general multiple effect evaporation plants in, for example, the sugar and paper pulp industries.

Barba et al [1973], have developed a mathematical model for an MSF process with brine recirculation. This model was used for on-line process computer control and applied to the Porto Torres desalination plant. The model supplies information for the optimal plant operation to meet the varying water demands of the refinery, which is using the distillate as process water. Stage to stage technique was used to solve the model.

Two programs were described by Hitchcock et al [1967]. The first carries out a performance calculation for the MSF process, while the

second performs design calculation for the MEE process. The authors have illustrated that four iterative loops are required to calculate a MSF process flowsheet. These loops are: one within each stage, one for each of the recovery and rejection sections, and one outside loop to adjust output and performance ratio to given values.

A rigorous mathematical model for MSF distillation process was developed by Medani et al [1980]. The temperature of the coolant stream leaving each stage is assumed, then the computation is started from the hot end to the cold end, then the calculated value of the coolant temperature entering is compared with that defined by the flowsheet calculation. This method is unreliable because of the numerical unstability problems, Flower et al [1982]. Medani et al have paid much attention to the performance characteristics of MSF process under changing operating conditions. Also, the nested iterative solution using the stage to stage technique was illustrated.

Rautenbach et al [1980], have developed a modular structure program for designing and/or simulating MSF plants. According to the considered flowsheet the required modules are linked by a master program. Stagewise computation is started with the hot end, where some variables are estimated, and a modified Regula Falsi method is used to update the estimated values. Several forms for simulating a recycle MSF plant are outlined. However, no information about the convergence characteristics of these forms is given.

Omar [1981], applied the stage to stage technique for simulating multi-stage flash plants with fixed configuration and different operating conditions.

General basic equations and initial values for iterative computation of individual stages and MSF process as a whole were illustrated by Homig [1978]. Using the stage to stage technique, this mathematical model was solved to design the FICHTNER company MSF reference plant. Also, the performance of this plant under different operating conditions was examined.

A rigorous mathematical model for the MSF process was developed by Glueck et al [1970]. This model can be used for steady state and dynamic simulation of a given process configuration. The model takes into account variations in heat transfer coefficient with condenser tube

geometry, tube surface fouling, effects of non-condensable gases, boiling point elevation, revaporization of product, thermal inertia of the flash vessel walls and tubes, and superheating of flashed vapour. To perform the flowsheet steady state calculations, a set of vapour space temperatures (T_v) are assumed, and the stage equations are solved, in turn producing a new estimation of (T_v), then the Newton Raphson method is used to update the estimated values. This model is mainly oriented toward performance evaluation rather than design. Unfortunately, no example has been given.

The performance and convergence characteristics of the stage to stage technique applied in the above programs have not been discussed. This point has been investigated by Helal [1985]. Helal has concluded that " the stage to stage approach has showed poor reliability characteristics, where it always diverges unless a good initial guess, close enough to the solution, is utilized". However, the general disadvantages of the technique may be defined as below.

4.3.1.c. Disadvantages Of The Procedure Oriented Approach.

The efficiency of the PO approach is seriously affected by the following two major problems:

1. Nested iteration structure. 2. Rigid information structure.

The first problem may be illustrated by assuming that the control loop used to handle design specification in Figure (4.2), takes 10 iterations to converge. At each of these ten iterations, the accelerated substitution loop used to converge the tear stream may need 5 iterations to converge. If the mathematical model of the evaporator unit requires 3 to 4 iterations to be solved, thus, the evaporator unit module would be encountered 150 - 200 times. More complex flowsheets with several layers of nested iteration loops, may require a great deal of time to converge, and in fact, may never converge, Locke [1982].

Finding suitable convergence tolerances for the various nested iteration loops is really a problem. Too tight tolerance in the deeper levels leads to excessive CPU times, whereas with a convergence criterion not tight enough may lead to unstable or oscillating system, and, consequently, to convergence problems on the outer iteration levels.

Rigid information structure is the second major disadvantage of

the PO approach. By definition, the direction of flow of information is parallel to that of physical process streams. In other words, each unit module is written to calculate specific outputs from specific inputs. In order to specify an output and calculate an input, the user must either use a different versions of the unit module or add a control block around the unit to adjust the input variables until the required output is obtained, Westerberg et al [1979]. Therefore, this approach is not flexible enough to perform all the different calculations which the designer is faced with.

Two alternative approaches have been considered to overcome the fundamental problems described above. They are: the simultaneous modular approach, and the equation oriented approach.

4.3.2. Simultaneous Modular Approach.

Using this approach, the problem is solved in two computation levels. First, the module level, in which the same unit models as the procedure oriented approach are required. Second, the flowsheet level, in which the linearized equations relating the outputs to the inputs of each unit, the connection equations between the units, and the specification equations are solved simultaneously.

Therefore, this approach is a hybrid of the procedure oriented approach, and the equation oriented approach (illustrated in the next section), and it combines some of the good features of both techniques, such as:

- No great additional investment in software would be required, because the already existing modules can be used to perform the module level calculations.
- No need for costly control loops to converge the design specifications, because the design specification equations are handled directly on the flowsheet level.
- Storage requirements for this technique would be less than that required by the equation oriented approach, because the number of equations in the flowsheet level would be smaller.

Stewart et al [1977] have developed a simultaneous modular approach based algorithm for the simulation of multiple effect evaporator system with backward feed. The solution is performed in two

steps. All connecting streams are torn and treated as two separate streams, an input and an output stream. The intermediate stage pressure values are assumed. By giving the parameters and inputs to each effect, the output variables are calculated using the available evaporator model. In the second step, the coefficients (β_j & α_j) are calculated by relating the vapour (V_j) (produced by an effect (j)) to;

i. Vapour required by the effect ($\bar{V}_{j-1}$) as;

$$\beta_j = \frac{\partial \bar{V}_{j-1}}{\partial V_j} \tag{4.1}$$

ii. Pressure difference over the effect (P_{j-1}-P_j) as;

$$\alpha_j = \frac{\partial V_j}{\partial (P_{j-1} - P_j)} \tag{4.2}$$

Using these coefficients a linear equation relating the pressure perturbation to the above variables is developed for each effect. Then the linear equations for the entire flowsheet are solved simultaneously. The resulting pressure perturbation values are used to start the next iteration.

The work of Stewart et al was extended by Ayangbile et al [1984]. They discussed a generalized cascade algorithm for a steady state simulation of multiple effect evaporation with heat recovery features and arbitrary configuration. The algorithm was tested for different feed arrangements (forward, backward, and mixed feed). However, no flowsheet with heat recovery was presented in their article.

Writing the linearized models for the simultaneous modular method can be difficult. If a poor approximation of the linearized equations is used, this approach may fail or at least require many iterations to converge, Westerberg et al [1979].

4.3.3. Equation Oriented Approach.

Equation Oriented (EO) approach has been proposed as another alternative for the procedure oriented approach. In this approach, the process unit model equations, connection equations, and specifications are expressed in the form of one large system of linear and nonlinear equations. This system is then solved iteratively for all the unknown variables.

Using this approach, the drawbacks associated with the more traditional procedure oriented approach can be avoided. Simultaneous solution of all the process equations gives:

* Great flexibility in the selection of specifications.
* No need for nested iteration loops, where only one level of iteration is required.
* Straightforward solution for the problems with recycle streams.

Many aspects involved in equation based flowsheeting are discussed in detail by Westerberg et. al. [1979], Shacham et. al. [1982], and Stadtherr et al [1982].

4.4. THE NUMERICAL STATEMENT OF THE PROBLEM.

The equation based process flowsheeting requires the solution of large systems of linear and nonlinear algebraic equations defined by equation 3.1. There are a number of numerical methods for solving that system.

4.5. NUMERICAL SOLUTION OF LARGE SYSTEM OF NONLINEAR EQUATIONS.

A detailed mathematical discussion of various methods for solving a system of nonlinear equations will not be presented here. This detailed discussion is available in standard numerical texts (e.g. Ortega and Rheinboldt [1970]). Also, a good review can be found in a paper by Sargent [1980]. In this section, only the techniques which are relevant to this work will be reviewed in some detail. These techniques are:

[1] Successive Substitution.

[2] Simultaneous Linearization
   * Newton
   * Quasi-Newton

[3] Direct Linearization Method

4.5.1. Successive Substitution.

By deciding for which variable each equation would be solved, equation (3.1) may be solved using the successive substitution (SS) technique. The variable for which an equation is solved, is called the output variable of the equation. By writing the chosen output variables vector on the left hand side of the rearranged system, equation (3.1) may take the following equivalent form:

$$X = \Phi (X) \tag{4.3}$$

Using the SS technique, the above equation is solved iteratively as follows:

$$X^{k+1} = \Phi (X^k) \tag{4.4}$$

where, k is an iteration counter, and X^{k+1} is the vector of the output variables. So, by guessing X^0, the vector of the output variables is calculated as X^1, and the process is repeated until a specified tolerance is satisfied.

The output variable set must be such that:

- Each equation has only one output variable assigned to it.
- Each assigned variable appears as the output variable of only one equation.

If the model equations contain a number of variables more than the number of equations, some variables would not be assigned as output for any equation, these variables are called "design variables". On the other hand, if the number of equations is greater than the number of variables, the system is over specified, i.e. either some equations are redundant or the set is inconsistent so that no solution exists.

By specifying the design variables, the mathematical model is uniquely defined and the solution can be started. However, the problem is to identify the design variables, the output variable for each equation, and to determine the solution order of these equations.

Rudd and Watson [1968] have discussed a design variable selection algorithm to choose suitable design variables, an output variable for each equation, and the "precedence order" in which the equations should be solved.

Simplified mathematical models were derived by Guneratne [1973], for representing the main seawater distillation processes, namely, the multiple effect evaporation, the vapour compression, and the multi-stage flash. Application of Rudd's ordering algorithm shows that the models can be solved by means of a suitable choice of design variables, and by using each equation of the model in turn to evaluate the output variable. Various computer programs were written, based on these models.

Schweitzer [1978], has suggested a technique named "reverse synthesis" in which, the equation output variables, the design variables, and the solution order of the problem relationships, are determined by inspection. As an illustrative example, design of two forward effect evaporators were considered. The technique shows feasibility for the considered simple problem, however, for more complicated problem the analysis by inspection may become impractical and a more systematic approach must be used.

The main disadvantages of the successive substitution method are:

[1] The method is sometimes unstable and diverges towards infinity rather than converging to definite value, Rose [1974].

[2] The method has only first order convergence rate to the final solution, Perkins [1979].

4.5.2 Simultaneous Linearization Techniques.

4.5.2.a. Newton's Method.

In the process flowsheeting area, Newton method for solving large system of nonlinear equations, with sparse matrix techniques is gaining attention very rapidly. The Newton Raphson (NR) method is based upon the local linearization of equations (3.1) using the first order Taylor expansion, which can be written in the following matrix notation;

$$F(X^{k+1}) = F(X^{k}) + J(X^{k}) \times (X^{k+1} - X^{k}) \qquad (4.5)$$

Where;

k :The previous iteration number.

$k+1$:Current iteration number.

$J(X)$:The matrix of partial derivatives of F with respect to X (Jacobian matrix).

X^{k+1} :The vector of variables to be calculated at the

current iteration.

Newton's formula is obtained by setting $F(X^{k+1})$ to zero, and solving the resulting equation for X^{k+1}.

$$X^{k+1} = X^k - [J(X^k)]^{-1} \times F(X^k) \tag{4.6}$$

as an alternative, equation (4.6) may be written in the following form;

$$J(X^k) \times (X^{k+1} - X^k) = - F(X^k) \tag{4.7}$$

The equations constructing the matrix form (4.7) are linear.

If the initial estimate vector X^0 is not too far from the final solution of the system (3.1), X^*, Newton's method is probably the most efficient method in terms of the number of iterations required for the solution of the system of equations. Near the solution the convergence of Newton's method is quadratic, i.e., the number of significant figures in the estimate of the solution is doubled in each iteration.

This method has been applied by many workers to simulate and/or design evaporation processes. "EVAP" is a specialized flowsheeting program for the simulation and design of multiple effect evaporators in the pulp mill process. This program was written by Waite [1982]. Shewchuk [1982], has developed a similar flowsheeting program for performing steady state heat and mass balance calculations for the MEE process found in the pulp and paper industry. The program was designed as a modular simultaneous system. By using NR method, Hayakawa et al [1973] has solved the mathematical model for all stages constructing an MSF process simultaneously. Suitable partial load operation curves, and information necessary for determining the fouling factor as design value were obtained. Holland [1975] proposed the use of the Newton Raphson method for solving simultaneously the set of algebraic equations which describes the performance of a multiple effect evaporator in general. Radovic et al [1979] have developed a mathematical model based on the approach of Holland to perform design and analysis calculations for five effect forward feed evaporator system. This process is adopted for the evaporation of sugar solution.

However, the following disadvantages for NR technique are generally cited:

1. The Jacobian matrix must be recalculated at every iteration. The partial derivatives can be evaluated numerically or analytically (if possible). This is a very time consuming step and represents a serious limitation to the method.
2. Since all variables are iterated, they must be initialized. For large problems this may be impractical.
3. The iteration process can diverge from poor starting values.
4. This method usually takes all the core space available on most machines, even with using sparse matrix methods.

4.5.2.b. Quasi-Newton Methods;

[a] Broyden's Method:

Broyden's method [1965] is one of the modifications of the Newton Raphson method. It is designed to reduce the number of function evaluations. The Jacobian matrix in equation (4.7) is evaluated only once, and on subsequent iterations corrections to the approximate inverse of the Jacobian matrix are computed from the values of the vector function F. However, the convergence of this method is superlinear instead of quadratic convergence, this means that the convergence is accelerated near the solution.

Quasi-Newton methods are generally represented by the following form:

$$X^{k+1} = X^k - H^k \cdot F^k \tag{4.8}$$

where H is a matrix approximating the inverse of the Jacobian. This matrix is unique, and Broyden proposed the following form for updating it:

$$H^{k+1} = H^k - \frac{(H^k Y^k + t^k P^k)\, P^{k^T} H^k}{P^{k^T} H^k Y^k} \tag{4.9}$$

Where:

$$Y^k = F(X^{k+1}) - F(X^k) \tag{4.10}$$

$$P^k = H^k \cdot F^k \tag{4.11}$$

t^k is a relaxation factor chosen such that the norm of $F(X^{k+1})$ is less than the norm of $F(X^k)$, so, the problem is prevented from diverging. The value of t^k is obtained as follows;

$$t^k = 1 \qquad \text{if;}$$

$$\left[\sum_{i=1}^{n} f_i^2 (X^{k+1})\right] \quad < \quad \left[\sum_{i=1}^{n} f_i^2 (X^k)\right] \tag{4.12}$$

Otherwise, t^k is computed as follows:

$$t = \frac{(1 + 6\,\theta)^{0.5} - 1}{3\,\theta} \tag{4.13}$$

$$\theta = \frac{\sum_{i=1}^{n} f_i^2 (X^{k+1})}{\sum_{i=1}^{n} f_i^2 (X^k)} \tag{4.14}$$

$$\text{And} \quad X^{k+1} = X^k + t^k (P^k) \tag{4.15}$$

Updating the inverse of the Jacobian is one drawback of Broyden's method, because the approximation of the inverted Jacobian matrix tends to be a dense matrix, even with a very sparse initial Jacobian matrix, Hlavacek et al [1985]. As mentioned before, Helal et al [1986] have used this technique to accelerate the convergence rate of the outermost computational loop in the simulation of MSF process.

[b] Schubert's Method;

Schubert's modification of Broyden's method (Schubert [1970]), shares the superlinear convergence characteristic of the original method, and it also maintains the sparsity pattern of the Jacobian matrix. This is achieved by updating the Jacobian matrix instead of its inverse.

Newton's method and the Schubert update are combined together in a hybrid algorithm proposed by Lucia et al [1983]. This algorithm is used for approximating quantities involving physical properties derivatives, (see the article for more details). The authors compared the performance of the proposed (hybrid) approach with three other methods in simulating five effect evaporation process. These methods are: partial Newton method, in which certain physical properties derivatives are neglected from the Jacobian matrix; the Schubert update, and a finite difference (f.d) Newton's method, in which the partial derivatives are approximated numerically by perturbation.

The results obtained for this problem are tabulated in Table (4.1). These results show that Schubert's method is the worst from the points of view of the number of iterations required, and the thermodynamic routine calls . Also, for this particular problem, neglecting the physical properties derivatives is a simple and economical strategy.

Table (4.1)

Method	Number of iterations required	Number of thermodynamic routine calls
f.d.Newton	5	24
Hybrid	13	14
Partial Newton	16	17
Schubert	41	43

4.5.3. Direct Linearization Method.

In the direct linearization method, a set of nonlinear equations, (equation 3.1) are represented by an equivalent set of linear equations in the form:

$$\mathbf{A} \times \mathbf{X} = \mathbf{B} \qquad (4.16)$$

where:

A : The coefficient matrix.

X : Unknown variables.

B : The constants vector.

This may be achieved by approximately linearizing the nonlinear terms of the equations.

To solve the linear form (4.16), all variables $\mathbf{X}^0$ are initialized, the matrix elements are calculated, then by using a linear technique (e.g. Gaussian elimination) **A** is solved. The process is repeated until some convergence criterion is achieved.

The concepts of this technique were applied to the material and energy balance equations describing an MEE system by Hirth et. al. [1971]. They performed simulation and design computations for a number of fixed configuration plants using a FORTRAN IV program. This program

allows for including different heat recovery features. The applicability of the program is limited by a number of restrictions built in it. These restrictions include: the maximum number of effects to be solved is ten, and the feed stream may be split between only two feed vaporizers.

Design calculations of multiple effect evaporator system using direct linearization method was described by Lambert et al [1987]. Constant values are given to all nonlinear terms (e.g. Enthalpies, U's, and BPR) which are based on the previous iteration results. The cross product of A and T in the heat transfer equation (equation 3.7) was eliminated by defining AT as a new variable. As a result, equation (4.16) is formed and the solution started iteratively. Different types of design problems were suggested, unfortunately none of them was performed. The authors concluded that the developed algorithm is stable and simple to program. The same technique was also used by Kurby, et. al. [1982] to calculate the optimal design of MEE process.

The performance of the direct linearization technique was tested against other approaches for solving sets of nonlinear equations by Koko, et al [1987]. They found that the direct linearization method did not get more complicated as the number of effects increases, whereas the scant and the successive substitution methods did not converge for large sets of equations. These nonlinear methods would not converge unless the initial elements were close enough to the answer.

Huang et al [1969], have developed a mathematical model and computer program for simulation and optimum design of a VTE desalting plant with a fixed configuration. The plant consists of a number of blocks, each block includes one evaporator unit, a preheat unit, and a flash unit. The material and energy balance equations representing the different units are manipulated and combined together to yield a set of (n+1) independent simultaneous equations {where: n is the number of effects} in (n+1) unknowns. The unknown variables are the steam flowrate and the vaporization rate of each effect. The solution is achieved iteratively by inverting the matrix of the model equations.

Direct linearization method has many desirable characteristics such as the computation stability, algorithm simplicity, convergence possibility under a wide range of starting points, Lambert et al [1987]. However, the rate of convergence depends to a great extent on the formulation of the problem in the matrix. Second order convergence can

be obtained by choosing the linear equation coefficients such that they are identical to the partial derivatives of the nonlinear equations with respect to the appropriate variables, Westerberg, et. al. [1979]. In addition, the convergence speed depends on the assumed initial values and the kind of the problem being solved.

4.6. EXPLOITING THE PROBLEM MATHEMATICAL MODEL STRUCTURE.

The storage requirements and computation effort for solving a set of n equations are proportional to n^2, Shacham [1984]. Therefore, decomposing a large system of equations into a number of small subsets (with smaller n) has clear advantages.

As shown in the previous chapter, the system of equations representing thermal distillation process behaviour tends to be sparse, i.e. each equation contains only a few variables (less than ten). This *numerical nature* of the problem may be exploited by decomposition. This type of decomposition or partitioning will be referred here to as *algebraic decomposition.*

Also, because of the nature of the physical construction of distillation process flowsheets (i.e. consisting of units and streams, like any other chemical plant), the process set of equations usually consists of a number of loosely combined subsets of equations. These subsets of equations may be grouped according to the unit types, or to the variable types. By such decomposition, the *physical structure nature* of the problem may be exploited to improve the computation performance. This decomposition is referred to here as *physical decomposition.*

4.6.1. Algebraic Decomposition.

Using this technique, a large set of algebraic equations can be decomposed (or partitioned) into a number of irreducible (i.e. can not be further partition) subsets of equations. These subsets can be further decomposed by "tearing". The principle concepts of tearing and partitioning techniques are illustrated by Ledet and Himmelblau [1970] and Sargent [1978].

Ledet and Himmelblau [1970], compared several algorithms for partitioning and tearing techniques. A complete computer program for determining the precedence order of a system of equations is presented

in their article. Using this program the occurrence matrix for triple effect evaporator problem was formed and analyzed. The system cannot be decomposed successfully by a linear sequence of calculations because of the nonlinearity of some of its equations. They concluded that the precedence order obtained by the program for this particular simple problem is neither better nor faster than the classical trial and error method discussed in many textbooks for unit operations.

Equations tearing algorithms have only limited use, Shacham [1984]. This is because:

- The uncertainty about the convergence reliability of the obtained solution strategy. This has been emphasized by Lin and Mah [1978]. They pointed out that because of a very long chain of computations existing between the guessed tear values and the residuals in the tear equations, sensitivity problems can arise that may cause divergence even for initial guesses that are very near to the solution.
- Tearing system of nonlinear equations tends to make them more nonlinear and consequently more difficult to solve, Mach [1972].
- Such algorithms usually include procedures for detecting the sparsity pattern of the problem, which may make the algorithm more complicated and sometimes not reliably efficient.

4.6.2. Physical Decomposition.

"Physical decomposition" was devised as another economical technique for solving large and sparse set of equations. This technique takes the advantages of the regular structure of the problem at hand. Here grouping the equations can be either according to stage or by variable types. Decomposition may be performed in conjunction with linearization by NR technique or alternatively by direct linearization technique.

The equilibrium stage problem in a chemical process can be considered as a determination of a set of stage temperatures, interstage flowrates and compositions which will satisfy all material balances, equilibrium relations, and energy balances. The methods proposed by Naphtali et al [1971] and Kubicek et al [1976] to solve this problem require grouping the model equations according to the stage. This produces a large tridiagonal sparse Jacobian matrix. The elements of this matrix are themselves matrices. Using this technique, the computer

storage economy is strongly improved. However, the technique is often numerically unstable, mainly due to a build up of truncation error, Friday et al [1964].

Matrix formulation of the equilibrium stage problem was first proposed by Amundson et al [1958]. Mass balance equations on each component are grouped in a tridiagonal matrix (TDM) to calculate the composition. Vapour flowrates through the column are obtained from another group for heat balance equations. These matrices of linear equations are solved simultaneously. Unfortunately, the advantages of the TDM structure were not used during the computational procedure. The submatrices are solved using full matrix inversion techniques which are inefficient from computing time and storage points of view. Wang and Henke [1966] improved the previous method by arranging the mass balance equations for each component in a TDM form. Then the Thomas algorithm [1981] is used to solve each matrix equations.

A new method for the simulation of MSF process was developed by Helal et al [1986]. In this method the nonlinear equations describing the process are linearized. The linearized enthalpy balance equations are arranged in a TDM form, which is solved by Thomas [1981] algorithm. The rest of the model equations are solved one by one. The method was tested for three cases of specification for recirculation plant flowsheet (I. performance calculation, II. fixed product flowrate, and III. fixed steam flowrate), and compared with the traditional stage to stage technique. The method gives better stability and rapid convergence. However, apart from the performance problem, the solution was only obtained by nested iteration loops. This is because each equilibrium equation is solved iteratively, and in case II for example, the plant production capacity D and the maximum brine temperature T_{max} are specified. Therefore, to solve the problem, the performance loop is nested with another outer loop (control loop) that iterates on the two variables D and T_{max}. So, the basic advantages of the simultaneous approach, namely, the specification flexibility and unnested iteration loops are not achieved. Another additional problem is related to the expense associated with computing the simplified model which is used to predict the initial guess for the complex model. This expense may be large, and could offset the computational speed due to the TDM advantages.

The processes in the above four articles, (e.g. Helal [1986]), have a fixed configuration, which made it possible to cast the mathematical model in a TDM form. However, the type of the process units and the process flowsheet topology are varied from one problem to another. These variations usually reflect sets of equations which have different structures and do not follow a fixed matrix pattern (e.g. tridiagonal). Therefore, Tierney and Bruno [1967] have proposed another decomposition form. In this form, the matrix **J**, and the columns **X** and **F** in equation (4.7) are partitioned as follows:

$$\begin{bmatrix} E_t & E_v \\ H_t & H_v \end{bmatrix} * \begin{bmatrix} C_t \\ C_v \end{bmatrix} = - \begin{bmatrix} D_m \\ D_e \end{bmatrix} \tag{4.17}$$

Which can be rewritten as two equations:

$$E_t \cdot C_t + E_v \cdot C_v = - D_m \tag{4.18}$$

$$H_t \cdot C_t + H_v \cdot C_v = - D_e \tag{4.19}$$

Where:

E_t ,E_v : Temperature and flowrate correction matrices for material balance error

H_t ,H_v : Temperature and flowrate correction matrices for energy balance error.

C_t : Temperature variation vector.

C_v : Flowrate variation vector.

D_m : Deviation or error in material balance equations.

D_e : Deviation or error in energy balance equations.

Equations (4.18) and (4.19) are based on the error in the material and energy balances, of the equilibrium stage, respectively.

4.7. REQUIREMENTS IN THE PRESENT WORK.

From the above outlined literature survey it may be inferred that the need for a specialized flowsheeting program for the simulation and design of thermal desalination processes is confirmed. This program system should include the following points:

1. Flexibility: the program must be sufficiently flexible to solve the given flowsheet under different specifications.
2. Generality: the program should be able to perform design and simulation calculations for different thermal desalination process types with different configurations.
3. Computer memory: the program should employ a technique of solution which reduces the memory requirements.
4. Reliability (or robustness): the program should be capable of solving a large number of different problems, starting from a wide range of initial guesses.
5. Computing time: the required computing time to obtain the numerical solution of the problem at hand should be economically feasible.

In fact, the combination of some or all of the above characteristics in one algorithm is expected to produce a highly practical and economical specialized flowsheeting program.

4.8. THE APPROACH USED IN THIS WORK.

From the above analysis it may be recognized that a technique based on solving all equations simultaneously, (e.g. Newton method), would probably provide the most flexible solution procedure. However, long computational time, and large computer storage requirements associated with this technique may make it uneconomical in solving many problems. Alternatively, decoupling the effect of certain variables and equations, then solving iteratively the selected groups of equations in a particular sequence for composition, temperature, and pressure, seems to be a more economical approach.

Olivares [1983] has tried to simulate a double effect evaporation system using a method similar to the latter technique. In this method, the model equations are linearized and the advantage of the equations sparsity is taken by decomposing the problem equations into a number of small subsystems, according to the variable type, (i.e. one set for component variables, one for temperature variables, and one set for pressure variables).

Unfortunately, Olivares was faced by computational unstability problems. In fact, apart from Olivares's work, no information has been

published in the literature about using this technique in performing design and simulation calculations for thermal desalination processes. Therefore, at the beginning of the present study, enough time was spent to detect the possible reasons of the numerical unstability of Olivares's problem, (see Appendix B for more details). By solving this problem, and a large number of different small problems, Flower and Nafey [1986], it was clear that further development of this approach to solve different practical desalination plants is really worthwhile. This new approach is referred to as the Variable Type By Variable Type (VTBVT) technique. Details about the development steps of the VTBVT technique will be illustrated in the next chapter. A number of approximation assumptions are proposed to develop the VTBVT technique. To justify these assumptions, another computer program based on the traditional Newton Raphson method (which solves the mathematical model without approximation) is written.

4.9. CONCLUSION.

In this chapter, the problems of performing the simulation and design calculations of thermal desalination processes are defined. The general computational approaches for solving these problems are illustrated. The available literature is classified according to these general approaches; and the convergence characteristics, advantages, and limitations of each approach are discussed.

Using the equation oriented approach, the evaporation process flowsheeting requires a solution of large systems of linear and nonlinear algebraic equations. Different numerical techniques which have been used in solving these large systems of equations are reviewed. Also, the advantages and limitations of each technique are discussed. Techniques for exploiting the numerical and physical structures of the problems in order to solve them more efficiently are illustrated.

From this literature survey it can be concluded that a specialized flowsheeting program for simulation and design of thermal desalination processes is needed. The requirement characteristics and the proposed computational approach of this program are outlined.

CHAPTER 5

VARIABLE TYPE BY VARIABLE TYPE [VTBVT] ALGORITHM SYNTHESIS

5.1. INTRODUCTION.

The development of the mathematical model describing the behaviour of the process at hand and the subsequent solution of this model are fundamental steps in process flowsheeting. In chapter 3 the mathematical models for various thermal desalting units were developed for steady state operating conditions. In chapter 4 previous different solution strategies for these models were outlined. In this chapter the development of VTBVT alternative method for solving these mathematical models will be illustrated. This development is referred to as "algorithm synthesis"

The sparsity and the weak nonlinearity of the model equations are among the characteristics of the thermal desalination process mathematical models, see chapter 3. The proposed approach in this work takes the advantages of these characteristics by grouping the model equations according to the variable type. This is achieved in three steps, viz: linearization, arranging and decomposing the mathematical model according to the variable type (i.e. component, temperature, and pressure). These steps will be illustrated in detail in section 5.2. The concepts of these steps are applied to various thermal desalination units. The linear mathematical models for these units are presented in Appendix (C). In section 5.3, the degrees of freedom of the different thermal desalination units are predicted. The computational sequence of the proposed technique is illustrated in section 5.4. Finally, the main points of the chapter are concluded in section 5.5.

5.2. STEPS OF THE PROPOSED TECHNIQUE.

The proposed VTBVT approach involves three major steps viz: *first*, the nonlinear equation set $F(X)$ of equation (3.1) are linearized using the first order Taylor approximation, equation (4.7). This step

can be illustrated by writing equation (4.7) in the following form:

$$J(X^k) * X^{k+1} = J(X^k) * X^k - F(X^k) \qquad (5.1)$$

where k is an iteration counter.
Each row i (i.e. equation i) of the matrix form (5.1) can be written in the following form:

$$\text{let } f_i(X^k) \Rightarrow f_i$$

$$\frac{\partial f_i}{\partial (X_1^k)} \cdot X_1^{k+1} + \frac{\partial f_i}{\partial (X_2^k)} \cdot X_2^{k+1} + \frac{\partial f_i}{\partial (X_3^k)} \cdot X_3^{k+1} + \cdots$$

$$= \frac{\partial f_i}{\partial (X_1^k)} \cdot X_1^k + \frac{\partial f_i}{\partial (X_2^k)} \cdot X_2^k + \frac{\partial f_i}{\partial (X_3^k)} \cdot X_3^k + \cdots$$

$$- f_i \qquad (5.2)$$

In the linearized equation (5.2), the right and left hand sides contain a term for every variable reflected to by the corresponding equation in the set (3.1).

Second, the previous linearized equation (5.2) is simplified by cancelling the identical terms in both sides of the equation. In addition some elements are neglected. This neglect affects only the convergence path, without affecting the accuracy of the final results, this point will be illustrated afterwards.

Probably the best way to make the previous two steps clear is to consider the following nonlinear equation as an example:

$$f(T,C) : T_1 \cdot C_1 + T_3 \cdot C_3 - T_4 \cdot C_4 = 0 \qquad (5.3)$$

where T and C are variables.

First this equation can be linearized using the form (5.2) producing the formula below:

let $f(T,C)^k \rightarrow f$ for simplicity

$$\frac{\partial f}{\partial (T_1^k)} \cdot T_1^{k+1} + \frac{\partial f}{\partial (T_3^k)} \cdot T_3^{k+1} + \frac{\partial f}{\partial (T_4^k)} \cdot T_4^{k+1}$$

$$+ \frac{\partial f}{\partial (C_1^k)} \cdot C_1^{k+1} + \frac{\partial f}{\partial (C_3^k)} \cdot C_3^{k+1} + \frac{\partial f}{\partial (C_4^k)} \cdot C_4^{k+1}$$

$$= \frac{\partial f}{\partial (T_1^k)} \cdot T_1^k + \frac{\partial f}{\partial (T_3^k)} \cdot T_3^k + \frac{\partial f}{\partial (T_4^k)} \cdot T_4^k$$

$$+ \frac{\partial f}{\partial (C_1^k)} \cdot C_1^k + \frac{\partial f}{\partial (C_3^k)} \cdot C_3^k + \frac{\partial f}{\partial (C_4^k)} \cdot C_4^k$$

$$- (T_1^k C_1^k + T_3^k C_3^k - T_4^k C_4^k) \qquad (5.4)$$

using equation (5.3) and (5.4), the next simple form can be written:

$$(C_1^k) \cdot T_1^{k+1} + (C_3^k) \cdot T_3^{k+1} - (C_4^k) \cdot T_4^{k+1} + (T_1^k) \cdot C_1^{k+1}$$

$$+ (T_3^k) \cdot C_3^{k+1} - (T_4^k) \cdot C_4^{k+1} = (C_1^k) \cdot T_1^k + (C_3^k) \cdot T_3^k$$

$$- (C_4^k) \cdot T_4^k + (T_1^k) \cdot C_1^k + (T_3^k) \cdot C_3^k - (T_4^k) \cdot C_4^k$$

$$- (T_1^k C_1^k + T_3^k C_3^k - T_4^k C_4^k) \qquad (5.5)$$

Following the cancellation of the identical terms, equation (5.5) may take one of the following forms:

$$(C_1^k) \cdot T_1^{k+1} + (C_3^k) \cdot T_3^{k+1} - (C_4^k) \cdot T_4^{k+1} + T_1^k \cdot (C_1^{k+1} - C_1^k) +$$

$$T_3^k \cdot (C_3^{k+1} - C_3^k) - T_4^k \cdot (C_4^{k+1} - C_4^k) = 0 \qquad (5.6,a)$$

Or

$$(T_1^k) \cdot C_1^{k+1} + (T_3^k) \cdot C_3^{k+1} - (T_4^k) \cdot C_4^{k+1} + C_1^k \cdot (T_1^{k+1} - T_1^+) +$$

$$C_3^k \cdot (T_3^{k+1} - T_3^k) - C_4^k \cdot (T_4^{k+1} - T_4^k) = 0 \qquad (5.6,b)$$

Near the solution the values of any variable at two successive iterations are approximately equal. So,

$$(C^{k+1} - C^{k}) \cong 0 \qquad (5.7,a)$$

and

$$(T^{k+1} - T^{k}) \cong 0 \qquad (5.7,b)$$

Therefore, these terms can be neglected from the above forms without affecting the final results, giving the following simple forms:

$$(C_1^k) \cdot T_1^{k+1} + (C_3^k) \cdot T_3^{k+1} - (C_4^k) \cdot T_4^{k+1} = 0 \qquad (5.8,a)$$

and:

$$(T_1^k) \cdot C_1^{k+1} + (T_3^k) \cdot C_3^{k+1} - (T_4^k) \cdot C_4^{k+1} = 0 \qquad (5.8,b)$$

Regarding the equations (5.6 & 5.8,a and b) it is worth noting that:

[1] If we have a nonlinear term of cross product of two* variables like (T*C) in an equation, (this situation occurs in the enthalpy balance and heat transfer equations for the evaporator units), this term can be linearized by one of the following forms:

{a} $$T * C = C^k \cdot T^{k+1} + T^k \cdot C^{k+1} - T^k \cdot C^k \qquad (5.9,a)$$

The convergence rate of this form is essentially of the second order. Because this form is driven using the Newton Raphson form, equation (4.7).

{b} $T * C = T^{k+1} \cdot C^k$ (from 5.8,a)

Or

$T * C = C^{k+1} \cdot T^k$ (from 5.8,b) $\qquad (5.9,b)$

This form representing the successive approximation of the nonlinear term (T * C), by giving constant values from the previous iteration.

Now, considering the above two forms (5.9,a & b), it is important to note that the only difference between them is the path of the iterative solution to the final solution. i.e. the

---

* Generally, starting with Taylor approximation it is possible to linearize the nonlinear terms of cross product of n variables as;

$$(X_1 * X_2 * X_3 * \cdots * X_n) = (X_2^k * X_3^k * \cdots X_n^k) * X_1^{k+1} + (X_1^k * X_3^k * \cdots X_n^k) * X_2^{k+1} + (X_1^k * X_2^k * \cdots X_n^k) * X_3^{k+1} + \cdots\cdots\cdots (X_1^k * X_2^k * X_3^k * \cdots) * X_n^{k+1} - (n-1) * (X_1^k * X_2^k * X_3^k * \cdots X_n^k) \qquad (5.8,c)$$

rate of the convergence. However, the final results of both forms are exactly the same as mentioned before.

[2] The choice of the proper form of equations (5.8,a & b) depends on the purpose of the calculation process. Equation (5.8,a) is used to calculate **T** variables by knowing **C** variables and vice versa, equation (5.8,b) is used.

The *third* step in the proposed VTBVT technique is the arranging and decomposing of a large system of the linearized equations into smaller subsystems according to the variable type. This step may be demonstrated by considering a system of linear and nonlinear equations describing one of the unit operations used in the thermal desalination process, say, flash unit module, Figure (3.2).

5.2.a System Of Linearized Equations.

The concepts of the linearization procedures, as explained above, are applied to the flashing brine enthalpy balance equation (3.15), total enthalpy balance equation (3.20), the heat transfer equation (3.23) and the equilibrium equation (3.26) for the flashing evaporator stage. The nonlinearity in the above equations is due to : first, the nonlinear nature of the enthalpy functions, overall heat transfer coefficient (U), boiling point rise (BPR), nonequilibrium allowance (NEA), etc····, with respect to T and X as shown in chapter 3. second, the cross product of two variables such as A * T. These two sources of nonlinearity will be handled in the light of the above linearization concepts as follows: First equation (3.15) can be rewritten as follows:

$$B_{i-1}\cdot h_{b,i-1} - B_i\cdot h_{b,i} - B_{i-1}\cdot H_{v,i} + B_i\cdot H_{v,i} = 0 \qquad (3.15)$$

using equation (5.2) the following second order convergence linearized form may be obtained (all the nomenclature have been explained in chapter 3)

$$\begin{aligned}
&(B^k_{i-1}\cdot Cp^k_{b,i-1})\cdot T^{k+1}_{b,i-1} - (B^k_i\cdot Cp^k_{b,i})\cdot T^{k+1}_{b,i} - ((B^k_{i-1} - B^k_i)\cdot \\
&Cp^k_v)\cdot T^{k+1}_{d,i} + (h^k_{b,i-1} - H^k_v)\cdot B^{k+1}_{i-1} + (H^k_v - h^k_{b,i})\cdot B^{k+1}_i \\
&= B^k_{i-1}\cdot Cp^k_{b,i-1}\cdot T^k_{b,i-1} - B^k_i\cdot Cp^k_{b,i-1}\cdot T^k_{b,i} - \\
&((B^k_{i-1} - B^k_i)\cdot Cp^k_v)\cdot T^k_{d,i} + (h^k_{b,i-1} - H^k_v)\cdot B^k_{i-1} + (H^k_v - h^k_{b,i})\cdot B^k_i \\
&- B^k_{i-1}\cdot h^k_{b,i-1} + B^k_i\cdot h^k_{b,i} + B^k_{i-1}\cdot H^k_{v,i} - B^k_i\cdot H^k_{v,i} \qquad (5.10,a)
\end{aligned}$$

Which can be written as:

$$(B^k_{i-1} \cdot Cp^k_{b,i-1}) \cdot T^{k+1}_{b,i-1} - (B^k_i \cdot Cp^k_{b,i}) \cdot T^{k+1}_{b,i} - ((B^k_{i-1} - B^k_i) \cdot Cp^k_v) \cdot T^{k+1}_{d,i}$$

$$+ (h^k_{b,i-1} - H^k_v) \cdot W^{k+1}_{i-1} + (H^k_v - h^k_{b,i}) \cdot W^{k+1}_i = Z1 \qquad (5.10,b)$$

where: $$Z1 = B^k_{i-1} \cdot Cp^k_{b,i-1} \cdot T^k_{b,i-1} - B^k_i \cdot Cp^k_{b,i-1} \cdot T^k_{b,i}$$

$$- ((B^k_{i-1} - B^k_i) \cdot Cp^k_v) \cdot T^k_{d,i} - S^k_{i-1} \cdot h^k_{b,i-1} + S^k_i \cdot h^k_{b,i} \qquad (5.10,c)$$

Alternatively, equation (5.10,a) may take the following form:

$$(h^k_{b,i-1} - H^k_v) \cdot W^{k+1}_{i-1} + (H^k_v - h^k_{b,i}) \cdot W^{k+1}_i + B^k_{i-1} \cdot Cp^k_{b,i-1} \cdot$$

$$(T^{k+1}_{b,i-1} - T^k_{b,i-1}) - B^k_i \cdot Cp^k_{b,i} \cdot (T^{k+1}_{b,i} - T^k_{b,i})$$

$$- ((W^k_{i-1} - W^k_i) \cdot Cp^k_v) \cdot (T^{k+1}_{d,i} - T^k_{d,i})$$

$$= - S^k_{i-1} \cdot h^k_{b,i-1} + S^k_i \cdot h^k_{b,i} \qquad (5.10,d)$$

Considering the above equation with the assumption that the values of the temperature variables at two successive iterations near the solution are equal, i.e.

$$T^k = T^{k+1} \qquad (5.10,e)$$

The following simple form may be used to calculate the component flowrates at the present iteration (k+1), by knowing the temperature variables from the previous iteration (k).

$$(h^k_{b,i-1} - H^k_v) \cdot W^{k+1}_{i-1} + (H^k_v - h^k_{b,i}) \cdot W^{k+1}_i = ZZ1 \qquad (5.10,f)$$

where:

$$ZZ1 = S^k \cdot (h^k_{b,i} - h^k_{b,i-1})$$

Second, following the same sequence as above the total enthalpy balance equation (3.20) can be linearized as follows:

$$(F_c \cdot Cp_c)^k_{i+1} \cdot T^{k+1}_{c,i+1} + (D \cdot Cp_d)^k_{i-1} \cdot T^{k+1}_{d,i-1} + (B \cdot Cp_b)^k_{i-1} \cdot$$

$$T^{k+1}_{d,i-1} - (F_c \cdot Cp_c)^k_i \cdot T^{k+1}_{c,i} - (D \cdot Cp_d)^k_i \cdot T^{k+1}_{d,i}$$

$$- (B \cdot Cp_b)^k_i \cdot T^{k+1}_{b,i} + (h_{c,i+1})^k \cdot F^{k+1}_{c,i+1} + (h_{d,i-1})^k \cdot D^{k+1}_{i-1}$$

$$+ (h_{b,i-1})^k \cdot B^{k+1}_{i-1} - (h_{c,i})^k \cdot F^{k+1}_{c,i} - (h_i)^k \cdot D^{k+1}_i - (h_{b,i})^k \cdot$$

$$B^{k+1}_i = Z2 \qquad (5.11,a)$$

where:

$$Z2 = (F_c \cdot Cp_c)^k_{i+1} \cdot T^k_{c,i+1} + (D \cdot Cp_d)^k_{i-1} \cdot T^k_{d,i-1}$$

$$+ (B \cdot Cp_b)^k_{i-1} \cdot T^k_{d,i-1} - (F_{c,i} \cdot Cp_c)^k \cdot T^k_{c,i} - (D \cdot Cp_d)^k_i \cdot T^k_d$$

$$- (B \cdot Cp_b)^k_i \cdot T^k_{b,i} + [Q_{loss}]^k \qquad (5.11,b)$$

The above second order linearized form (5.11,a) may be simplified by assuming that the values of the component variables, **C** at each two successive iterations near the solution are equal, i.e:

$$\mathbf{C}^k = \mathbf{C}^{k+1} \qquad (5.11,c)$$

By assuming appropriate expressions for the specific enthalpies so that the temperatures are explicit in the equation (5.11,a), the following linear approximation form can be set up:

$$h = a + b * T \qquad (5.11,d)$$

where a and b are particular constants for different streams. The simplified equation takes the following form:

$$(F_c \cdot Cp_c)^k_{i+1} \cdot T^{k+1}_{c,i+1} + (D \cdot Cp_d)^k_{i-1} \cdot T^{k+1}_{d,i-1}$$

$$+ (B \cdot Cp_b)^k_{i-1} \cdot T^{k+1}_{b,i-1} - (F_c \cdot Cp_c)^k_i \cdot T^{k+1}_{c,i} - (D \cdot Cp_d)^k_i \cdot T^{k+1}_{d,i}$$

$$- (B \cdot Cp_b)^k_i \cdot T^{k+1}_{b,i} = Z22 \qquad (5.11,e)$$

where:

$$ZZ2 = -(a_c \cdot F_c)^k_{i+1} - (a_d \cdot D)^k_{i-1} - (a_b \cdot B)^k_{i-1}$$

$$+ (a_c \cdot F_c)^k_i + (a_d \cdot D)^k_i - (a_b \cdot B)^k_i + Q_{loss}$$

a_b, a_c, a_d :particular constants for flashing brine, cooling water, and distillate water into and out of the stage (calculated using equation (5.11,d))

Third, in the same way, the heat transfer equation (2.23) takes the following linearized form:

$$(1 - E)^k \cdot T^{k+1}_{c,i+1} + E^k \cdot T^{k+1}_{d,i} - T^{k+1}_{c,i}$$

$$+ \left[- T^k_{c,i+1} \cdot \left[\frac{\partial E}{\partial F}\right]^k_c \cdot F^{k+1}_c + T^k_{d,i} \cdot \left[\frac{\partial E}{\partial F}\right]^k_c \cdot F^{k+1}_c\right]$$

$$= (1 - E)^k \cdot T^k_{c,i+1} + E^k \cdot T^k_{d,i} - T^k_{c,i} - T^k_{c,i+1} \cdot \left[\frac{\partial E}{\partial F}\right]^k_c \cdot F^k_c$$

$$+ T^k_{d,i} \cdot \left[\frac{\partial E}{\partial F}\right]^k_c \cdot F^k_c - ((1-E)^k \cdot T^k_{c,i+1} + E^k \cdot T^k_{d,i} - T^k_{c,i}) \qquad (5.12,a)$$

where $$E = 1 - e^{-U \cdot A / F_c \cdot Cp_m}$$

The above equation may be simplified to:

$$(1 - E)^k \cdot T^{k+1}_{c,i+1} + E^k \cdot T^{k+1}_{d,i} - T^{k+1}_{c,i} + \epsilon \cdot F^{k+1}_c \cdot (T^k_{d,i}$$

$$- T^k_{c,i+1}) = \epsilon \cdot F^k_c \cdot (T^k_{d,i} - T^k_{c,i+1}) \qquad (5.12,b)$$

where $$\epsilon = \left[\frac{\partial E}{\partial F}\right]_c = \frac{U \cdot A}{F^2_c \cdot Cp_m} \cdot e^{-U \cdot A / F_c \cdot Cp_m}$$

From the above equation and equation (5.10,e) the following linear equation can be used:

$$(1 - E)^k \cdot T^{k+1}_{c,i+1} + E^k \cdot T^{k+1}_{d,i} - T^{k+1}_{c,i} = 0 \qquad (5.12,c)$$

In the above equation, the heat transfer area is considered as a constant value. In other words this equation is suitable only for simulation calculations. However, in the design calculations, the heat

transfer area (A) is considered as a dependent variable. Therefore, the following form can be obtained:

$$(E)^k \cdot T^{k+1}_{d,i} + (1 - E) \cdot T^{k+1}_{c,i+1} - T^{k+1}_{c,i} + \left[\frac{U}{F \cdot Cp} \cdot (1 - E) \cdot (T_{d,i} - T_{c,i+1})\right]^k \cdot A^{k+1} = (E)^k \cdot T^k_{d,i} + (1 - E)^k \cdot T^k_{c,i+1} - T^k_{c,i} + \left[\frac{U}{F_c \cdot Cp_m} \cdot (1 - E)\right]^k \cdot (T_{d,i} - T_{c,i+1})^k \cdot A^k - (E)^k \cdot T^k_{d,i} - (T_{c,i+1} \cdot (1 - E))^k + T^k_{c,i} \qquad (5.12,d)$$

Following the cancellation of the identical terms in the above equation, the following form can be obtained:

$$(1 - E)^k \cdot T^{k+1}_{c,i+1} + E^k \cdot T^{k+1}_{d,i} - T^{k+1}_{c,i} + \mathcal{R} \cdot A^{k+1} = \mathcal{R} \cdot A^k \qquad (5.12,e)$$

where;

$$\mathcal{R} = \left[\frac{U}{F_c \cdot Cp_m} \cdot e^{-U \cdot A / F_c \cdot Cp_m}\right]^k \cdot (T^k_{d,i} - T^k_{c,i+1})$$

In equations (5.12, c) and (5.12, e) the overall heat transfer coefficient (U) is not an independent variable but may be computed, equation (A.14), by knowing the temperature and composition from the previous iteration. Also, it may be assigned a constant value. For performing design calculations with specified stage temperature decrement, (ΔT_s) the following equation is used:

$$T^{k+1}_{c,i} - T^{k+1}_{c,i+1} = \Delta T_s \qquad (5.12,f)$$

Now, equilibrium equation (3.26) can be linearized using the same sequence as follows:

$$T_{b,i} - T_{d,i} - Z3 = 0 \qquad (3.26,a)$$

where $Z3 = NEA + BPR$

Assuming Z3 is a function of T_b only we have:

$$\left[1 - \frac{\partial Z3}{\partial T_{b,i}}\right]^k \cdot T^{k+1}_{b,i} - T^{k+1}_{d,i} - Z3^{k+1} = \left[1 - \frac{\partial Z3}{\partial T_{b,i}}\right]^k \cdot T^k_{b,i} - T^k_{d,i} - Z3^k - T^k_{b,i} + T^k_{d,i} + Z3^k \qquad (5.13,a)$$

By cancelling the identical terms the following equation may be obtained:

$$\left[1 - \frac{\partial Z3}{\partial T_{b,i}}\right] \cdot T_{b,i}^{k+1} - T_{d,i}^{k+1} - Z3^{k+1} = - \frac{\partial Z3}{\partial T_{b,i}} \cdot T_{b,i}^{k} \qquad (5.13,b)$$

By giving constant values to Z3 terms which are estimated from the previous iteration, the following simple form may be obtained:

$$T_{b,i}^{k+1} - T_{d,i}^{k+1} = Z3^{k} \qquad (5.13,c)$$

To complete the mathematical model of the unit at hand, let us write the material balance equations (3.16 to 3.19) in the next form:

$$W_{b,i-1}^{k+1} + D_{i-1}^{k+1} - W_{b,i}^{k+1} - D_{i}^{k+1} = 0 \qquad (5.14)$$

And

$$\left.\begin{aligned} S_{c,i+1}^{k+1} - S_{c,i}^{k+1} &= 0 \\ W_{c,i+1}^{k+1} - W_{c,i}^{k+1} &= 0 \\ S_{b,i-1}^{k+1} - S_{b,i}^{k+1} &= 0 \end{aligned}\right\} \qquad (5.15)$$

5.2.b. Variables And Equations Ordering.

Having developed the linearized model for just one flash unit, Figure (3.2), the equations and variables may be grouped according to the variable type (i.e. component variables group, temperature variables group,.....). It should be mentioned here that the equations for only one flash unit are considered here for the sake of illustration. However, during the solution, the same steps are applied for the total flowsheet equations. For this particular configuration we have sixteen component and temperature variables but only five equations (5.10,b), (5.11,a), (5.12,b), (5.13,a), and (5.14) and three equalities (5.15). Evidently if the feed component and temperature parameters are specified, an additional eight equations can be written:

$$\left.\begin{aligned} W_{c,i+1}^{k+1} &= G1 & D_{i-1}^{k+1} &= G2 \\ W_{b,i-1}^{k+1} &= G3 & S_{c,i+1}^{k+1} &= G4 \\ S_{b,i-1}^{k+1} &= G5 & T_{c,i+1}^{k+1} &= G6 \\ T_{d,i-1}^{k+1} &= G7 & T_{b,i-1}^{k+1} &= G8 \end{aligned}\right\} \qquad (5.16)$$

where, G1 to G8 are specified constants.

So, this particular unit is represented by a set of sixteen equations in sixteen variables which can be written in the following matrix form:

$$[\ A\ ]\cdot[\ X\ ] = [\ B\ ] \qquad (5.17)$$

where:

A : is the coefficient matrix.

X : Variables to be calculated.

B : A vector evaluated from the previous iteration.

The above set of equations may be arranged according to the component and temperature variables. The arranged equations and variables are written as follows:

$$\left[\begin{array}{c|c} A\ 1 & D\ 1 \\ \hline A\ 2 & D\ 2 \end{array}\right] * \left[\begin{array}{c} C \\ \hline T \end{array}\right] = \left[\begin{array}{c} B\ 1 \\ \hline B\ 2 \end{array}\right] \qquad (5.18)$$

The submatrices D1 and A2 of the above coefficient matrix contain only very few elements. So, for efficient solution, the matrix sparsity should be exploited. This can be achieved by using the simplified forms defined by equations (5.10,f), (5.11,e), (5.12,c), and (5.13,c).

So, equation 5.18 may be represented by:

$$\left[\begin{array}{c|c} A\ 1 & 0 \\ \hline 0 & D\ 2 \end{array}\right] * \left[\begin{array}{c} C \\ \hline T \end{array}\right] = \left[\begin{array}{c} E1 \\ \hline E2 \end{array}\right] \qquad (5.19)$$

The above form , (5.19), can be decomposed into two independent smaller matrices, as follows:

$$[\ A\ 1] * [\ C\ ] = [\ E1\ ] \qquad (5.20\ a)$$

and;

$$[\ D\ 2] * [\ T\ ] = [\ E2\ ] \qquad (5.20\ b)$$

These equations can then be processed sequentially. There are two basic approaches to solve these equations: either by the use of further decomposition by "tearing" or by simultaneous solution using one of the standard technique of linear algebra, the latter is chosen in this work.

It should be pointed out here that:

[1] The second order linearized form, equation (5.18), provides speed at the expense of sparsity and reliability, while, the first order method provides reliability at the expense of speed. However, the linearized simple form, equation (5.20,a,b) considers a hybrid of the two strategies.

[2] By the VTBVT technique, the large problem may be decomposed into a number of small ones which are solved in sequence. As a result, the two main problems associated with Newton's method may now be overcome. This is because, first, the initial values need only to be guessed for the first matrix, so, the number of the estimated variables is reduced. Second, a large problem may become a number of small problems, so, the need for big computer memory will be reduced. Also, the computation effort will be reduced because this effort is proportional to the problem size.

[3] The proposed technique does not need any means for detecting the sparsity pattern, this makes the algorithm much simpler.

[4] Theoretically, the use of the linearized simple form equation (5.19), instead of the Taylor linearized form (5.18) usually slows down the convergence rate to the solution, Westerberg et al [1979]. However, practically it depends on the following factors as well:

   a. The initial guess for the solution of the equations.
   b. The number of equations. Generally, the number of iterations required to solve a system of linear equations increases as the number of equations becomes larger.
   c. It is also worth noting that, in the VTBVT method, the first matrix produces a better guess for the second matrix. This may lead to the accelerating of the convergence.

Some of the above points will be illustrated numerically in the results chapters numbers 7, 8, and 9.

Following the same sequence as that used in the previous section, the linearized models for various units in thermal desalination processes are developed, see Appendix {C}

5.3. THERMAL DESALINATION UNITS DEGREES OF FREEDOM.

Having developed the linearized models of the thermal desalination operation units, see Appendix (C), the degrees of freedom of each unit (and consequently the considered system) have to be defined so as to start the solution. The degrees of freedom are defined as "the number of the variables which must be arbitrarily fixed in order to completely define the system ", Perry et al [1973]. However, Kubicek, et al [1976] pointed out that the selection of the independent (specified) variables is not completely arbitrary, because this selection may lead to an underdetermined system of equation. This case takes place for instance by specifying a number of variables which eliminate all the dependent variables in a particular equation. Also, an inadequate selection of the independent variables may lead to a system of equations which do not yield a unique (or any) solution.

The general equation for calculating degrees of freedom of a model is:

$$N_d = N_v - N_e \qquad (5.21)$$

where:

N_d : Number of degrees of freedom.
N_v : Number of variables.
N_e : Number of independent equations.

Specification of N_d variables is equivalent to adding an additional N_d independent equations to the mathematical model. This makes the number of variables N_v and equations N_e consistent, and the solution of the model becomes feasible.

Table (5.1). Degrees of Freedom of the Units.

Unit	N_v	N_e	N_d
Flash stage	22	11	11
Evaporator	17	7	10
Condenser	14	8	6
Flash unit	11	6	5
Flow splitter	12	8	4
Flow mixer	12	4	8
liquid/liquid heat exchanger	16	7	9
Desuperheater	9	4	5
Compressor	6	3	3

Perhaps the most practical way to determine the number of degrees of freedom for a flowsheet is to predict the degrees of freedom of its constituent units, Westerberg et al [1979].

In the above table, the number of equations N_e, the number of variables N_v as well as the number of degrees of freedom N_d for all the units constructing different thermal desalination flowsheets are illustrated.

For a complete flowsheet consisting of a number of the above units , only the unit outlet stream variables should be considered to avoid taking the intermediate streams variables twice into account.

5.4. VTBVT COMPUTATIONAL PROCEDURES.

The algorithm using VTBVT technique for performing design and simulation calculations consists of the following steps:

Step (1). Assume an initial temperature profile $[\ \mathbf{T}\ ]^k$.

Step (2). Calculate and setup the elements of the component matrix, equation (5.20,a). These elements comprise enthalpy values, which are mainly function of temperature.

Step (3). Solve the component matrix for $\mathbf{C}^{k+1}$ using a sparse matrix routine with any linear technique like Gaussian

elimination.

Step (4). By knowing $[T]^k$ and $[C]^{k+1}$ calculate and setup the elements of the temperature matrix, equation (5.20,b). These elements comprise boiling point rise (BPR), NEA, overall heat transfer coefficient, all are functions of temperature and composition.

Step (5). Using the same spare matrix routine, solve the temperature matrix, equation (5.20,b), for T^{k+1}.

Step (6). Calculate and setup the pressure matrix elements.

Step (7). Using the sparse matrix routine, solve the pressure matrix for P^{k+1}.

Step (8). Repeat steps (2) through (7) until the specified convergence criterion is satisfied.

Step (9). Finish.

The structure and the operation of the developed programs which performing the above steps are outlined in the next chapter.

5.5. CONCLUSION.

In this chapter, the development of the linearized model equations for a flash stage unit is exemplified, and the detailed description of the proposed VTBVT technique is given. This linearized model has been designed to allow decomposition into a number of small sets of equations according to the variable type. The proposed technique provides an easily programmed, reduced memory, and requiring only a few initial guessed values method for solving thermal desalination process flowsheets. The convergence characteristics of this technique (such as stability, number of iterations to converge, computing time, sensitivity to starting values, and general ease of use) will be investigated in chapters 7, 8, and 9.

The model equations do not completely define the operation of the units, thus allowing constraints to be imposed. The degrees of freedom analysis of various thermal desalination units are performed.

The Computational sequence for the proposed technique is illustrated. The construction of the program which performs this computational sequence is illustrated in chapter 6.

CHAPTER 6

STRUCTURE AND OPERATION OF THE DEVELOPED PROGRAMS

6.1. INTRODUCTION.

Thermodynamic and physical properties and the linear mathematical equations utilized in modelling various unit operations of thermal desalination processes are presented in chapter 5 and the Appendices {A} and {C}. These equations are incorporated in two modular computer packages for determining the steady state solution of the main thermal desalination processes. The first package consists of two parts: the Data Structure Program (DSP), and the Calculation Program (CP). The CP involves decomposing the whole set of equations representing the problem at hand into three variable type subsets as explained in chapter 5. In other words, the CP uses the proposed VTBVT technique. The second package consists also of two parts: one for data reading and construction (NDSP), and the other for performing the calculations (NBCP). In this program the whole set of material and energy balances are solved by successive linearization using the standard second order Newton Raphson method, see Appendix {D}.

One of the major factors in the usefulness of any computer program is the ability of the user to: (1) determine how to use the program. (2) Understand the principles used in the program. (3) Trace the flow of data through the program and (4) see the calculations done by the program. To satisfy these user needs, the main lines of the first package documentation will be provided in this chapter, and details of the main points will be presented in Appendix {D}.

6.2. GENERAL DESCRIPTION OF THE FIRST PACKAGE.

As pointed out in chapter 4, the flowsheeting programs using the procedure oriented approach are based on modular constructions. In this approach, the mathematical models of the process units act upon input material and energy streams to produce output material and energy streams. Information is transferred into and out of the unit modules as a set of numerical values for the stream variables such as compositions, temperature, and pressure. This modular construction makes the above

approach simple, and the program may be easy to construct. Therefore, it seems reasonable to retain the modular structure also for the present equation oriented programs. In this program, in contrast to the above approach, each unit module returns the equations describing the process unit to the executive program which acts upon the total set of equations to solve it, regardless of their origin.

The organization and the solution of the problem at hand are controlled by the two parts of the package, see figure 6.1. The task of the first part (i.e. Data Structure Program (DSP)) is to interpret different thermal desalination process types with different configurations into a proper code by defining the variables and parameters which describe the state of these processes. While the equations relating the above variables and parameters and defining the operation of the process are set up and solved by the second part (i.e. Calculation Program (CP)) of the package. All the necessary subroutines to model the units in the configuration, to solve the resulting equation set, to retrieve physical properties information, and to channel input and output data to and from the database are available. Communication between various subroutines and the executive in each part of the package is carried out through a COMMON pool of storage in the form of linked lists. An intermediate data file communicates the two parts of the package. The main outlines of the functions of the constituent parts of figure 6.1, and the relation between them will be illustrated in the following sections.

6.3. THE DATA STRUCTURE PROGRAM (DSP).

This program allows the establishment of plant description and specification to be in a proper form for the subsequent calculation process. This is achieved by creating a number of arrays called lists. These arrays are dimensioned to include all the information and variable pointers for each stream and unit in the considered flowsheet. These arrays are resident in COMMON storage, so different subroutines may get access to them. The DSP is written in the FORTRAN 77 language.

6.3.1. General Organization Of The Data Structure Program (DSP)

As illustrated by Figure 6.2, the data structure program (DSP) has three major sections:

[1] Data input and verification section, in which the considered

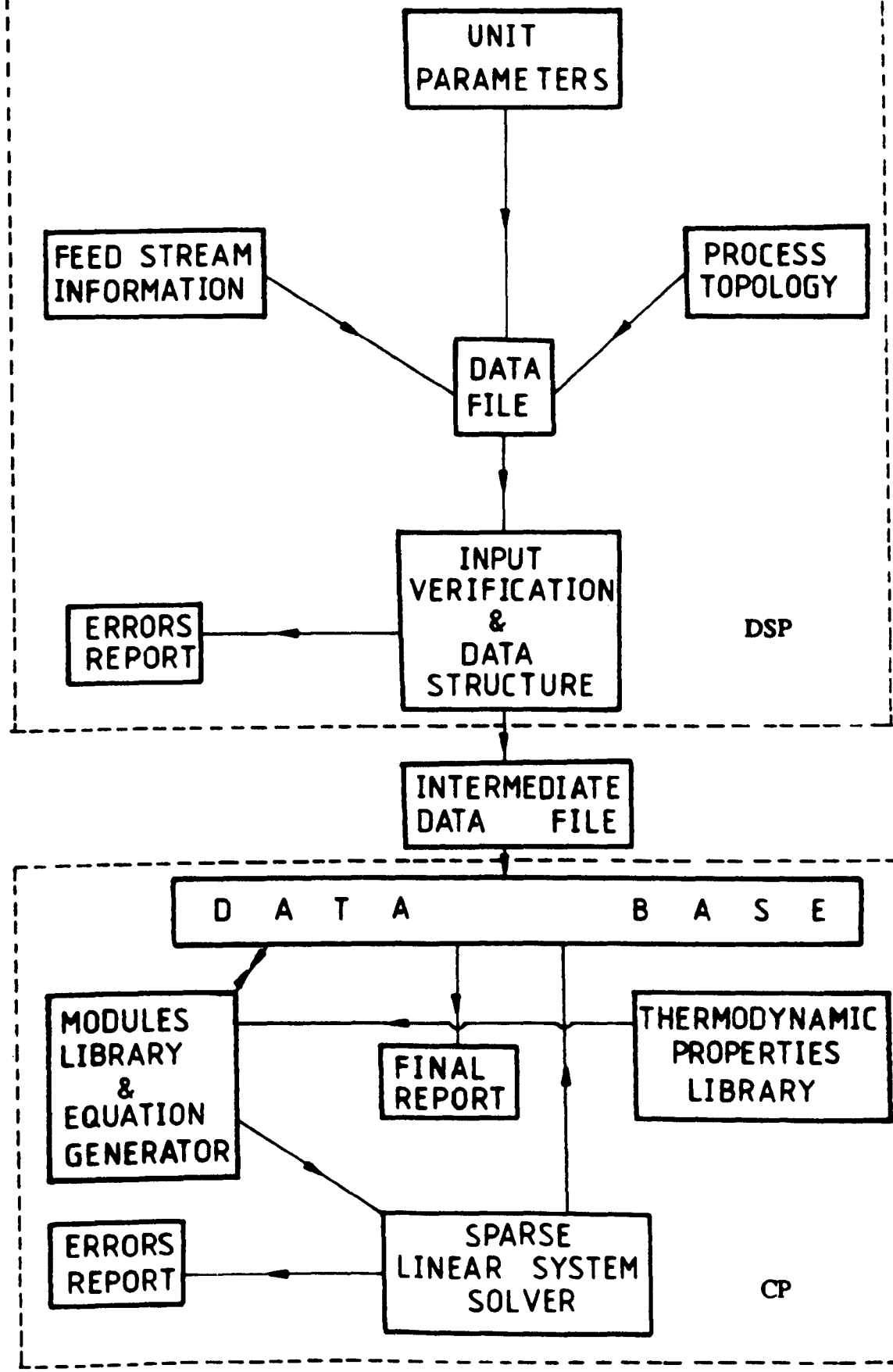

FIGURE 6.1. THE STRUCTURE OF THE DEVELOPED PROGRAM.

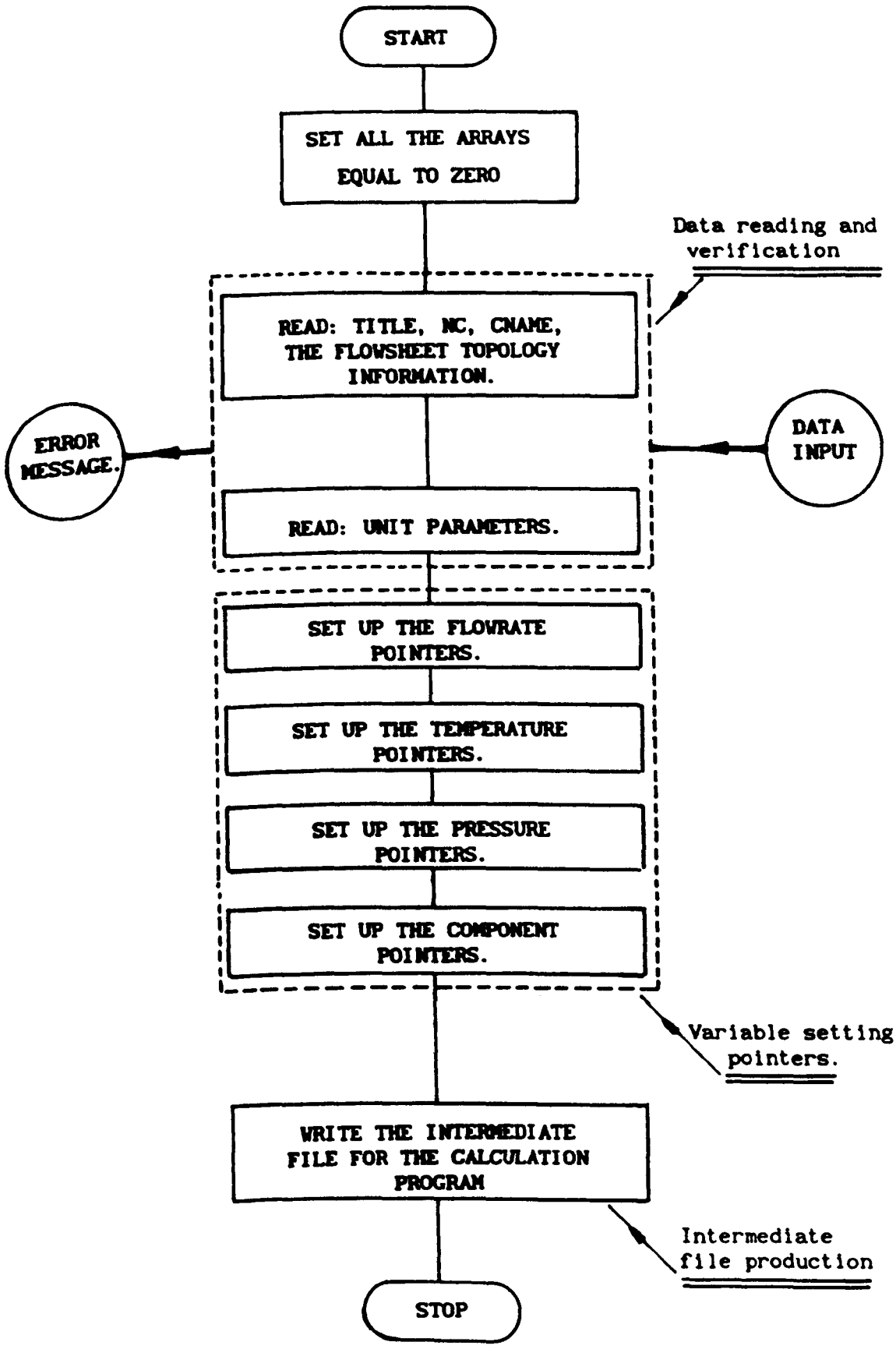

Figure (6.2), Data Structure Program Organization.

flowsheet may be specified by the following data:

(1) The process topology.

(2) The stream information.

(3) The unit parameters.

Generally, the input data to the DSP contains the following:

(a) The title of the process flowsheet.

(b) The required calculation mode (simulation or design)

(c) The number of components (NC), (usually two components)

(d) Number of the units in the considered flowsheet.

(e) Then for each unit, the following data is required;

(1) Unit name.

(2) Unit type.

(3) And for each output stream the following data is needed:

[a] Stream name.

[b] Destination unit name.

[c] Which input number to the destination.

(4) Unit parameters.

Table (6.1) shows all information related to various unit operations required to construct thermal desalination flowsheets. Also illustrated in Figure 6.3 is the convention by which the user should number the streams of the various units.

[2] In the second section, the given data are manipulated to set up the required flow rate, temperature, pressure, and component pointers for ease of data location. And, to identify the different elements of the considered process. Also, a number of lists for unit parameters, unit names, and stream names is established. This is illustrated in some detail in Appendix {D}.

[3] In the third section of the data structure program (DSP), all information, variable pointer lists, parameter and identification lists are written in an intermediate file to be handled by the calculation program (CP). The output file of the DSP is illustrated in Appendix {D}.

Table (6.1). Types and Operational Data for the Units.

Unit	Type	Parameters.
Boiling evaporator	400	□ U*A, heat losses, [simulation with known U] □ A, heat losses, [simulation with unknown U] □ heat losses, ξ [Design]
Flash evaporator	410	□ U*A, heat losses, [simulation with known U] □ A, heat losses [simulation with unknown U] □ Number of stages, heat losses, Δt_s [design] □ Number of stages, heat losses
Flow splitter	30	□ splitter ratio [α], [first output/input stream] or -1 [for unknown α]
Flow mixer	20	□ none
Flash unit	25	□-1 or saturated temperature (or pressure) of the flashed vapour.
Desuperheater	55	□ none
Compressor	45	□ T (saturated), ζ [for design] T (saturated), ω [for simulation]
Liquid/liquid heat exchanger	120	□ U, TTD [for design] U*A [for simulation]
Condenser	420	□ A*U , heat losses [simulation with known U] □ A, heat losses [simulation with unknown U] □ U {or liquid velocity, fouling allowance, OD, K, FF, }, [design with unknown U]
Feed	1	□ F, T, P, W, S □ -1, salt or water ratios of the total flowrate.
Pressure break	210	□ none
Temperature break	140	□ none
Temperature setter	130	□ Required Temperature value (K)
Pressure setter	220	□ Required Pressure value (kPa)
Fraction or ratio setter	15	□ reference component □ ratio of the first component to the reference component. □ ratio of the second component to the reference component.
Flowrate setter	10	□ The required flowrate value.
Component setter	5	□ Components 1 and 2

6.4. THE CONSTRUCTION OF THE CALCULATION PROGRAM [CP].

The numerical solution is achieved using this part of the package (i.e. the CP). This task is attained by using the data and the information given by the intermediate file, Appendix {D}, to set up a number of variable type sets of equations which model the behaviour of the considered process. These sets of equations are then iteratively solved to obtain the steady state solution of the process. The program consists of an executive and a library of unit modules as well as the necessary thermodynamic and physical properties subroutines. The

FIGURE 6.3. STREAM NUMBERING CONVENTION FOR THE UNITS.

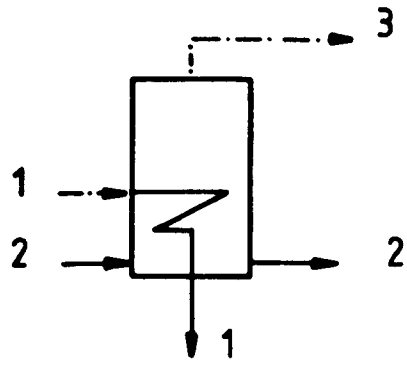

Boiling Evaporation Unit

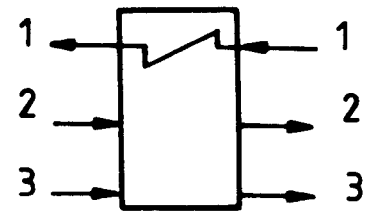

Flash Evaporation Unit

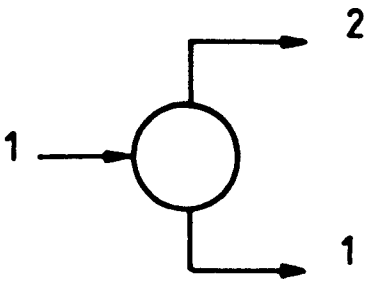

Flow Splitter

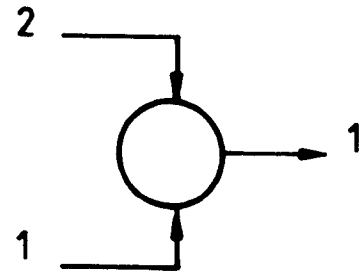

Flow Mixer

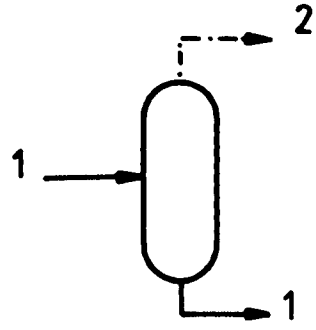

Flash Unit

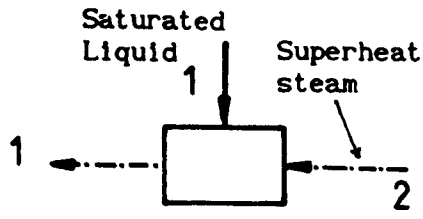

Desuperheater Unit

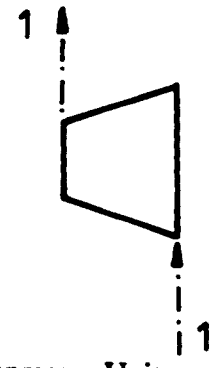

Compressor Unit

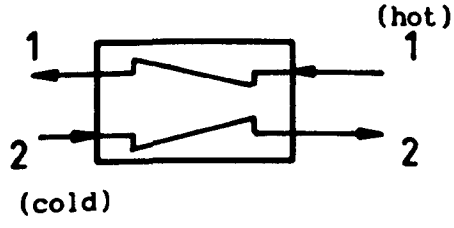

Liquid/Liquid heat exchanger Unit

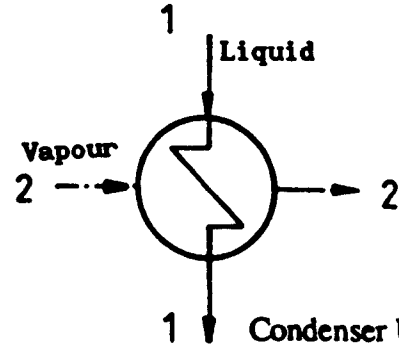

Condenser Unit

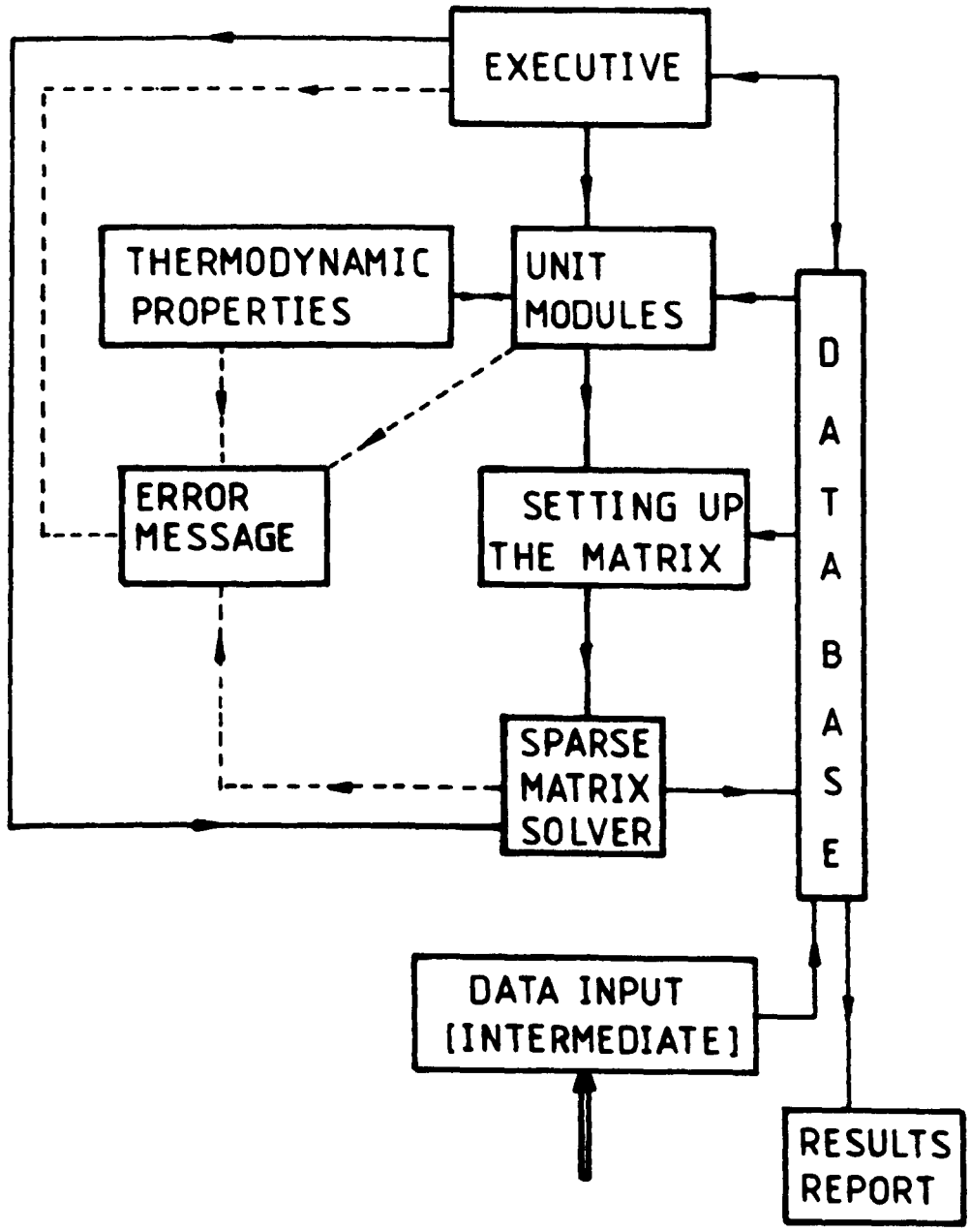

FIGURE 6.4. THE ORGANIZATION OF THE CALCULATION PROGRAM [CP].

executive gets access to the unit module library, calls sparse matrix solver, and channels input data from the intermediate file and the output results to the data base. The unit modules obtains access to the thermodynamic and physical property routines and set up the unit model equations. Communication between various parts of the program is carried out through a COMMON pool of storage. The general organization of this part of the package is illustrated by Figure (6.4). In Appendix {D} the organized units are considered in some detail.

6.5. CONCLUSION.

From the discussion presented in this chapter it may be concluded that: the program system is developed to simulate and design different thermal desalination processes. Its design emphasizes flexibility, modularity, conservation of computer time and store, and ease of use. The program allows easy and flexible definition of various units constructing different types and configuration of thermal desalination processes. Also, it allows great flexibility in the type of the constraints which may be imposed on the process. Each unit operation takes the form of an independent module or subroutine. These modules may then be combined in different ways to model the desired plant. These modules are designed to be easily expanded, modified, and/or updated. This modular structure of the package achieves the desired flexibility efficient, and easily understood code.

CHAPTER 7

DESIGN AND SIMULATION OF MULTI-STAGE FLASH DESALINATION PROCESS

7.1. INTRODUCTION

The Multi-Stage Flash (MSF) process has considerable promise as a technique suitable for producing large scale quantities of potable water, from seawater. Also, it has many technical and economical advantages (see chapter 2). Furthermore, in many instances, this technique has been considered as one of the most practical means for making extremely pure water for such applications as boiler feed make-up or industrial plant process supply. Therefore, this process may be regarded at the present time as providing the optimum solution of the problem of seawater conversion.

While the equations describing this countercurrent process, at steady state, appear to be quite simple, they are in fact nonlinear and highly interdependent. Therefore, the necessary calculations to solve these equations are iterative in nature and large in number.

Using the proposed Variable Type By Variable Type (VTBVT) technique, outlined in chapter 5, different problem types of MSF process will be exemplified in this chapter.

Section (7.2.) outlines the degrees of freedom of the MSF process and some forms of design and performance problems which can be solved by the developed program. This leads to the application of the program in design calculations to determine the stage heat transfer areas of the MSF processes. Design results of AL-KHOBAR II MSF desalination plant are presented in section (7.3). To build confidence in the developed program, it must be reliable, free of bugs, flexible, and its final results should be valid. These aspects are examined in section (7.4). Also, in sections (7.3) and (7.4) the convergence characteristics of the suggested technique as well as its stability under a wide range of initial temperature profiles during both design and performance calculations are illustrated. The capability of the developed program to

carry out a comprehensive and critical evaluation of the MSF performance under varying operating conditions is illustrated in section (7.5). This is achieved by calculating AL-KHOBAR II plant performance under changing feed seawater temperature and brine recirculation flowrate. The results of this study are used to plot a " performance map" which can be used in design and operation processes.

Iterations, convergence characteristics, and the reliability of the proposed computational technique are examined in section (7.6). This is performed by calculating the "FICHTNER" plant using VTBVT technique and Newton Raphson technique. Also, the final results of this plant (i.e.FICHTNER) using " equation oriented " approach ,(VTBVT), and that obtained by Homig [1978], using "sequential modular" approach (or stage to stage technique), are compared to examine the validity of the proposed technique, see section (7.7) for presentation of these results.

The calculations of once-through process, in section (7.8) serve two purposes; one, is to evaluate numerically this type of plant in comparison with the traditional recirculation type. The second is to show the competency of the program using VTBVT technique to simulate and/or design the once-through MSF process.

In all the above cases, the (VTBVT) method shows no need for accelerator technique for convergence. Obviously, such technique could be used to make the method even faster at a slight increase in programing complexity.

Finally, the main inferred points from the results of all the above sections are summarized in section (7.9). All the computations are performed on an Amdahl 580 computer.

7.2 DEGREES OF FREEDOM FOR BRINE RECIRCULATION MSF PLANTS

The overall flow for the brine recirculating plant is illustrated in chapter 2. Also, the connecting units of this plant have been analysed in chapter 5. This analysis comprises; determination of the stream variables numbers, unit model equations as well as the degrees of freedom for each separate unit. The final results of these analysis, related to the main units constructing a recirculation MSF plants, are summarized in Table (7.1). According to this table, eleven design variables are needed to be specified to obtain a consistent solution for

the simulation problem. However, in the design problem, where heat transfer areas for; heat recovery, and rejection sections then become dependent variables , thirteen degrees of freedom will be obtained, (assuming constant area for each of heat recovery and rejection sections). In other words, thirteen design variables are needed to be specified in order to have a matching variables and equations number, to start the solution.

Figure (7.1) shows how the unit modules are constructed by the developed program for designing (or simulating) the considered brine recirculation plant.

Table (7.1) Degrees of Freedom Analysis for a Brine Recirculation* MSF Plant.

Unit	No. of equations	No. of outlet stream variables
Flash stage	11 × N	11 × N
Blow down splitter	6	8
Reject seawater splitter	6	8
Mixer	4	4
Brine heater	8	7
Feeding steam		4
Feeding seawater		4
Temperature break		1

Total number of equations = 11 * N + 24

Total number of stream variables = 11 × N + 35

So, the flowsheet has d = (11 × N + 35) - (11 × N + 24) = 11 degrees of freedom.

where N is the total number of stages.

---

* In the case of once-through MSF process, there will be neither splitter units nor mixer unit (see Figure (7.2)). So, according to the above table, the number of equations will be 11 × N + 15. Therefore, the plant has 7 degrees of freedom (in the case of simulation calculations.)

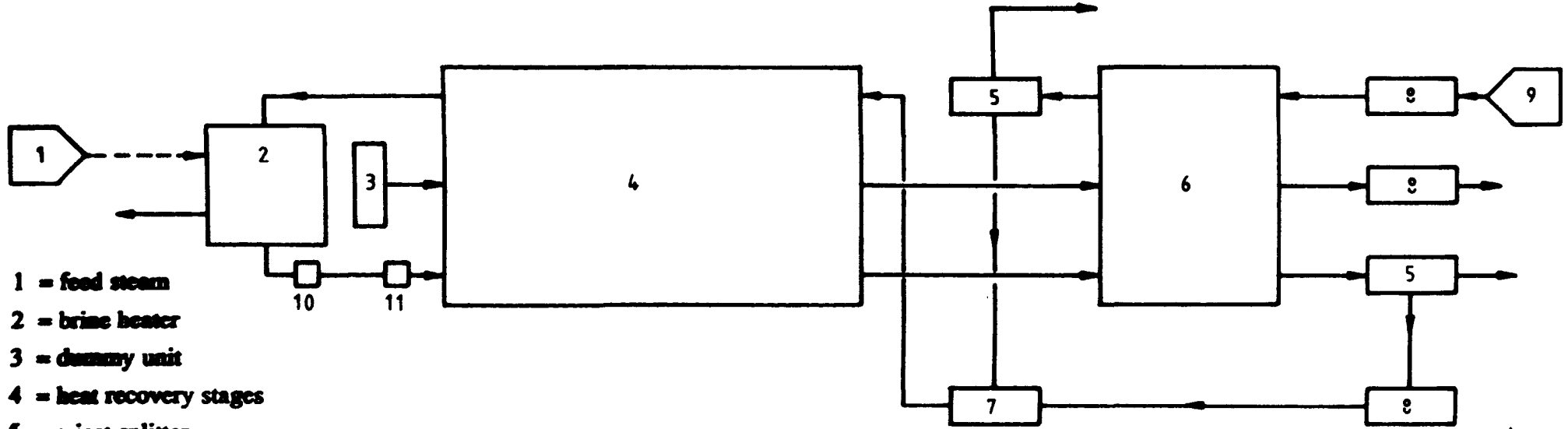

1 = feed steam
2 = brine heater
3 = dummy unit
4 = heat recovery stages
5 = reject splitter
6 = heat rejection stages
7 = mixer
8 = pump
9 = feed seawater
10 = temperature brake
11 = temperature setter

FIGURE 7.1. BRINE RECIRCULATION MSF PROCESS.

FIGURE 7.2. ONCE THROUGH MSF PROCESS.

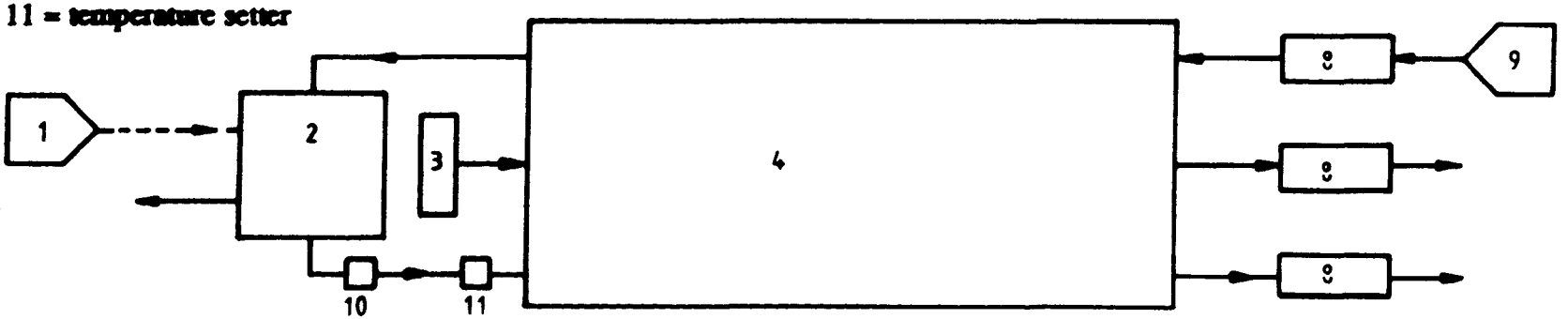

7.2.1. Forms Of Design And Performance Problems:

In order to place a high degree of confidence in the program, a large number of problems under different specifications needs to be solved and verified against independent data. Table (7.2) shows some of the possible design variables sets that can be chosen to simulate or design an MSF desalination plant of recirculation and once through types.

Once the designer has assigned specific values to any set of the design variables and parameters listed in Table (7.2), the values of the state variables may be obtained by solving the mathematical model relations. A change of any of the assigned values, e.g. the maximum brine temperature, or feed seawater temperature, will result in a new design differing more or less in design or in performance from the one calculated before.

One of the interesting applications of the developed program is to calculate the response of state variables by varying one condition at a time. So, by doing this for every possible process condition, in turn, a series of response curves may be obtained. A usual examination of these curves shows the affecting values of the operating parameters from the economical point of view. In fact, several forms of performance calculations under changing operating conditions of an existing plant are possible using the developed program. This point will be discussed later in more detail.

From the above information and discussion it may be seen that the demand for great flexibility has been fulfilled by permitting six basically different types of calculation cases. Three of these cases are evaluation calculations and the rest are different types of design calculations. Four of these cases will be exemplified in the following sections.

Table (7.2)

Different Combinations of Specified Variables and Parameters for MSF Plants.

Case	Specified Variables and Parameters																			
	X_f	T_f	P_f	F_f	T_s	P_s	M	D	C_b	T_c	T_b	$\alpha 1$	$\alpha 2$	T_{max}	R	A_{rej}	A_{rec}	A_h	ΔT_s
I	■	■	■	□	■	■	■	■	■	■	■	■	□	■	□	□	□	□	□
II	■	■	■	■	■	■	□	□	□	□	□	■	■	■	□	■	■	■	□
III	■	■	■	□	■	■	□	□	□	□	□	■	■	□	■	■	■	■	□
IV	■	■	■	□	■	■	□	■	□	□	□	■	□	■	□	□	□	□	■
V	■	■	■	□	■	■	□	■	□	-	■	-	-	■	□	-	□	□	□
VI	■	■	■	■	■	■	□	□	□	-	□	-	-	■	□	-	■	■	□

Where;

Case	Referred to as;
I	Design calculations of brine recirculation MSF process.
II	Simulation calculations of brine recirculation process.
III	Performance calculations with constant brine recirculation flow rate.
IV	Design calculations with specified stages temperature decrement
V	Design calculations of once-through MSF.
VI	Performance calculations of once-through MSF.

■ :Specified variables and parameters.

□ :Calculated variables and parameters.

X_f :Seawater salinity

T_f :Feed seawater temperature.

P_f :Feed seawater pressure.

F_f :Feed seawater flowrate.

C_b :Brine recycle concentration ratio.

T_c :Cooling water temperature.

R :Brine recirculation flowrate.

ΔT_s :Stage temperature decrement.

$\alpha 1$:Reject splitter ratio.

$\alpha 2$:Blowdown splitter ratio.

T_s :Steam temperature.

P_s :Steam pressure.

M :Makeup flowrate.

D :Plant production.

T_{max} :Top brine temperature.

T_b :Blowdown temperature.

A_{rej} :Heat rejection stage area.

A_{rec} :Heat recovery stage area.

A_h :Brine heater area.

7.3. DESIGN OF AL-KHOBAR II MSF DESALINATION PLANT:

In this section, the design calculations of Al-KHOBAR II MSF desalination plant in Saudi Arabia will be considered to achieve three main objectives. First, to exemplify the capability of the developed program using the proposed VTBVT technique to perform design calculations for large practical MSF plants. Furthermore, to investigate the convergence characteristics and the stability of the proposed technique during the design calculations. Finally, to determine the required heat transfer areas, temperature and flowrate in various parts of AL-KHOBAR II MSF desalination plant.

There are two main approaches to design MSF desalination process. Firstly, by assuming equal temperature drop per stage, Homig [1978]. Secondly, by assuming equal condenser area per stage, Steinbruchel et al [1980]. The developed program in this work has the capability of performing both approaches as illustrated in chapter 5. However, the second approach has been used routinely by many engineering firms because of the increase of the engineering and manufacturing costs associated with building non identical stages. AL-KHOBAR II plant was designed with equal stage heat transfer area, Helal [1986].

This particular problem contains 114 variables. However, 101 independent equations are generated by the program modules. Therefore, 13 design variables must be specified to start the solution of the mathematical model. Table (7.3), contains full details of the design data given by Omar [1981] and used in this study. Having a consistent mathematical model the solution can be started by predicting an initial temperature profile for the first matrix (i.e. the component matrix), following the computational sequence shown in chapter 5.

7.3.1. The convergence characteristics of MSF process design:

The steady state computations are started by assuming a linear temperature profile (400 - 2.0 x NT), as an initial guess profile, where NT is the temperature variable number. The solution is obtained in nine iterations and 0.71 second of computing time. The distillate, flashing brine, flowrate profiles (FDOUT, FBOUT) and temperature (TDOUT, TBOUT) profiles computed at the end of the fifth, and last iterations, as well as the initial distillate and flashing temperature profiles are listed in Table (7.4). The convergence behaviour of the distillate temperature

Table (7.3). List of the Specified Variables and Parameters for AL-KHOBAR II Plant Design, Omar [1981].

A. Specified Variables:

Variable	Symbol	Value	Units
Seawater salinity	X	57000.00	ppm
Feed seawater temperature	T_f	308.15	K
Feed seawater pressure	P_f	100.00	kPa
Steam temperature	T_s	370.15	K
Steam pressure	P_s	100.00	kPa
Make-up flowrate $\times 10^{-3}$	M	5640.24	kg/hr
Plant production $\times 10^{-3}$	D	914.67	kg/hr
Brine recycle concentration ratio	C_b	1.18	
Cooling water temperature	T_c	315.68	K
Blowdown Temperature	T_b	315.68	K
Splitting ratio of the reject cooling water	$\alpha 1$	0.5014	
Top brine temperature	T_{max}	363.15	K

B. Specified parameters:

Variable \ Section	Brine heater	Heat recovery	Heat rejection
Recycle brine velocity (m/s)	1.999	1.999	1.899
Fouling allowance $\times 10^3$ $(kcal/hr.m^2.K)^{-1}$	0.1863	0.1394	0.2382
Tube outside diameter (m)	0.02199	0.02199	0.0239
Tube material thermal Conductivity, (kcal/hr.m.K)	25.00	43.00	13.99
Terminal temperature difference (K)	6.96	-	-
Flooding factor	16.000	16.000	16.000

(TDOUT) and flowrate (FDOUT) profiles during the iteration is illustrated in Figures (7.3.A,B). It is observed that (TDOUT) and (FDOUT) profiles change only slightly after the fourth iteration. As Table (7.4) shows, the results obtained by the end of the fifth iteration are close to the final solution. These results could be considered sufficiently accurate, if a large value of the predescribed tolerance is permissible. The convergence criterion used for this problem is;

$$\text{Error} = \sum_{i=1}^{N} [(\text{FDOUT})_i^{k+1} - (\text{FDOUT})_i^{k}]^2 / N \leq \varepsilon \qquad (7.1)$$

where;

FDOUT : Distillate flowrate out of each stage.

i : Stage number.

k : Iteration number

N : Total number of stages.

ε : Predescribed tolerance
$= 5 \times 10^{-4}$ in this problem.

It is worth mentioning here that an adequate accuracy in the calculated stage heat transfer area is obtained by using the above equation as convergence criterion. This statement becomes more clear by giving attention to Table (7.5), where the successive values of heat transfer area for brine heater, heat recovery, and heat rejection sections are given.

Figure (7.4) illustrates the stability of the developed technique, the error (defined by 7.1) decreases dramatically as the solution is approached. Also, the technique is stable under a wide range of initial guessing temperature profiles, as will be illustrated in the next section.

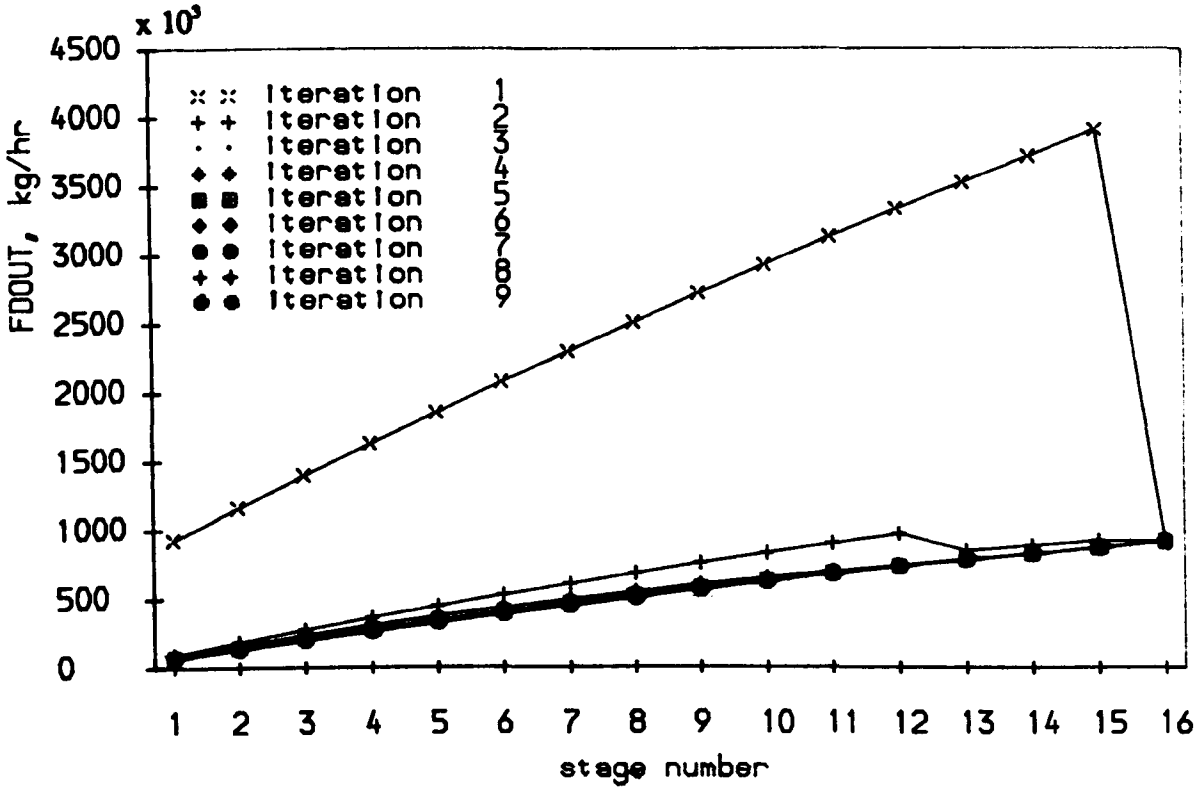

FIG. (7.3,a) CONVERGENCE OF THE DISTILLATE FLOWRATE ALONG THE PLANT. (design calculation)

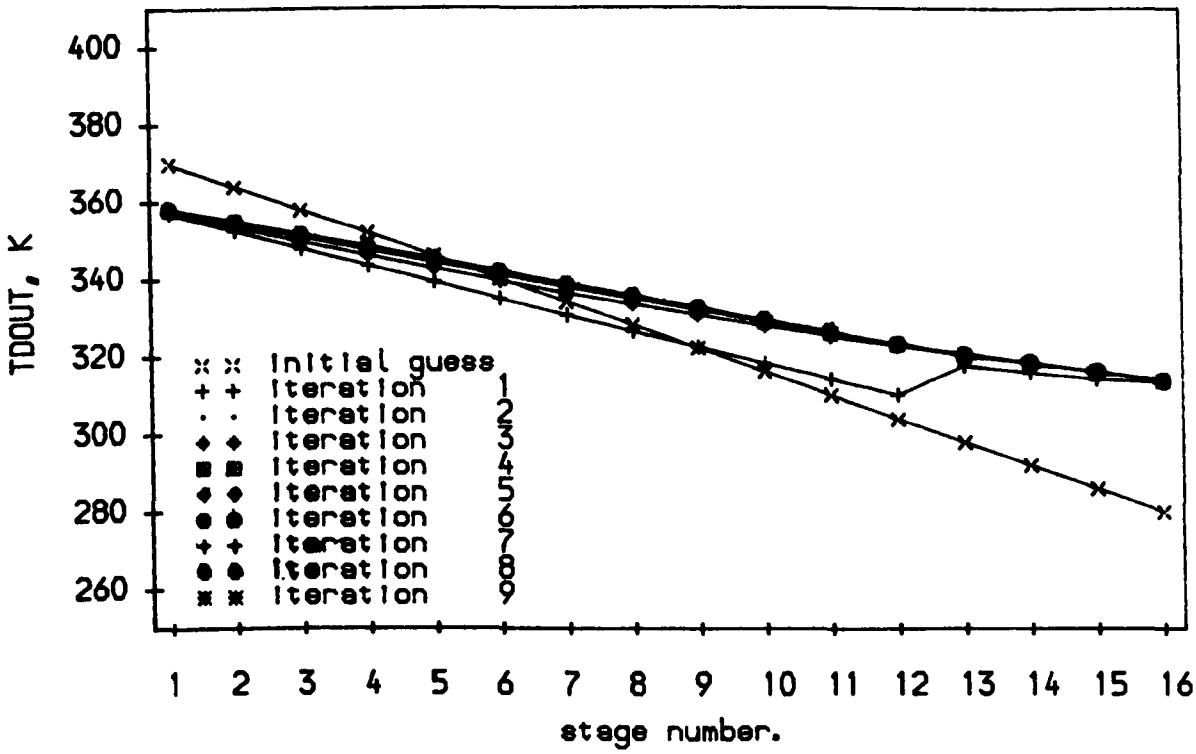

FIG. (7.3,b) CONVERGENCE OF THE DISTILLATE TEMPERATURE ALONG THE PLANT.

Table (7.4). Initial Guess And Some Successive Iterations (design calculations)

St No.	Initial Guess		Iteration 5				Iteration 9			
	TDOUT	TBOUT	TDOUT	TBOUT	FDOUT	FBOUT	TDOUT	TBOUT	FDOUT	FBOUT
	[K]		[K]		$x10^{-3}$ [kg/hr]		[K]		$x10^{-3}$ [kg/hr]	
1	370.00	368.00	358.24	359.78	69.46	12012.70	358.28	359.81	68.66	12013.35
2	364.00	362.00	354.85	356.44	137.36	11944.79	354.93	356.51	135.96	11946.05
3	358.00	356.00	351.51	353.15	203.71	11878.44	351.61	353.24	201.89	11880.12
4	352.00	350.00	348.21	349.90	268.52	11813.64	348.32	350.00	266.44	11815.57
5	346.00	344.00	344.96	346.70	331.80	11750.36	345.07	346.81	329.62	11752.39
6	340.00	338.00	341.74	343.54	393.58	11688.58	341.86	343.65	391.43	11690.58
7	334.00	332.00	338.58	340.43	453.87	11628.28	338.69	340.53	451.87	11630.14
8	328.00	326.00	335.46	337.37	512.72	11569.43	335.56	337.46	510.96	11571.05
9	322.00	320.00	332.39	334.35	570.17	11511.99	332.47	334.43	568.71	11513.30
10	316.00	314.00	329.36	331.38	626.26	11455.90	329.42	331.44	625.13	11456.88
11	310.00	308.00	326.38	328.45	681.01	11401.14	326.42	328.49	680.26	11401.75
12	304.00	302.00	323.44	325.57	734.47	11347.68	323.46	325.59	734.10	11347.91
13	298.00	396.00	320.54	322.73	786.69	11295.47	320.54	322.73	786.69	11295.32
14	292.00	290.00	318.61	320.42	828.87	11253.28	318.61	320.42	828.88	11253.14
15	286.00	284.00	316.28	318.08	871.38	11210.77	316.28	318.08	871.38	11210.62
16	280.00	378.00	313.89	315.68	914.67	11167.49	313.89	315.68	914.67	11167.34

Table (7.5) The Successive Values of Heat Transfer Area During The Iterations.

Iteration No.	Brine heater area (m^2)	Heat recovery area (m^2)	Heat rejection area (m^2)
1	9692.83	- 23461.70	-*2837.27
2	1771.60	- 5392.60	2809.40
3	3676.50	- 1845.10	3573.00
4	3485.56	1342.55	3636.44
5	3492.51	3337.88	3637.67
6	3492.91	3964.77	3637.62
7	3493.73	4013.41	3637.63
8	3493.92	4013.87	3637.62
9	3493.88	4013.69	3637.59

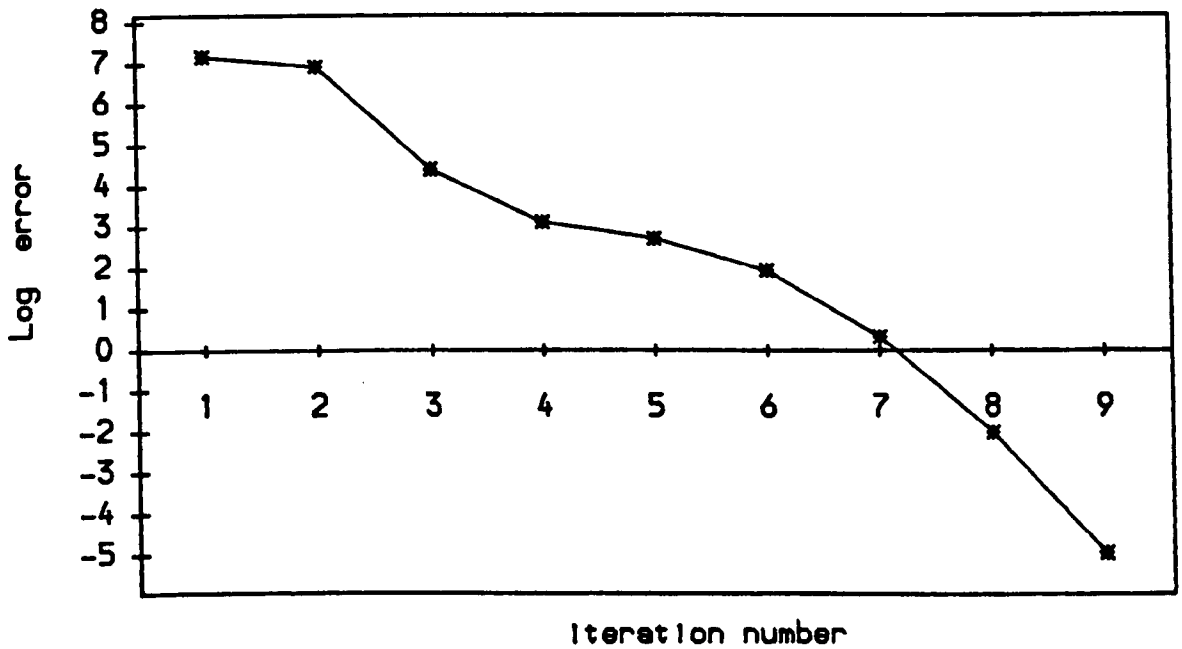

FIG. (7.4) CONVERGENCE STABILITY OF THE VTBVT TECHNIQUE

---

* The calculated variables may vary considerably from iteration to another, and some values may be outside the range of physical feasibility, e.g. negative flowrates and/or temperatures. If the temperature driving force goes negative, the area must also become negative to maintain the sine of the heat transfer (to satisfy the heat balance equation).

7.3.2. Sensitivity Of The VTBVT Technique To Initial Starting Values:

The convergence behaviour and the solution stability of the design calculations, under a wide range of initial temperature profiles are studied in this section. Some typical results of this study are illustrated graphically by Figures (7.5) to (7.8). In Figures (7.5.A,B), the error in the initial assumed temperature profile is approximately 30% more than the final temperature results. While in Figures (7.6.A,B), the initial guess is taken as 90 % of the final results profile. In the Figures (7.7.A,B), the solution is started by; (the final results + (0.5 x NT)). In all these cases the convergence is observed to be rapid. Just 6 to 7 iterations and between 0.4 to 0.5 second of CPU time are needed to reach the final solution. However, with unsatisfactory starting temperature values, Figures (7.8.A,B), ten iterations are enough to reach the solution. The increase of the number of iterations in this case may be attributed to the fluctuations in the temperature and flowrate profiles during the first and the second iterations. On the basis of this study, it may be deduced that; first, the VTBVT technique is stable under a wide range of starting values. Second, better estimates on the first approximation will give more rapid convergence.

7.3.3. The Plant Design Numerical Results:

The computational results of AL-KHOBAR II MSF plant are tabulated in Tables (7.6), and (7.7). In Table (7.6) the temperature profiles of the cooling water (TCOUT), the distillate (TDOUT) and the flashing brine (TBOUT) as well as the distillate (FDOUT) and flashing brine (FBOUT) flowrates are tabulated versus the stage number. Furthermore, the main design parameters such as the boiling point rise (BPR), the non equilibrium temperature correction (CORR), terminal temperature difference (TTD), logarithmic mean temperature difference (LMTD), heat transfer load (QLOAD), stage heat transfer area (A), and finally the overall heat transfer coefficient (U) are listed.

While Table (7.7) comprises all the main information required to describe the process design and the operation of the plant. This table includes some of the specified and the calculated variables.

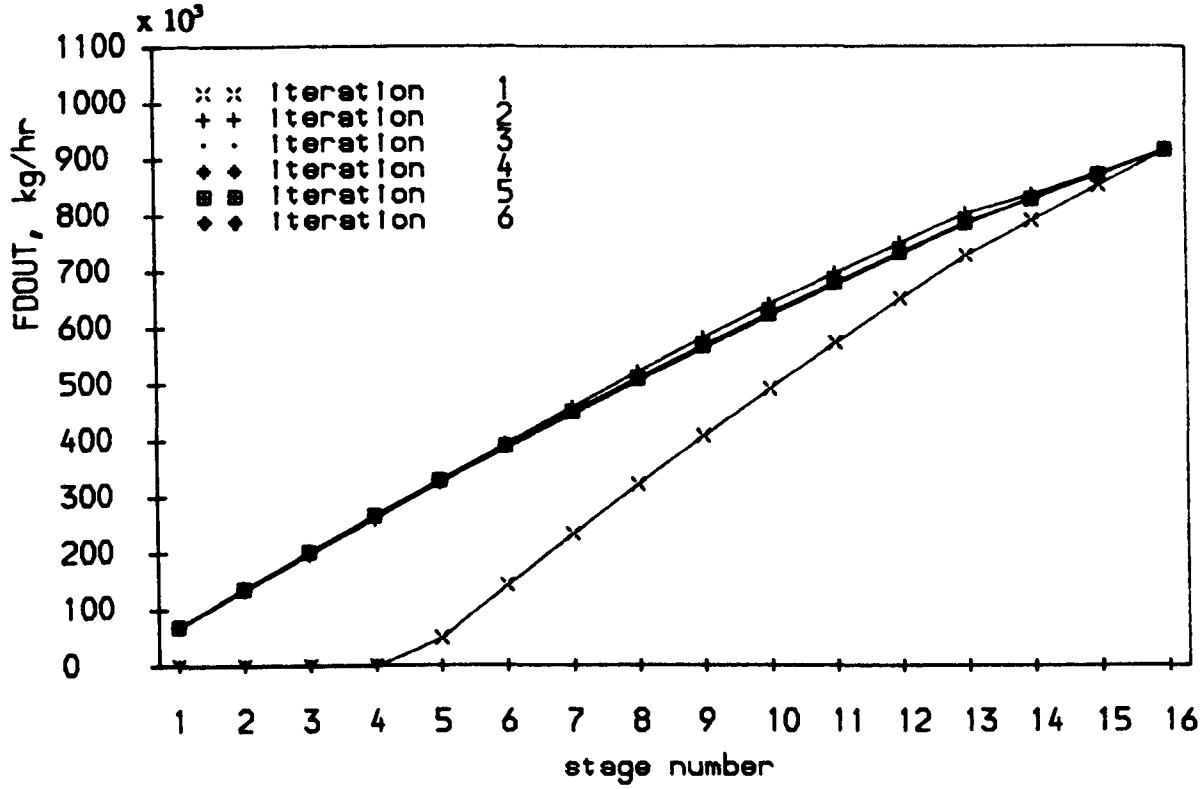

FIG. (7.5,a) CONVERGENCE OF THE DISTILLATE FLOWRATE ALONG THE PLANT. (design calculation)

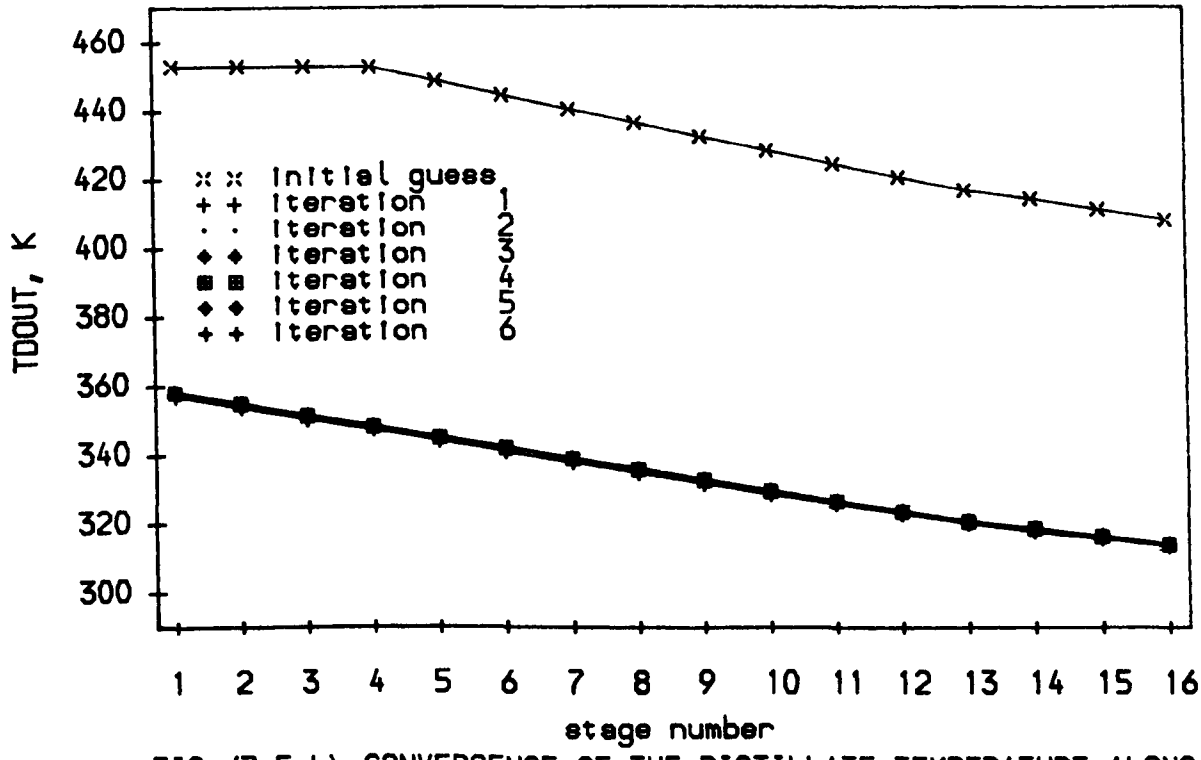

FIG. (7.5,b) CONVERGENCE OF THE DISTILLATE TEMPERATURE ALONG THE PLANT.

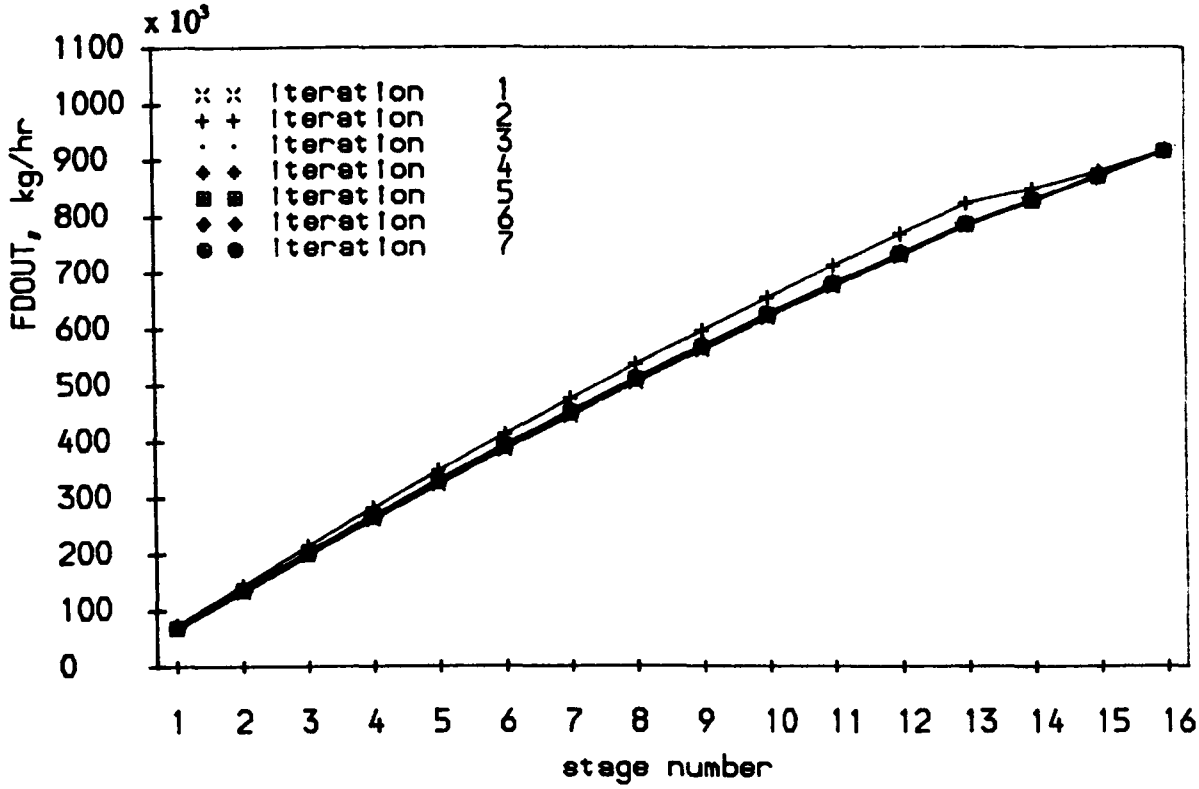

FIG. (7.6,a) CONVERGENCE OF THE DISTILLATE FLOWRATE ALONG THE PLANT. (design calculation)

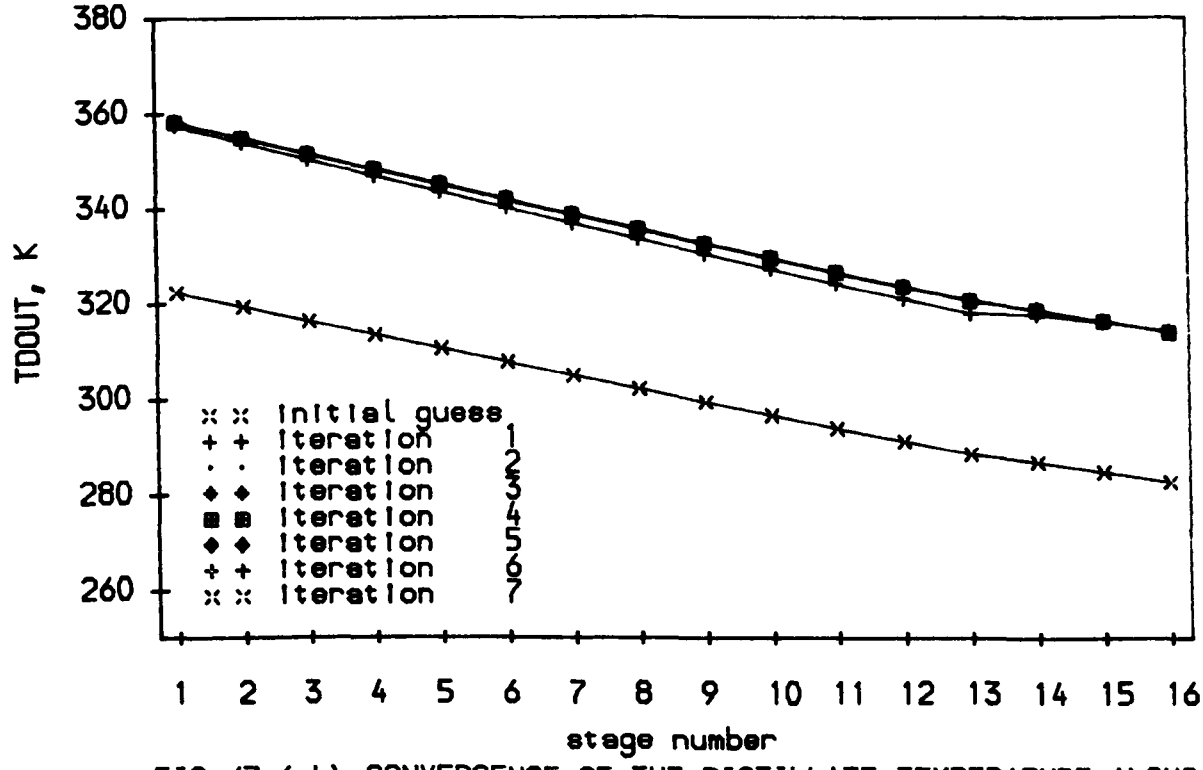

FIG. (7.6,b) CONVERGENCE OF THE DISTILLATE TEMPERATURE ALONG THE PLANT.

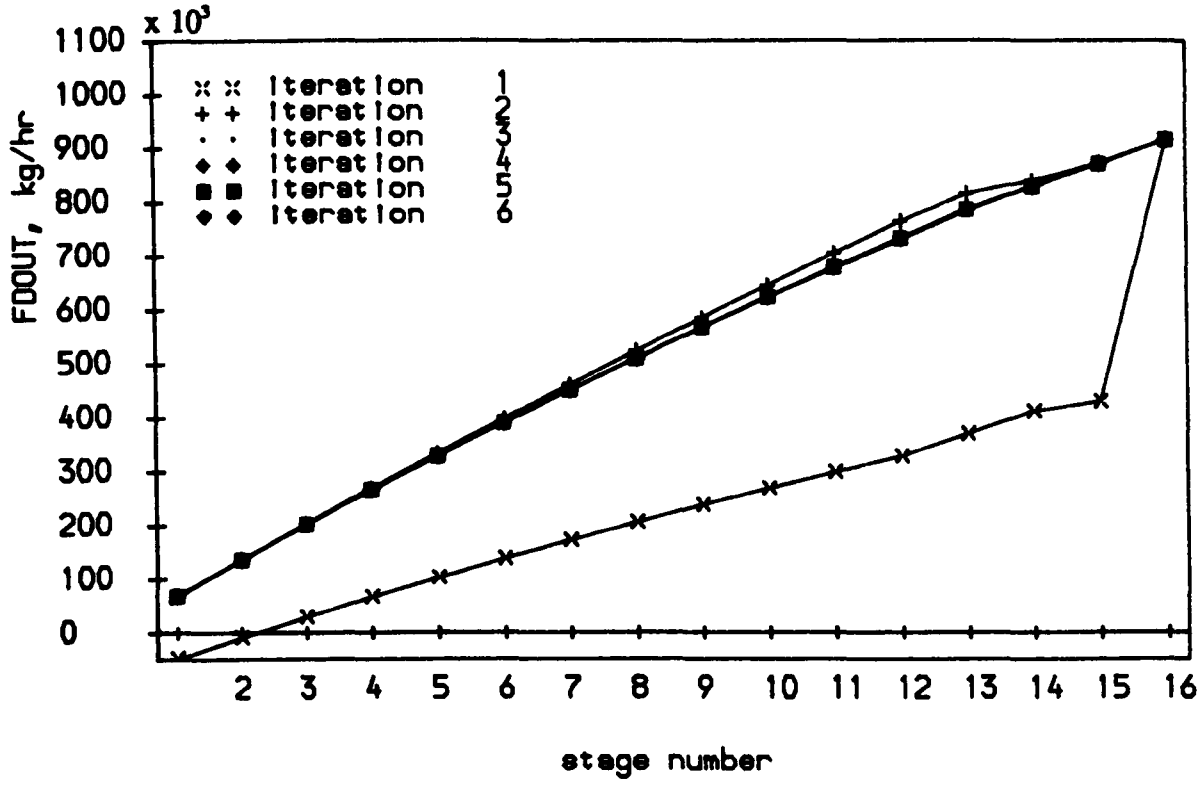

FIG. (7.7,a) CONVERGENCE OF THE DISTILLATE FLOWRATE ALONG THE PLANT. (design calculation)

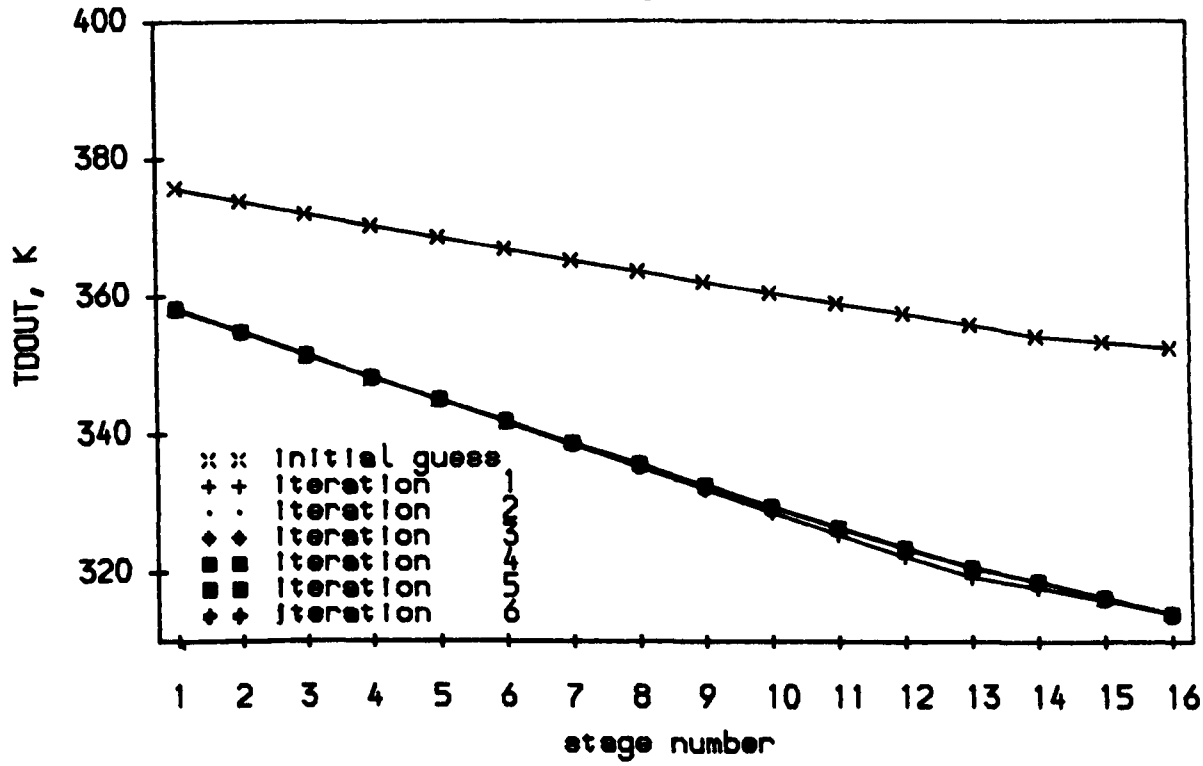

FIG. (7.7,b) CONVERGENCE OF THE DISTILLATE TEMPERATURE ALONG THE PLANT.

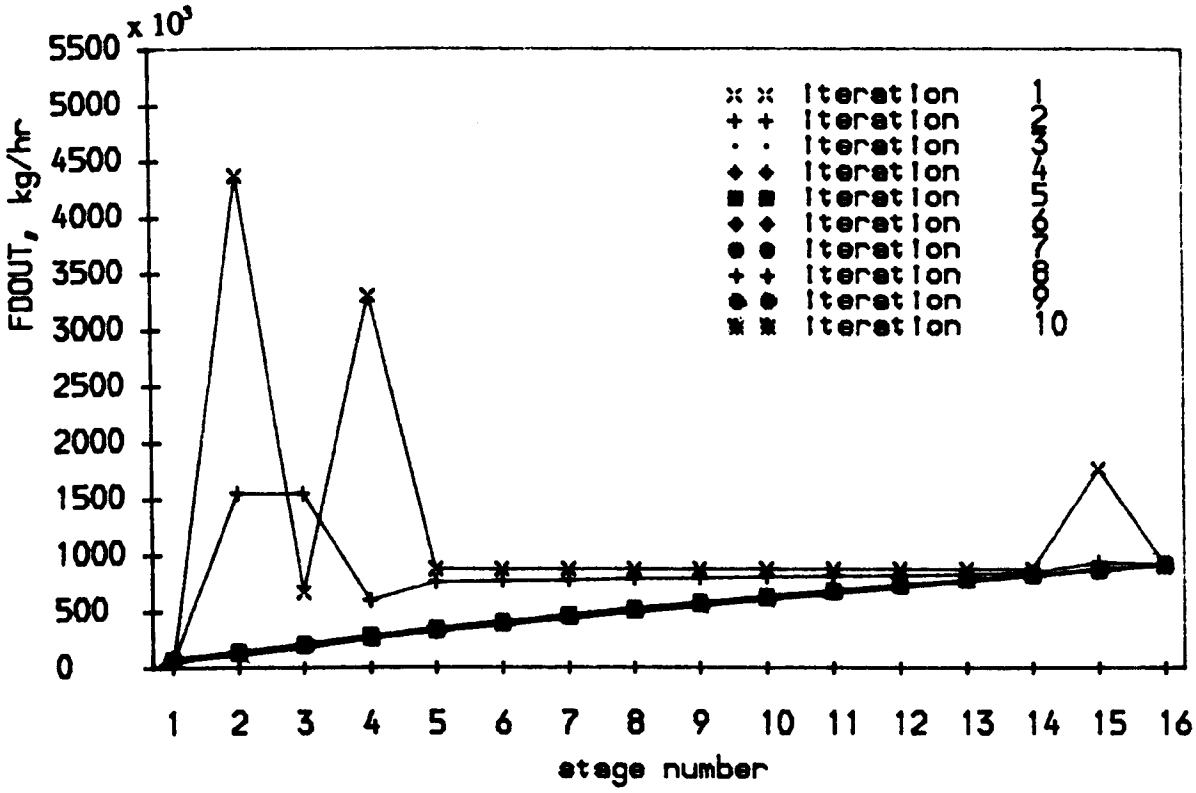

FIG. (7.8,A) CONVERGENCE OF THE DISTILLATE FLOWRATE ALONG THE PLANT. (design calculation)

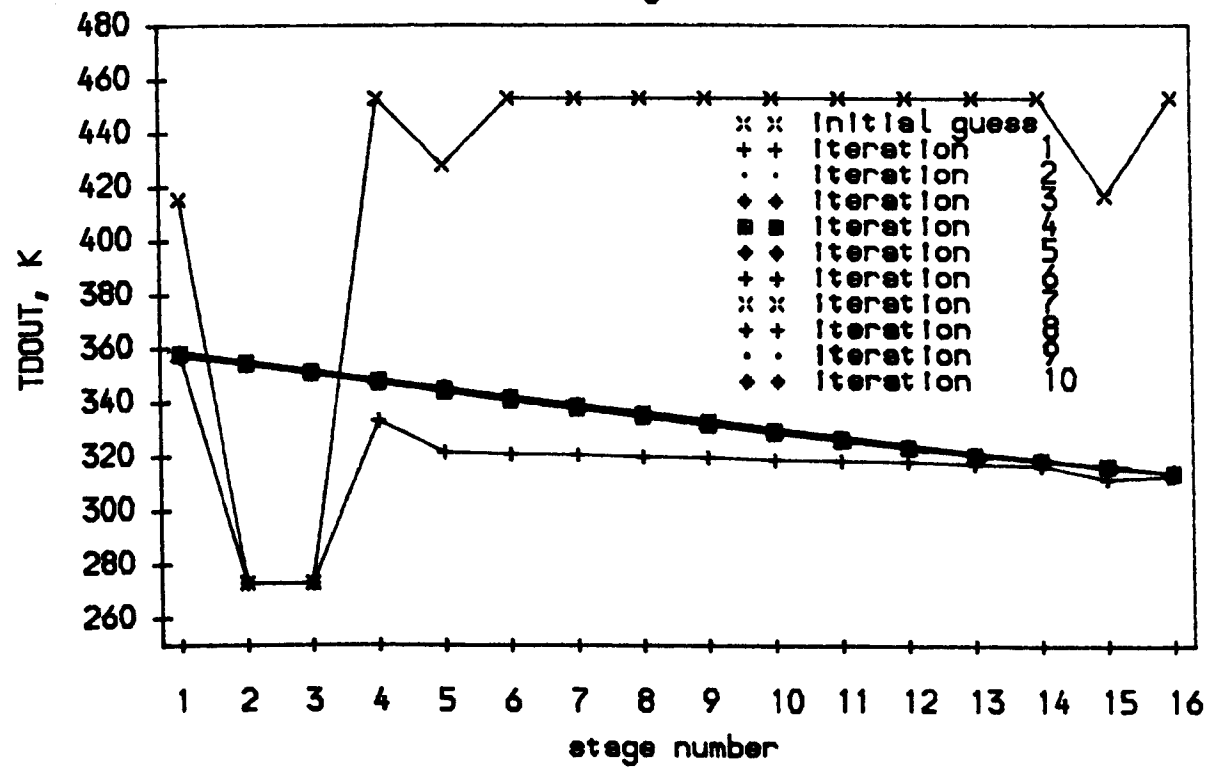

FIG. (7.8,B) CONVERGENCE OF THE DISTILLATE TEMPERATURE ALONG THE PLANT.

Table (7.6). Distribution Of The Main Variables Along AL-KHOBAR II Desalination Plant.

St	TCOUT	TDOUT	TBOUT	FDOUT	FBOUT	BPR	CORR	TTD	LMTD	QLOAD	AREA	U
No	[K]	[K]	[K]	$x10^{-3}$ [kg/hr]		[K]	[K]	[K]	[K]	$x10^{-3}$ [kJ/hr]	[m^2]	[kJ/hr. m^2.K]
1	356.29	358.28	359.81	68.66	12013.35	0.98	0.56	1.98	3.39	157846.37	4013.69	11606.86
2	352.94	354.93	356.51	135.96	11946.05	0.97	0.62	1.98	3.38	156268.75	4013.69	11533.16
3	349.62	351.61	353.24	201.89	11880.12	0.95	0.68	1.98	3.36	154593.50	4013.69	11454.81
4	346.34	348.32	350.00	266.44	11815.57	0.94	0.74	1.98	3.35	152827.50	4013.69	11371.93
5	343.09	345.07	346.81	329.62	11752.39	0.92	0.81	1.98	3.33	150989.25	4013.69	11284.57
6	339.88	341.86	343.65	391.43	11690.58	0.91	0.88	1.98	3.32	149081.62	4013.69	11192.88
7	336.71	338.69	340.53	451.87	11630.14	0.90	0.94	1.98	3.30	147122.31	4013.69	11096.89
8	333.58	335.56	337.46	510.96	11571.05	0.88	1.01	1.98	3.29	145125.12	4013.69	10996.72
9	330.49	332.47	334.43	568.71	11513.30	0.87	1.08	1.98	3.27	143091.81	4013.69	10892.46
10	327.44	329.42	331.44	625.13	11456.88	0.86	1.16	1.98	3.26	141025.06	4013.69	10784.26
11	324.44	326.42	328.49	680.26	11401.75	0.85	1.23	1.98	3.24	138940.56	4013.69	10672.16
12	321.47	323.46	325.59	734.10	11347.91	0.83	1.30	1.99	3.23	136850.50	4013.69	10556.21
13	318.55	320.54	322.73	786.69	11295.32	0.82	1.37	1.99	3.22	134752.87	4013.69	10436.61
14	315.68	318.61	320.42	828.88	11253.14	0.81	1.00	2.93	4.03	107440.62	3637.88	7322.56
15	313.23	316.28	318.08	871.38	11210.62	0.80	1.00	3.05	4.18	110190.19	3637.88	7252.16
16	310.72	313.89	315.68	914.67	11167.34	0.79	1.00	3.17	4.33	112926.37	3637.88	7177.70

Table (7.7)

General Specification Results for AL-KHOBAR II Plant.

Parameter	Value	Unit
Brine heater:		
Mean tube length	7.5	m
Brine temperature increase by heater	6.86	K
Log. mean temperature difference	10.02	K
Overall heat transfer coefficient	9364.30	$kJ/m^2.hr.K$
Heat load of brine heater $\times 10^{-5}$	3278.0	kJ/hr
Heat transfer area required	3494.0	m^2
Heating steam required $\times 10^{-3}$	143.55	kg/hr
Number of tubes in brine heater bundle	3035.00	
Brine heater pressure drop	26.75	kPa.
Terminal temperature difference	6.96	K
Heat Recovery Section:		
Pressure drop	344.70	kPa.
Heat Rejection Section:		
Pressure drop	80.9	kPa.
The complete Plant:		
Plant production $\times 10^{-3}$	914.667	kg/hr
Recycle ratio, (kg recycle/kg product)	13.2	
Concentration ratio of recycle stream	1.18	
Maximum brine temperature	363.15	K
Steam economy	6.37	
Make-up flowrate $\times 10^{-3}$	5640.24	kg/hr
Blowdown flowrate $\times 10^{-3}$	11167.30	kg/hr
Splitting ratio of the reject seawater splitter	0.5014	
Splitting ratio of the blow down splitter	0.5768	
Feed seawater flowrate $\times 10^{-3}$	11249.1	kg/hr
Total condenser surface area	62824.0	m^2
Specific condenser surface area	0.0687	$m^2 \times hr/kg$

Table (7.8) Specifications Needed for Al-KHOBAR II Plant, Performance Calculations*

Variables	Symbol	Value	Units
Feed seawater flowrate $\times 10^{-3}$	F_f	1249.1	kg/hr
Seawater salinity $\times 10^{-3}$	X_f	57.00	ppm
Seawater temperature	T_f	308.15	K
Feed seawater pressure	P_f	100.00	kPa
Steam temperature	T_s	370.15	K
Steam pressure	P_s	100.00	kPa
Blowdown splitter ratio	$\alpha 2$	0.5768	
Reject splitter ratio	$\alpha 1$	0.5014	
Top brine temperature	T_{max}	363.15	K
Brine heater transfer area	A_h	3493.88	m^2
Heat recovery stage area	A_{rec}	4013.69	m^2
Heat rejection stage area	A_{rej}	3637.59	m^2

7.4. SIMULATION CALCULATIONS oF AL-KHOBAR II MSF PLANT:

The stability and the convergence characteristics of the proposed VTBVT technique during the design calculations of AL-KHOBAR II were underlined in the previous section. In this section, the convergence behaviour, the stability of the model to the initial guesses, and the accuracy of the final results of performance calculations, for Al-KHOBAR II plant using the VTBVT technique, will be investigated. And in the mean time, the capability of the developed package to perform simulation calculations for MSF process, which is in fact a typical multi-stage countercurrent separation process, will be illustrated.

In the design mode, as can be realized from the previous section, the distillate product (D) was fixed, while the feed seawater (F), the heat transfer area (A), and the splitting ratio of the recycle stream ($\alpha 2$) were among the results. By contrast, in the simulation mode, F, A,

---

* The plant parameters used are exactly the same as those tabulated in Table (7.3).

and α_2, are fixed. And the distillate product will be one of the results. So, to examine the performance of the designed (or existing) plant under the design operating conditions, the proper specifications are taken from the design calculations output presented in the previous section. These specifications are tabulated in Table (7.8). Eleven additional equations will be established by these specifications to make the equations and variables numbers match.

7.4.1. The Convergence Aspects of The Performance Calculation:

In this section, some convergence aspects (such as the sensitivity of the model to starting values and the rate of convergence), of the performance calculations using VTBVT technique are examined. Three runs are executed using different initial temperature profiles, and the convergence behaviour is recorded. First, in Figures (7.9.A,B), the initial temperature profile is taken as (450 - 0.1 x NT) (where, NT is the temperature variable number). Second, (400. - 0.1 x NT) is taken as initial temperature approximation, and the successive TDOUT and FDOUT are plotted in Figures (7.10.A,B). Third, in Figures (7.11.A,B). the temperature starting values are (350 - 0.1 x NT). These figures illustrate that the solution is obtained after 6 to 7 iterations, each of which requires about 0.07 second.

On this basis, it can be inferred that; first, the convergence rate of the VTBVT technique in the performance calculations is not significantly affected by the value of the starting temperature profile. Second, the technique is remarkably insensitive to the starting values.

The influence of the problem size (i.e. the number of variables (or equations) and consequently the number of arithmetical operations required to be performed) on the performance of the VTBVT technique is investigated. This is attained by considering different sizes of the MSF process, ranging from 16 to 33 stages. The results of this study are represented in Figure (7.12). An interesting point to note in this figure is that the convergence rate does not seem to depend greatly on the plant size. Conversely, as shown in Table (7.9), the computer CPU time is proportional to the number of stages. Also, it should be pointed out here that, the solution does not get significantly more complicated as the number of stages increases.

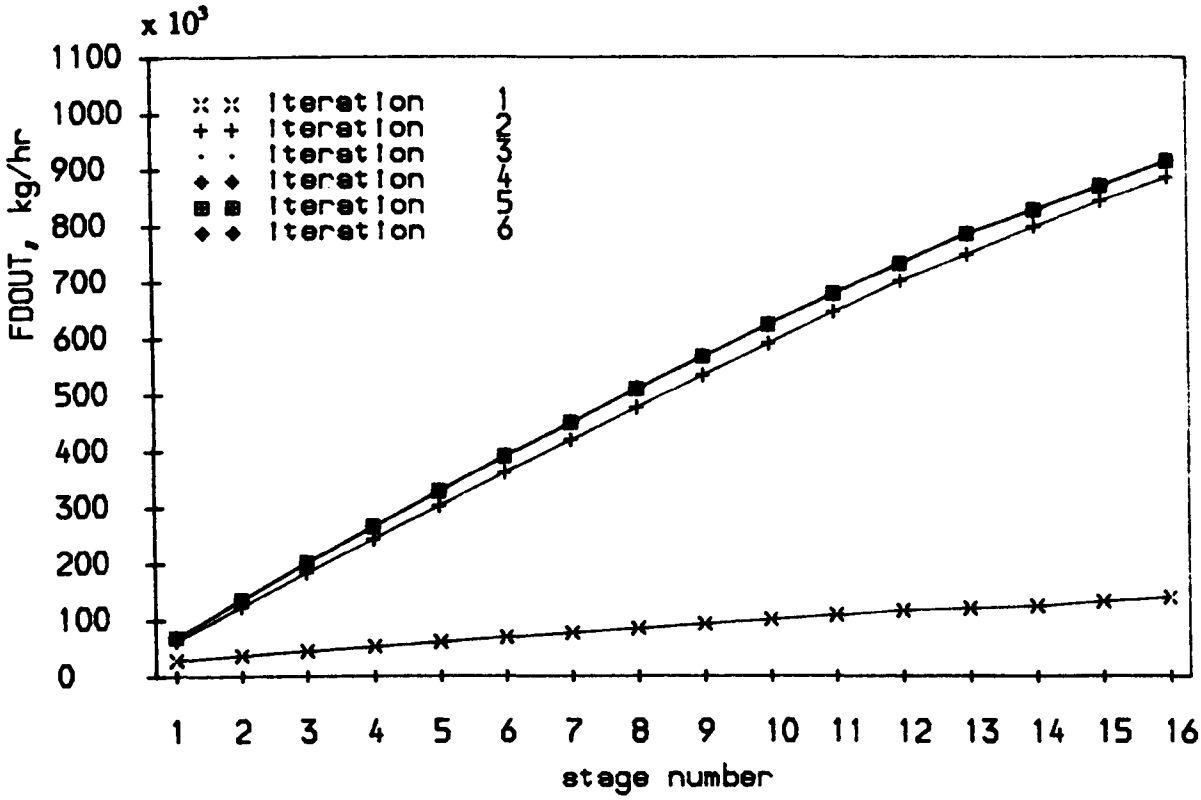

FIG. (7.9,a) CONVERGENCE OF THE DISTILLATE FLOWRATE ALONG THE PLANT. (performance calculation)

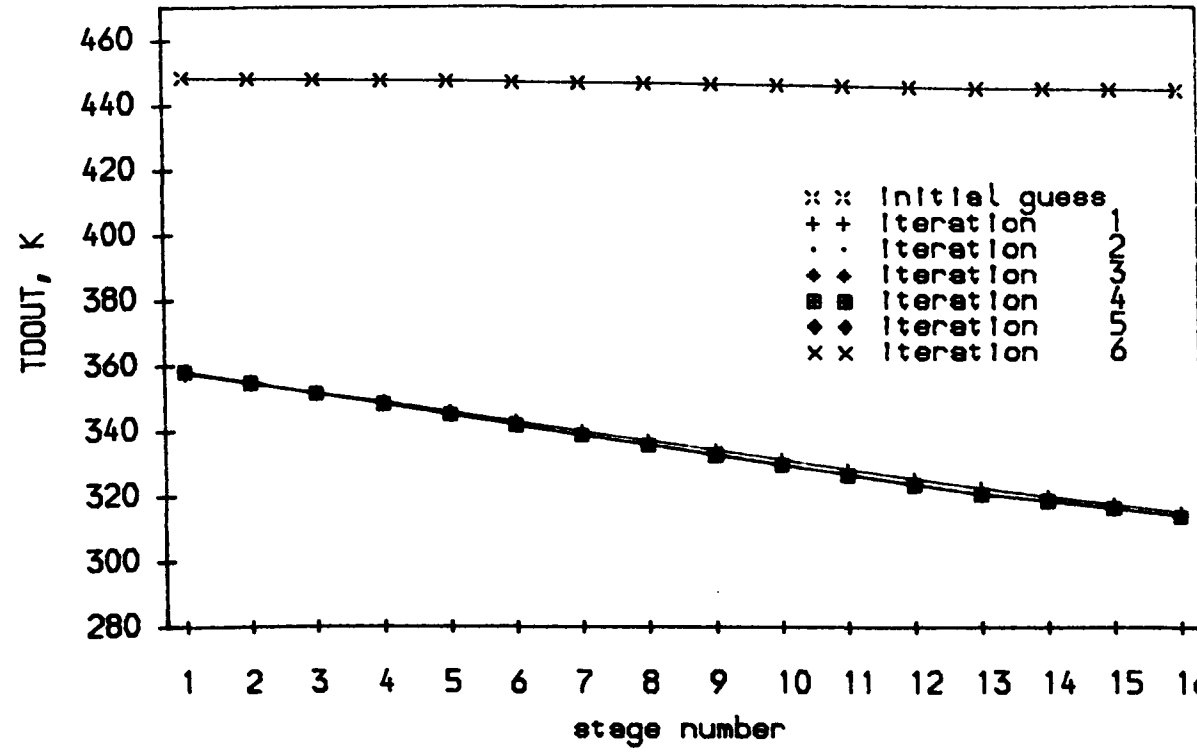

FIG. (7.9,b) CONVERGENCE OF THE DISTILLATE TEMPERATURE ALONG THE PLANT.

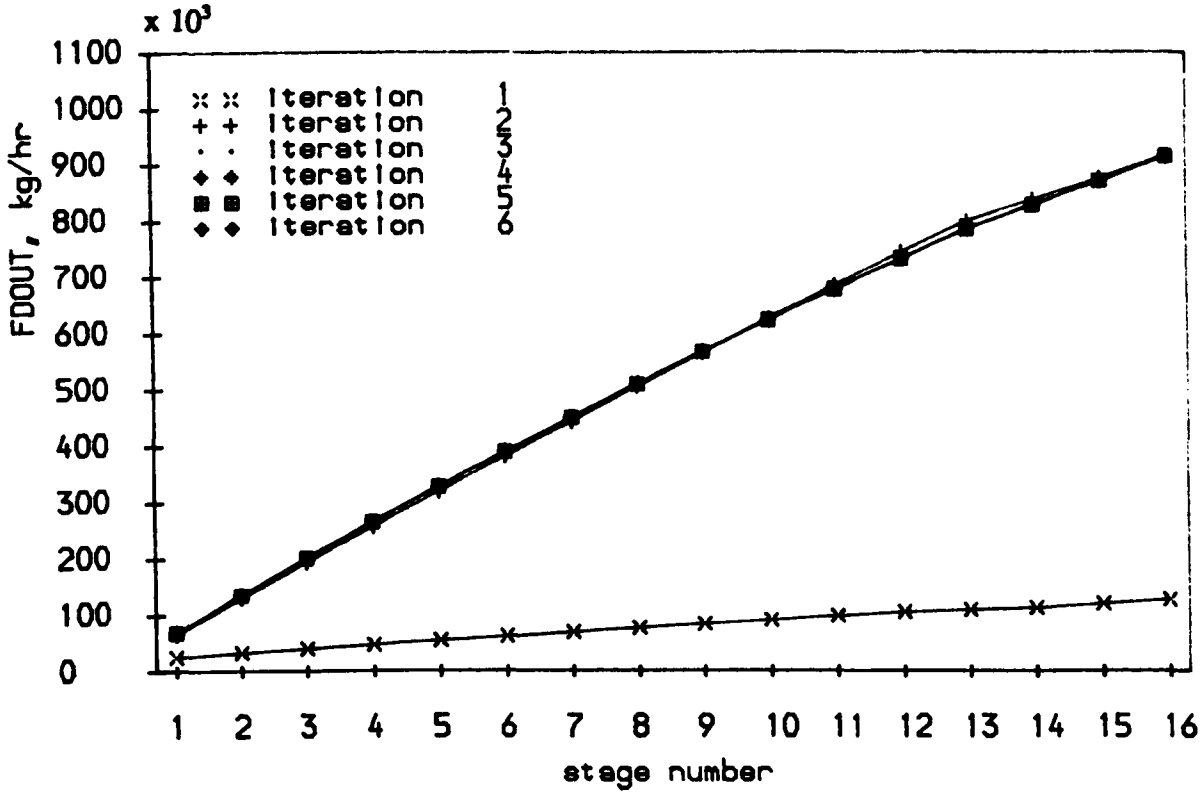

FIG. (7.10,a) CONVERGENCE OF THE DISTILLATE FLOWRATE ALONG THE PLANT. (performance calculation)

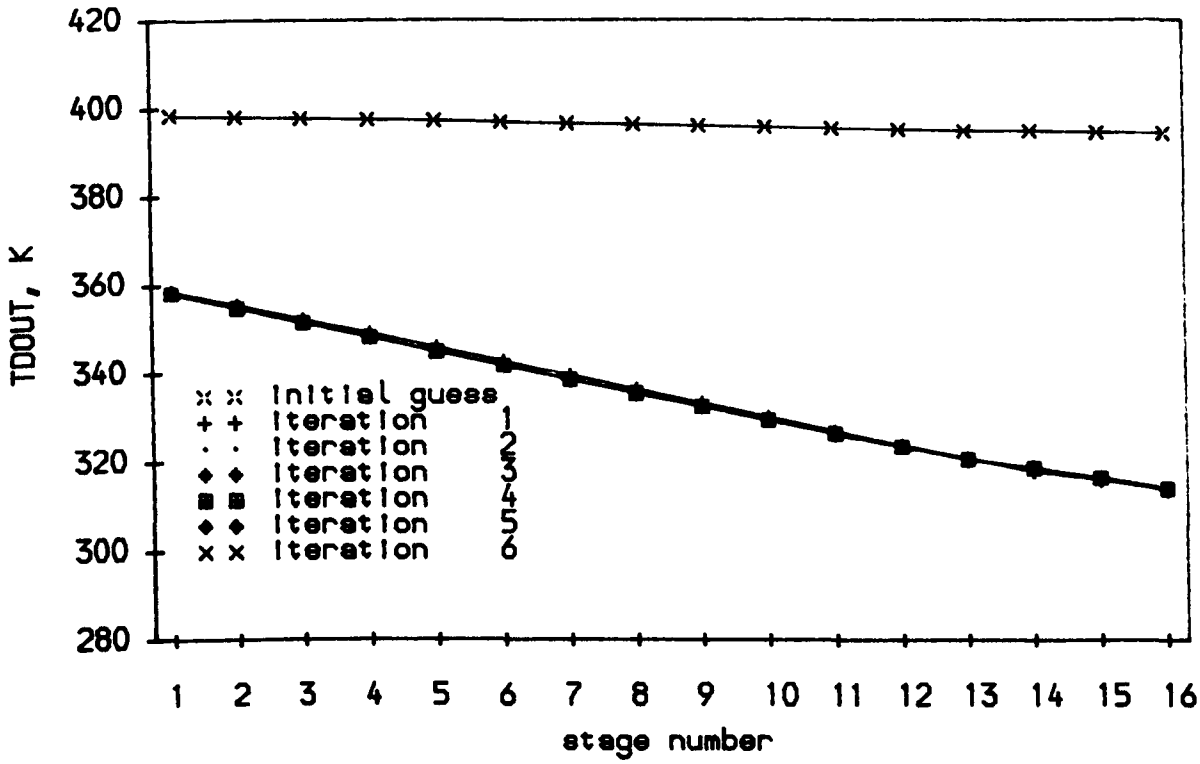

FIG. (7.10,b) CONVERGENCE OF THE DISTILLATE TEMPERATURE ALONG THE PLANT.

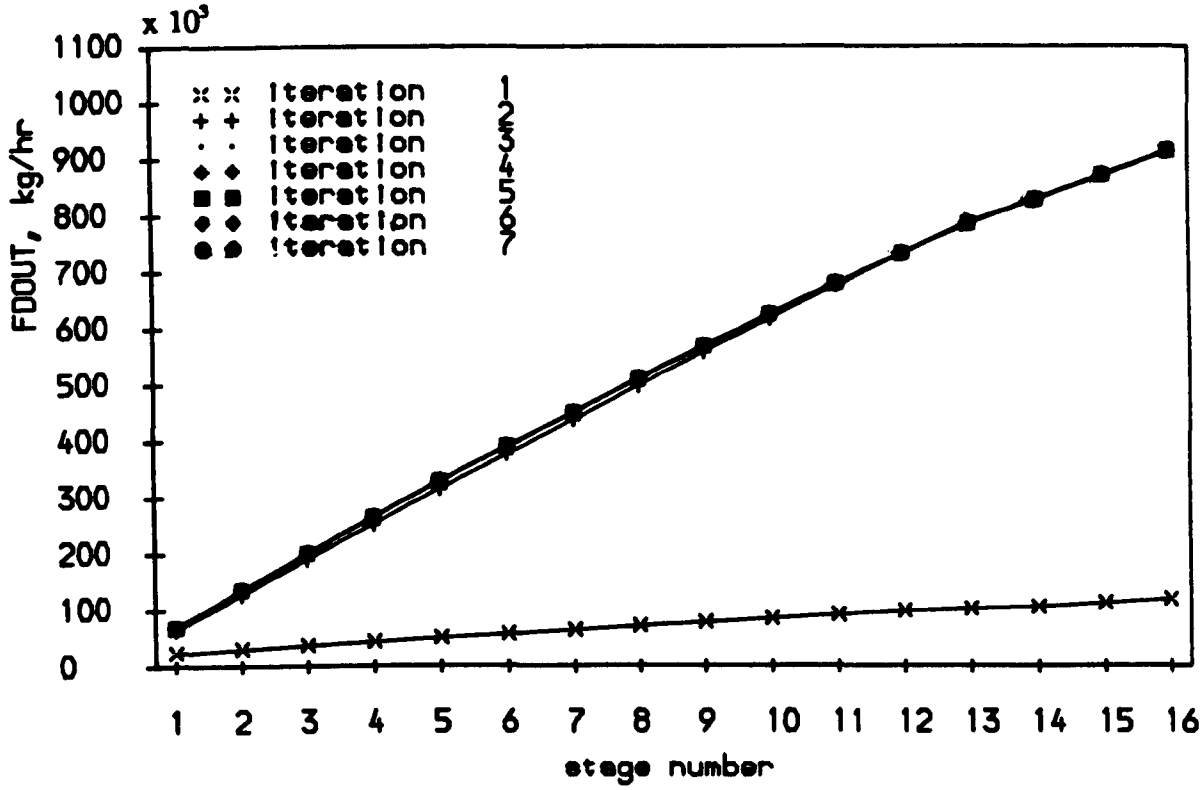

FIG. (7.11,a) CONVERGENCE OF THE DISTILLATE FLOWRATE ALONG THE PLANT. (performance calculation)

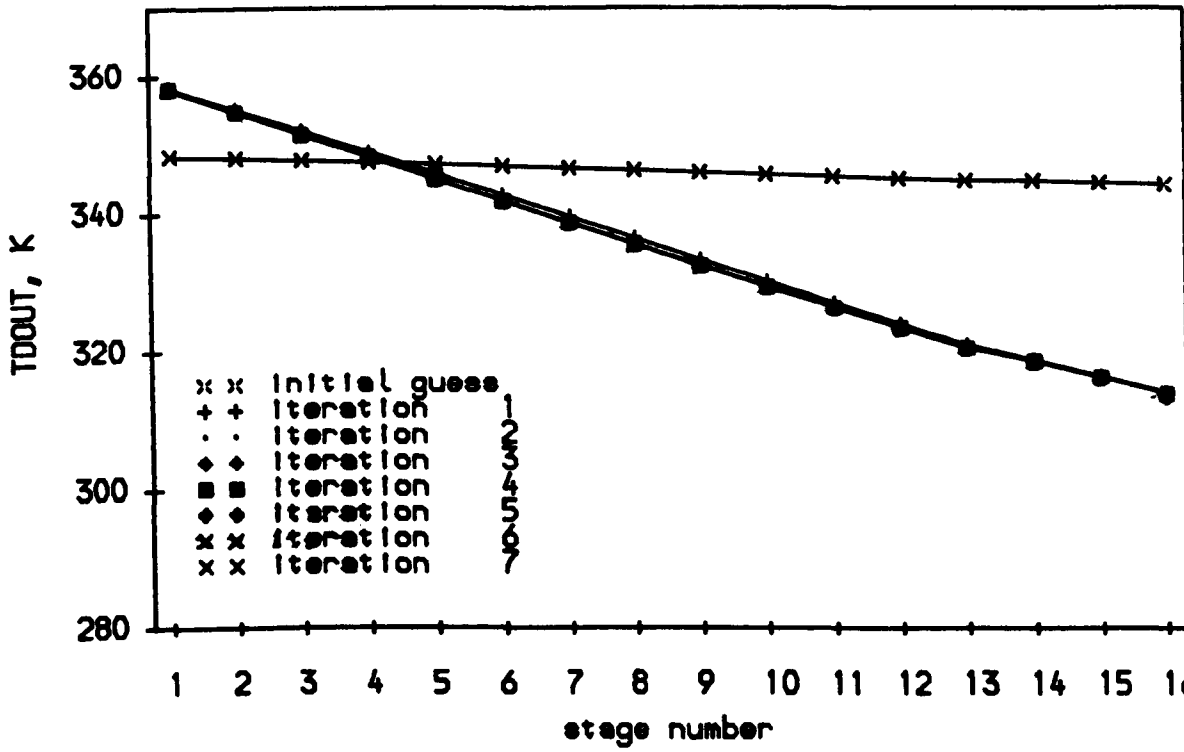

FIG. (7.11,b) CONVERGENCE OF THE DISTILLATE TEMPERATURE ALONG THE PLANT.

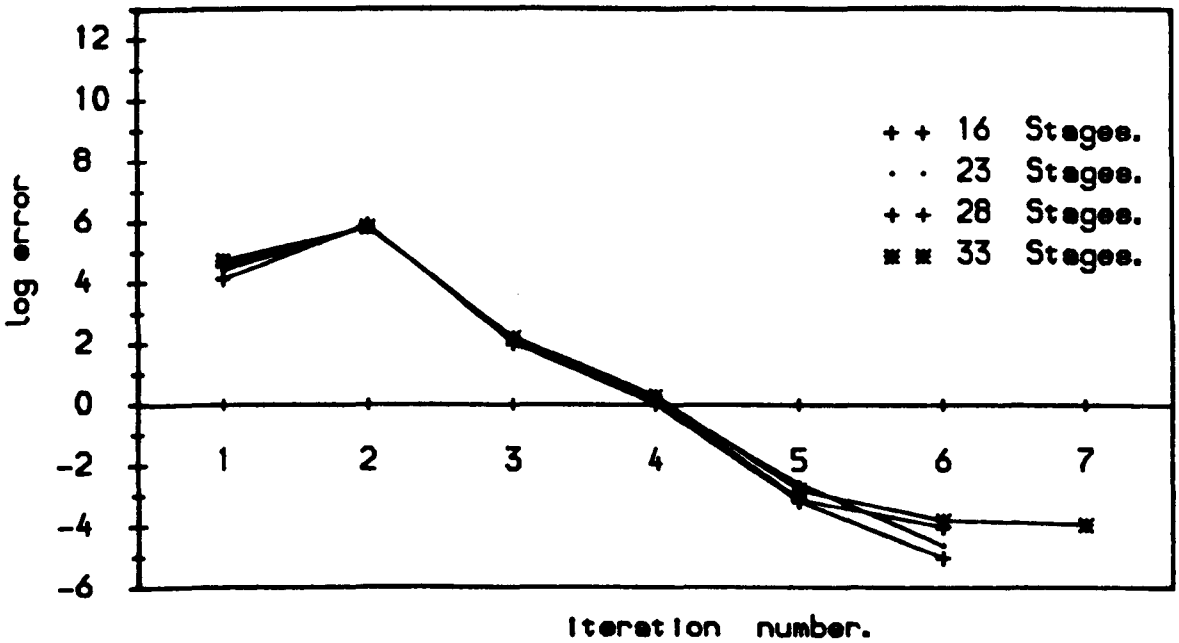

FIG. (7.12) EFFECT OF THE NUMBER OF STAGES ON THE CONVERGENCE CHARACTERISTICS

Table (7.9). Relation Between Computation CPU time and the Plant Size.

No. of stages	CPU time, sec.
16	0.39
23	0.52
28	0.64
33	0.87

7.4.2. Comparison of Design And Simulation Convergence Rates.

The convergence rates of the VTBVT technique in performing both the design and the simulation calculations are compared. Starting at the same initial values (120% of the final temperature profile), the behaviour of both modes are plotted in Figure (7.13). This figure shows that the convergence of the design problem is slightly faster than that of the simulation problem. This is probably because different specified variables are used in the two problems. Also, the heat transfer equation has a different formulation in both problem types, see chapter 5.

Table (7.10). Comparison Between The Temperature Profiles for AL-KHOBAR II MSF Plant as Calculated by the Design and The Performance Calculations.

Stage	TDOUT (K)			TBOUT (K)			TCOUT (K)		
NO.	Des.	Per.	Err.	Des.	Per.	Err.	Des.	Per.	Err.
1	358.28	358.28	0.00	359.81	359.81	0.00	356.29	356.29	0.00
2	354.93	354.92	0.01	356.51	356.51	0.00	352.94	352.94	0.00
3	351.61	351.61	0.00	353.24	353.24	0.00	349.62	349.62	0.00
4	348.32	348.32	0.00	350.00	350.00	0.00	346.34	346.34	0.00
5	345.07	345.07	0.00	346.81	346.80	0.01	343.09	343.09	0.00
6	341.86	341.86	0.00	343.65	343.65	0.00	339.88	339.88	0.00
7	338.69	338.69	0.00	340.53	340.53	0.00	336.71	336.71	0.00
8	335.56	335.56	0.00	337.46	337.46	0.00	333.58	333.58	0.00
9	332.47	332.47	0.00	334.43	334.42	0.01	330.49	330.49	0.00
10	329.42	329.42	0.00	331.44	331.44	0.00	327.44	327.44	0.00
11	326.42	326.42	0.00	328.49	328.49	0.00	324.44	324.43	0.01
12	323.46	323.46	0.00	325.59	325.59	0.00	321.47	321.47	0.00
13	320.54	320.54	0.00	322.73	322.73	0.00	318.55	318.55	0.00
14	318.61	318.61	0.00	320.42	320.42	0.00	315.68	315.68	0.00
15	316.28	316.28	0.00	318.08	318.08	0.00	313.23	313.23	0.00
16	313.89	313.89	0.00	315.68	315.68	0.00	310.72	310.72	0.00

Des. : Design Calculations

Per. : Performance calculations.

Err. : Error = Des.- Per.

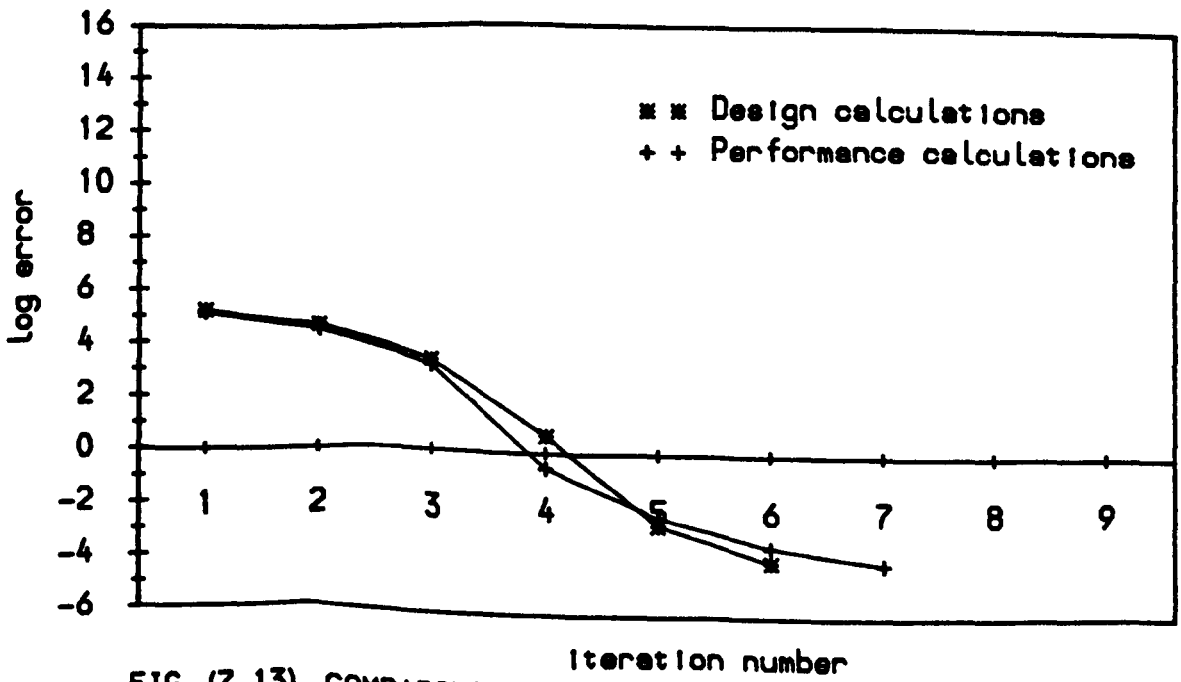

FIG. (7.13) COMPARING THE CONVERGENCE CHARACTERISTICS OF THE DESIGN AND PERFORMANCE CALCULATIONS OF AL-KHOBAR II PLANT.

Table (7.11). Comparison Between the Calculated Flowrate Profiles Along AL-KHOBAR II MSF Plant Using the Design And The Performance Calculations.

Stage	FDOUT (kg/hr) x 10^{-3}			FBOUT (kg/hr) x 10^{-3}		
No.	Des.	Perf.	Err.	Des.	Perf.	Err.
1	68.66	68.66	0.00	12013.35	12013.44	-0.09
2	135.96	135.97	-0.01	11946.05	11946.13	-0.08
3	201.89	201.90	-0.01	11880.12	11880.20	-0.08
4	266.44	266.46	-0.02	11815.57	11815.64	-0.07
5	329.62	329.64	-0.02	11752.39	11752.46	-0.07
6	391.43	391.45	-0.02	11690.58	11690.65	-0.07
7	451.87	451.88	-0.01	11630.14	11630.21	-0.07
8	510.96	510.97	-0.01	11571.05	11571.12	-0.07
9	568.71	568.72	-0.01	11513.30	11513.38	-0.08
10	625.13	625.14	-0.01	11456.88	11456.96	-0.08
11	680.26	680.26	0.00	11401.75	11401.84	-0.09
12	734.10	734.10	0.00	11347.91	11348.00	-0.09
13	786.69	786.67	0.02	11295.32	11295.43	-0.11
14	828.88	828.85	0.03	11253.14	11253.25	-0.11
15	871.38	871.36	0.02	11210.62	11210.74	-0.12
16	914.67	914.64	0.03	11167.34	11167.46	-0.12

7.4.3. Simulation And Design Results Accuracy:

So far the emphasis was focused on the stability and the efficiency of the proposed technique. In this subsection, the results reproducibility, and the program output accuracy, are examined. The reproducibility means that the output of one problem type, (e.g. design), can be used as input to another type, (e.g. simulation) and the solution gives almost identical results for both problem types. As pointed out before, the input data for the simulation problem is taken from the output results of the design problem (section 7.3). So, it is expected, theoretically at least, that the output results of both problem types will be the same. To examine this point, variables of primary interest, produced by simulation calculations and those produced by the design calculations, (presented in section 7.3), are arranged for comparison in Tables (7.10) and (7.11). First, Table (7.10), includes the distillate, flashing brine, and cooling (or recycle) water temperature profiles (TDOUT, TBOUT, and TCOUT respectively) produced by both the design and the simulation calculations. It can be seen that the

temperature profiles are approximately identical, where the maximum fractional error* is $(3.082 \pm 6.165) \times 10^{-5}$. Second, Table (7.11) shows that the maximum fractional error in the distillate flowrate profile (FDOUT) along the plant is about $(7.354 \pm 14.7) \times 10^{-5}$ and the flashing brine flowrate profile (FBOUT) has $(1.075 \pm 17.909) \times 10^{-5}$ as a maximum fractional error. These errors may be because both types of calculations (simulation and design) takes a different way to the final solution, therefore, different values of round off errors are generated in both routes, which lead to a slightly different final answer. In fact, these fractional errors do not show any clear trend, and they are too small to be of any significance. So, these accuracy comparisons indicate that the program outputs of the simulation and the design problem are accurate and also illustrate the reproducibility of the results.

7.5. PERFORMANCE OF AL-KHOBAR II PLANT UNDER CHANGING OPERATING CONDITIONS

MSF plants are always designed to operate under certain operating conditions. However, often these operating conditions have to be varied. For example, the brine flowrate may be changed due to some failure or because of a change in the fresh water requirements. Also, in some cases the plant production has to be varied as a result of a change in the total plant flashing range (top brine temperature minus blowdown temperature). This may be due to a change in quantity or quality of the heating steam and/or because of seasonal and daily variations of the feed seawater temperature.

Investigation of a plant under such new conditions is, in fact, a part of the designer's task to be sure that a safe and practical plant is built and operated. Also, it is a part of the operator's duty for operating the plant to its best advantages. In other words, the behaviour investigation of an existing (or a fully designed) plant, is an interesting problem for the designer and/or the operator as well.

---

* Fractional error = error range =

$$\frac{\left[\begin{array}{l}\text{difference between}\\ \text{the two values}\end{array}\right] \pm \left[\begin{array}{l}\text{The maximum round in}\\ \text{the last decimal place}\end{array}\right]}{\left[\begin{array}{l}\text{the average of the}\\ \text{two values}\end{array}\right]}$$

In fact, this problem is considered one of the most straightforward applications, of the simulation mode, of the developed program. To illustrate this applicability, investigations of the impact of changing some operating conditions, such as, brine recirculation flowrate (R), and feed seawater temperature (T_f), on the plant performance and productivity are discussed in this section. This is performed by running the program for case III, in Table (7.2), using the specification data listed in Table (7.12), as a reference case. A previously obtained solution may be used as a starting point for a new solution and thus the number of required iterations can be reduced.

7.5.1. Performance Map For AL-KHOBAR II Plant:

This investigation is performed by assuming a variation in both seawater temperature (T_f), (from 23 C to 38 C), and the recirculated brine flowrate (R), (from 70 % to 110 % of the reference value). All the other assigned independent variables remain the same as those of the reference case tabulated in Table (7.12). A summary of the computer output is shown in Table (7.13). In this table, the significant variables of operating and controlling the plant are represented. It should be noted that the flow quantities in this table (i.e steam, water production, recycle brine and feed seawater, flowrates) are expressed as a ratio of the reference case quantities. These ratios, (namely; water production ratio (D_r), brine recirculated flowrate ratio (R_r) and steam flowrate consumption ratio (S_r)), as well as variation range of feed seawater temperature (T_f), are represented graphically in the shape suggested by Van [1970], in Figure (7.14), which is referred to as "performance map" of AL-KHOBAR II plant.

Using this performance map, many investigations can be done quickly and accurately. For example, prediction of the plant performance and controlling variables can be performed, when the plant is operated under constant steam consumption policy, constant water production policy, or constant recycle brine flowrate, in the face of changing feed seawater temperature. In fact, these investigations can be attained not only for the design capacity (100 % load), but also for "off design" capacities (i.e. enhanced and partial capacity).

By operating the plant under the design conditions, which are represented in the performance map by "Design Point", the plant production, as expected, will be the full design capacity. However, any

Table (7.12), Specification List of The Performance Calculations of AL-KHOBAR II Plant Under a Constant Brine Recirculation Policy*.

Variable	Symbol	Value	Units
Seawater salinity	X_f	57000.00	ppm
Feed seawater temperature	T_f	308.15	K
Feed seawater pressure	P_f	100.00	kPa
Steam temperature	T_s	370.15	K
Steam pressure	P_s	100.00	kPa
Brine recirculation flowrate flowrate $\times 10^{-3}$	R	12082.10	kg/hr
Reject seawater splitter ratio	$\alpha 2$	0.5014	
Blowdown splitter ratio	$\alpha 1$	0.5768	
Heat recovery stage heat transfer area	A_{rec}	4013.69	m^2
Heat rejection stage heat transfer area	A_{rej}	3637.59	m^2
Area of the brine heater	A_h	3493.88	m^2

deviation of feed seawater temperature (or any other operating parameter) will affect the plant production. So, to get back the design production value, new different values of controlling variables should be reset. For instance, variables represented by points "A" or "B" in the performance map, may be used if the feed seawater temperature changes to 30 C (303.15 K) or approximately 39 C (312.15 K) respectively. Similarly, the plant can be operated for constant water production of, say, 90 % of the design capacity (i.e. partial load case), in face of changing seawater temperature, by changing the controlling variables to fulfill the conditions of any point along the line "CD" according to the value of "T_f". In the same manner, the plant

---

* In this case, the used parameters are the same as those tabulated in Table (7.3)

Table (7.13). Effect of Varying Seawater Temperature And Brine Recirculation Flowrate on The Performance of AL-KHOBAR II Plant.

Feed seawater temperatur T_f [K]	313.15	313.15	313.15	313.15	313.15	308.15	308.15*	308.15	308.15	308.15	303.15	303.15	303.15	303.15	303.15	298.15	298.15	298.15	298.15	298.15
Recycle brine flowrate R x 10^{-3} [kg/hr]	13290.4	12082.10	10873.89	9665.68	8457.47	13290.4	12082.1	10873.89	9665.68	8457.47	13290.40	12082.10	10873.89	9665.86	8457.47	13290.40	12082.10	10873.89	9665.68	8457.47
R_r	(1.1)	(1.0)	(0.9)	0.8)	0.7)	(1.1)	(1.0)	(0.9)	(0.8)	(0.7)	(1.1)	(1.0)	(0.9)	(0.8)	(0.7)	(1.1)	(1.0)	(0.9)	(0.8)	(0.7)
Brine heater outlet temperature [K]	362.75	363.83	364.89	365.90	366.84	362.0	363.23	364.45	365.54	366.57	361.41	362.72	263.89	365.17	366.28	360.72	362.19	363.50	364.79	365.99
Brine heater inlet temperature [K]	356.26	357.44	358.63	359.78	360.89	355.07	356.29	357.71	358.97	360.17	353.86	355.32	356.74	358.11	359.43	352.63	354.21	355.75	357.25	358.67
Flashing brine temperature (out of the heat recovery section) [K]	327.01	326.63	326.33	326.01	325.66	323.09	322.72	322.46	322.10	321.72	319.17	318.85	318.49	318.09	317.66	315.27	314.92	314.52	314.08	313.62
Brine blowdown temperature [K]	320.55	320.08	319.73	319.36	318.99	316.06	315.68	315.30	314.90	314.49	311.59	311.18	310.75	310.31	309.86	307.10	306.69	306.22	305.73	305.23
Make-up temperature [K]	320.58	320.06	319.89	319.71	319.52	315.88	315.68	315.52	315.32	315.10	311.63	311.22	311.01	310.79	310.56	307.14	306.73	306.51	306.27	306.01
Seawater reject temperature [K]	320.61	320.05	320.09	320.10	320.11	315.68	315.68	315.7	315.78	315.78	311.67	311.66	311.30	311.32	311.32	307.20	306.79	306.83	306.85	306.85
Feed seawater flowrate x 10^{-3} [kg/hr]	12253.6	11170.21	10080.59	8484.14	7880.86	12340.00	11249.10	10153.9	9051.31	7941.24	12424.70	11328.88	10228.15	9114.29	8002.45	12507.50	11406.96	10300.84	9186.07	8062.59
F_r	1.0893	0.993	0.8961	0.7987	0.7006	1.0970	1.000	0.930	0.8046	0.7059	1.1045	1.0071	0.9092	0.8107	0.7114	1.11187	1.0140	0.9157	0.8166	0. 7167
Product water flowrate 10^{-3} [kg/hr]	901.39	846.22	785.036	718.54	645.84	976.56	914.64	117.2	776.78	698.20	1050.15	983.76	913.26	835.73	751.72	1122.08	1051.46	976.31	893.62	803.42
D_r	0.9855	0.9252	0.9587	0.7856	0.7061	1.0677	1.0	0.9282	0.8493	0.7634	1.1482	1.0756	0.9984	0.9137	0.8214	1.2268	1.1496	1.0674	0.9770	0. 8784
Heating steam flowrate x 10^{-3} [kg/hr]	148.83	134.04	118.10	102.50	87.33	160.75	144.33	127.0	110.18	93.78	172.799	155.06	136.44	118.160	100.500	185.00	165.92	145.90	126.29	107.27
S_r	1.0312	0.9287	0.8183	0.7102	0.6051	1.1138	1.0	0.8805	0.7634	0.6498	1.1973	1.0743	0.9453	0.8186	0.8963	1.2818	1.1946	1.0109	0.8750	0.7433

R_r: Brine recirculation flowrate ratio

D_r: Water production ratio

* (Design point)

S_r: Steam flowrate consumption ratio

F_r: Feed seawater flowrate ratio

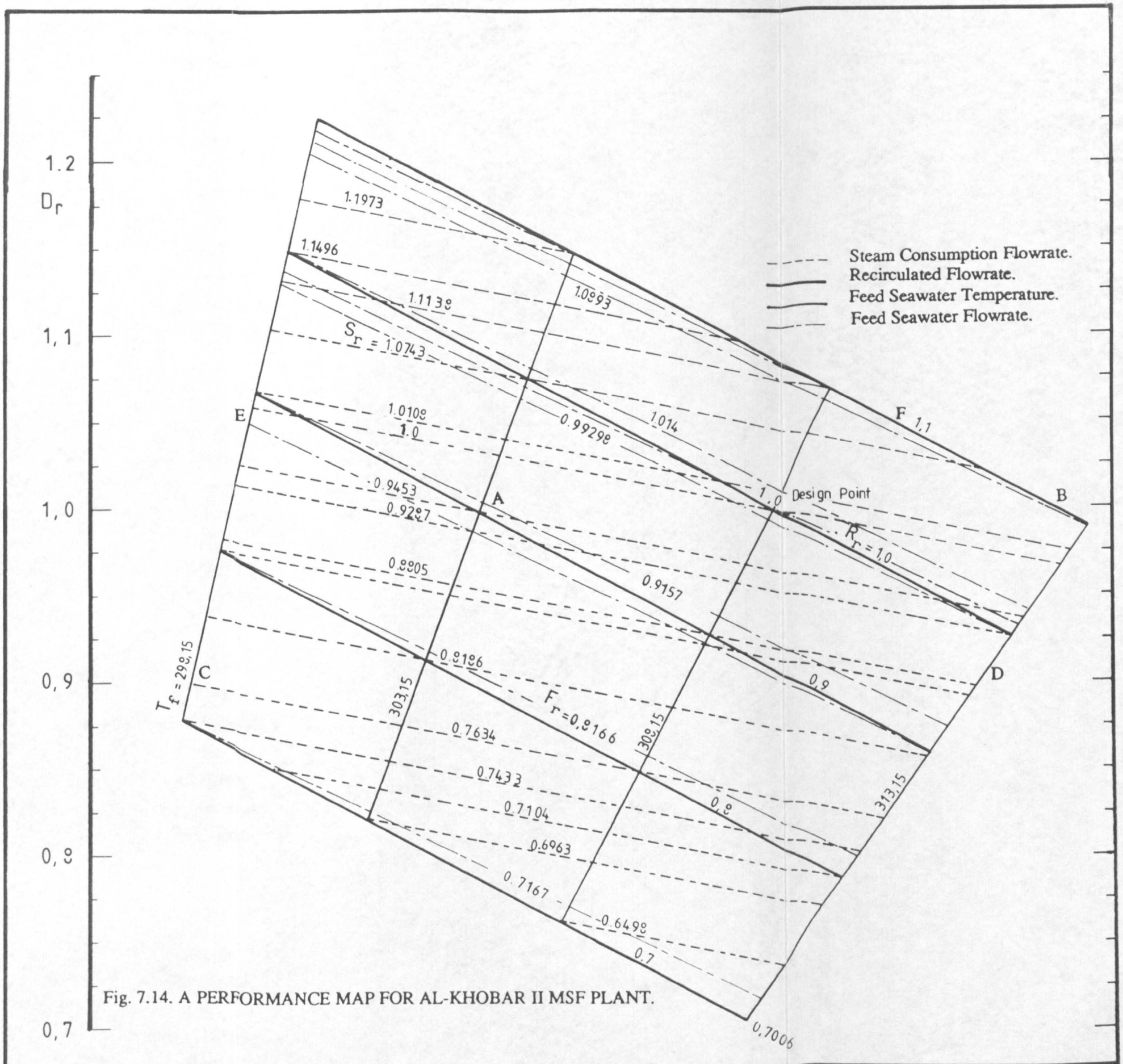

Fig. 7.14. A PERFORMANCE MAP FOR AL-KHOBAR II MSF PLANT.

production can be enhanced to say, 105 % of the design capacity, by running the plant under the controlling specifications of any point along the line "EF" depending on the value of feed seawater temperature.

As it can be seen from the performance map, Figure (7.14), in the case of constant water production, the required steam consumption, feed seawater flowrate (and consequently cooling water flowrate), and recycle brine flowrate (and thereby the pumping power), increase by increasing feed seawater temperature (T_f). Therefore, the operation cost in the summer season will be much higher than that in the winter season. It should be mentioned here that the "off design" operating conditions (i.e. partial load or enhanced capacity) may be applied under a certain practical limitations. These limitations have been illustrated in some details by Medani et al [1980], and Arad et al [1973].

With reference to operating the plant under constant recirculation brine flowrate policy, the required steam consumption flowrate, feed seawater flowrate, as well as the distillate product water flowrate decrease by increasing feed seawater temperature. Therefore, under this operating policy, the plant production in summer, when more water is needed, is much less than that in winter. It should be pointed out here that Soliman [1981] proved that; for optimum design, the recirculation flowrate should remain constant regardless of the feed seawater temperature.

As illustrated by the performance map, Figure (7.14), the decreasing slope of constant steam consumption flowrate ratio lines (S_r), with increasing seawater temperature, is less than the decreasing slop of constant brine recirculation flowrate ratio lines (R_r). Therefore, with constant steam consumption policy, which is mainly suitable for operating dual purpose plant, much smaller changes occur in the plant production, with increasing T_f, than those obtained under constant recirculated brine flowrate policy.

7.6. THE VALIDITY OF THE PROPOSED TECHNIQUE.

To justify the approximation assumptions proposed in chapter 5 to develop the VTBVT technique, FICHTNER reference plant, Homig [1978], is solved using two equation forms (4.7 and 5.20). The first form represents Newton Raphson (NR) method which solves the model without approximations, the second form represents the VTBVT approach.

The main differences between AL-KHOBAR II (KH) plant which is solved in the previous sections and FICHTNER (FI) plant may be summarized as:

I. AL-KHOBAR II plant belongs to the low top brine temperature class, whereas FICHTNER belongs to the high top brine temperature class. And the production capacity of (KH) plant is much larger than that of the (FI) plant.

II. The number of stages in (FI) plant is greater than that of (KH) plant. As a result, the performance of the first plant is higher than that of the second.

III. AL-KHOBAR II and FICHTNER plants have been designed for different feed seawater concentrations (5.7 % for (KH) and 3.5 % for (FI)). Thus, the brine concentration ratio* (which depends on the maximum allowable brine salinity in the brine heater tubes (64000 ppm at present) for the second plant is higher than that of the first.

So, the solution of FICHTNER plant may show the capability of the developed program to design and/or simulate plants with different design specifications and different location sits. Another important reason for considering FICHTNER plant is the availability of the plant results using stage to stage (STS) technique, Homig [1978]. So, more confidence can be gained by comparing the results obtained by the proposed VTBVT technique with the available STS technique, (see next section).

Figure (7.1), shows the flowsheet representing this type of plants (i.e. recirculation type), and full details of the input data used are given in Table (7.14).

7.6.1. Effect of The Approximation Assumptions on the Rate of Convergence:

FICHTNER MSF plant is represented by 171 equations. In order to solve this system of equations, one must supply good initial estimates for all the variables (in case of Newton's method), or just for temperature variables (in case of VTBVT method).

---

* Concentration ratio :the ratio of the total dissolved solids in any stream in a desalination plant to that in the feed stream.

Table (7.14). Design Data For FICHTNER MSF Desalination Reference Plant, Homig [1978]

General specifications:	
Type of the plant	Brine recycle-cross tube
Chemical treatment	Sulphuric acid
Number of evaporator stages	30
Number of heat recovery stages	27
Number of heat rejection stages	3
Flow Rates $\times 10^{-3}$ (kg/hr)	
Seawater feed flowrate	3895.00
Distillate product rate	500.00
Recycle stream flowrate	2702.00
Reject cooling seawater	2702.00
Salinity in seawater (g/kg)	35.00
Temperature (K)	
Seawater temperature	333.15
Top brine temperature	393.15
Heating steam temperature	400.15

Heat transfer area, A (m^2) and the overall heat transfer coefficient, U ($kJ/hr.m^2K$)

Stage	A	U	Stage	A	U
1	472.72	12658.0	2	473.87	12632.0
3	475.25	12604.0	4	476.86	12572.0
5	478.70	12536.0	6	480.78	12496.0
7	483.06	12453.0	8	485.59	12406.0
9	488.36	12356.0	10	491.37	12301.0
11	497.63	12244.0	12	498.15	12182.0
13	501.92	12117.0	14	505.97	12047.0
15	510.29	11974.0	16	514.90	11897.0
17	519.81	11816.0	18	525.03	11731.0
19	530.57	11642.0	20	536.45	11549.0
21	542.68	11451.0	22	549.28	11349.0
23	556.27	11243.0	24	563.67	11132.0
25	571.51	11017.0	26	579.8	10897.0
27	588.59	10772.0	28	711.99	10734.0
29	752.35	10580.0	30	776.93	10413.0

Fouling Factors ($m^2.hr.K/kcal$)	
Brine heater	0.0001512
Heat recovery section	0.0001163
Heat rejection section	0.0001163

Tube specifications:

Plant section	Tube length (m)	Number of tubes	Outside diameter (mm)	Inside diameter (mm)	Thermal conduct-ivity	Tube material
Brine heater	6.6	3564.0	16.0	14.0	25.0215	CU NI 30
Heat recovery	2.66	3942.0	16.0	14.0	42.9923	CU NI
Heat rejection	3.88	3834.0	16.0	14.0	42.9923	CU NI

The progress of the convergence of the distillate flowrate (FDOUT) and the distillate temperature (TDOUT) profiles along the plant using NR method are shown in Figures (7.15). At the second iteration, the shapes of the distillate flowrate and the distillate temperature profiles are well established. At the third iteration the solution is nearly converged and the remaining iteration only performs fine adjustments to satisfy the convergence criterion.

With respect to Figures (7.16) it is observed that the convergence of the steady state performance calculations using VTBVT technique is very rapid by the end of the second iteration, and the rest of the iterations, however, are carried out to realize the tight convergence criteria.

From the previous figures it may be concluded that; using Newton Raphson approach, the obtained solution is accurate up to $\varepsilon = 5 \times 10^{-4}$($\varepsilon$ = accuracy allowance) by the end of the fourth iteration (where equation (7.1) is used as a convergence criterion). Similarly, using the proposed VTBVT technique, this problem is solved maintaining the same degree of accuracy and starting at nearly the same point, (0.9 of the final results profiles) to yield results precisely the same as those produced by Newton's method (as will be illustrated by the end of this section), after five iterations. This may confirm the validity of the assumption proposed in chapter 5, that the linearized equations can be simplified by neglecting the insignificant changing for some variables during the iterations without affecting the rate of convergence so much.

Furthermore, one of the advantages of the VTBVT technique is the reduction of the dimension of the problem from 171 equations, to two smaller problems (74 equations for component matrix and 97 equations for temperature matrix). Since the computational effort is proportional to the square of the dimension of the problem, see Gorczynski [1977], quite substantial saving in computer time is achieved by using the VTBVT technique. Comparison of the total CPU times shows that the solution by VTBVT technique reduces the CPU time consumed to about one fifth of that required by Newton's method, (where CPU time = 0.44 sec. for the VTBVT technique and 2.5 sec. for Newton's method)

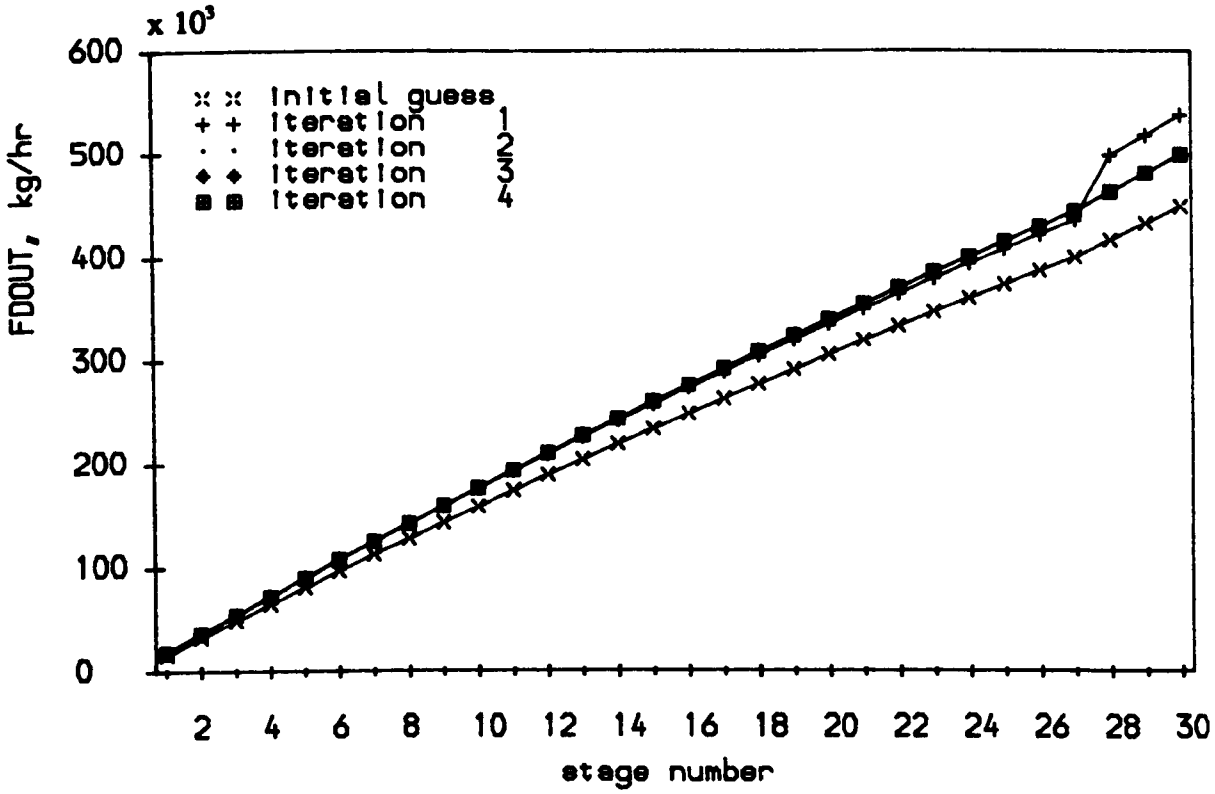

FIG. (7.15,a) CONVERGENCE OF THE DISTILLATE FLOWRATE ALONG THE PLANT. (performance calculation ,Newton)

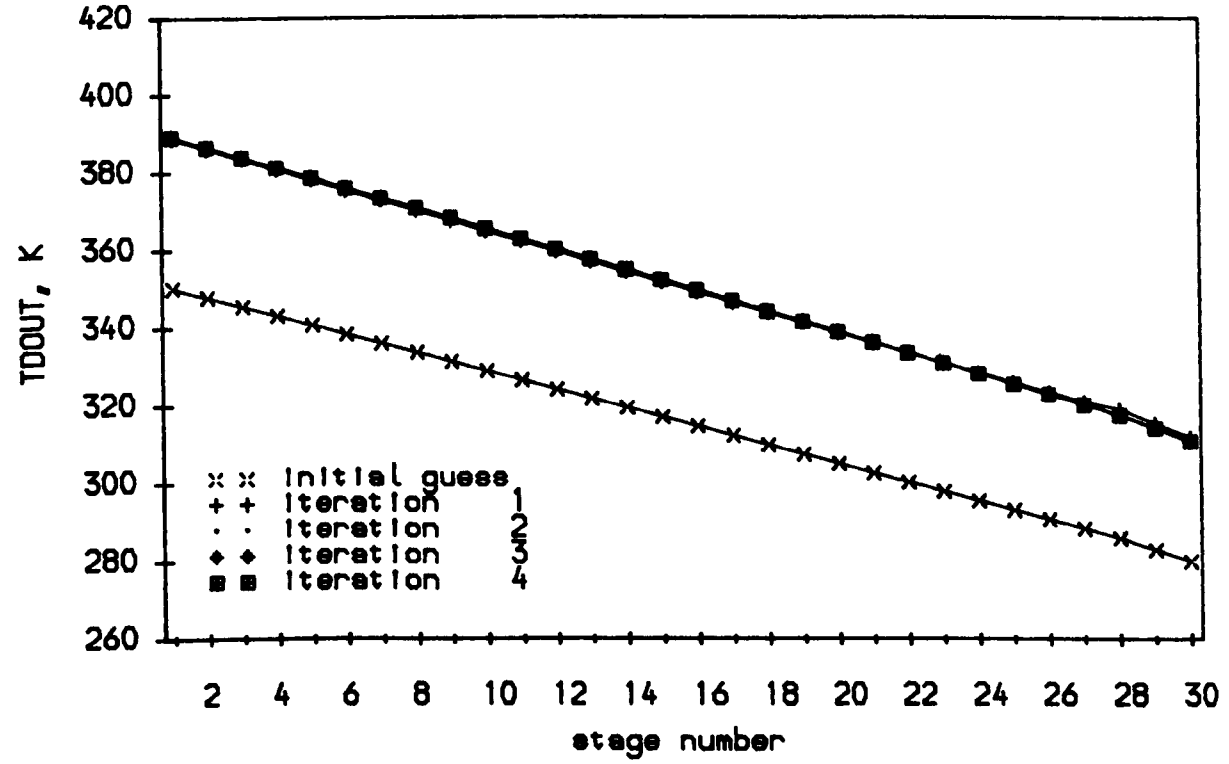

FIG. (7.15,b) CONVERGENCE OF THE DISTILLATE TEMPERATURE ALONG FICHTNER MSF-DESALINATION PLANT (Newton)

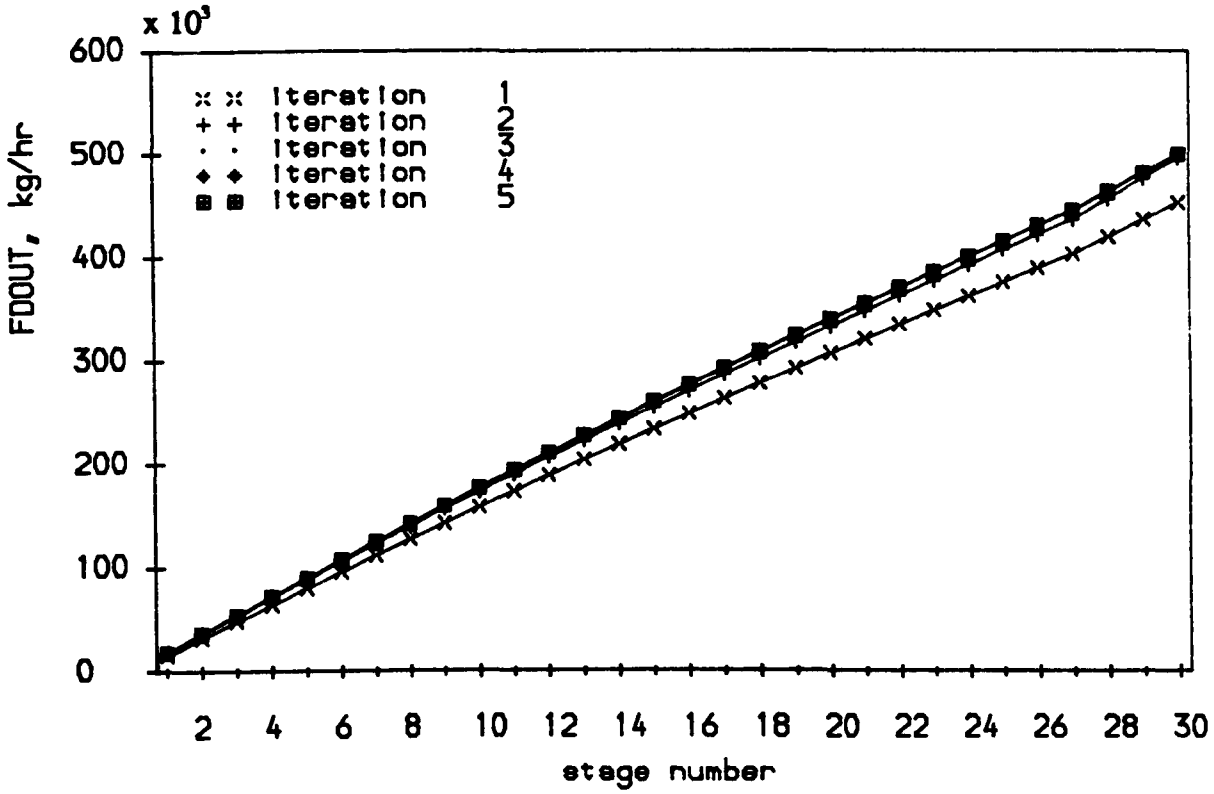

FIG. (7.16,a) CONVERGENCE OF THE DISTILLATE FLOWRATE ALONG THE PLANT. (performance calculation, VTBVT)

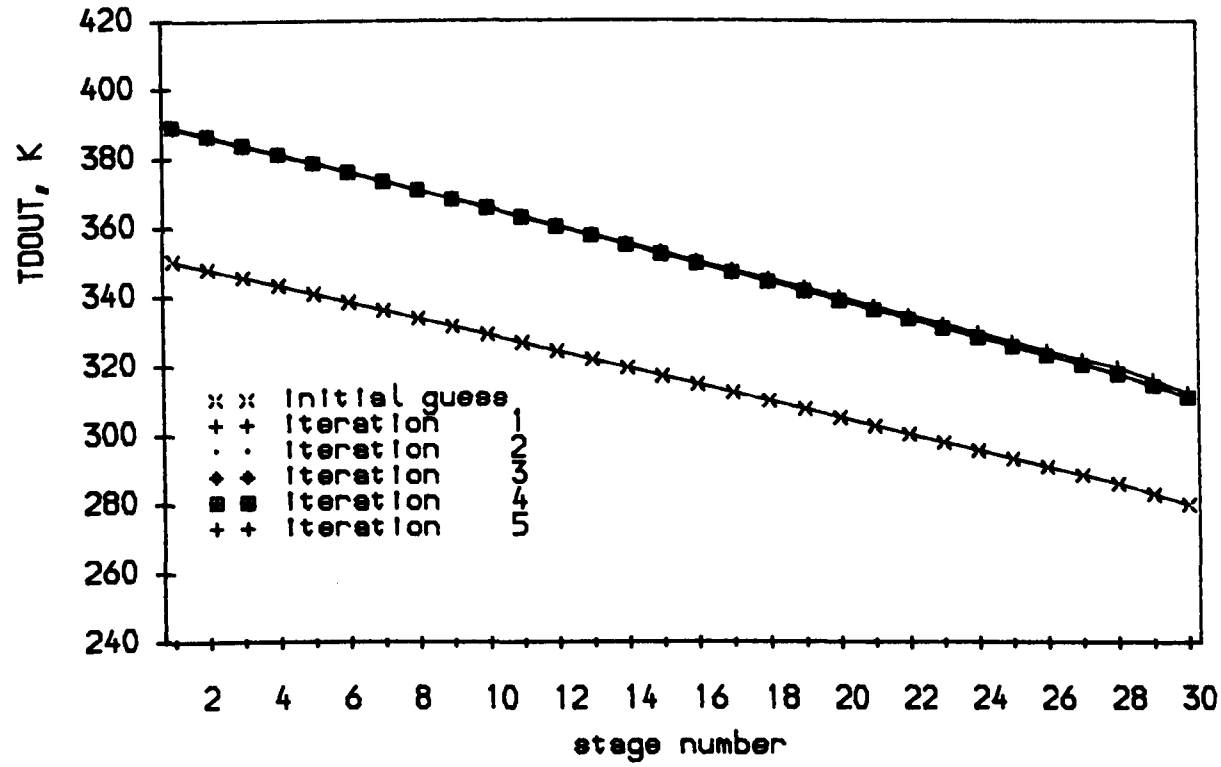

FIG. (7.16,b) CONVERGENCE OF THE DISTILLATE TEMPERATURE ALONG FICHTNER MSF-DESALINATION PLANT

7.6.2. Effect of The Approximation Assumptions on the Accuracy of the Final Results:

To examine the accuracy of the final results produced by the VTBVT technique, the results before the approximation assumptions (i.e. from the Newton algorithm) and that produced under the approximation assumptions (i.e. from VTBVT algorithm) are compared. These results are tabulated in Tables (7.15) and (7.16). These two tables show that the tabulated results are highly consistent. Agreement is observed up to fourth and sixth significant figures. The maximum fractional error is $(6.367 \pm 6.367) \times 10^{-6}$ for the distillate temperature (TDOUT), $(2.631 \pm 5.226) \times 10^{-6}$ for flashing brine temperature (TBOUT), $(4.09 \pm 81.84) \times 10^{-5}$ for the distillate product flowrate (FDOUT) and $(4.341 \pm 0.542) \times 10^{-6}$ for the flashing brine flowrate (FBOUT).

In fact, as mentioned before, it is impossible to end the calculations using two different algorithms each of them adopting a different numerical technique, at exactly the same results. This may be because the course of the computation is different in both techniques, thereby the amount of rounding off error is different as well. Also, the accuracy of the final solution as measured by the stopping criterion is varied from method to method although in each case the iteration is terminated as soon as this convergence criterion becomes less than the tolerance arbitrary chosen. In this particular example, the tolerance chosen is 5×10^{-4}, and the convergence criterion at the final iteration is 3.7015×10^{-4} for Newton's method, compared to, 3.6236×10^{-4} for the VTBVT method. As a result, a very small deviation between the two results is introduced.

Table (7.15) Comparison between the Temperature Profiles in FICHTNER MSF Desalination Plant as Calculated by VTBVT and NEWTON RAPHSON Techniques

Stage No.	TDOUT (K)			TBOUT (K)		
	VTBVT	NR.	DIFF.	VTBVT	NR.	DIFF.
1	389.366	389.366	0.000	390.532	390.532	0.000
2	386.739	386.739	0.000	387.909	387.909	0.000
3	384.104	384.104	0.000	385.281	385.281	0.000
4	381.461	381.461	0.000	382.649	382.648	0.001
5	378.812	378.812	0.000	380.013	380.013	0.000
6	376.158	376.157	0.001	377.376	377.375	0.001
7	373.499	373.499	0.000	374.737	374.737	0.000
8	370.836	370.836	0.000	372.097	372.097	0.000
9	368.171	368.170	0.001	369.458	369.457	0.001
10	365.503	365.502	0.001	366.819	366.818	0.001
11	362.834	362.833	0.001	364.180	364.180	0.000
12	360.164	360.163	0.001	361.544	361.543	0.001
13	357.494	357.493	0.001	358.910	358.909	0.001
14	354.825	354.823	0.002	356.278	356.277	0.001
15	352.156	352.155	0.001	353.649	353.648	0.001
16	349.489	349.488	0.001	351.024	351.023	0.001
17	346.823	346.822	0.001	348.402	348.401	0.001
18	344.160	344.159	0.001	345.784	345.783	0.001
19	341.499	341.498	0.001	343.169	343.169	0.000
20	338.841	338.840	0.001	340.560	340.559	0.001
21	336.186	336.185	0.001	337.954	337.954	0.000
22	333.534	333.534	0.000	335.353	335.353	0.000
23	330.886	330.886	0.000	332.757	332.756	0.001
24	328.242	328.242	0.000	330.164	330.164	0.000
25	325.601	325.601	0.000	327.577	327.577	0.000
26	322.964	322.964	0.000	324.994	324.994	0.000
27	320.331	320.332	-0.001	322.415	322.415	0.000
28	317.629	317.629	0.000	319.164	319.165	-0.001
29	314.339	314.339	0.000	315.922	315.923	-0.001
30	311.041	311.042	-0.001	312.683	312.683	0.000

DIFF. : Difference = VTBVT value - NR value

Table (7.16), Comparison between The Calculated Flowrate Profiles Along FICHTNER MSF Desalination Plant Using VTBVT and Newton Raphson (NR) Techniques.

Stage No.	FDOUT x 10^{-3}[kg/hr]			FBOUT x 10^{-3}[kg/hr]		
	VTBVT	NR.	DIFF.	VTBVT	NR.	DIFF.
1	18.355	18.356	-0.001	3878.039	3878.034	0.005
2	36.584	36.585	-0.001	3859.810	3859.805	0.005
3	54.683	54.682	0.001	3841.711	3841.707	0.004
4	72.646	72.647	-0.001	3823.748	3823.743	0.005
5	90.471	90.472	-0.001	3805.923	3805.918	0.005
6	108.156	108.159	-0.003	3788.238	3788.231	0.007
7	125.697	125.700	-0.003	3770.697	3770.689	0.008
8	143.093	143.099	-0.006	3753.301	3753.291	0.010
9	160.342	160.350	-0.008	3736.052	3736.040	0.012
10	177.444	177.452	-0.008	3718.950	3718.937	0.013
11	194.397	194.405	-0.008	3701.997	3701.984	0.013
12	211.197	211.209	-0.012	3685.197	3685.181	0.016
13	227.847	227.857	-0.010	3668.547	3668.532	0.015
14	244.345	244.355	-0.010	3652.049	3652.035	0.014
15	260.693	260.702	-0.009	3635.700	3635.687	0.013
16	276.889	276.898	-0.009	3619.504	3619.491	0.013
17	292.938	292.943	-0.005	3603.456	3603.446	0.010
18	308.834	308.840	-0.006	3587.560	3587.550	0.010
19	324.585	324.587	-0.002	3571.809	3571.802	0.007
20	340.186	340.190	-0.004	3556.208	3556.199	0.009
21	355.641	355.645	-0.004	3540.753	3540.744	0.009
22	370.952	370.958	-0.006	3525.441	3525.432	0.009
23	386.121	386.126	-0.005	3510.273	3510.263	0.010
24	401.151	401.155	-0.004	3495.243	3495.234	0.009
25	416.041	416.046	-0.005	3480.353	3480.343	0.010
26	430.795	430.801	-0.006	3465.599	3465.588	0.011
27	445.417	445.421	-0.004	3450.977	3450.969	0.008
28	463.697	463.701	-0.004	3432.697	3432.688	0.009
29	481.761	481.763	-0.002	3414.633	3414.627	0.006
30	499.642	499.643	-0.001	3396.751	3396.746	0.005

DIFF. : Difference = VTBVT value – NR value

7.7. Comparison With Published Techniques:

A comparison with some existing computer programs, for obtaining the steady state solution of MSF desalination process, is the main purpose of this section. In fact, it is difficult to obtain a definitive comparison of the performance of two different algorithms using two numerical techniques, and perhaps different simplifying assumptions

However, a number of conclusions can be derived from such a comparison.

Two examples are considered in this section. The first one illustrates the comparison between the results obtained by using stage to stage (STS) technique for the simulation of the FICHTNER, MSF desalination reference plant, Homig [1978], and those obtained in the previous section using VTBVT technique. The second example considered is the performance calculation of AL-KHOBAR II MSF desalination plant in Saudi Arabia. This plant was calculated by Helal [1985] using a tridiagonal matrix (TDM) algorithm for solving the linearized model representing the plant.

The numerical results for the first comparison (VTBVT. and STS), are listed in Tables (7.17) and (7.18) where it can be noticed that the agreement is really remarkable, as the maximum fractional error is $(-6.59 \pm 0.599) \times 10^{-4}$ for flashing brine temperature (TBOUT), $(1.438 \pm 2.877) \times 10^{-2}$ for boiling point rise (BPR), $(0.188 \pm 3.77 \times 10^{-2})$ for NEA, $(4.287 \pm 7.8 \times 10^{-3}) \times 10^{-3}$for (FDOUT), and $(6.158 \pm 5.889 \times 10^{-3}) \times 10^{-3}$ for flashing brine flowrate (FBOUT). This deviation is thought to be due to simplification adopted by Homig by performing the calculations using simple average value methods (e.g. mean specific heat, and mean latent heat of vaporization were used). Unfortunately no information has been given by Homig about the convergence characteristics of the used computational approach (STS).

The second example in this section is the performance calculations of AL-KHOBAR II plant. This plant is solved in section (7.4), and was solved by Helal [1985]. Because the physical properties correlations used in both programs are different, it is unpractical to compare the numerical results produced by the two algorithms. However, the applied numerical technique in both algorithms may be evaluated by comparing the convergence rate of both techniques. Helal obtained a solution, for AL-KHOBAR II plant, accurate to 16×10^{-5}, after eleven iterations by using a program specifically written for the simulation of MSF process only, and taking the advantages of arranging the equations representing the plant in a tridiagonal matrix. In comparison, this problem is solved maintaining the same degree of accuracy in only seven iterations.

Table (7.17) Comparison Between The Temperature Profiles Along the FICHTNER Plant as Calculated by The VTBVT and Stage to Stage (STS) Techniques.

STAGE	TDOUT [K]			TBOUT [K]			BPR [K]			NEA [K]		
NO.	VTBVT	STS	dif.	VTBVT	STS	dif.	VTBVT	STS	dif.	VTBVT	STS	dif.
1	389.37	389.34	0.03	390.53	390.53	0.00	0.96	0.95	0.01	0.21	0.24	-0.03
2	386.74	386.70	0.04	387.91	387.91	0.00	0.95	0.94	0.01	0.22	0.27	-0.05
3	384.10	384.06	0.04	385.28	385.29	-0.01	0.94	0.93	0.01	0.24	0.30	-0.06
4	381.46	381.42	0.04	382.65	382.68	-0.03	0.93	0.92	0.01	0.26	0.33	-0.07
5	378.81	378.78	0.03	380.01	380.06	-0.05	0.92	0.91	0.01	0.28	0.37	-0.09
6	376.16	376.49	-0.33	377.38	377.44	-0.06	0.91	0.91	0.00	0.31	0.40	-0.09
7	373.50	373.49	0.01	374.74	374.82	-0.08	0.90	0.90	0.00	0.34	0.44	-0.10
8	370.84	370.85	-0.01	372.10	372.20	-0.10	0.89	0.89	0.00	0.37	0.47	-0.10
9	368.17	368.20	-0.03	369.46	369.58	-0.12	0.88	0.88	0.00	0.41	0.51	-0.10
10	365.50	365.56	-0.06	366.82	366.97	-0.15	0.87	0.87	0.00	0.44	0.54	-0.10
11	362.83	362.91	-0.08	364.18	364.35	-0.17	0.86	0.86	0.00	0.48	0.58	-0.10
12	360.16	360.26	-0.10	361.54	361.73	-0.19	0.85	0.85	0.00	0.53	0.62	-0.09
13	357.49	357.61	-0.12	358.91	359.11	-0.20	0.84	0.84	0.00	0.57	0.66	-0.09
14	354.82	354.97	-0.15	356.28	356.49	-0.21	0.83	0.83	0.00	0.62	0.70	-0.08
15	352.16	352.32	-0.16	353.65	353.87	-0.22	0.82	0.82	0.00	0.67	0.74	-0.07
16	349.49	349.67	-0.18	351.02	351.26	-0.24	0.81	0.81	0.00	0.72	0.78	-0.06
17	346.82	347.01	-0.19	348.40	348.64	-0.24	0.80	0.80	0.00	0.77	0.82	-0.05
18	344.16	344.36	-0.20	345.78	346.02	-0.24	0.79	0.79	0.00	0.83	0.86	-0.03
19	341.50	341.71	-0.21	343.17	343.40	-0.23	0.79	0.78	0.01	0.89	0.91	-0.02
20	338.84	339.06	-0.22	340.56	340.78	-0.22	0.77	0.77	0.00	0.94	0.95	-0.01
21	336.19	336.40	-0.21	337.95	338.16	-0.21	0.76	0.76	0.00	1.00	1.00	0.00
22	333.53	333.75	-0.22	335.35	335.55	-0.20	0.76	0.75	0.01	1.06	1.04	0.02
23	330.89	331.09	-0.20	332.76	332.93	-0.17	0.75	0.74	0.01	1.12	1.09	0.03
24	328.24	328.44	-0.20	330.16	330.31	-0.15	0.74	0.73	0.01	1.19	1.14	0.05
25	325.60	325.74	-0.14	327.58	327.69	-0.11	0.73	0.72	0.01	1.25	1.19	0.06
26	322.96	323.12	-0.16	324.99	325.05	-0.06	0.72	0.71	0.01	1.31	1.24	0.07
27	320.33	320.46	-0.13	322.42	322.45	-0.03	0.71	0.70	0.01	1.38	1.29	0.09
28	317.63	317.67	-0.04	319.16	319.20	-0.04	0.70	0.69	0.01	0.84	0.84	0.00
29	314.34	314.37	-0.03	315.92	315.95	-0.03	0.68	0.68	0.00	0.90	0.90	0.00
30	311.04	311.06	-0.02	312.68	312.70	-0.02	0.67	0.67	0.00	0.97	0.97	0.00

dif. (difference) = VTBVT value - STS value

assumptions. Table (7.18) Comparison between the Calculated Flowrate Profiles Along FICHTNER MSF Plant Using VTBVT And Stage to Stage (STS) Techniques.

Stage NO.	FDOUT x 10^{-3} kg/hr			FBOUT x 10^{-3} kg/hr		
	VTBVT	STS	DIF.	VTBVT	STS	DIF.
1	18.355	18.39	-0.035	3878.039	3876.27	1.769
2	36.584	36.61	-0.026	3859.810	3858.05	1.760
3	54.683	54.67	0.013	3841.711	3839.99	1.721
4	72.646	72.57	0.076	3823.748	3822.09	1.658
5	90.471	90.31	0.161	3805.923	3804.35	1.573
6	108.156	107.89	0.266	3788.238	3786.77	1.468
7	125.697	125.32	0.377	3770.697	3769.34	1.357
8	143.093	142.61	0.483	3753.301	3752.05	1.251
9	160.342	159.74	0.602	3736.052	3734.92	1.132
10	177.444	176.73	0.714	3718.950	3717.93	1.020
11	194.397	193.58	0.817	3701.997	3701.08	0.917
12	211.197	210.29	0.907	3685.197	3684.36	0.837
13	227.847	226.87	0.977	3668.547	3667.79	0.757
14	244.345	243.31	1.035	3652.049	3651.35	0.699
15	260.693	259.61	1.083	3635.700	3635.04	0.660
16	276.889	275.79	1.099	3619.504	3618.87	0.634
17	292.938	291.84	1.098	3603.456	3602.82	0.636
18	308.834	307.76	1.074	3587.560	3586.90	0.660
19	324.585	323.56	1.025	3571.809	3571.10	0.709
20	340.186	339.23	0.956	3556.208	3555.42	0.788
21	355.641	354.79	0.851	3540.753	3539.87	0.883
22	370.952	370.22	0.732	3525.441	3524.44	1.001
23	386.121	385.54	0.581	3510.273	3509.12	1.153
24	401.151	400.74	0.411	3495.243	3493.92	1.323
25	416.041	415.82	0.221	3480.353	3478.84	1.513
26	430.795	430.79	0.005	3465.599	3463.87	1.729
27	445.417	445.64	-0.223	3450.977	3449.01	1.967
28	463.697	463.93	-0.233	3432.697	3430.73	1.967
29	481.761	482.05	-0.289	3414.633	3412.61	2.023
30	499.642	500.00	-0.358	3396.751	3394.66	2.091

7.8. NUMERICAL EVALUATION OF ONCE-THROUGH VERSUS BRINE RECIRCULATION MSF PLANT DESIGN:

So far, the stress in the previous sections was concentrated on brine recirculation MSF process. The most fundamental type of this process is the once-through (OT) MSF process. However, this type of process (i.e. OT) does not seem to have received enough numerical investigation in the available literature. Therefore, in this section the once-through, (OT), process is evaluated numerically with comparison with the brine recirculation process. The later type is represented by AL-KHOBAR II plant, designed in section (7.3). Seven design variables (assuming constant heat transfer area), as well as the top brine temperature need to be specified, (see section 7.2), to design a once-through MSF process. To design an equivalent once-through plant to AL-KHOBAR II brine recirculation plant on the basis of the production and the operating conditions, the numerical values of the needed design variables, (X_f, T_f, P_f, T_s, P_s, D, T_b , and T_{max}), are taken from Table (7.3). In this case, (case A), the maximum brine temperature is 90 C. However, since the seawater concentration factor {the ratio of total dissolved solids to the dissolved solids in standard seawater, (34483 ppm), Dukler [1971]}, in this case, is equal to about 1.65, the maximum brine temperature may be taken as much as 120 C (for acid treated feed), Simpson [1967]. This is considered here as (case B), (using the same specification as case A except that T_{max} = 120 C)

Table (7.19), Brine Recycle and Once-through Processes Main Results.

Parameter		Once-though		Brine recycle
	Case	A	B	
	T_{max}	90 (C)	120 (C)	
Specific heat x 10^3 transfer area (m^2 hr/kg)		63.24	38.67	72.8
Specific heat consumption (kJ/kg)		377.73	222.19	355.48
Makeup flowrate x 10^{-5}		120.014	73.2553	56.4023

By running the program for these two cases, the solution is obtained in 6 iterations, and 0.46 second CPU time. The accuracy of the

final answer is controlled by using the same convergence criterion as used in section 7.3, (equation 7.1), for AL-KHOBAR II plant. Table (7.19) gives the main points in the computed results. In the light of the results obtained, the following points may be inferred;

[A] To produce the same capacity, the makeup flowrate required by the once-through plant is about two times (case A) or 25 % (case B) greater than that required by the brine recirculation MSF plant. This is one of the reasons why once-through process is not used in large scale desalting of seawater.

[B] The specific heat transfer area required by (OT) process is about 13 % (case A) or 35 % (case B) which is less than that needed for brine recirculation MSF plant. This may be because of the possible large flashing temperature range and the lower boiling point elevation in the (OT) process.

[C] The specific heat demand in the brine heater of (OT) process is about 5.9 % (case A) higher and about 37.5 % (case B) which is less than that demanded for the brine recirculation plant. This may be attributed to the difference of adopted T_{max}.

[D] The (OT) process has a simple plant operation with few process controls.

[E] The (OT) low brine concentration, in some cases, provides scale free operation, and even it is possible to operate without chemical treatment for extended periods of time, Steinbruchel [1980].

So, in brief, the operating cost for (OT) system is much higher than that required for brine recirculation process. However, the capital cost for the second process is much higher than the first. Therefore, the optimum choice between the two process configurations should be based on the minimum total cost according to the plant location site.

7.9. CONCLUSIONS:

The main deduced points in this chapter may be summarized under four different titles, viz; design and simulation calculations, evaluation of the proposed technique and the approximation assumptions, brine recirculation and once-through MSF process, and finally, the developed programs and the proposed technique characteristics.

I. Design and Simulation (or performance) calculations:

[a] For a given number of stages, the program system using VTBVT technique computes design variables such as: area, externally supplied steam rate, stage temperatures and flowrates, etc..., such results are directly useful in design analysis.

[b] The convergence rate of the simulation calculations is not significantly affected by the use of unsatisfactory initial values. With very poor initial approximation only six to seven iterations are needed to obtain the correct solution. On the contrary, a better estimate on the first approximation for the design problem will give more rapid convergence.

[c] The required number of iterations for both simulation and design calculations are not affected significantly by increasing the process units (stages). Also, the computation does not get more complicated as the plant size increases. Conversely, of course, the computational time requirements are increased as the number of stages increases.

[d] The transition from simulation problem (with fixed unit operation conditions) to a design problem (with some design or operating specifications instead) has little effect on the required number of iterations. In other words, the convergence of the design problem (6 iterations) is slightly faster than that of the simulation problem (7 iterations), starting the solution in both calculation types at the same point.

[e] By taking the input parameters for the simulation calculations of Al-KHOBAR II plant from the output of the design calculations for the same plant, the accuracy comparison of the final results of both calculation type indicates a very good agreement between the results. This may illustrate the flexibility, and reproducibility of the program and the accuracy of the results.

[f] The ability of the developed program to carry out performance calculations under different operating conditions is

exemplified. The effect of changing feed seawater temperature and the brine recirculation flowrate on the performance and the reproducibility of the considered AL-KHOBAR II plant are studied. The results of this study are used to plot a "performance map" for this plant. This map can be used by both the designer and the operator for many and accurate investigations, of the plant performance and the controlling variables. This may show one aspect of many possible practical applications of the simulation calculations.

II. Evaluation of The Proposed Technique And The Approximation Assumptions:

[a] One of the advantages of the proposed VTBVT technique is: a large problem can be divided to a number of small problems. Thereby, the initial values need only to be guessed for the first matrix. Instead, all the problem variables need to be initialized for Newton Raphson technique.

[b] On the basis of the number of iterations, the (NR) method is slightly faster (4 iterations) than the VTBVT technique (5 iterations), starting at the same initial guessing, (0.9 of the final results). However, the proposed VTBVT may still be a faster technique in terms of computing time. CPU time required for FICHTNER plant simulation by (NR) method is five times CPU time needed by the VTBVT technique to carry out the same calculation type for the same plant.

III. Brine Recirculation and Once-through MSF Process:

The design of once through process is evaluated numerically in comparison with the recirculation brine process. The once-through flashing process has many advantages over the second process such as; first, it is a simple plant operation with few process controls. Furthermore, it requires a lower heat transfer surface. And finally, its low brine concentration may provide scale free operation. Besides, like any other desalination process, it has a number of disadvantages. Therefore, the choice between the two processes should be based on the minimum total operating costs according to the plant location site prices.

IV. The Developed Algorithms And The Proposed Technique Characteristics:

[a] Example problems presented in this chapter show that the developed

program using VTBVT technique has several advantages. Besides competing very well with existing methods (e.g. Tridiagonal matrix model by Helal [1985], and stage to stage calculation program by Homig [1978]) the program is flexible enough to be used as a design and/or simulation tool for either a recirculating or once-through MSF configurations, under a wide range of design constrained and operating parameters. Also, the VTBVT algorithm is simple and easy to program.

[b] From the performance and the results reported in this chapter, the reader may realize that the developed program using VTBVT technique is fast, stable, reliable, efficient, and has more convergence characteristics than the developed program using NR method. In fact, all these characteristics make the proposed VTBVT technique feasible.

CHAPTER 8

DESIGN AND SIMULATION OF MULTIPLE EFFECT EVAPORATION [MEE] PROCESSES.

8.1. INTRODUCTION:

In the field of thermal desalination, the Multiple Effect Evaporation (MEE) process is one of the main techniques. In this chapter the developed program, using the proposed VTBVT technique, is used to solve some of the problems facing the evaporator designer and the plant operator.

Usually the designer seeks to determine the heat transfer area and the best flowsheet configuration from the economical point of view. Section (8.2) illustrates the capability of the program to perform the design calculations for different configurations of an MEE plant.

The accuracy, the efficiency, and the validity of the developed program using the VTBVT technique are examined in sections (8.3) and (8.4). This is performed by comparing the convergence behaviour and the final results of both the design and the simulation calculations of ten effects with heat recovery system. Moreover, the performance calculations for the same MEE desalination plant is performed using Newton Raphson (NR) technique to examine the validity of the assumptions proposed in chapter 5 to develop the VTBVT technique. This is achieved by comparing the behaviour during the iterative solution and the accuracy of the final results of both techniques (NR & VTBVT) (See Appendix {E} for presentation of these results). The stability of the VTBVT technique under a wide range of the initial guess is examined, see Appendix {F}. This is achieved by solving the above performance problem, starting with four different initial linear temperature profiles.

In section (8.5) the examination of the behaviour of an existing (or detailed design) plant under operating conditions other than those used for the design calculations is illustrated. Three different performance calculation cases are considered. The solution of these cases (or the combination of some of them) demonstrates how the

developed package can be used to predict the right operating conditions for the "off design" problems. For example, what changes in the operating conditions must be performed if it is desired to operate a plant under a "partial load" conditions ?. Discussion of this point is presented in the subsection (8.5.2). Also, presented in the subsection (8.5.3), is the answer of the question "how to keep a constant water production rate in the face of changing the plant configuration by bypassing one of its effects and its associated preheaters".

Section (8. 6) contains a summary of all the results obtained in this chapter and conclusions about it.

8.2. DESIGN OF MULTIPLE EFFECT EVAPORATION WITH IMPROVED HEAT ECONOMY.

The cost of the product water of any desalination plant can be reduced by reducing the energy and the capital costs of that plant. One of the most important questions which may face the designer is: how the energy consumption of a considered plant can be reduced ?. In other words how to improve the steam economy (kg product/kg steam) of a plant.

In fact, the steam economy of a multiple effect evaporator is primarily a function of the number of its effects. However, another important factor which is the subject of this section, is the heat exchange between the various plant streams and especially the recovery of the heat from the evaporator outlet streams.

Five different flowsheet problems are used to illustrate the capability of the developed program to perform a steady state calculation to determine the proper heating areas of evaporators and heat exchangers. The solution of these problems may also show the efficiency of the program to tell the designer *how* much surface would be necessary; *where* this surface should be located in the flowsheet; *which* type of the heat recovery units can perform properly; and *how* good a heat economy can be attained at the beginning stage of the design calculation so as to avoid doing lengthy calculations, some of which may prove later to be a waste of time.

The multiple effect evaporation system can be designed with effects of varying size. However, unless there are strong reasons for the contrary, it is usually desirable to make all the effects identical (i.e. with equal heat transfer area). This makes the maintenance much

easier and lowers the capital cost.

The design calculation discussed here is concerned with six effect seawater desalination plant with equal heat transfer area. The basic configuration is arranged as in Figure (8.1). In such a plant the direction of feed flow through the evaporators is forward. This flowsheet contains fifty nine variables, out of which are 19 for the component variables, 16 for the temperature variables, 1 area variable, and 23 for the pressure variables. However, the program generates 14 equations for the component matrix, 13 equations for the temperature matrix and generates 20 equations in the pressure matrix. Having defined the degree of freedom of the system, the design calculation is started based on the data given in Table (8.1), producing results, some of which are tabulated in Table (8.2).

Table (8.1). Design Data For Six Effect Evaporators.*

Steam temperature.	373.15	K
Seawater feed temperature.	302.50	K
Cooling water temperature.	302.50	K
Saturated temperature of vapour from the last effect.	319.2611	K
Rate of product x 10^{-3}	453.587	kg/hr
The dissolved salt in feed	3.5	%
The dissolved salt in cooling water	3.5	%
The dissolved salt in the exit brine	7.0	%
Steam pressure	101	kPa
Feed water pressure	101	kPa
Cooling water pressure	101	kPa

* Estimated values of overall heat transfer coefficient of the preheaters are fed into the input data as follows; Sherwood [1963].

- For water/water heat exchangers U = 4088 $kJ/m^2K.hr$
- For water/condensing vapour heat exchangers U = 7155 $kJ/m^2K.hr$

In the process described by the flowsheet Figure (8.1), the seawater feed temperature enters the first effect at the normal seawater temperature (as shown in Table (8.1)). It can be seen from Table (8.2), that the plant under this operating condition has low steam economy. In fact, this is because the feedwater is preheated up to its boiling temperature by the supplied steam in the first effect. At the same time, a considerable amount of that heat leaves the evaporators in the form of discharged vapour and hot condensate. So, by recovering the heat loss,

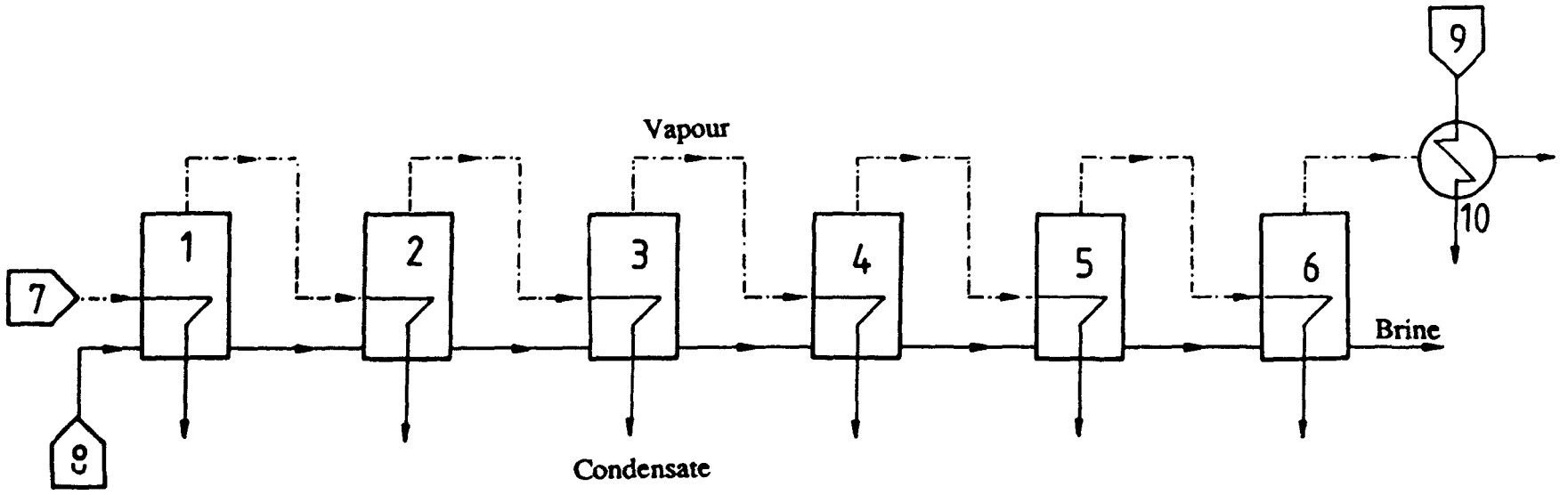

FIGURE 8.1. FORWARD FEED, SIX EFFECTS EVAPORATION SYSTEM.

1-6 : Effect 1 to Effect 6
7 : Steam
8 : Feed 1 (Seawater)
9 : Feed 2 (Cooling water)
10 : COND

the steam economy of the plant should be improved. Practically, it would be beneficial to preheat the feed as much as possible by recovering heat from some of these streams.

(Table 8.2). Some of The Final Results of Design of MEE With Different Heat Recovery Systems

Process / Variable	Figure (8.1)	Figure (8.2)	Figure (8.3)	Figure (8.4)	Figure (8.5)
Steam consumption $\times 10^{-3}$ kg/hr	148.792	109.615	84.7146	86.8115	123.859
Product water $\times 10^{-3}$ kg/hr	453.578	453.578	453.578	453.578	453.578
Steam economy kg water/kg steam	3.04	4.13	5.35	5.22	3.66
Cooling water flowrate $\times 10^{-3}$	4201.75	3367.75	2132.15	2386.76	3688.51
Heat transfer/ effect (m^2)	2139.44	1968.01	1752.89	1733.30	1278.86
Heat recovery units area (m^2)					
COND1	4758.39	1027.32	1027.32	1025.88	1027.32
COND2		3813.74	2414.54	2702.85	4176.96
VB1			791.95	829.23	402.81
VB2			784.52	835.76	402.83
VB3			779.91	857.25	504.82
VB4			778.14	883.38	504.82
VB5			779.47	915.22	1021.02
Total (m^2)	4758.39	4841.06	7355.85	8049.57	8040.58
Condensate heat exchanger area m^2					
HEX1		115.26	94.50		69.3
HEX2		176.95	175.05		69.3
HEX3		246.93	246.07		305.14
HEX4		304.51	310.12		414.48
HEX5		328.88	368.94		
Total (m^2)		1172.53	1194.68		858.22

From the practical point of view, the maximum brine feed temperature, on the one hand must be less than the condensation temperature of the heating steam, and it should be as high as possible on the other hand. However, it depends upon the scale control method used, and the concentration range selected for the plant, Simpson [1967].

Below, for illustration, four alternatives are presented to improve the plant heat economy. The solution of these alternatives may demonstrate the capability of the developed package to perform the design calculation for a number of different cases including various combinations of the heat recovery feature.

8.2.1. Heat Recovery From Intermediate Condensate.

Some of the heat losses may be recovered by pumping the feed seawater through a number of heat exchangers, which brings its temperature up by recovering the sensible heat contained in the intermediate condensate from each effect (except the first effect). The heated feed is then entered into the fist effect. This process is illustrated by Figure (8.2).

In general, the latent heat available from the final vapour stream V6, is more than the heat required by the feed stream at the temperature of the final effect. Therefore, the extra latent heat is taken up by an auxiliary condenser (COND2) with its own separate cooling water stream. The cooling water of the primary condenser is the feed stream to the evaporation system.

In this situation the specifications include the heat exchanger approach temperatures (the temperature difference at the limiting ends of the exchanger). A 2.778 K (5 F) minimum approach temperature is used, Sherwood [1963]. And the rest of the specifications are as shown before in Table (8.1).

Using these specifications the problem is solved for the steady state of the system and the required heat exchanger area in nine iterations. Some of the results are tabulated in Table (8.2). As the results indicate, by using the condensate heat exchangers, the steam economy is improved and the heat transfer area per effect is reduced, however, more heat transfer area is needed for the feed heaters.

1 - 6 : Effect 1 to Effect 6
9 : FEED2
12-16 : HEX1 to HEX5

7 : STEAM 8 : FEED1
11 : COND1
10: COND2

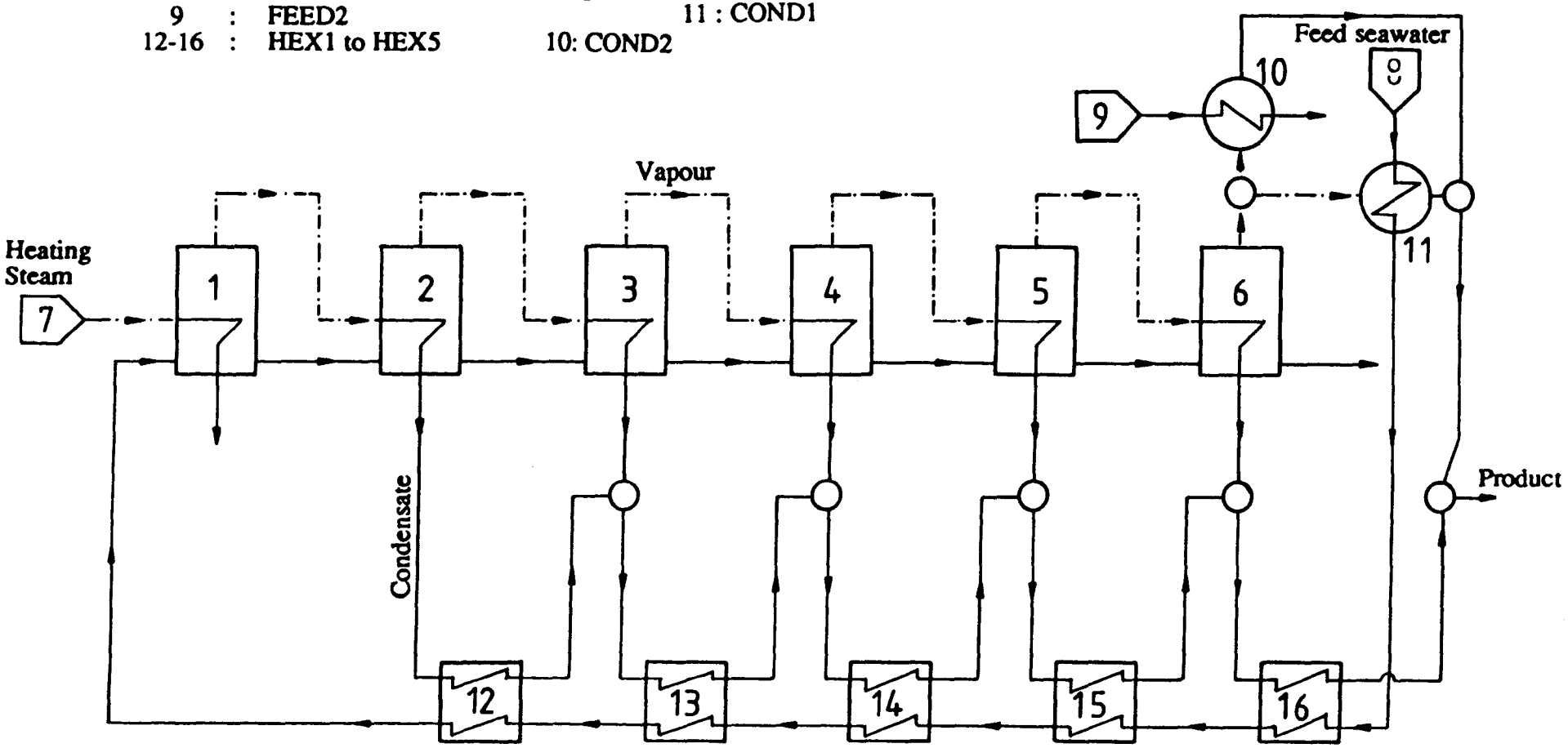

FIGURE 8.2. MEE SYSTEM WITH HEAT RECOVERY FROM THE INTERMEDIATE CONDENSATE.

8.2.2. Preheating By Vapour Bleed.

It is possible also to preheat the feed water using a certain amount of vapour bleed from each effect to raise up the feed water temperature to 2.778 K (5 F), (the temperature approach), less than the vapour temperature of that effect. Figure (8.3) illustrates the same multiple effect evaporator series. The feed seawater is preheated by passing through a series of external heat exchangers in which vapour bleed is used as a heating medium. The same specifications in Table (8.1) are used as in the previous problem. Some of the results obtained are presented in the fourth column of Table (8.2). As the results illustrate, the steam consumption is 84.7146 $\times$ 10^3kg/hr representing a reduction by a factor of 1.29 on the comparable figure for the previous flowsheet, Figure 8.2.

8.2.3. Heat Recovery By Product Vaporization:

The third alternative in this series, shows the possibility to improve the economy by vaporization of the condensate streams at reduced pressure. The flowsheet illustrated in Figure (8.4), consists of the same units as the previous flowsheet Figure (8.3). Here the condensate heat exchangers are replaced by five flash units where heat is recovered from the discharging condensate streams by flashing. Also, using the same specification as the previous example, the problem is solved after 8 iterations.

Interesting results can be seen from Table (8.2). On one hand, the steam consumption increases over the previous process (preheating by vapour bleed) by just a factor of 1.024, on the other hand 100 % saving of the condensate heat exchanger areas is achieved. Therefore, compared with vapour bleed preheating process, the heat recovery process by flash tanks could be equally profitable even if the improvement in steam economy is somewhat smaller, because it may cost less for heat exchangers.

8.2.4. Effect of The Flowsheet Configuration On The Process Economy

In order to select the necessary modifications which bring the steam economy up, several different configurations can be considered. The objective of the present example, which is the last example in this series, is to show that different configurations of vapour and liquid distribution and heat recovery system, in connection with the evaporation plant, can be easily accounted for with the aid of the

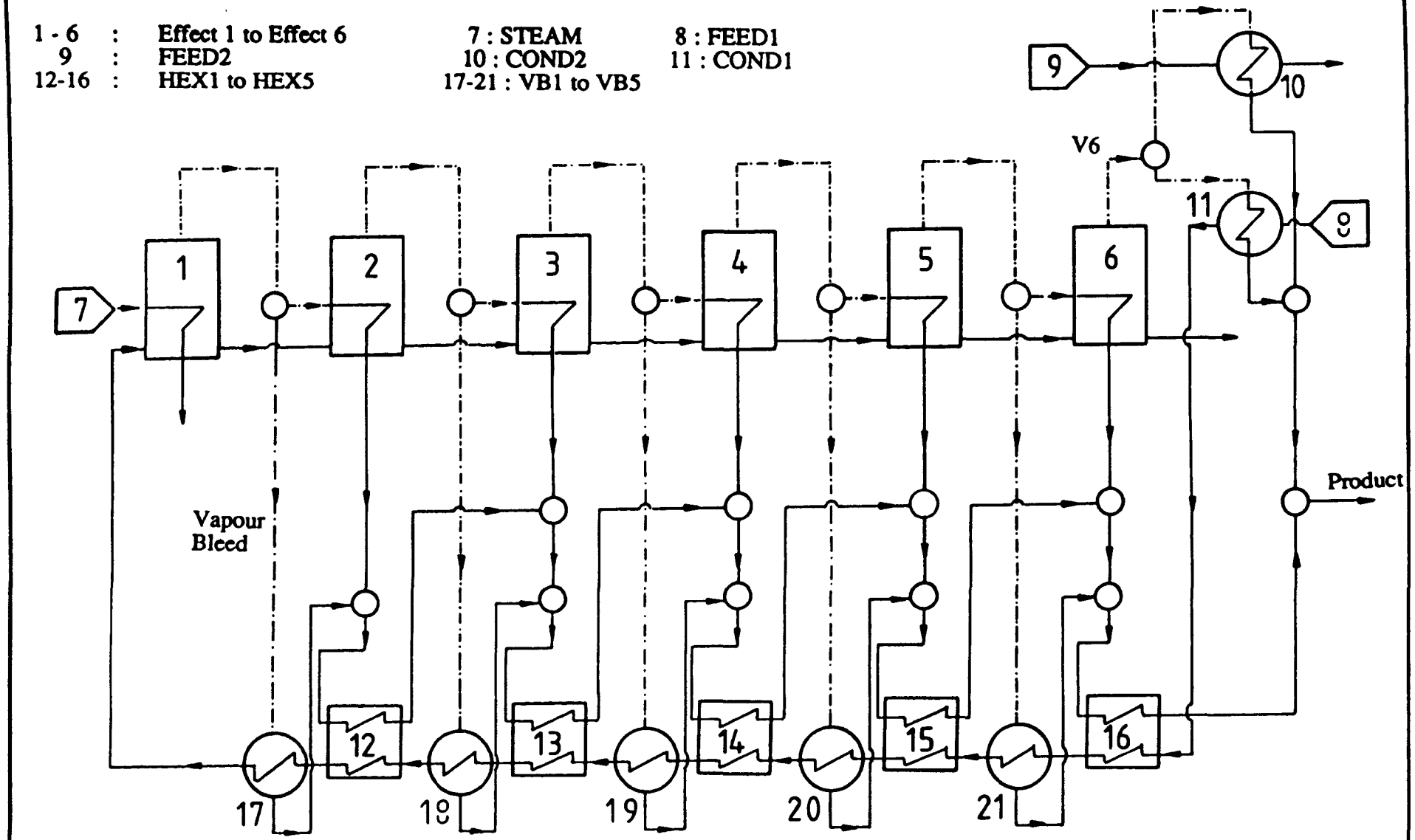

FIGURE 8.3. MEE SYSTEM WITH INTERMEDIATE CONDENSATE AND VAPOUR BLEED HEAT RECOVERY SYSTEM.

1 - 6	:	Effect 1 to Effect 6	10	:	COND2
7	:	STEAM	11	:	COND1
8	:	FEED1	12-16	:	FLASH1 to FLASH5
9	:	FEED2	17-21	:	VB1 to VB5

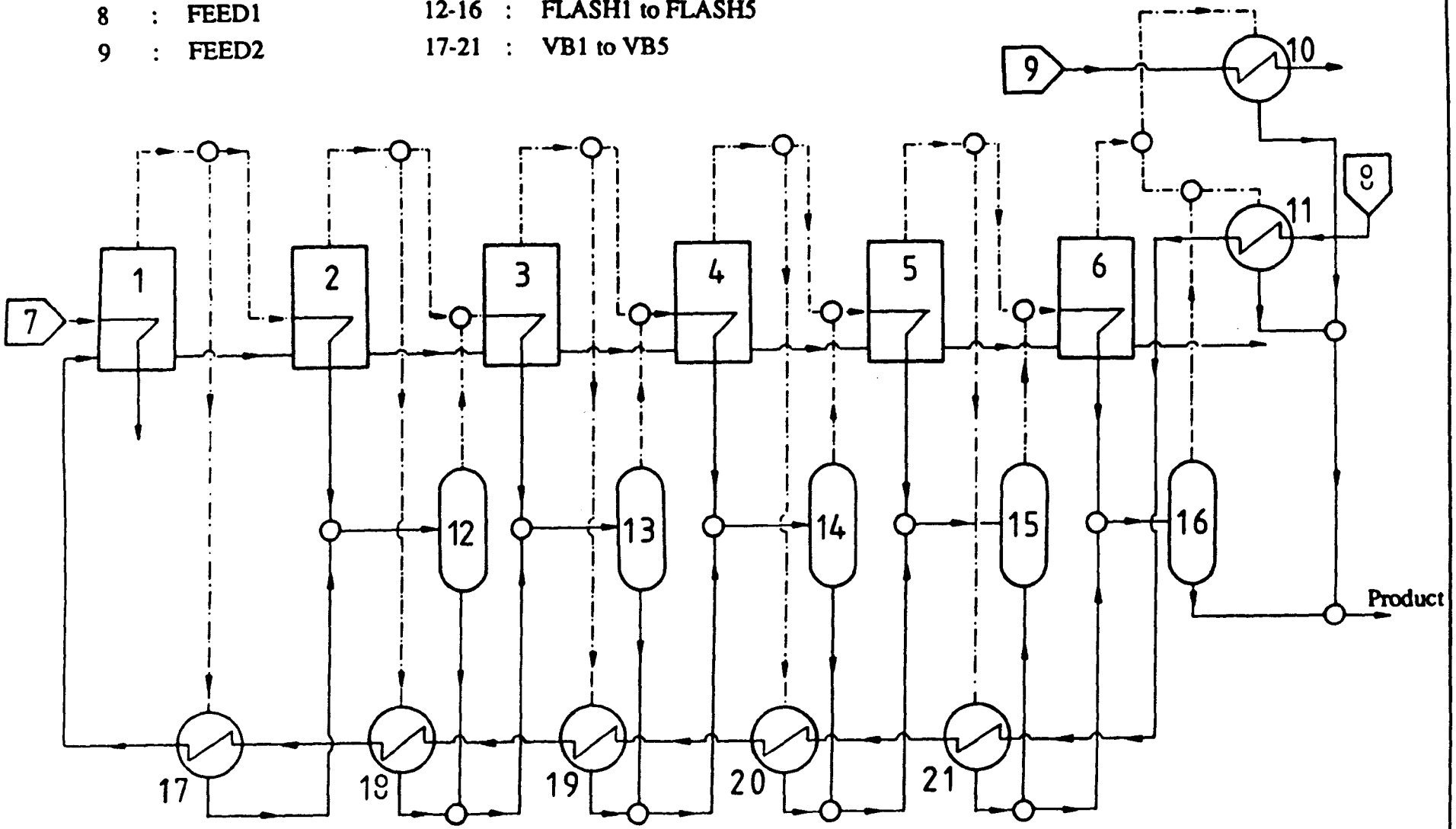

FIGURE 8.4. MEE WITH VAPOUR BLEED AND PRODUCT VAPORIZATION HEAT RECOVERY SYSTEM.

flexible developed program.

According to Figure (8.3) (heat recovery by vapour bleeding) an interesting variation of this type of configuration can be achieved as illustrated in Figure (8.5). This system may be examined (or computed) because the distribution of the heating steam (with its high temperature) to two evaporators instead of just one may improve the heat transfer coefficient and consequently lower steam consumption.

By adopting the same specifications given in Table (8.1) the results are obtained after 8 iterations. Some of the final results are presented in Table (8.2). These results show that the steam consumption is 123.859×10^3 kg/hr, a 1.46 increasing factor on the configuration of figure (8.3). This may be because the steam consumption by a multiple effect evaporator increases with decreasing the number of effects in sequence. However, as the results indicate, the evaporator heat transfer area is 1278.86 m^2, a 0.27 reduction factor on the configuration shown in Figure (8.3).

From the previous analysis the following points can be concluded;

* It may be clear from the considered examples that the design study would normally involve consideration of several alternative configurations. So quick calculations for these alternatives provides a good point of departure in the calculation of the full plant design. In fact, the flexibility of the developed program makes it a very powerful instrument for a better understanding of the way in which changing the various parameters affects the operation of an evaporation plant. For example, the effect of using different heat recovery units within a system and/or the effect of the changing of the configuration of the plant on the economy of the process can be quickly determined. It is thus possible to study a series of alternative possibilities in the design of a new plant or in the design of the rebuilding of an existing plant.

** The results show that the effect of heat recovery on steam economy can be quite big but it also depends on how the heat is recovered and reused.

1 - 6 :Effect 1 to Effect 6 7 : STEAM 8 : FEED1
9 :FEED2 10 : COND2 11 : COND1
12-15 :HEX1 to HEX4 16-20 : VB1 to VB5

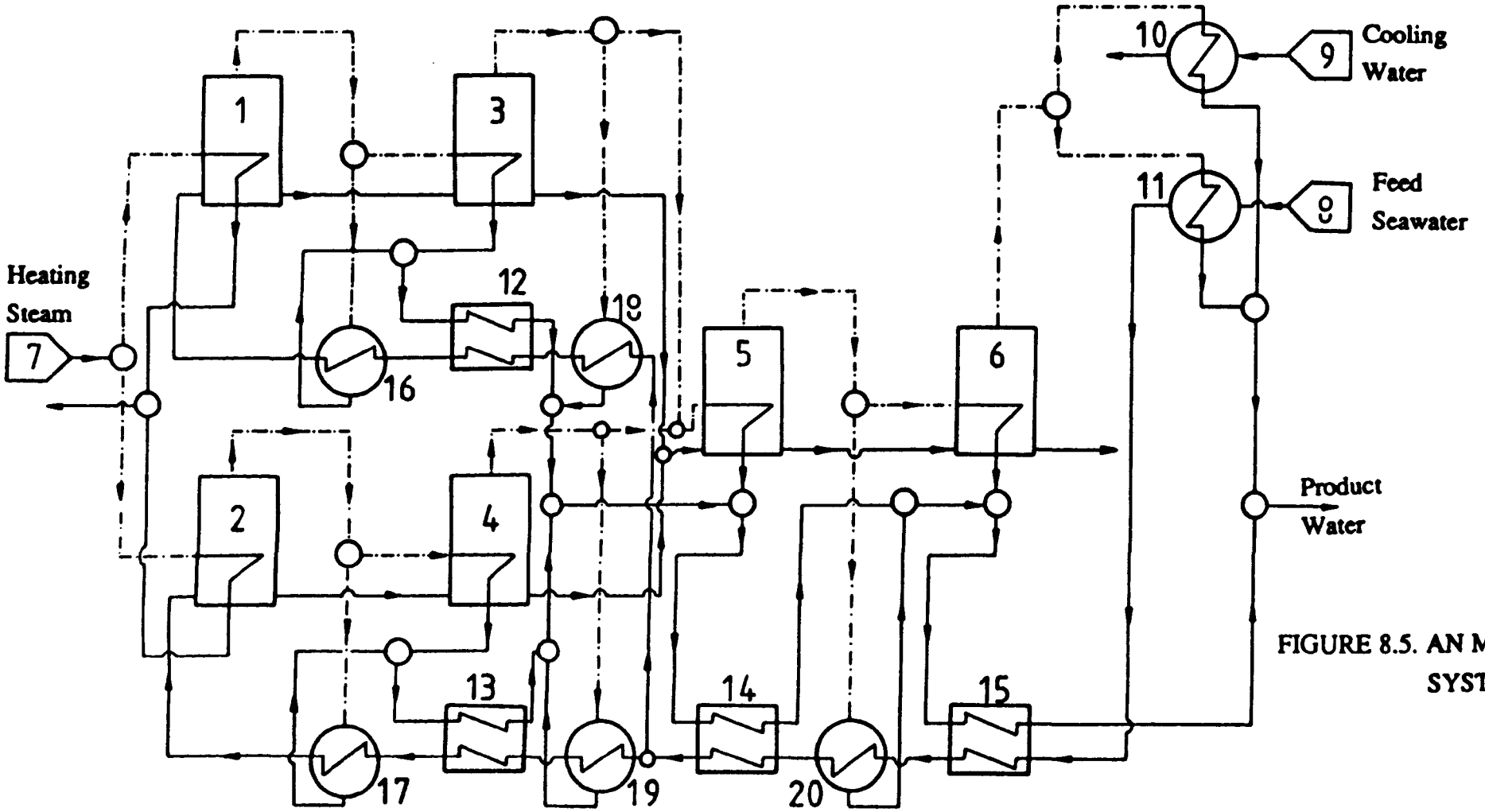

FIGURE 8.5. AN MEE SYSTEM.

8.3. DESIGN CALCULATION OF TEN EFFECT EVAPORATORS WITH HEAT RECOVERY SYSTEM.

The main objectives of this section is to examine the convergence behaviour of the developed program (using the VTBVT technique) in performing a design calculation of a multiple effect evaporator (MEE) system. It is also hoped to clarify the capability of the program to perform the design calculation of a large scale multiple effect evaporator desalination plant with heat recovery system.

The design of ten effects evaporation system with heat recovery by intermediate condensate and vapour bleeding, Figure (8.6), will be considered in this section as an example. This example is taken from Sherwood [1963]. In fact, this problem is chosen because: first, as indicated in the previous section, the combination between a MEE system and a number of heat recovery units, in particular, intermediate condensate and vapour bleed heat exchangers, produces one of the most interesting flowsheet from the economical point of view. Secondly, this plant is considered one of the largest size of this type (multiple effect evaporator system) in the seawater desalination field. So, more confidence can be gained in the developed program as well as the proposed technique by solving such a plant.

The mathematical model of this system requires a total of 203 linear and nonlinear algebraic equations, for 203 stream variables (65 component variables, 82 temperature variables, one area variable, and 55 pressure variables). However, the program generates 61 linearized equations for the component matrix, 79 equations for temperature matrix, and 52 equations for the pressure matrix. Having defined the number of generated equations and variables, the degree of freedom of the system can be defined. To start the solution, a number of variables matching the degree of freedom should be specified. To produce 453.587 $\times$ 10^3kg/hr, the design data given in the previous section, Table (8.1), is used.

8.3.1. The Convergence Behaviour Of The Design Calculation:

The convergence properties of the developed program, (using the proposed VTBVT technique), for the solution of the design problem considered here, can be illustrated by Table (8.3). The table shows a list of the successive values of some variables, such as, vapour temperature (TVOUT), vapour flowrate (FVOUT) out of each effect, and the

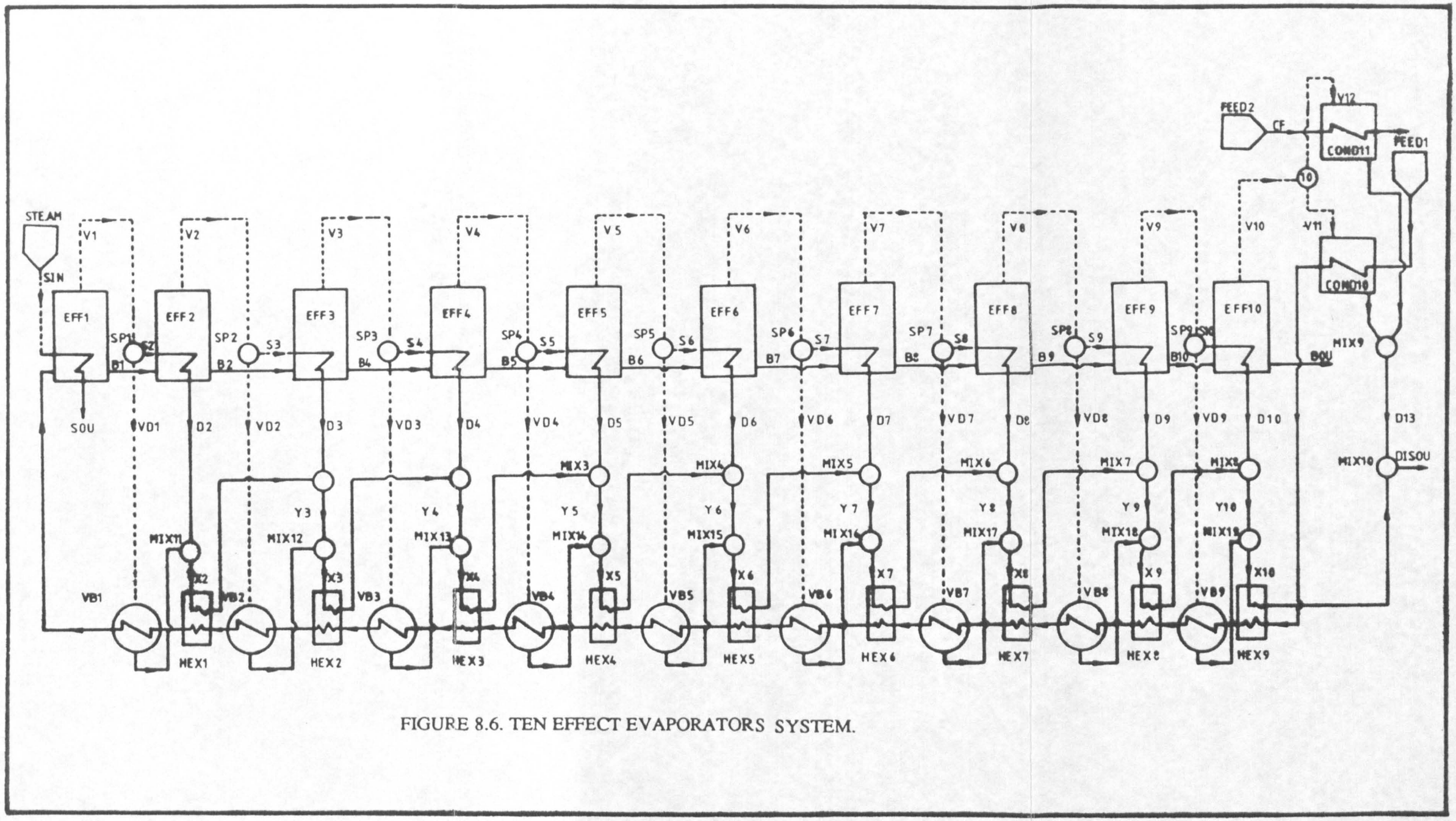

FIGURE 8.6. TEN EFFECT EVAPORATORS SYSTEM.

evaporator area of heat transfer.

Starting with the initial guessing values given in Table (8.3,a) the final solution is reached within the tolerance of $0.5*10^{-4}$, after 8 iterations, and the total CPU time required to solve the problem on the Amdahl 580 computer is approximately 0.52 second.

The progress of the convergence of FVOUT and TVOUT during the iteration process along the plant may become clearer by giving attention to Figure (8.7), the vapour flow rate profile is brought into existence at the second iteration. And at the third iteration, the solution is nearly converged. The remaining five iterations merely perform fine adjustment to satisfy the convergence criterion. With reference to Figure (8.8) it is noticed that the solution is approached very rapidly by the end of the first iteration. This is achieved although the initial guess is far from the final solution.

An interesting observation that can be noticed from the above figures and the results obtained in the previous section for the flowsheet Figure (8.3) (6 effects) is that the number of iterations required to obtain the final solution for ten effect evaporators is the same as that required for just 6 effect evaporators (see the previous section). Therefore, it can be concluded that the increase in the number of units (of the same type) does not increase the number of iterations. However, the CPU time required increases with increasing the number of variables (i.e. the size of the problem) because the arithmetic operations increase as well. Another simple conclusion that can be derived from Table (8.3) and Figures (8.7) & (8.8) is that the vapour flow rate variables (FVOUT) converge to the accuracy of $4.04 * 10^{-5}$, in 8 iterations; in comparison the area of heat transfer variable is converged to the accuracy of $6.6 * 10^{-4}$, by the end of the 7th iteration and to accuracy of $5*10^{-5}$, after 8 iterations, which in fact seems too tight. So the accuracy of the vapour flow rate can be used as a stopping criterion for the design calculation (as well as the performance calculation) to produce an accurate enough evaporator heat transfer area.

Table (8.3)

(8.3.A), Vapour Temperature Profiles (TVOUT) Along the Plant During the Iteration, [K]

Effect number	Initial guess	Iteration No. 1	Iteration No. 3	Iteration No. 8
1	399.700	368.070	367.862	367.502
2	399.500	362.937	362.562	362.899
3	399.300	357.742	357.245	358.128
4	399.100	352.490	351.917	353.178
5	398.900	347.165	346.566	348.041
6	398.700	341.751	341.176	342.707
7	398.500	336.254	335.753	337.168
8	398.300	330.670	330.294	331.417
9	398.100	325.009	324.802	325.450
10	397.900	319.261	319.261	319.261

(8.3.B), Vapour Flowrate Profiles (FVOUT) along the Plant During the Iteration [kg/hr $\times 10^{-3}$]

Effect number	Iteration No. 1	Iteration No. 2	Iteration No. 4	Iteration No. 8
1	63.835	47.793	47.688	47.692
2	59.780	47.497	47.466	47.449
3	55.702	47.145	47.186	47.150
4	51.605	46.714	46.815	46.769
5	47.489	46.184	46.326	46.276
6	43.357	45.533	45.686	45.643
7	39.209	44.747	44.869	44.846
8	35.047	43.811	43.848	43.859
9	30.873	42.716	42.599	42.664
10	26.690	41.448	41.104	41.240

(8.3.C), Evaporator Heat Transfer Area During the Iterative Solution

Iteration	Area (m^2)
Initial guess	397.
1	-1.668×10^{7}
2	0.127×10^{7}
3	1.438×10^{3}
4	1.814×10^{3}
5	1.800×10^{3}
6	1.8061×10^{3}
7	1.8049×10^{3}
8	1.805×10^{3}

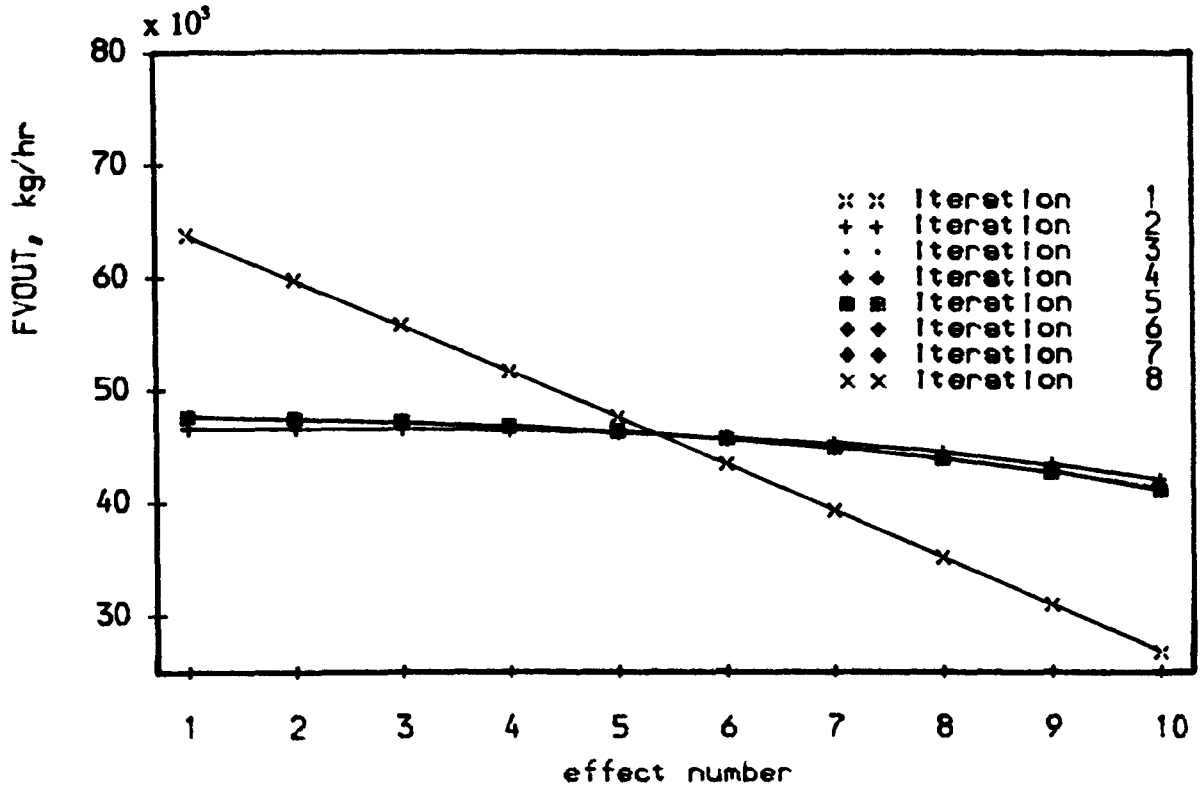

FIG. (8.7) CONVERGENCE OF THE VAPOUR FLOWRATE ALONG THE FLOWSHEET.

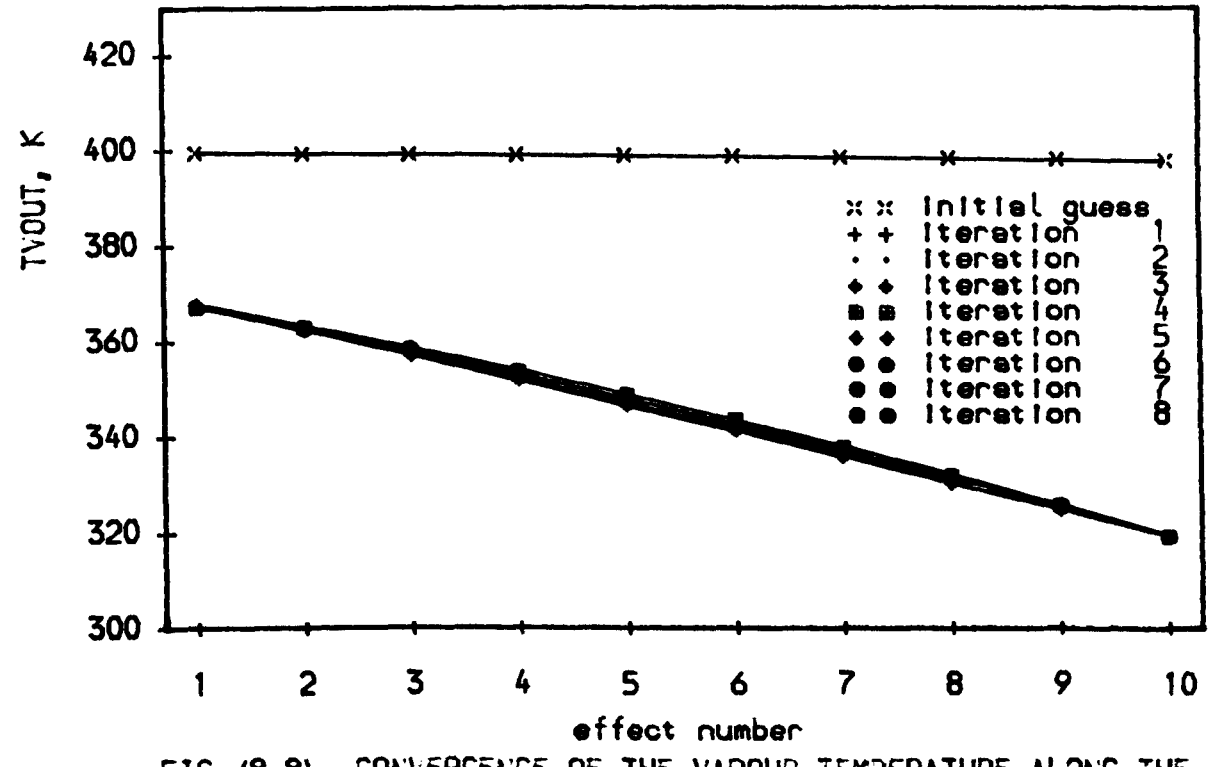

FIG. (8.8) CONVERGENCE OF THE VAPOUR TEMPERATURE ALONG THE FLOWSHEET.

Table (8.4) contains the calculated heat transfer areas and the duties of all the units constructing the plant. Among the results produced, is the steam consumption (53.3716×10^3 kg/hr.) which represents a reduction by a factor of 1.58 on the comparable figure for the 6 effects evaporation system, with the same heat recovery unit types (Flowsheet Figure (8.3) in the previous section). In fact the reduction of the steam consumption is achieved at a sacrifice of increasing the evaporator heat transfer area by a factor of 1.4 on the same plant.

A complete output report of the final results of all the variables (components, temperature, pressure) for all the streams out of all the plant units is shown in Appendix {G}.

8.4. THE PERFORMANCE CALCULATION OF TEN EFFECT EVAPORATORS WITH HEAT RECOVERY SYSTEM.

As illustrated in the previous sections, the designer of an evaporator system is usually interested in performing a steady state calculation to determine the proper heating areas of evaporators, heat exchangers, as well as the proper design configuration (vapour and liquid streams) for a particular process. However, one of great interest for the customer, the operating engineer, as well as the design engineer, is the question of how a given, i.e. a complete designed or already existing, plant will perform if one or more of the parameters, like capacity, and/or sea water feed temperature etc..., are changed.

The capability of the developed program (using the proposed VTBVT technique) to find an accurate answer to questions such as the above one within reasonable computing time will be illustrated in this and the subsequent sections.

To exemplify the efficiency of the developed package to carry out the calculations of different cases of an MEE plant simulation, the designed plant in the previous section (ten effect evaporators with heat recovery system, Figure (8.6)) is considered.

Table (8.4)

(8.4. A) Vapour Bleed Heat Exchangers Design Results

unit name	area (m^2)	load (kJ/hr) $\times 10^{-7}$	LMTD (K)
VB1	484.37	1.602	4.622
VB2	478.90	1.575	4.596
VB3	474.26	1.552	4.574
VB4	470.31	1.533	4.556
VB5	467.02	1.517	4.540
VB6	464.61	1.504	4.528
VB7	461.80	1.439	4.517
VB8	459.81	1.483	4.508
VB9	458.15	1.476	4.501

$U = 7155$ kJ/hr.m^2. K

(8.4. B) Design Results of the Primary and Auxiliary Condensers

unit name	area (m^2)	load (kJ/hr) $\times 10^{-7}$	LMTD (K)
COND10 (Primary)	915.53	5.096	7.780
COND11 (Auxiliary)	861.72	4.797	7.780

(8.4. C). Design Results of the Evaporator Units

unit name	U [kJ/hr.m^2. K] $\times 10^{-2}$	load (kJ/hr) $\times 10^{-7}$	$\Delta T_{eff.}$ [K]
EFF1	131.226	12.05	5.086
EFF2	127.280	9.239	4.023
EFF3	123.191	9.267	4.168
EFF4	118.950	9.280	4.322
EFF5	114.548	9.270	4.483
Eff6	109.977	9.232	4.650
Eff7	105.231	9.159	4.821
Eff8	100.304	9.045	5.995
EFF9	95.191	8.884	5.170
EFF10	89.888	8.871	5.344

$A_{eff} = 1805$ m^2

(8.4, D) Condensate Heat Exchanger Areas

Unit name	Area (m^2)
HEX1	44.76
HEX2	86.19
HEX3	124.88
HEX4	161.28
HEX5	195.63
HEX6	228.18
HEX7	259.03
HEX8	288.28
HEX9	316.01

U = 4088 $kJ/m^2.hr.K$

As demonstrated in the previous section, 202 variables are comprised by 72 streams that belong to this particular plant. However, only a total of 192 equations are generated by the program. So, to start the solution a number of variables matching the degree of freedom of the system have to be specified. They are four component variables, three temperature variables as well as three pressure variables.

Different combinations of the specified variables (each includes ten specified variables) can be used to start the solution of different simulation cases, as will be shown in the following section.

The principle objectives of this section are: firstly, the investigation of the capability of the developed program and the proposed technique to perform the performance calculations for such a large MEE desalination plant; secondly, studying the behaviour of the proposed VTBVT technique during its progress to the final solution of the performance evaluation problem. And comparing this behaviour with that of the solution during the design calculations (presented in the previous section). Thirdly, the analysis of the accuracy of the results by comparing the final results obtained by the performance calculations and that obtained in the previous section using the design calculations.

Some of the specifications used in this section to carry out the performance calculation (case I) were used in the design problem, Table (8.1), and the remainder of the specifications are obtained from the results of the design calculations, Table (8.4).

In fact, it should be mentioned here that this type of calculations, "formal performance calculations", is most appropriate for sensitivity analysis of the performance of the plant under any change of the operating conditions.

8.4.1. The Behaviour Of The VTBVT Technique During The Performance Calculations Of Ten Evaporators With Heat Recovery System:

To start the solution of this problem, using the proposed VTBVT technique, 82 temperature variables are guessed. Table (8.5) shows the initial values of the vapour temperature profile (TVOUT) along the plant, and some of the succeeding values, as well as the final temperature profile results. While, Table (8.6) comprises some of the successive values of the vapour flowrate out of each effect along the plant, the numerical values listed in the above tables are plotted in Figures (8.9, a,b). As shown in Figure (8.9,a) the vapour temperature profile (TVOUT) is guessed as a linear profile, which is far from the final solution. It is also noted that all the successive profiles are approximately linear with different slopes. The final trend of the temperature profile is well established after 6 iterations. By the end of the 7th iteration the solution is almost converged. The remainder of the fourteen iterations merely performs fine adjustment to satisfy the convergence criterion.

The steady progress of TVOUT to the final solution may become clear by giving attention to Figure (8.10,a) which illustrates the convergence progress of the TVOUT variable out of only one effect (effect number 5).

Table (8.5)

Vapour Temperature Profiles (TVOUT) along the Plant During the Iteration, [K]

Effect number	Initial guess	Iteration No. 2	Iteration No. 7	Iteration No. 14
1	399.700	375.494	367.694	367.500
2	399.500	371.730	363.072	362.892
3	399.300	368.060	358.292	358.116
4	399.100	364.489	353.346	353.163
5	398.900	361.024	348.228	348.022
6	398.700	357.675	342.931	342.685
7	398.500	354.460	337.454	337.144
8	398.300	351.426	331.800	331.392
9	398.100	348.721	326.001	325.424
10	397.900	346.761	320.200	319.237

Table (8.6)

Vapour Flowrate Profiles (FVOUT) along the Plant During the Iteration [kg/hr × 10^{-3}]

Effect number	Iteration No. 1	Iteration No. 2	Iteration No. 7	Iteration No. 14
1	37.868	64.196	47.912	47.728
2	33.824	62.012	47.636	47.483
3	29.769	59.720	47.311	47.183
4	25.703	57.323	46.906	46.799
5	21.629	54.804	46.395	46.303
6	17.549	52.098	45.749	45.666
7	13.463	48.983	44.946	44.866
8	9.373	44.804	43.949	43.879
9	5.281	37.641	42.659	42.687
10	1.189	21.946	40.695	41.283

Figure (8.9,b) explains the convergence attitude of the vapour flow rate (FVOUT) distribution along the plant. About seven iterations and 0.45 second of the computer time are required for setting up the vapour flow rate profile. By the end of the 14th iteration and after total CPU time of 0.74 second, the final distribution of FVOUT along the plant is obtained. Following the same way of illustration, the response of the vapour flow rate out of the fifth effect is recorded and plotted as shown in Figure (8.10,b)

8.4.2. Comparing The Design And The Performance Calculations Behaviour.

The design and the performance calculations using the VTBVT technique start at the same initial values. Also, the solution is computed to the same accuracy (i.e. using the same convergence criterion). However, Figures (8.11) shows that the rate of convergence of the design calculations is faster (8 iterations, 0.52 second CPU time) than that of the performance calculations (14 iterations, 0.74 second CPU time). This difference in the rate of convergence may be due to the fact that in both types of the calculation, different forms of the linearized heat transfer equations of the evaporators are used. Also, in the problem of performance calculations, the heat transfer equations for the heat exchangers are adopted (where the heat transfer area is specified). Instead, in the design problem, the relation between the output streams temperatures are related by the specified approach temperatures (see chapter 5 for more details). Therefore, different

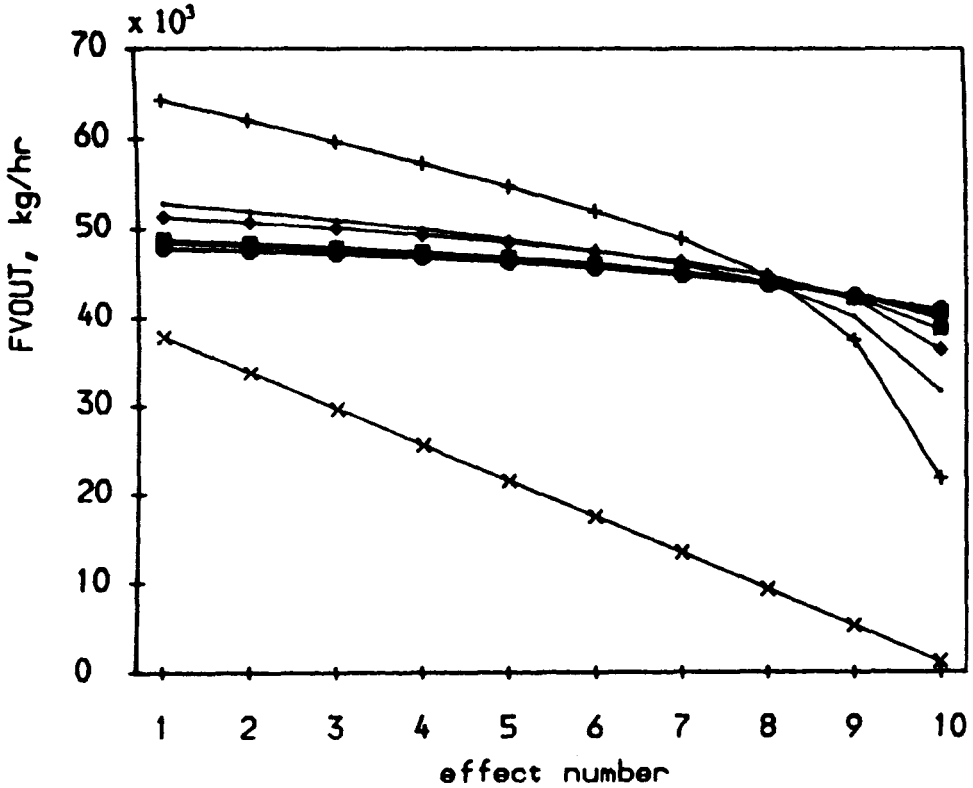

(b) FVOUT vs The Number of Effects

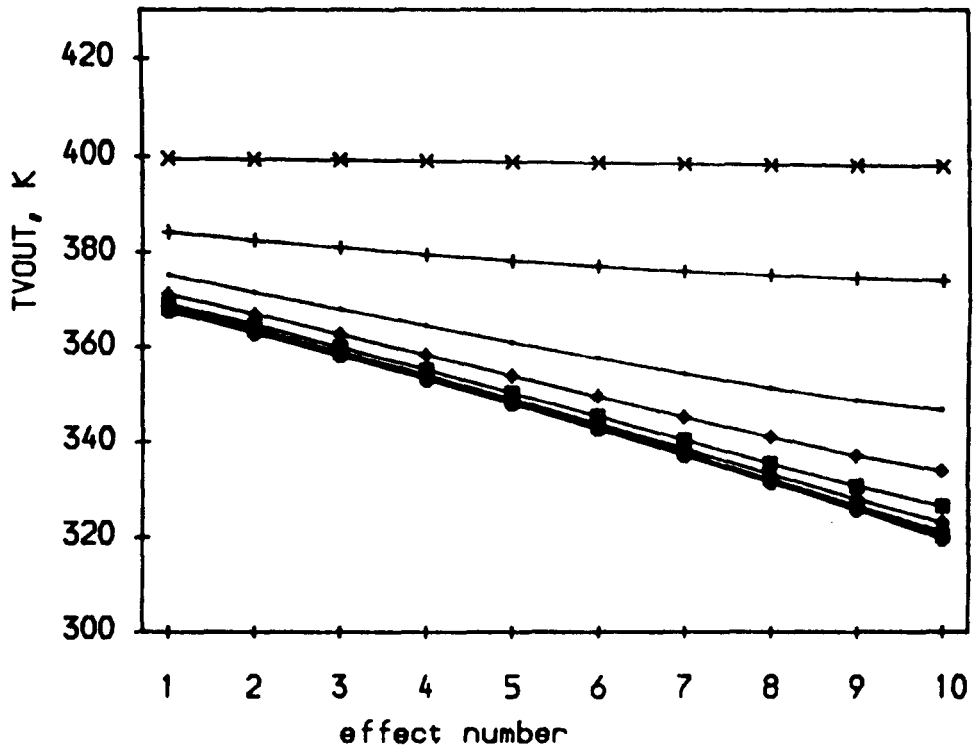

(a) TVOUT vs The Number of Effects

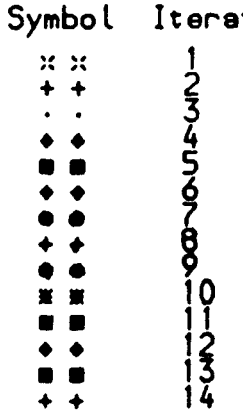

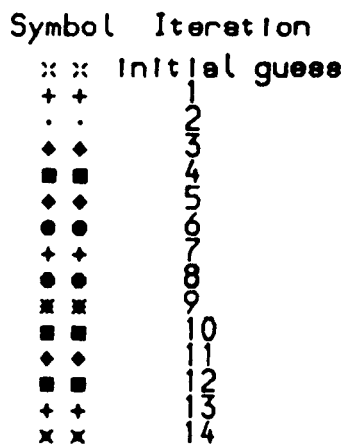

FIGURE 8.9. THE CONVERGENCE BEHAVIOUR OF THE VTBVT TECHNIQUE DURING THE PERFORMANCE CALCULATIONS OF MEE SYSTEM.

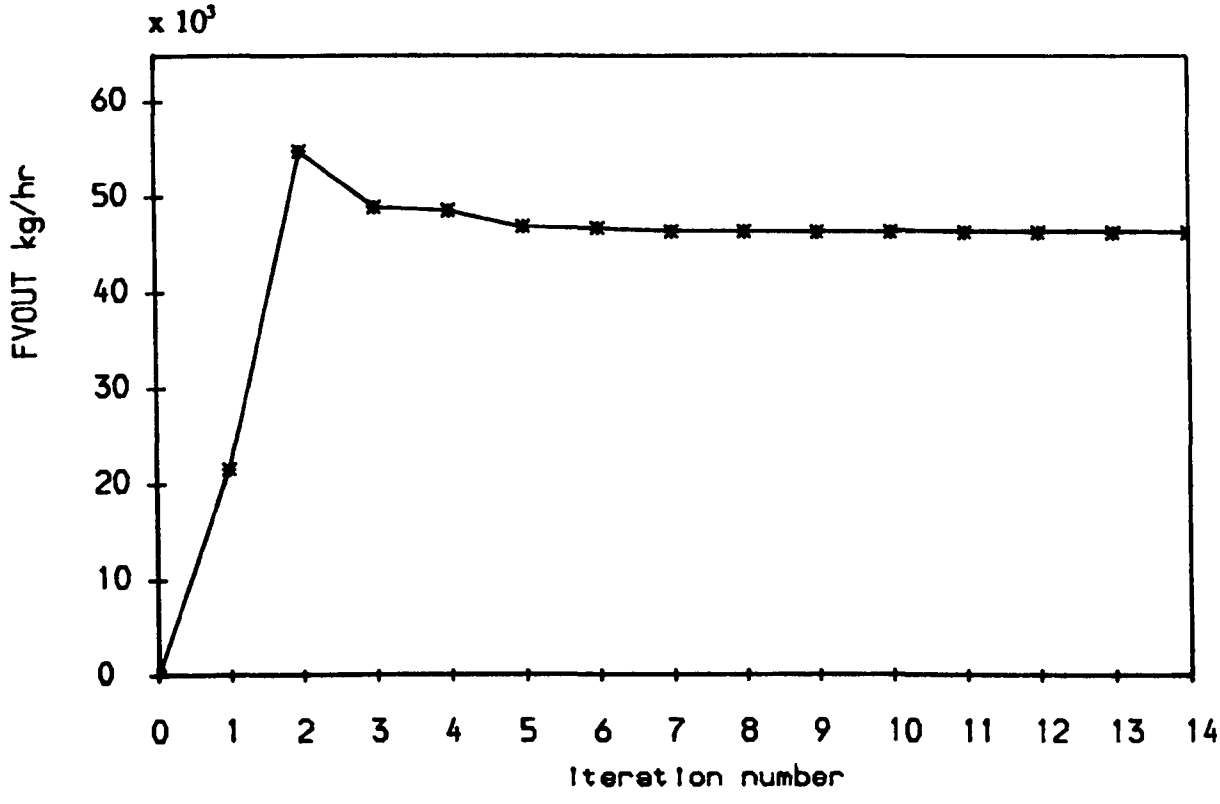

FIG. (8.10,b) CONVERGENCE OF VAPOUR FLOWRATE OUT OF THE EFFECT NUMBER 5 (CASE'I', VTBVT)

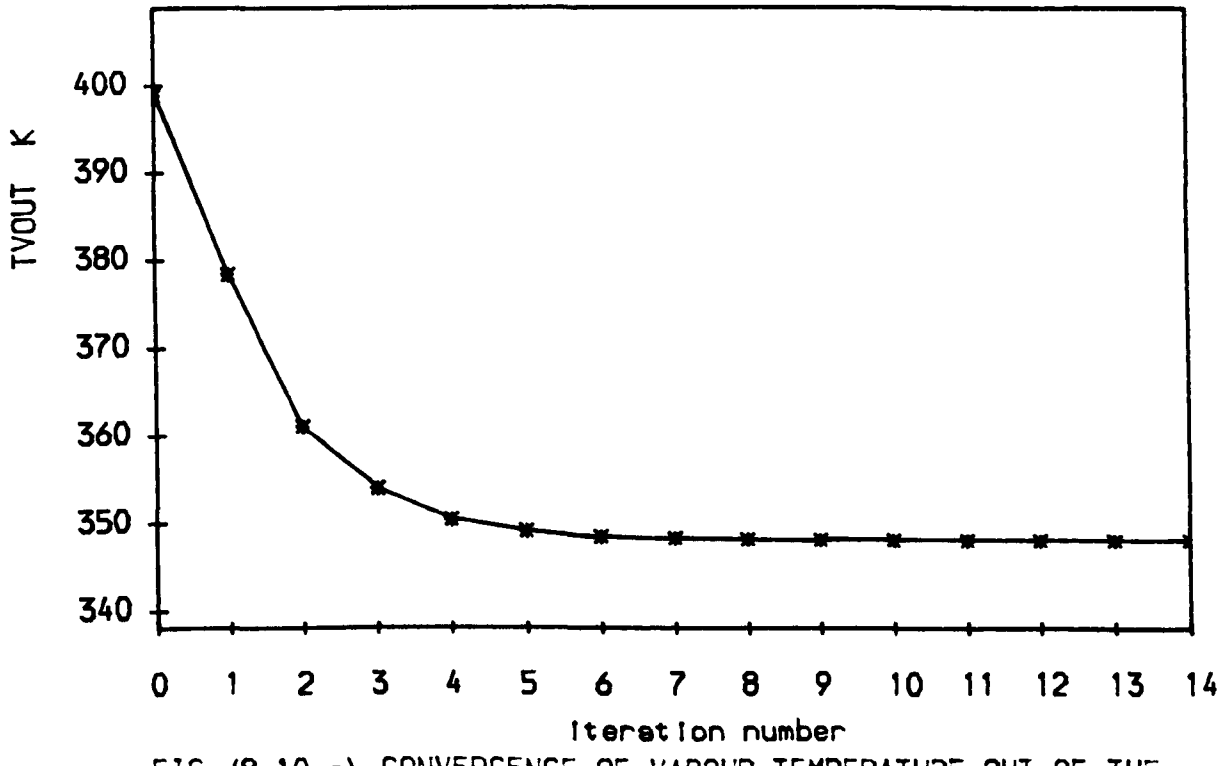

FIG. (8.10,a) CONVERGENCE OF VAPOUR TEMPERATURE OUT OF THE EFFECT NUMBER 5 (CASE'I',VTBVT)

representations of a mathematical model can produce different rates of convergence.

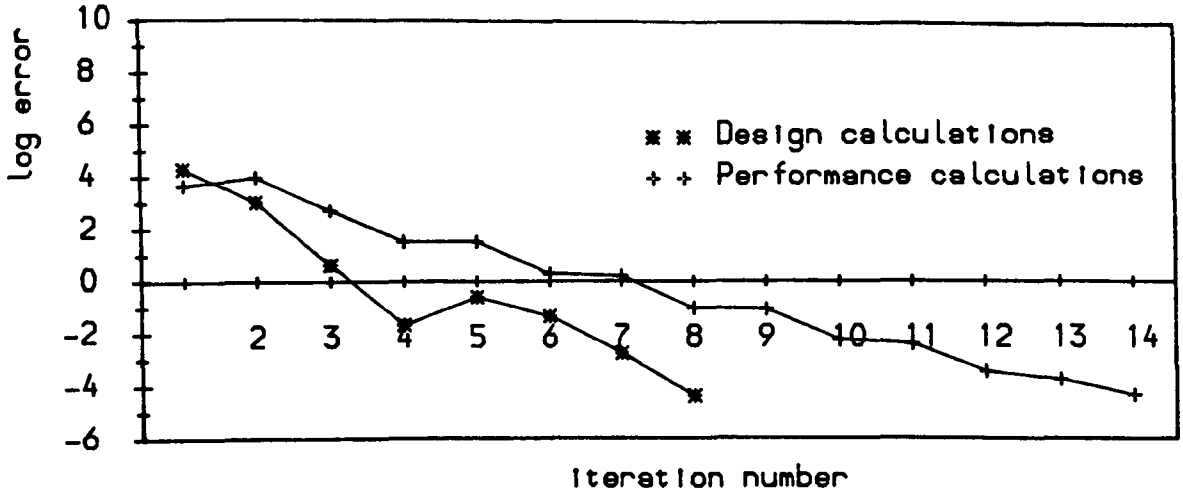

FIG. (8.11) THE CONVERGENCE BEHAVIOUR OF THE VTBVT TECHNIQUE

8.4.3 Comparing The Final Results of The Design And Performance Calculations:

The proper specifications for the simulation problem are taken from the output of the design calculations, as mentioned before. More confidence can be gained in the validity and the flexibility of the developed program and the proposed technique if the output results of both types of calculations (design & simulation) are matching each other (within acceptable fractional error).

In this section, the reproducibility of the performance calculation results will be examined. This can be achieved by comparing the final results of the design and performance calculations. Tables (8.7) and (8.8) give the numerical results of this comparison. Table (8.7) shows the brine temperature profile (TBOUT), vapour temperature profile (TVOUT) along the plant as well as the absolute error between both types of calculation. In Table (8.8) the calculated brine flow rate, vapour flowrate and the absolute error are listed as a function of the effect number. From the results tabulated in both tables it is quite clear that the results of the design and the simulation calculations are in good agreement, where the maximum fractional error for TBOUT is $(7.36 \pm 0.61) \times 10^{-5}$, $(7.622 \pm 0.61) \times 10^{-5}$ for TVOUT and $(6.347 \pm 0.004) \times 10^{-4}$ for FBOUT, $(1.0421 \pm 0.0048) \times 10^{-3}$ for FVOUT.

In fact, this very small deviation in the final results should be

expected because both types of calculation follow a different path to the final solution. The design calculation path is much shorter (8 iterations) than that followed by the performance calculations (14 iterations). As a result, the number of the mathematical operations is different, and thereby, the amount of round off error is different as well. Furthermore, as introduced previously in chapter 7, although the

Table (8.7) Comparison between the Temperature Profiles for an MEE Plant as Calculated by the Design and the Simulation Calculations

EFFECT NO.	TBOUT (K)			TVOUT (K)		
	DESIG.	SIMUL.	ERROR	DESIG.	SIMUL.	ERROR
1	368.064	368.062	0.002	367.502	367.500	0.002
2	363.479	363.474	0.005	362.899	362.892	0.007
3	358.729	358.720	0.009	358.128	358.116	0.012
4	353.803	353.791	0.012	353.178	353.163	0.015
5	348.692	348.677	0.015	348.041	348.022	0.019
6	343.388	343.370	0.018	342.707	342.685	0.022
7	337.883	337.862	0.021	337.168	337.144	0.024
8	332.171	332.148	0.023	331.417	331.392	0.025
9	326.246	326.222	0.024	325.450	325.424	0.026
10	320.106	320.083	0.023	319.261	319.237	0.024

DESIG.= design calculation

SIMUL.= simulation calculation

ERROR = DESIG.-SIMUL.

Table (8.8) Comparison between the Calculated Flowrate Profiles along an MEE Plant Using the Design and Simulation Calculations.

EFFECT NO.	FBOUT × 10^{-3} kg/hr			FVOUT × 10^{-3} kg/hr		
	DESIG.	SIMUL.	ERROR	DESIG.	SIMUL.	ERROR
1	859.4919	859.4561	0.0359	47.692	47.728	-0.036
2	812.0430	811.9729	0.0701	47.449	47.483	-0.034
3	764.8931	764.7910	0.1021	47.150	47.183	-0.033
4	718.1240	717.9919	0.1321	46.769	46.799	-0.030
5	671.8479	671.6890	0.1589	46.276	46.303	-0.027
6	626.2061	626.0229	0.1831	45.643	45.666	-0.023
7	581.3601	581.1570	0.2031	44.846	44.866	-0.020
8	537.5010	537.2781	0.2229	43.859	43.879	-0.020
9	494.8369	494.5911	0.2458	42.664	42.687	-0.023
10	453.5969	453.3091	0.2878	41.240	41.283	-0.043

Table (8.9)

The Convergence Characteristics of The VTBVT Technique

[a] Design Calculations

Iteration	Error
1	21083.34
2	1105.35
3	4.1688
4	0.0211
5	0.2452
6	0.04488
7	0.0017168
8	0.00004045

[b] Performance Calculations

Iteration	Error
1	4817.78
2	9673.81
3	520.354
4	32.8621
5	32.06822
6	1.088605
7	1.056326
8	0.091893
9	0.082398
10	0.0056413
11	0.0039291
12	0.0003511
13	0.0001766
14	0.00004524

$$\text{Error} = \sum_{i=1}^{N} (\text{FVOUT}^{k+1} - \text{FVOUT}^{k})_i^2 \qquad (8.1)$$

Where;

N : Total number of effects

i : The present effect number

FVOUT : Vapour flowrate out of an effect.

iterations are terminated as soon as the convergence criterion is satisfied, the stopping point is varied from one path to another. In this particular case, the chosen convergence criterion is 0.5×10^{-4} and the results show that the stopping criterion for the design calculation is 0.4045×10^{-4} on the contrary, 0.4524×10^{-4} for the simulation calculation, see Tables (8.9,a and b).

The performance calculation for the same desalination plant, Figure (8.6), is performed using Newton Raphson technique, with the same specifications used in the previous section. This is performed to examine the validity of the proposed assumptions for developing the VTBVT technique. Newton's method converges to the final solution faster (6 iterations) than the VTBVT technique (14 iterations). However, the computation time required by the VTBVT technique to perform the performance problem is only one third of that required by Newton's method. This great advantage may make the VTBVT technique more practically attractive.

Extensive testing is applied to the computer program to ensure confidence, reliability and efficiency of the proposed technique in solving the MEE problems. In this aspect, the final results obtained by NR and the VTBVT techniques are highly consistent, taking into consideration the effect of the round off error and the stopping criterion. For a further discussion of the above points, see Appendix {E}.

The VTBVT technique shows much stability, where the solution always converged, starting with any linear temperature profile as an initial guess between 300 - 450 K, see Appendix {F} for more details.

8.5. SIMULATION STUDY CASES OF MEE PLANTS.

One of the main aims of the simulation of thermal desalination plants is to study the behaviour of an existing (or detailed design) plant under operating conditions other than those used for the design calculations. Such study would produce good information for the plant operators to make the most efficient use of the plant and to avoid conditions which could affect the production rate of the plant.

There are many "off design" conditions which may arise during the operation of an MEE plant. For instance, when the plant is new (or

after retubing the heat transfer surface) the effect of the fouling factors are practically zero. Under these conditions, operation at the design temperature range would lead to an output above the design value. If the seawater feed rate to the plant is not correspondingly increased, the maximum brine concentration could exceed the maximum allowed value.

Similarly, if the fouling inside an operating plant exceeds the design values, this would lead to a decrease in the design output of the plant. So, to keep the product constant, the reduction of the overall heat transfer coefficient (due to increasing the fouling) should be compensated for by increasing the steam consumption. Also, it would be required to compensate the increase in the steam consumption by increasing the cooling water flow rate. Equally, the same situation can arise if the feed sea water temperature increases.

Furthermore, if one of the effects of the plant (and/or its associated heat exchangers) is bypassed to be isolated for cleaning or retubing without having to shut the plant down, the required operating conditions should be correctly predicted to keep the production of the plant constant.

Besides the solution of the above problems, the answer to the question of what changes in the operating conditions must be performed if it is desired to operate a plant under "partial load" conditions can be obtained by the developed program.

As introduced in section (8.3), ten variables are required to be specified to perform the performance calculations for the MEE plant shown in Figure (8.6). For illustration purpose three different combinations, each includes 10 variables are presented in Table (8.10). The solution of these cases (or combination of some of them) demonstrates how the developed package, using the proposed VTBVT technique, can be used to predict the right operating conditions for the "off design " problems mentioned above.

Table (8.10), Different Specifications for the MEE Plant, Figure (8.6)

Case No.	Specified terminal variables	Purpose
I	F_f , X_f , T_f , P_f , F_c , X_c T_c , P_c , T_s , P_s	Performance Calculations
II	X_f , T_f , P_f , F_c , X_c , T_c P_c , T_s , P_s , D	Calculating feed seawater for a known product flowrate
III	F_f , X_f , T_f , P_f , X_c , T_c P_c , T_s , P_s , D	Calculating the cooling water flow-rate for known water product

8.5.1. The Convergence Characteristics of Cases II And III:

Discussion of the convergence behaviour of the iterative solution for case I (performance calculations) is presented in section (8.4). Ten plant evaporators with heat recovery system were used to exemplify that behaviour. Following the same way of illustration (for the same plant) the characteristics of the convergence behaviour of the solution for cases II and III will be clarified in this section.

The convergence attitude of the iterative solution for case II is represented by Figures (8.12, a,b). In Figure (8.12,a) the progress of the convergence for the vapour temperature profile along the plant, is illustrated. While, Figure (8.12,b) explains the convergence behaviour of the vapour flow rate profiles during the iterations. As can be seen from Table (8.11) and Figure (8.13), to reach the solution within the error 0.961×10^{-2}, ten iterations and 0.58 second are required. And for more tight tolerance of 0.1488×10^{-4}, fifteen iterations and a total of 0.76 second CPU time will be sufficient.

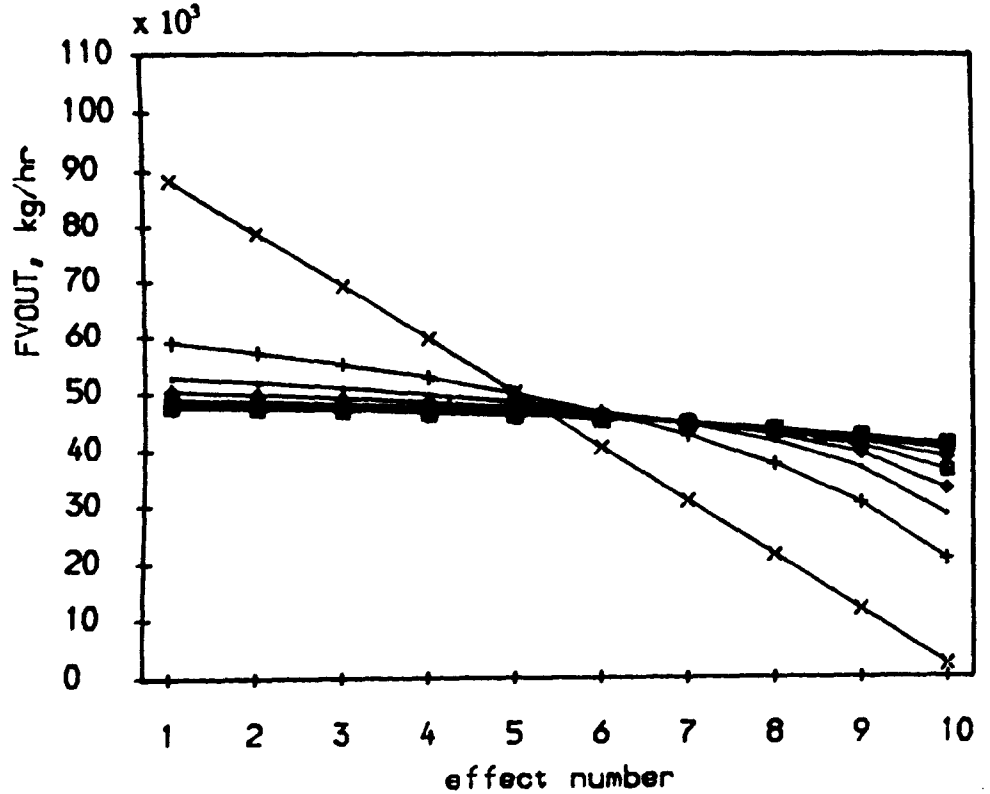

(b) FVOUT vs The Number of Effects

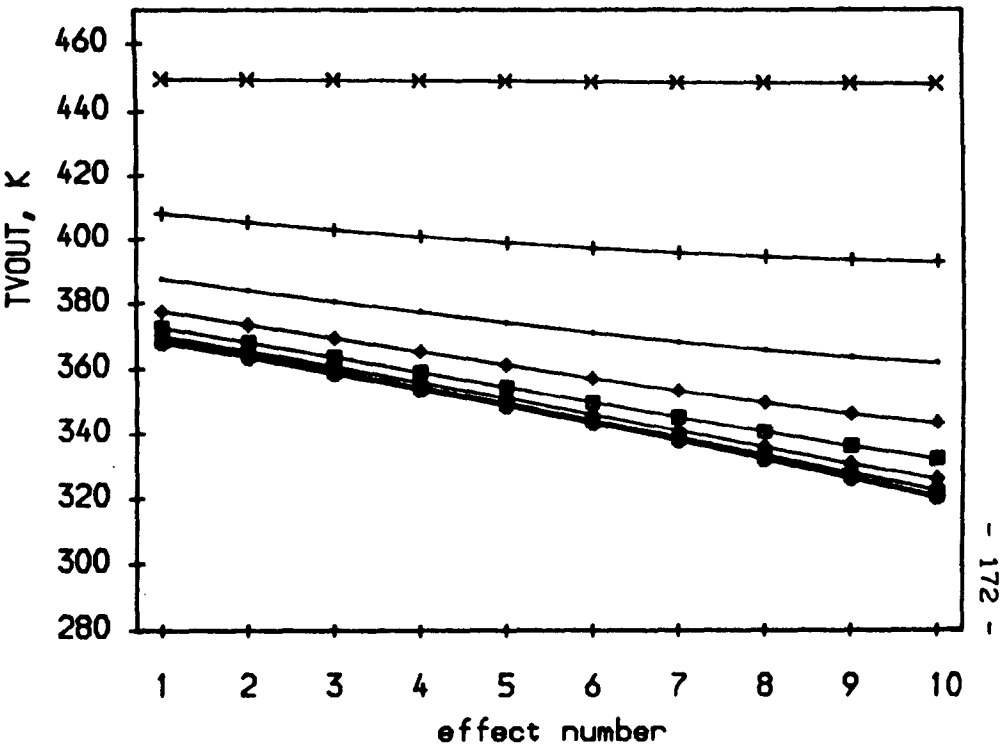

(a) TVOUT vs The Number of Effects

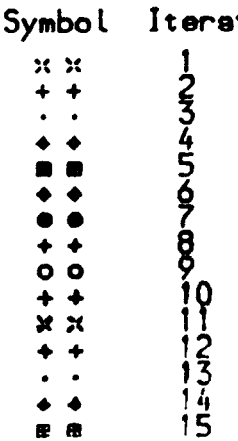

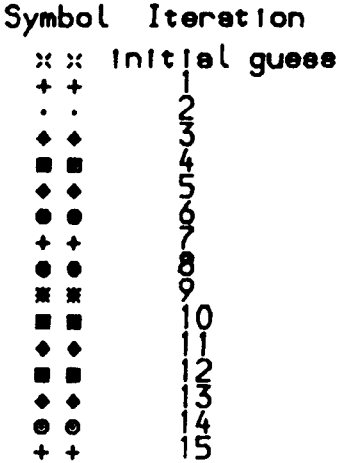

FIGURE 8.12. THE CONVERGENCE BEHAVIOUR OF CASE II.

Table (8.11)

Convergence Characteristics of The VTBVT Technique During the Solution of Cases II and III

Iteration number	Error = $\sum_{i=1}^{N} (FVOUT^{k+1} - FVOUT^{k})_i^2$	
	Case II	Case III
1	27249.582	4817.7813
2	2700.859	1911.5400
3	219.985	450.518
4	44.565	110.785
5	18.968	26.4835
6	8.350	6.2809
7	2.846	1.4839
8	0.6412	0.3531
9	0.09021	0.08419
10	0.009611	0.01982
11	0.001334	0.004832
12	0.0004114	0.001185
13	0.0001883	0.000306
14	0.00006106	0.0001269
15	0.00001488	0.00002559

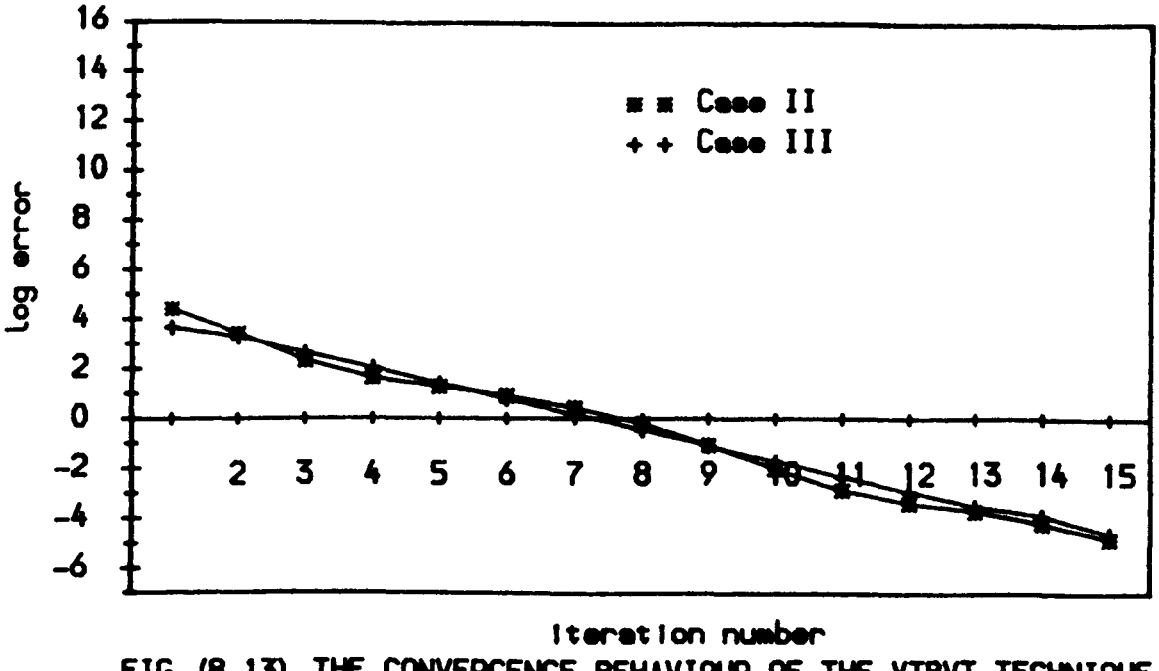

FIG. (8.13) THE CONVERGENCE BEHAVIOUR OF THE VTBVT TECHNIQUE

With respect to case III in table (8,10), the convergence behaviour is represented by plotting the numerical results in Table (8.11) in Figure (8.13). According to this figure, the solution converges almost exponentially after the second iteration. The final solution is reached in 0.79 second CPU time.

On the basis of the above results, it may be concluded that: first, the rates of convergence of the three case studies in Table (8.10) are almost similar (14 - 15 iterations), therefore, it can be deduced that the direction of the flow information (the specifications) does not considerably change the convergence rate of the VTBVT technique; Second, the final results of all the above cases (I, II, III) are in remarkable agreement, this may confirm the validity and the reproducibility of the results.

8.5.2 Studying The behaviour Of The MEE System Under Partial Loads:

In this subsection, an attempt is made to present an answer to the question raised in the beginning of this section: i.e. 'what changes in operating conditions must be performed if it is desired to operate the plant under a " partial load" conditions ?'. In fact, to answer the above question properly a sort of parametric analysis of the effect of reducing the production flow rate of an MEE on the required feed seawater, cooling water flow rate, the temperature distribution, salt concentration, steam requirements, and other parameters is presented.

The simulation calculation is conducted under the assumption that the MEE desalination plant shown in Figure (8.6) is operated under partial load conditions (80%, and 60% of the design load). The number of units and the specifications of the heat transfer areas are as shown in Table (8.4). On one hand the quantity of fresh water to be produced is regarded as a given condition, on the other hand, the feed and the cooling flow rates are regarded as unknown parameters. So, a combination of case II (calculate the required feed seawater for a specified product flow rate) and case III (calculate the required cooling water flow rate for a specified product flowrate) in Table (8.10) is required to perform the calculations as follows:

[1] Assume the saturation vapour temperature (or pressure) at the last effect T_N^o, solve the computer program for case II to predict the required feed seawater F_f, salt concentration at

the last effect X_N, and a new value of the last effect temperature T_N^k.

[2] Using T_N^k and X_N run the program for case III to calculate the cooling water flow rate F_C and a new value of the last effect temperature T_N^{k+1}

[3] The steps (1) and (2) are repeated until $T_N^{k+1} = T_N^k$.

Table (8.12)

Some Changing of The Operating Conditions

Under Partial Loads

Parameter \ Load	100 %	80 %	60 %
P_N (kPa)	10.1219	15.2995	23.6121
ΔT (K)	53.918	45.581	36.266
D $\times 10^{-3}$, kg/hr	453.587	362.8696	272.1522
S $\times 10^{-3}$, kg/hr	53.3467	40.4963	29.1675
Performance ratio	8.5	8.86	9.33
$F_c \times 10^{-3}$, kg/hr	853.862	237.856	13.203
$F_f \times 10^{-3}$, kg/hr	907.17	610.448	427.881

where;

P_N :Pressure at the last effect.

S :Steam consumption.

T_s :Steam temperature.

F_c :Cooling water flowrate

F_f :Feed water flowrate

ΔT :Operating temperature range = $T_s - T_N$

D :Distillate output flowrate.

Table (8.12) shows the results of these calculations, from which the following points can be concluded;

[A] The performance ratio increases by decreasing the plant capacity.

[B] The steam consumption decreases as the load decreases.

[C] According to these calculations, the lower limits of the accuracy required for the feed, cooling water, and the steam flow rate controller limits can be determined.

[D] The operating temperature range ΔT decreases by decreasing the load.

[E] The relationship between the maximum possible vacuum pressure at

the last effect and the partial load conditions is clarified, where, the vacuum pressure increases as the load decreases.

[F] By this calculation the limits, to which the reduction of the plant capacity is possible and reasonable can be determined according to the maximum allowed salt concentration.

8.5.3. Determination Of The New Operating Conditions For An MEE After Bypassing One Or More Of Its Units.

Practically, it is possible to bypass any operation unit(s) of an MEE system to separate it for cleaning or maintenance without having to shut the plant down. This subsection discusses how to keep a constant water production rate in the face of changing the configuration of the plant by isolating one of its effects. The ten effect evaporator with heat recovery system, Figure (8.6), is computed assuming the complete removal of the fourth effect and its associated preheaters. The final results have been reached within the tolerance (0.5×10^{-4}) in 16 iterations, and CPU 0.72 second. These results show that under the design conditions an output of 453.857×10^3 kg/hr could still be achieved by increasing the steam consumption to 58.7792×10^3 kg/hr representing an increase by a factor of 1.1 on the comparable figure for the normal plant. The maximum brine temperature required is about 0.8 C lower than that when the plant is operating normally, and the cooling water flow rate required is increased to 1482.26×10^3 kg/hr which represents an increase on the normal plant by a factor of 1.74. In conclusion, using the developed program, the operating conditions required to meet the changing in the plant configuration due to bypassing one or more of its units can be determined accurately.

8.6. CONCLUSION.

In this chapter the developed modular program using the proposed VTBVT technique is used to design and simulate a Multiple Effect Evaporator (MEE) process.

The flexibility of this program makes it a very powerful instrument for studying a series of alternative possibilities in the design of a new plant or the design of the rebuilding of an existing plant. Six different configurations are studied to determine the effect of the heat recovery on the steam economy. The results show that the effect can be quite big but it also depends on how the heat is recovered and reused.

In general, it is found that the convergence of the performance calculations is always reached after (14-16) iterations using the proposed technique and usually independent of the size of the problem or of the information direction. However, the CPU time required increases with increasing the number of variables (i.e. the size of the problem). The rate of convergence of the design calculation is faster (8 iterations)

To confirm the validity of the solution procedure followed in each of the considered three case studies, specifications for case II and III are taken from the final results of case I. The same solution is then reproduced by running the program for case II and III

To show the practicability of the simulation studies, the behaviour of the MEE plant under a partial load is illustrated. In this case the control variables to be adjusted are the pressure at the last effect, top brine temperature, cooling water flow rate and feed water flowrate. By these calculations the limits, to which the reduction of the plant capacity are possible and reasonable can be determined according to the maximum allowed salt concentration.

In another practical application, the developed program is used to calculate the required changes in the operating conditions to keep a constant water production rate in the face of changing the plant configuration by isolating one or more of its units for cleaning or maintenance without having to shut the plant down.

CHAPTER 9

THE ECONOMIC IMPROVEMENT OF THE DISTILLATION PROCESSES BY COMBINING DIFFERENT SYSTEMS

9.1. INTRODUCTION:

Thermal efficiency is one of the main important means which can provide a sizable reduction in the desalted water cost. The process thermal efficiency may be improved by combining the advantages of different desalination processes in one hybrid system (e.g. MEE/VC or MEE/VC/MSF), and/or by combining seawater distillation processes and power plants, as illustrated in chapter 2.

In this chapter, the capability of the developed program using the proposed VTBVT technique to deal with problems related to these hybrid systems will be illustrated in three sections. In section 9.2 the impact of some design parameters and plant configuration on the evaporation cost of the Vapour Compression process (VC) will be performed.

Another important application of the program is to simulate an existing process when there is an operating problem or a possible improvement is being considered. Also, the effect on the process due to changing one or more units can be examined before the actual change to ensure that the operating problem will be corrected and to find the cheapest means of achieving the desired improvement. This application will be demonstrated in section 9.3 , by studying the conversion of an existing Multiple Effect Evaporation (MEE) plant to VC system to improve its energy consumption. In this section two alternatives are proposed and a technical and economical comparisons are performed.

Furthermore, the program may be used to learn as much as possible about a complicated process by trying various modifications, and examining the sensitivity of the process economy to key parameters and data before building a pilot or demonstration plant for the process. To show the potentiality of the developed package to carry out these types of calculations, a large VTE/VC/MSF demonstration plant is designed in section 9.4. Finally the main conclusions of the above three sections are summarized in section 9.5 .

9.2. ENERGY CONVERSATION BY VAPOUR COMPRESSION EVAPORATION

Because of the dramatic increase of the energy costs during the last fifteen years, it has become very important to choose the most economical way to improve the evaporation economy. Mechanical Vapour Compression (VC) is one of the proven means to significantly reduce energy required for an evaporation system, Minton [1986]. The operating principles of VC evaporation are illustrated in chapter 2.

In fact, the technical and the economical justification for integrating a vapour compressor with an evaporation process will never be a trivial exercise, because: energy, construction material costs, and configuration vary considerably from one location to another, and from one plant type to another. Therefore, each design case (or project) has to be treated individually. In each case, a number of design parameters should be manipulated, and different configurations must be examined in order to achieved an optimized design for the given operating conditions.

Thus, a flexible, fast, and reliable tool for testing many alternatives is required, if the job is to be completed accurately in a reasonable length of time. Different types of calculations using different combinations of specified variables (see Table (9.1)), can be performed by the developed program using the proposed VTBVT technique.

In this section, the impact of some design parameters on the operating and capital costs of different VC configurations will be investigated, case 1 in Table (9.1).

Table (9.1)

Different Combinations Of Specified Variables For VC System

Case	1		2	3	4
Problem Type / Parameters	Total Design		Partial design	Partial design around a given BHP	simulation, given Feed Flow rate
	A	B			
F_f	■	□	□	■	■
T_f	■	■	■	■	■
X_f	■	■	■	■	■
X_N	■	■	■	■	□
D	□	■	■	□	□
$A_{eff.}$	□	□	■	□	■
BHP	□	□	□	■	■
$[T \text{ or } P]_{ou,c}$	■	■	■	■	■
T_s	■	■	■	■	■

where; ■ : Given Variable □ : Calculated variable

X_N : Outlet concentration $A_{eff.}$: Area of the effect.

BHP : Brake horsepower.

T_s : Make-up steam temperature.

$T_{ou,c}$: Compressor outlet saturation temperature.

9.2.1. Design Specifications:

In order to have consistent numbers of variables and equations for the mathematical model of the considered VC process, the following design variables, Table (9.2), are used in the design calculations, except when a sensitivity analysis is involved.

Table (9.2)

Design Specifications Of The VC System

Steam temperature (K)	375.15
Feed temperature (K)	300.00
Feed concentration	3.5 %
Feed flowrate $\times 10^{-3}$ (kg/hr)	157.72
Brine concentration	7.0 %
Polytropic efficiency	85 %
Suction pressure (kPa)	41.608
$\Delta T_{approach}$	6.0 C°

9.2.2. Economic Evaluation:

The detailed cost calculation of a VC process usually requires knowledge of the energy, capital, operating labour, spare parts, and maintenance cost over the assumed life of the plant. In fact, the aim of this work is not to search extensively into the detailed cost calculations, but rather to present a parametric analysis of the behaviour of the VC operating and capital costs under different design conditions and parameters. Table (9.3) shows capital cost equations of the installed equipment. Some of these equations are fitted to data reported by Chauvel [1981]. All these equations are based on CE plant cost index (April 1987).

The total venture cost, as defined by Rudd and Watson [1968], is used to estimate the overall economies. The parameters of the following equation were calculated by Guimaraes [1980];

Total venture cost (TVC) , ($/year) =

0.5 (total operating cost) + 0.35 (total capital cost)

And the evaporation cost ($/kg) =

$$\frac{\text{TVC}}{\text{(kg water evaporated/hr)(8000 hr/year)}}$$

Table (9.3), Cost Data

No.	Unit	Equation	Reference
1	Evaporator (VTE)	= 4135 $A^{0.786}$ A ; area (m^2)	**
2	Flash stage	= 2805 $A^{0.65}$ A ; area (m^2)	Ali [1983]
3	Heat exch	= 1224 $A^{0.57}$ A ; area (m^2)	Sherwood [1963]
4	Pump	= 65. $Q^{0.825}$ Q ; m^3/hr	**
5	Compressor	= 10684 $(BHP)^{0.652}$ for BHP ≤ 1236 = 12625 $(BHP)^{0.652}$ for BHP > 1236	Guimaraes [1980]

Steam : 9.0 $/ton

Electricity 0.04 $/kWh

** fitted to the data reported by Chauvel [1981]

9.2.3. Design Parameters Affecting Costs:

Mechanical vapour compressors can be integrated in principle with any type of evaporation process (by boiling or by flashing), Minton [1986]. However, the total economic feasibility is one of the main effective limits. Following, are three of the main design parameters affecting any VC process economy.

9.2.3.A. Temperature Differential (or Compression Ratio):

In the considered VC process, Figure (9.1), the evaporator working pressure is assumed fixed, and the make-up steam temperature is assigned different values. Thus, variable temperature difference ΔT is obtained. The effect of these ΔT values on the process economy is illustrated in Table (9.4) from which the most important results may be

summarized as follows:

Table (9.4)

Impact Of Temperature Differential On The Design Results

ΔT K	$S_m \times 10^{-3}$ kg/hr	A_{eff}	BHP	$T_{do} = T_s$ K	$S_f \times 10^{-3}$ kg/hr	P_2/P_1	$E_c \times 10^3$ \$/kg
24.1	10.325	382.87	6433.6	375.15	95.28	2.613	4.17
19.1	11.038	483.12	5146.9	370.15	94.74	2.185	3.73
14.1	11.714	654.43	3885.1	365.15	94.21	1.816	3.30
9.1	12.355	1013.84	2649.0	360.15	93.68	1.501	2.92
4.1	12.961	2248.32	1438.6	355.15	93.17	1.233	2.80

Volume flowrate = 303.15 m^3/hr

where;

S_m : Make-up steam S_f : Heating steam to the first effect

E_c : Evaporation cost P2/P1: Compression ratio.

T_s : Steam temperature T_{do} : Outlet distillate temperature.

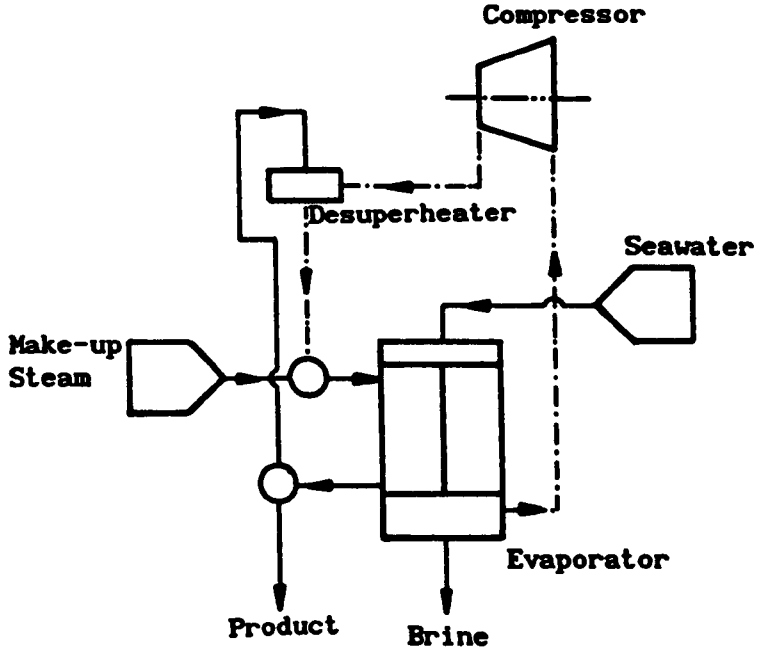

Fig. 9.1. a VC Process.

[1] The advantage of operating the VC system at high temperature difference (i.e. high compression ratio) is a reduction in evaporator tube surface, but this is achieved at the expense

of the compressor capital cost and horsepower required.

[2] Make-up steam consumption is inversely proportional to the temperature difference, but the latter is proportional to the total saturated steam input to the evaporator. As ΔT decreases, the amount of water to the desuperheater unit decreases as well.

[3] To achieve reasonable evaporation cost, the compression evaporation process must operate with very low temperature difference ΔT. However, ΔT can not be chosen freely, because it depends on several aspects such as, pressure drop, temperature driving force, and BPR (Boiling Point Rise). These aspects have to be compensated.

[4] The absolute value of the vapour pressure is also decisive for the economic feasibility for a VC system. Obviously, it is possible to operate the evaporator under vacuum conditions. However, in this case the compressor volume and the horsepower increase significantly.

[5] Economics of VC system are commonly judged by comparison with steam operated evaporation system. The Performance Ratio (PR) of VC system may be calculated by the following equation, El-Sayed [1986].

$$PR = \frac{D * \lambda}{\text{heat input to VC system}} \qquad (9.1)$$

$$= \frac{\lambda}{\frac{\omega}{\eta * D} + \frac{Q_{aux}}{D}} \qquad (9.1,a)$$

where;

$$\eta_{max} = \frac{T_h - T_i}{T_h}$$

= Thermal efficiency of the heat engine used to drive the compressor

D : Distillate flowrate.

λ : Average latent heat of vaporization.

ω : Work

Q_{aux}: Auxiliary heat supplied to the evaporator.

T_h : Heating steam saturated temperature.

T_i : Feed temperature to the VC system.

Thus, the PR for the considered VC system would be equal to 7.36 . This is based on the following values:

ω = 170348 kJ/hr D = 78860 kg/hr Q = 23251900. kJ/hr

λ = 2252 kJ/kg $\eta \cong$ 20.0 %

Now, assuming the performance ratio for the thermal operated MEE process represented by:

0.85 * Number of effects

So, at least nine evaporation effects are needed to have the same performance as the VC system.

9.2.3.B. The Number Of Effects:

Using the design specifications tabulated in Table (9.2), four multi-effect vapour compression systems with different numbers of evaporators (2,4,6, and 8 effects), but without heat recovery, Fig. (9.2) are designed using the proposed technique.

Increasing the plant number of effects usually has two opposite influences on the product water cost: first, the compressed vapour volume flowrate is reduced. So, the compressor size and the required horsepower are reduced. Second, the capital cost increases, because of increasing the plant heat transfer area, see Table (9.5). Therefore, a compromise between these two opposite results due to increasing the

Table (9.5), Impact of changing The Plant Number Of Effects On The Main Calculated Parameters

Parameter \ No.of effects	2	4	6	8
Area of H. Transfer, m^2	2*378.0	4*394.0	6*418.0	8*447.0
Volume flow rate, m^3/hr	1550.0	814.0	570.0	450.0
Compressor BHP	3290.0	1728.0	1210.0	955.0
Make-up steam $\times 10^{-3}$ kg/hr	13.0	14.6	14.8	15.0

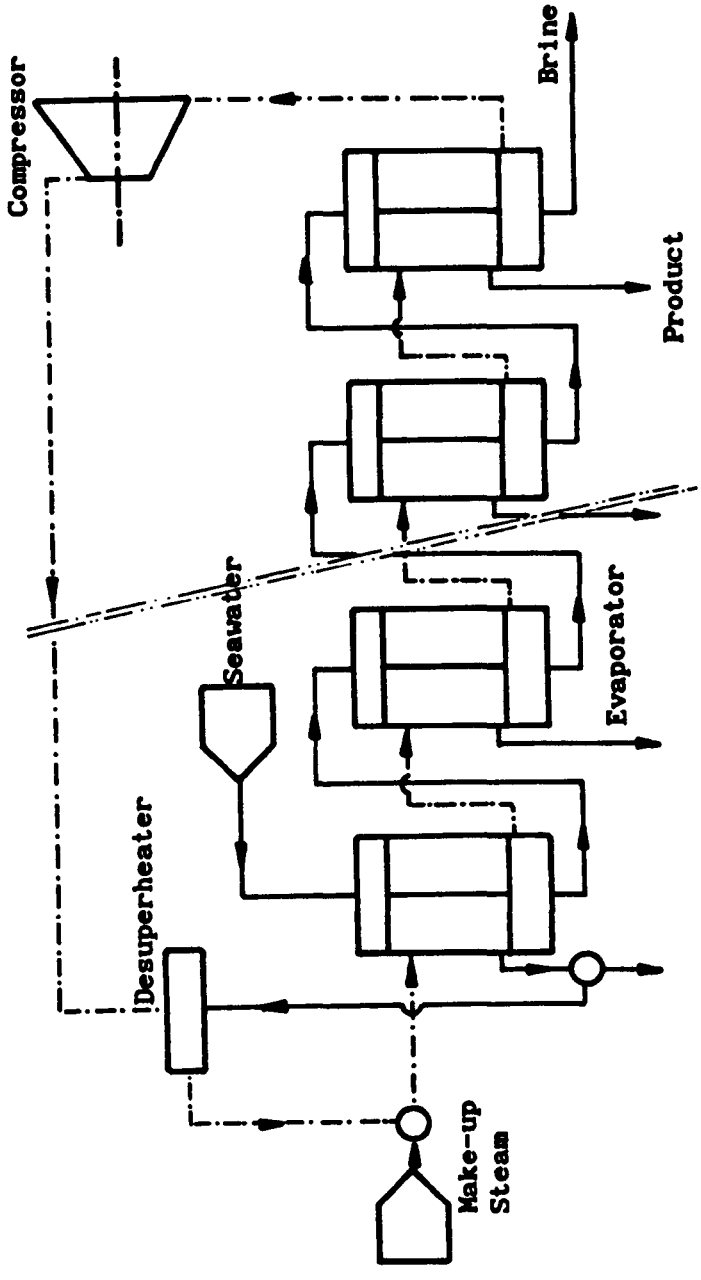

Fig. 9.2. Multi Effect Vapour Compression System.

plant number of effects must be performed to determine a particular number of effects at which the evaporation cost of the product is a minimum. Figure (9.3, a,b), shows the relation between the number of effects and the evaporation cost at different steam and electricity prices. From this figure it can be seen that: under the given specifications, the evaporation cost/ton, of the product water reduces as the number of effects increases, until between four and five effects, (depending on the power cost), then the evaporation cost starts rising with increasing the number of effects. Figures (9.3, a,b.), show also

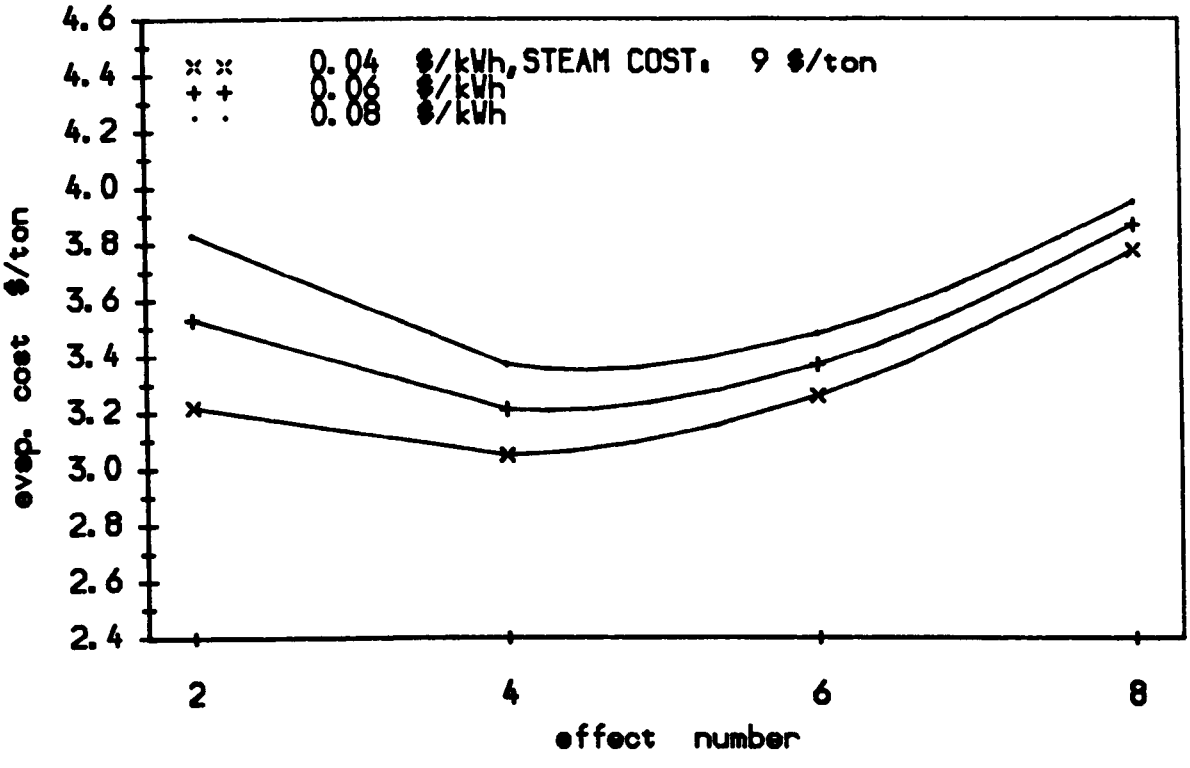

FIG. (9.3,a) EVAPORATION COST VS. THE NUMBER OF EFFECTS AT DIFFERENT ELECTRICITY PRICE

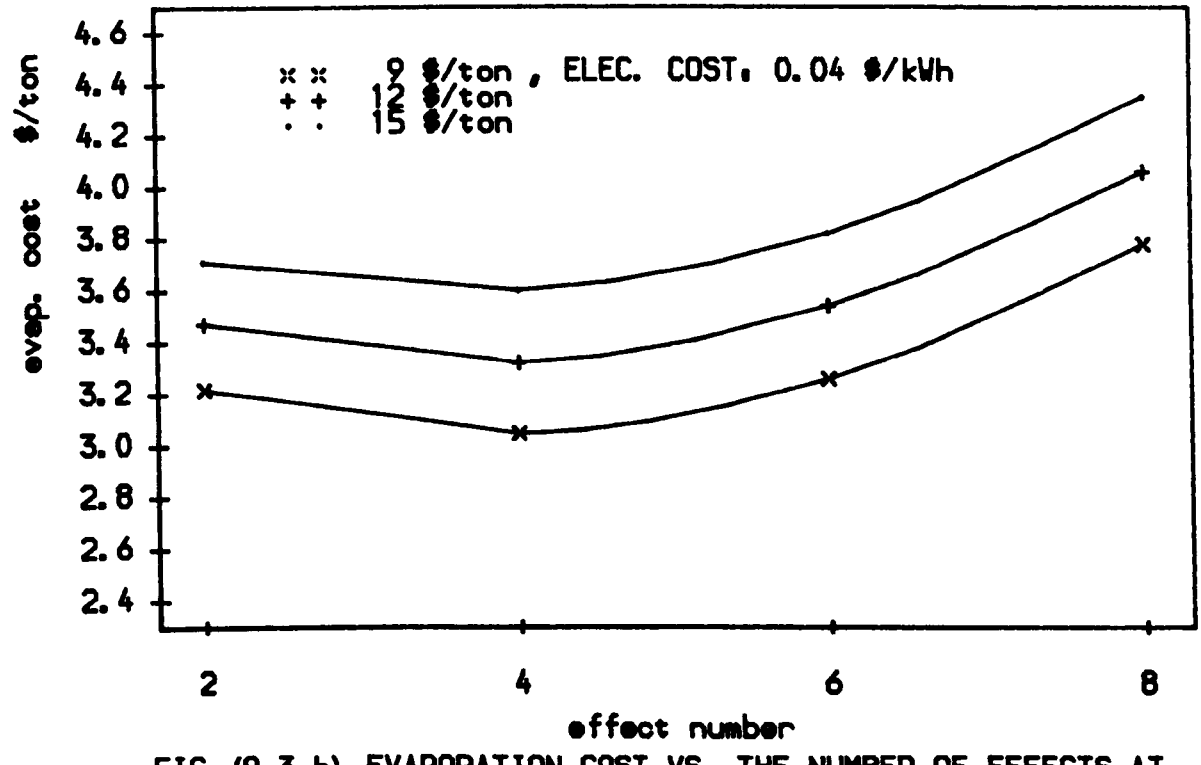

FIG. (9.3,b) EVAPORATION COST VS. THE NUMBER OF EFFECTS AT DIFFERENT STEAM PRICES

that the optimal number of evaporation in one energy cost situation is no longer such under increased energy cost conditions, where the optimal number is slightly shifted by increasing the electricity cost to 0.08 $/kwh.

9.2.3.C. Heat Recovery And Plant Configurations:

In the process described by Figure (9.1), the feed seawater enters the evaporator unit at whatever temperature that comes from the sea. The preheating of the feed will be accomplished by an extra heating steam inside the evaporator. In such a plant, effective heat recovery may be desirable. This may be achieved by preheating the feed as much as possible by recovering heat from the exit streams.

Below is a numerical evaluation of four of the most popular arrangement configurations for the VC process. The comparison between these arrangements, which is the aim of this subsection, helps in selecting the most suitable plant type and configuration under the given conditions, Table (9.2).

The hot streams are cooled using feed/condensate and feed/brine heat exchangers in a parallel arrangement as Figure (9.4) shows, or in a sequence arrangement as shown in Figure (9.5). Alternatively, the hot exit streams are cooled by flashing under reduced pressure of one or more stages (5 stages are used in this study), and the released vapour used to preheat the feed stream, Figure (9.6), or by accommodating three effects between the discharge and suction sides of the compressor and using bleed, liquid/liquid feed heaters, Figure (9.7). The advantages of both multiple-effect evaporation and mechanical vapour compression are obtained by such a process. The compressed vapour volume flowrate is only about one third of a single effect VC system, this reduces the required compressor size significantly.

Table (9.6), summarizes the results obtained by the developed program for the design calculations for the above four arrangements.

Generally, heat recovery lowers the make-up steam requirement and reduces the evaporator area used for preheating. However, in this particular problem, it seems that because of the high equipment costs, saving in the required steam and evaporator area (with comparison with VC system without heat recovery, Table (9.4)) is not significant in the

Fig. 9.4. VC With Heat Recovery (parallel heat exchanger).

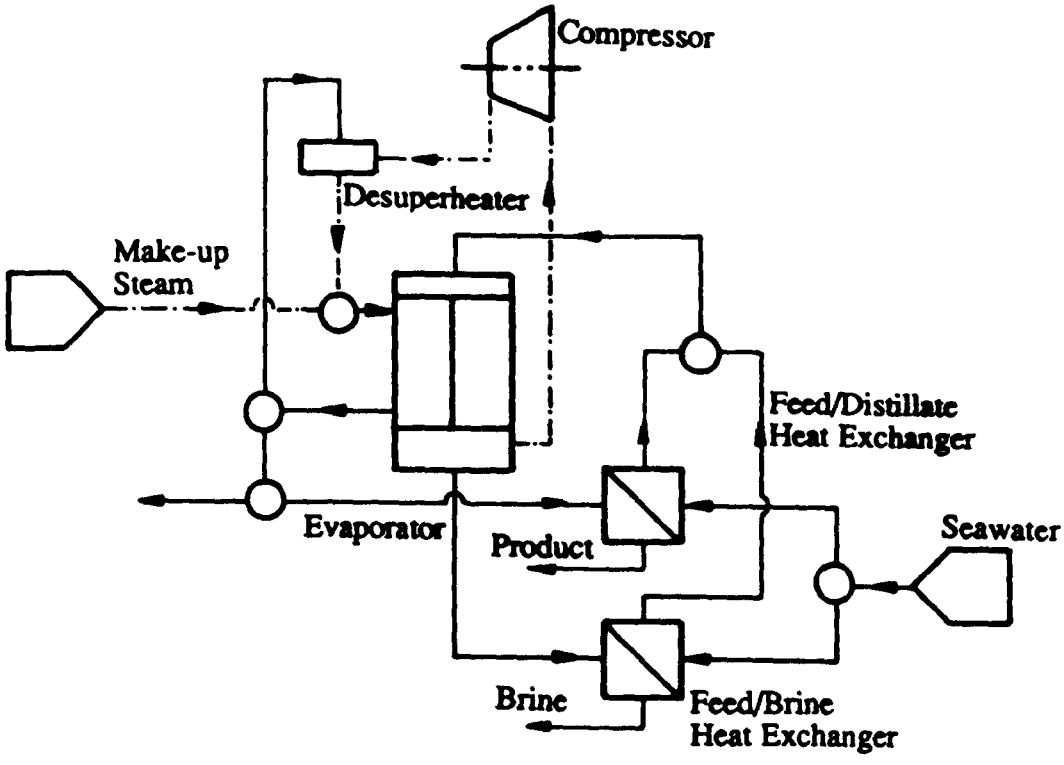

Fig. 9.5. VC With Heat Recovery (heat exchangers in sequence)

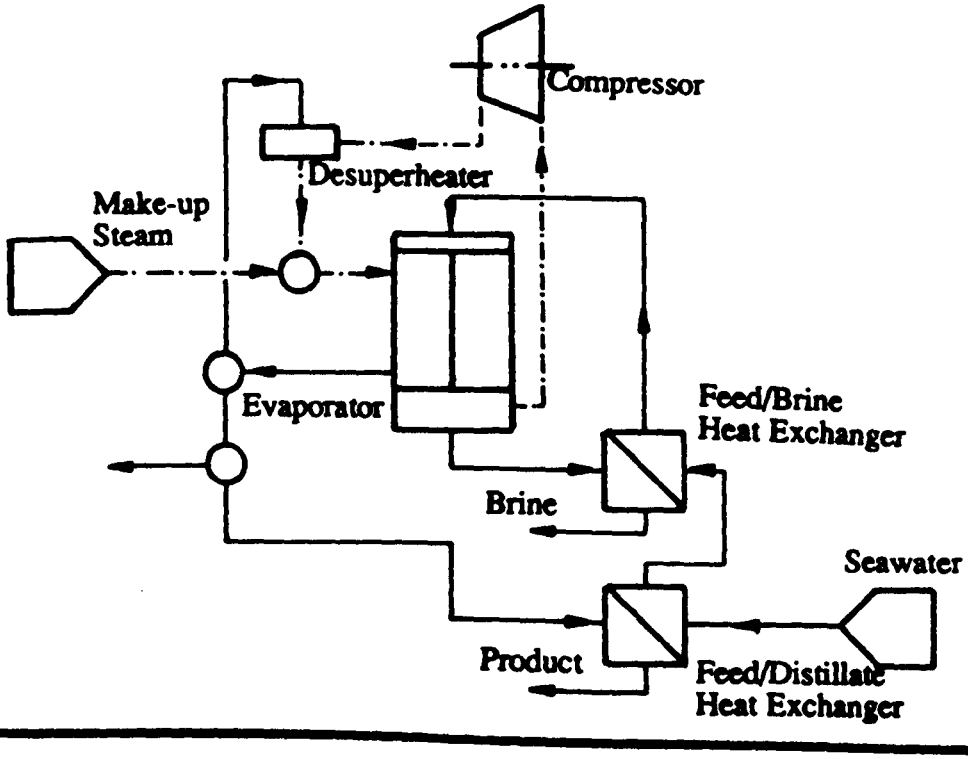

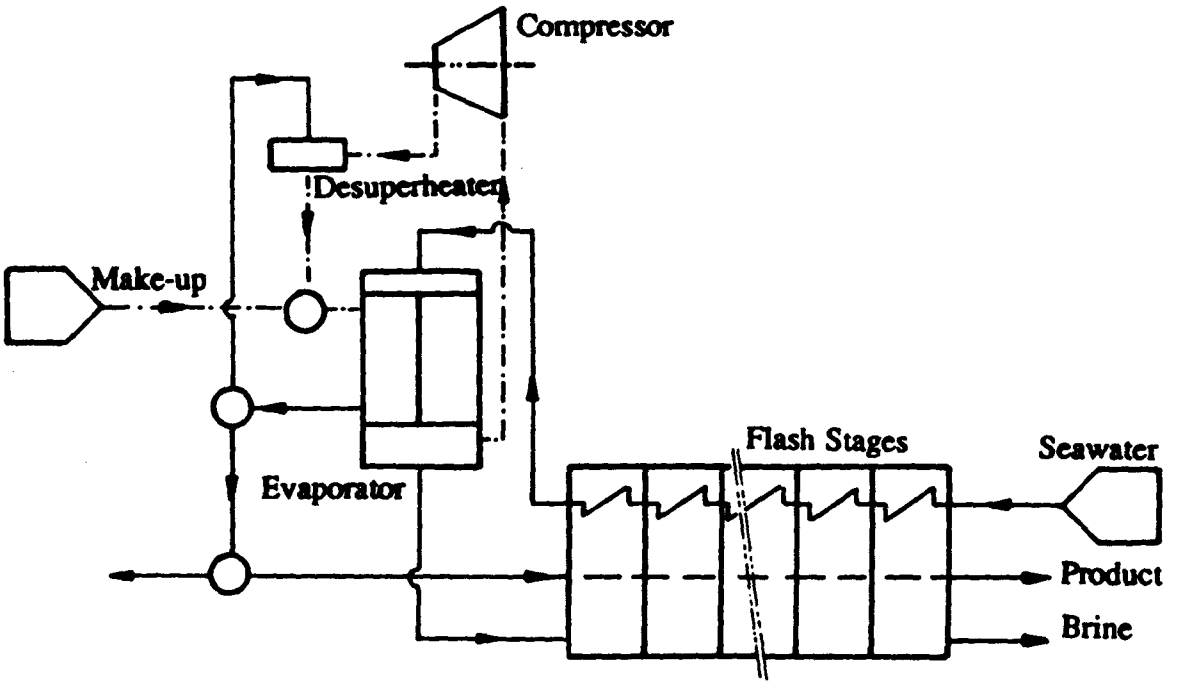

Fig. 9.6. VC/MSF System.

Fig. 9.7. 3 VTE/VC/heat Recovery System.

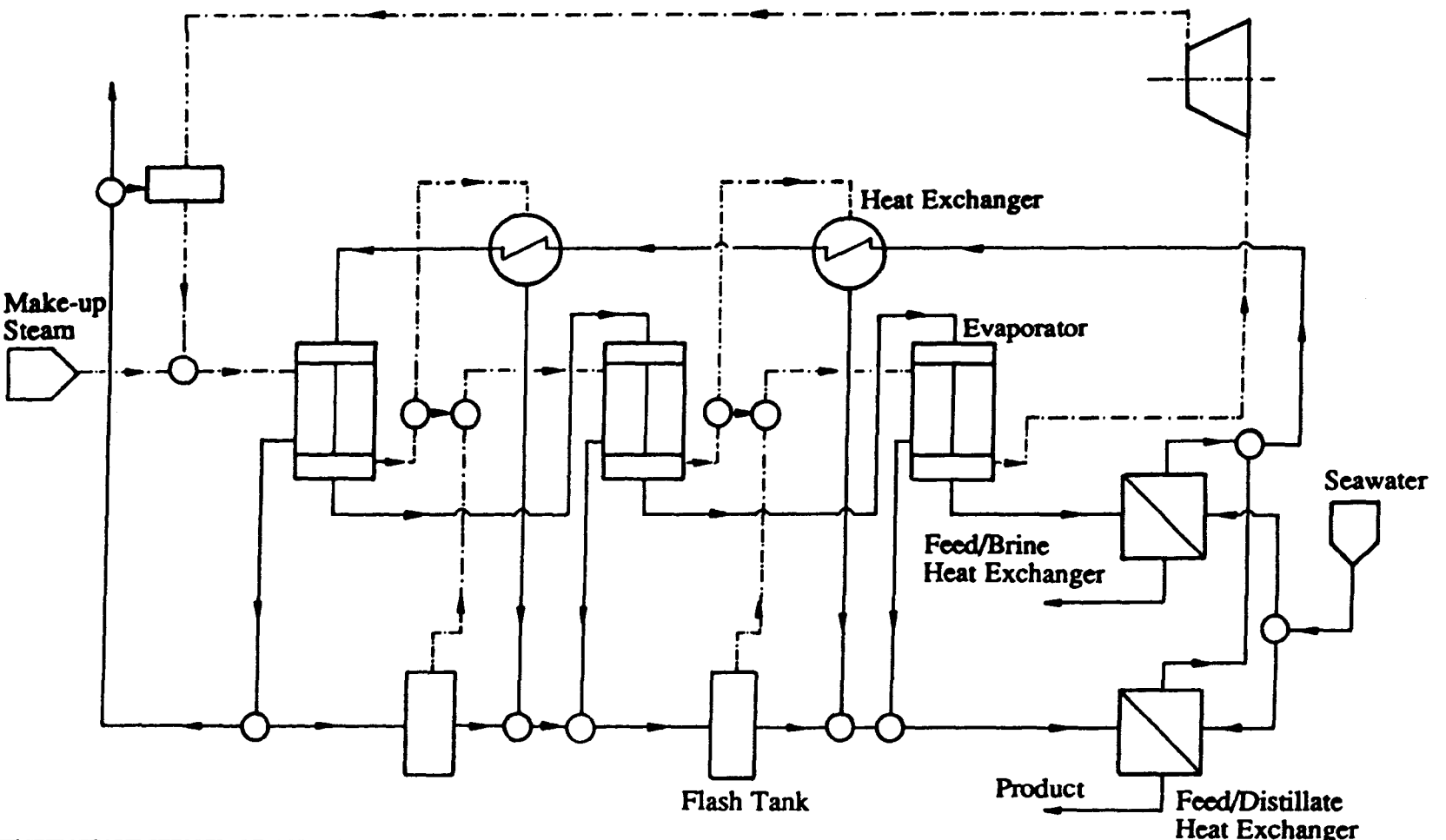

Table (9.6). Technical and Economical Comparison Between Four Different Configurations

Parameter	Fig.9.4		Fig.9.5	Fig.9.6	Fig.9.7
	α=0.5	α=0.6			
Evaporator area (m^2)	350.0	349.9	348.0	331.0	3*313.5
Compressor (BHP)	6434.0	6434.0	6434.0	6199.0	1818.0
Make-up steam x 10^{-3} (kg/hr)	2.24	2.12	1.7	0.645	6.3
Feed/distillate heat Exchanger area (m^2)	42.6	46.6	58.64	---	47.2
Feed/brine heat Exchanger area(m^2)	45.4	40.5	49.47	---	42.0
Flash stages Area (m^2)	---	---	---	87.9	---
Bleed heat exchanger Area (m^2)	---	---	---	---	87.4 169.6
Evaporation cost ($/ton)	3.7	3.69	3.67	3.52	2.3

where α : split ratio

first three configurations. On the contrary, the evaporation cost reduces significantly by the fourth configuration.

From the above discussion it may be concluded that: first, the examples in this subsection may show the flexibility and ease of use of the program in both defining and solving VC systems for a wide range of different configurations. Second, the results of the parameters affecting the evaporation cost, show the capability of the developed program to perform the first approximation for ΔT, number of effects, the plant configuration of vapour compression plant before making more precise estimations when exact design information may become available.

9.3. ENERGY IMPROVEMENT OF AN EXISTING MEE PLANT:

Since 1973, the world has grown more and more energy conscious. and in view of this, processes already applied have been investigated systematically, and existing plants configurations and/or construction have been reconsidered for the purpose of efficient use of energy.

In this section, the applicability of the developed program (using VTBVT technique) in this area will be exemplified by examining the transformation of an existing Multiple Effect Evaporator (MEE) process into Mechanical Vapour Compression (MVC) process. Also in this section, the economical feasibility of different proposed alternatives will be considered.

9.3.1. The Different Layouts

The arrangement of the basic layout uses the conventional multiple effect evaporation technology, while the proposed alternative flowsheets are based on vapour compression process. The concepts of these flowsheets are described below.

9.3.1.A. The Basic Flowsheet:

In the basic flowsheet Figure (9.8), the direction of the feed flow through the evaporation is forward. Seawater enters the plant as cooling water for the last condenser, part of it is discharged again to the sea after going through the condenser, and the remainder is circulated through the plant as distiller feed, heated on its way before entering the first evaporator in two liquid/liquid feed heaters and two bleed heat exchangers.

Presented in Table (9.7), are the design specifications of this flowsheet. This flowsheet was designed by Howe [1974]. Using the proposed VTBVT technique, it is designed after 14 iterations and 0.34 second CPU time.

The more significant design results for the basic flowsheet are tabulated in Table (9.8)

Consider the designed flowsheet as an existing plant. Then by performing the simulation calculations for this existing plant, the final results predicted by the design calculations are obtained (this point has been illustrated in more detail in section 8.4).

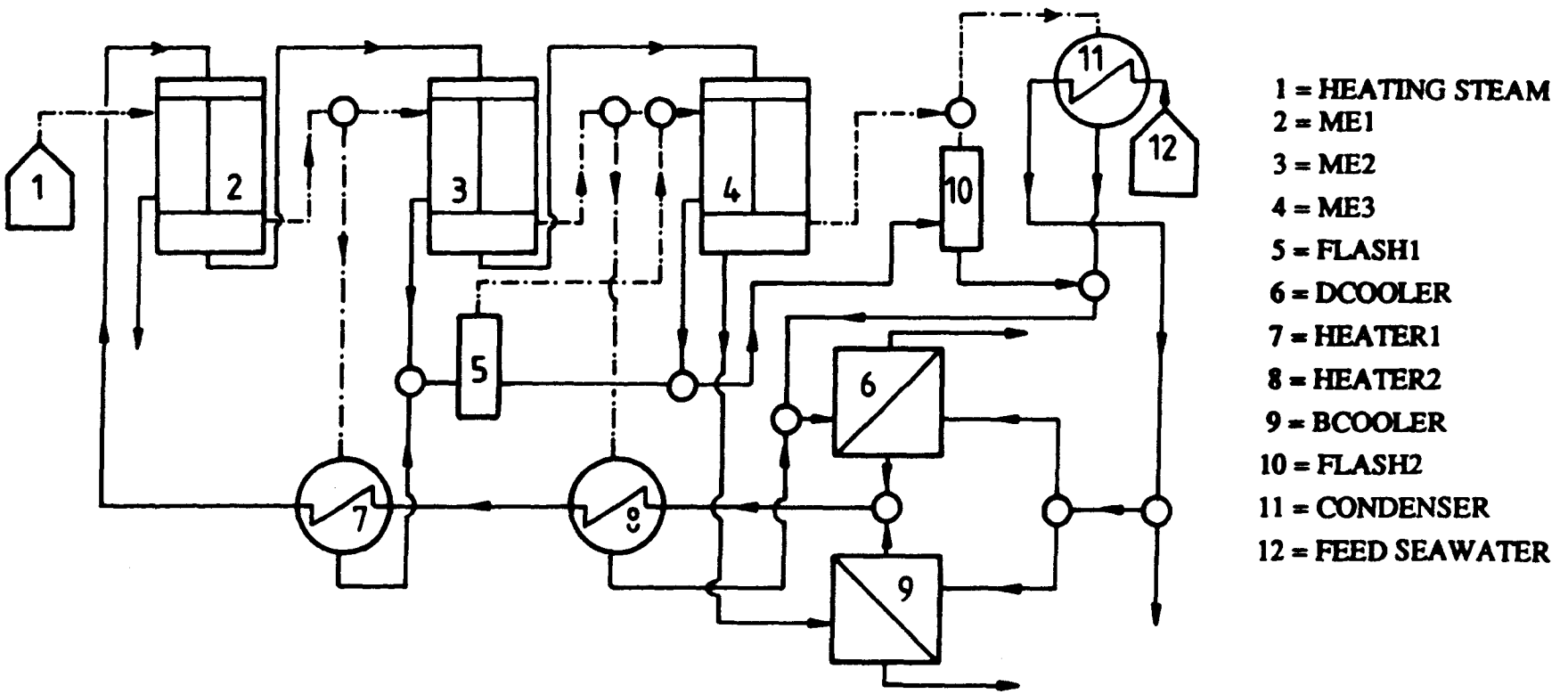

FIGURE 9.8. TRIPLE EFFECT DISTILLER PLANT (Basic Layout)

Table (9.7). Design Specifications Of The Triple Effect Distiller Plant

Heating steam temperature	381.483	K
Seawater feed temperature	294.26	K
Rate of product $\times 10^{-3}$	453.597	kg/hr
Feed salt concentration	3.5 %	
Brine concentration ratio	2.0	
Vacuum pressure in the last effect	88.036	kPa.
Heating steam pressure	137.896	kPa.
Feed water pressure	100.	kPa.

Heat Exchanger	Temp. approach.	U $kJ/m^2.K.hr$
heater1	4.44	7155.
heater2	5.27	7155.
condenser	21.38	7155.
Dcooler	9.94	6484.
Bcooler	9.94	5400.

From the next results it may be seen that: first, the feed seawater is about 22 times larger than the distillation production rate required. This may be because the MEE process (as all the thermal energy desalination processes) requires a large amount of cooling water to reject all input energy in excess of the minimum reversible separation energy to a heat sink (the sea), Dodge [1960], Genthner [1979]. Therefore, high pretreatment and pumping costs are required. Second, the required condenser heat transfer surface is nearly the same as the heat transfer area required by more than two effects. Thus high capital, operating and maintenance costs are the main characteristics of this flowsheet. Therefore, the following two alternatives are proposed as a possible way of improving an existing MEE economical performance.

Table (9.8)

Basic Flowsheet Significant Results

Unit Name	Δt (K)	Load*10^{-6} (kJ/hr)	U * 10^{-2} (kJ/m^2hr.K)	Area m^2
ME1	19.6	394.2	251.72	798.8
ME2	17.4	307.0	250.60	798.8
ME3	18.4	275.7	187.87	798.8
	LMTD	load ×10^{-6}	U	Area
Heater 1	11.4	69.64	7155	852.01
Heater 2	14.9	98.16	7155	923.33
Condenser	25.30	349.90	7155	1930.99
Bcooler			6484	126.21
Dcooler			5400	146.91

Steam Consumption × 10^{-3} = 176.42 kg/hr

Seawater flowrate × 10^{-3} = 10271.90 kg/hr

9.3.1.B. Alternative 1

Figure (9.9), shows the first alternative layout. A vapour compressor and a desuperheater unit are the only additional components to the basic plant. In the last condenser, a portion of the vapour stream is condensed giving the heat of condensation to the feed seawater stream. The remainder of the vapour stream is compressed polytropically (assuming 85% polytropic efficiency) to the saturation pressure of the heating steam, and then desuperheated in the desuperheater unit to the steam saturated temperature.

The areas of heat transfer and the overall heat transfer coefficients of all the units maintained, are equal to those of the basic flowsheet. While, the compressor horsepower and the required make-up stream for keeping up the basic plant production, are calculated. So, this problem may be considered as a partial design calculation (or a combination of simulation and design calculations), case 2 of Table (9.1). A converged solution for this alternative is

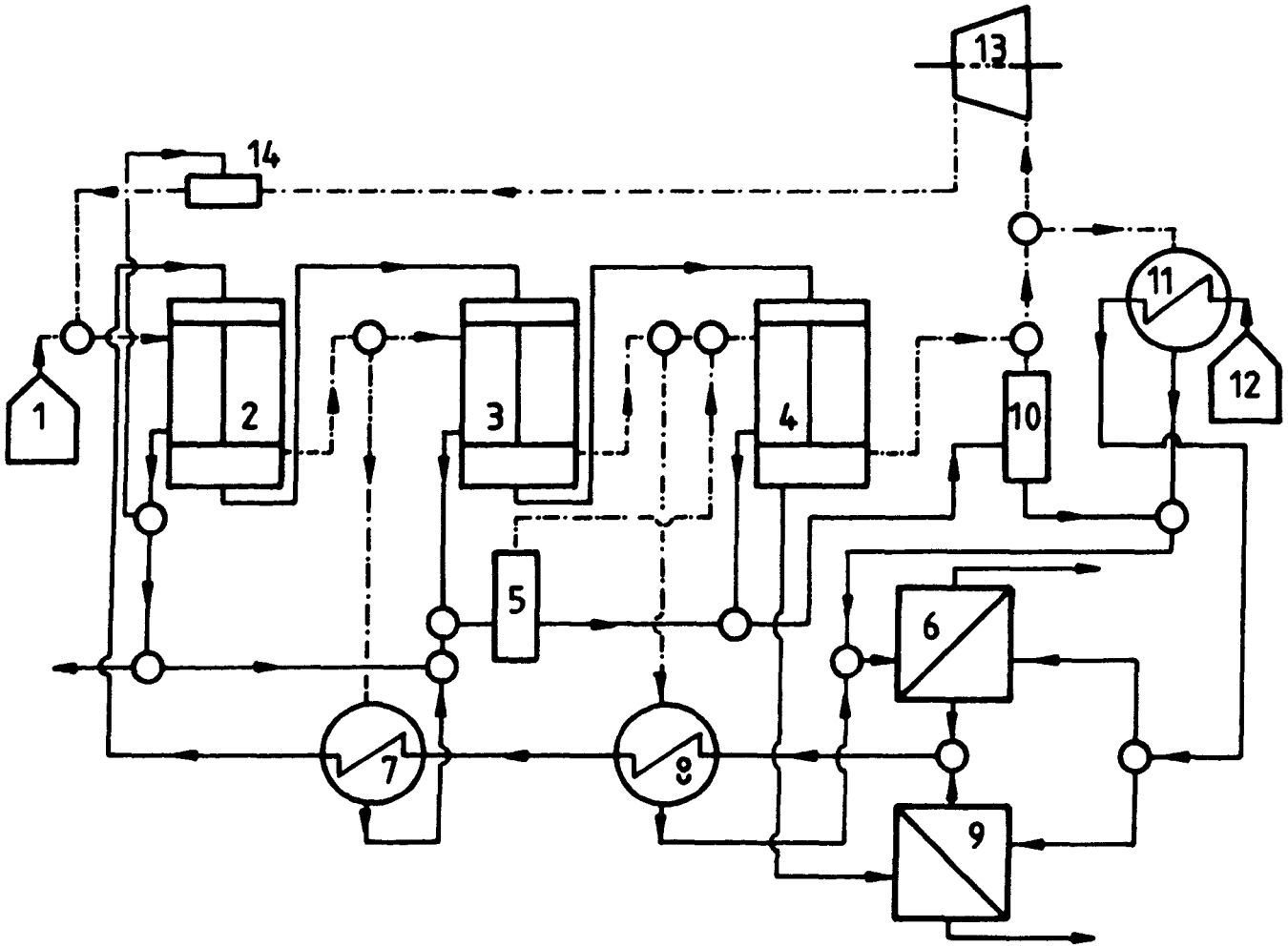

1 = HEATING STEAM
2 = ME1
3 = ME2
4 = ME3
5 = FLASH1
6 = DCOOLER
7 = HEATER1
8 = HEATER2
9 = BCOOLER
10 = FLASH2
11 = CONDENSER
12 = FEED SEAWATER
13 = COMP

FIGURE 9.9. ALTERNATIVE CONFIGURATION NO. 1.

obtained after 9 iterations, and 0.22 second CPU time. The main significant results are grouped in Tables (9.9,10,11)

9.3.1.C. Alternative 2

In this alternative, the last condenser in the previous alternative, Figure (9.9), is completely removed, and the feed seawater is pumped directly through the brine and distillate feed heaters. The layout of this proposal is shown in Figure (9.10). Using the VTBVT technique the final results are obtained after 11 iterations, and 0.27 second of CPU time. Some interesting results of this analysis are tabulated in Tables (9.9,10,11).

9.3.2. The Arrangements Comparison:

Comparison of the main evaluation criteria and operating costs for the respective processes are given in Tables (9.9,10,11). From these tables the following points may be deduced:

[1] The second alternative needs about one-thirteenth of the steam needed for the basic layout, however, the first alternative just requires about one-sixteenth of that amount.

[2] The pumped feed seawater to the first or the second alternatives represents only about 9% of that needed by the basic flowsheet, (existing plant).

[3] The exit temperatures (brine & distillate streams) for the proposed alternatives do not change significantly from those of the basic layout.

[4] In the basic layout about 97% of the energy costs is steam cost and about 3% is for auxiliary power cost. Regarding alternative 1, the steam cost represents only 38% of the energy running cost and the remaining 62% for the power cost. Likewise, the bulk of the running energy cost for the second alternative is for the power cost (83 %) and only about 17% for the steam cost.

[5] The specific energy running cost for both alternatives 1 and 2 are reduced by about 50% of that of the basic plant.

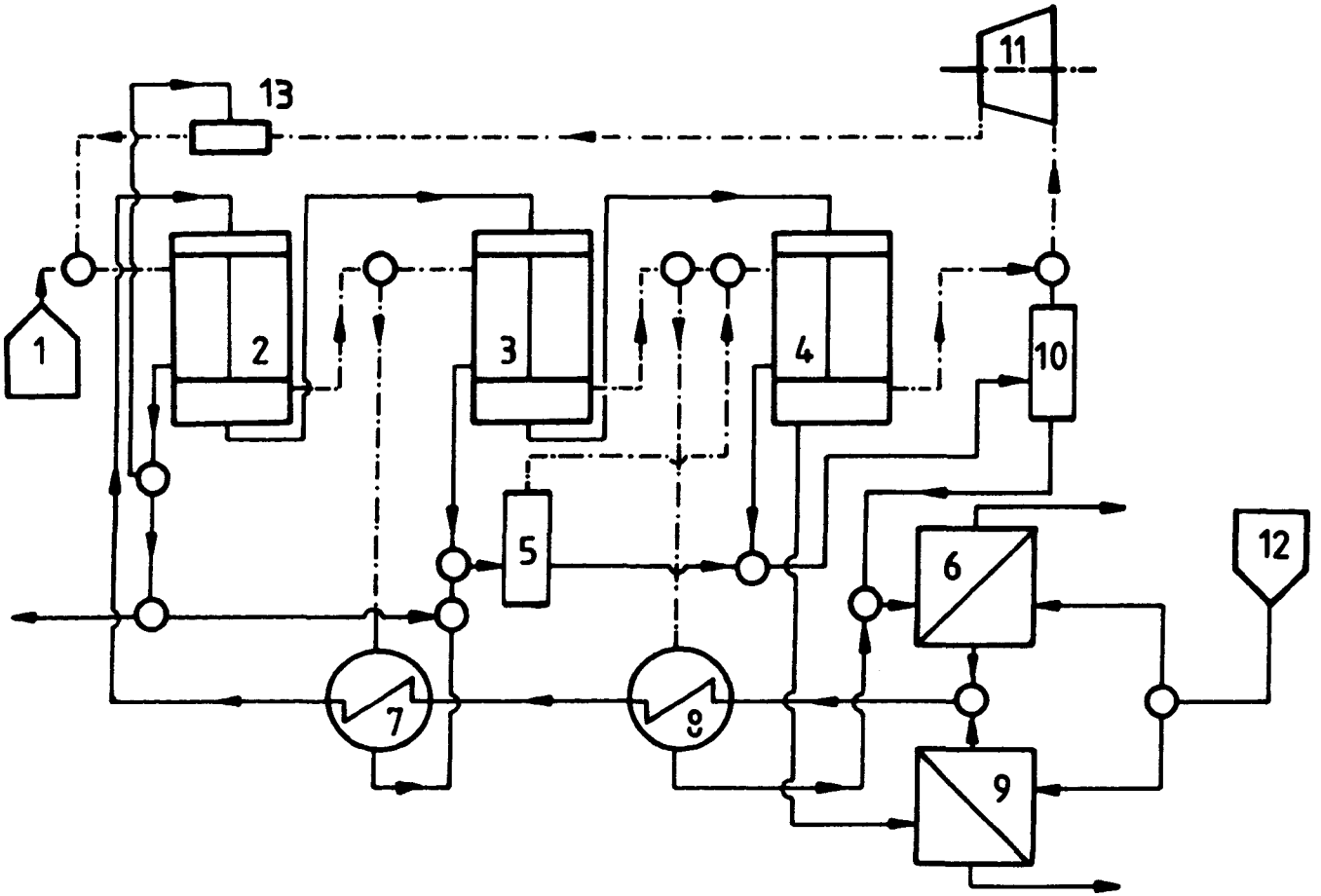

1 = HEATING STEAM
2 = ME1
3 = ME2
4 = ME3
5 = FLASH1
6 = DCOOLER
7 = HEATER1
8 = HEATER2
9 = BCOOLER
10 = FLASH2
11 = COMP

FIGURE 9.10. ALTERNATIVE CONFIGURATION NO. 2.

Table (9.9), Technical Data Of Studied Configurations

Feature Compared	Unit	Basic Layout	Alternative	
			1	2
Steam consumption x 10^{-3}	kg/hr	176.42	31.23	13.26
Seawater intake x 10^{-3}	kg/hr	10271.9	907.2	907.2
Reject cooling water x 10^{-3}	kg/hr	9364.67	--	--
Make-up seawater x 10^{-3}	kg/hr	907.2	907.2	907.2
Distillate output x 10^{-3}	kg/hr	453.6	453.6	453.6
Brine output x 10^{-3}	kg/hr	453.6	453.6	453.6
Compressed vapour x 10^{-3}	kg/hr		120.79	148.2
Salt concentration factor		2	2	2
Output brine temperature	K	318.6	324.6	316.
Output distillate temperature.	K	323.3	331.2	321.
Compressed vapour temperature.	K		620.7	624.3
Feed stream temperature to the first effect	K	356.8	358.86	356.5
Energy requirement for main drives	kW			
Feed seawater pump (H = 45 m)*		1064.	94.	94.
Distillate pump (H = 30 m)*		31.	31.	31.
Brine pump (H = 30 m)*		31.	31.	31.
Compressor			11351.	1396.
Total energy requirement		1126.	11507.	1412.

* Assumed total head

Table (9.10), Specific Values For The Studied Configurations

Value	Unit	Basic Layout	Alternative	
			1	2
Steam consumption/kg distillate	kg/kg	0.389	0.069	0.029
Seawater demand/kg distillate	kg/kg	22.600	2.000	2.000
Power demand/kg of distillate	kW/kg	2.480	25.360	31.140

Table (9.11), Operating Cost** For The Different Configurations

Item Compared	Unit	Basic Layout	Alternative	
			1	2
Steam cost	$/year	12,702,240.	2,248,560	954,720
Power Cost	$/year	360,320	3,682,240	4,519,680
Total Running Cost	$/year	13,062,560	5,930,800	5,474,400
Specific Energy Running Cost	$/ton	3.6	1.634	1.51

** Running Hours = 8000.0 hr/year
Assuming Steam Cost = 9.0 $/ton
Assuming Power Cost = 0.04 $/kw

9.3.3. Conclusion.

On the basis of the above discussion the following two points may be concluded: first, vapour compression technique aims specifically at improving the plant overall energy efficiency by reducing (or eliminating) the required cooling water and the make-up steam consumption. As a result, significant reduction of the running cost can be achieved. Second, vapour compressor can be installed in an existing MEE plant with a minimum of modification and thus a limited capital overcost.

9.4. DESIGN OF A COMBINED VTE/VC/MSF SYSTEM.

Combined VTE/VC/MSF systems have the advantages of: first, higher process temperature, because seawater is usually at its minimum concentration when the temperature is maximum (in VTE system); second, more favourable heat exchange in (MSF) part, because the feed seawater is preheated in more stages than is commonly used in the VTE process. Thus heat is transferred at a higher temperature differential, and consequently, less heat transfer surface is required for the feed heating. Third, high performance ratio, which is achieved by the vapour compressor unit. Therefore, the energy requirements and the capital investments for combined VTE/VC/MSF process are reduced significantly in comparison with processes using VTE or MSF process on their own.

A VTE/VC/MSF system was studied by the U.S. Office of Saline Water, Hunter [1968]. A simplified flowsheet for this plant is shown in Figure (9.11). As shown in this flowsheet, a waste heat boiler recovers the heat from gas turbine exhaust. Steam at two energy levels is generated. One level is low pressure saturated vapour and the other high pressure superheated steam. The latter is used to drive a back pressure steam turbine, which is coupled to an electric generator producing all the required auxiliary power for the facility. The exhaust steam from the back pressure turbine is combined with the steam from the lower pressure boiler. This steam is used as the heat input to the first effect in the desalination plant, see chapter 2 for more details.

Using the developed program (with the proposed VTBVT technique), many configurations of this type can be computed, various modifications can be tried, and the sensitivity of the process economics to design and operating parameters can be determined. Here, the design calculation for the desalination part of the configuration shown in Figure (9.11), is demonstrated. Also, the effect of the unit heat losses on the plant design results is considered.

9.4.1. The Problem Size.

A total of 239 equations are required to model this flowsheet. This number consists of the linearized mass and energy balance equations generated by the unit subroutines, (228 equations), and the design specifications of the plant, (11 equations). Table (9.12), shows the number of equations, variables, and degrees of freedom for the component, the temperature, and the pressure matrices.

FIGURE 9.11 A COMBINED VTE/VC/MSF SYSTEM.

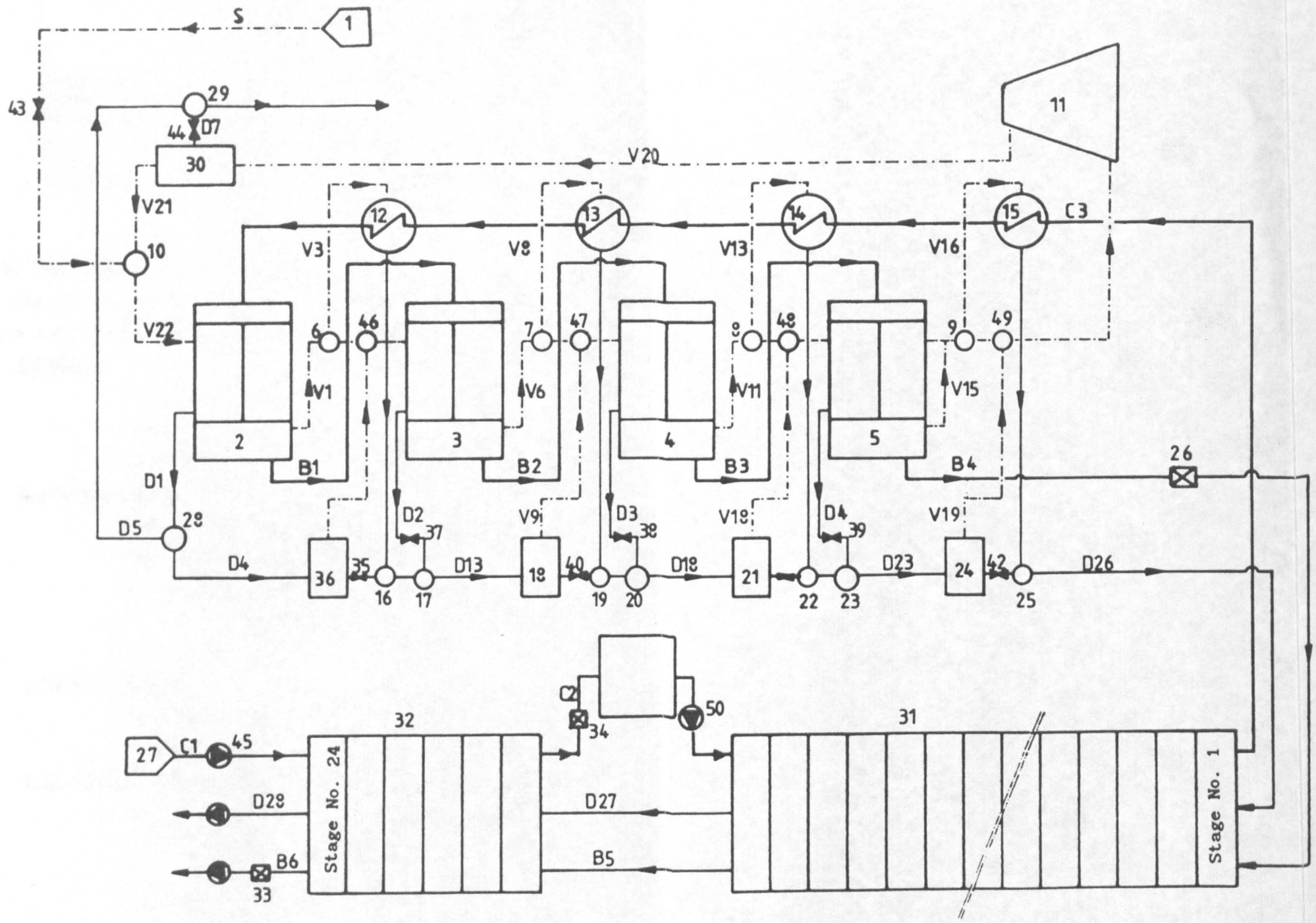

1 = STEAM
2 = VTE1
3 = VTE2
4 = VTE3
5 = VTE4
6 = SP4
7 = SP5
8 = SP6
9 = SP7
10 = MX2
11 = COMP
12 = HEX1
13 = HEX2
14 = HEX3
15 = HEX4
16 = MX3
17 = MIX4
18 = FT2
19 = MX5
20 = MX6
21 = FT3
22 = MX7
23 = MX8
24 = FT4
25 = MX9
26 = CS1
27 = FEED
28 = SP2
29 = SP3
30 = DSUB
31 = REC
32 = REJ
33 = TS3
34 = TS2
35 = VL1
36 = FT1
37 = VL2
38 = VL3
39 = VL4
40 = VL5
41 = VL6
42 = VL7
43 = VL8
44 = VL9
45 = PUMP1
46 = MX10
47 = MX11
48 = MX12
49 = MX13
50 = PUMP2

Table (9.12). The model equations, variables, and degrees of freedom

Matrix	No. of Generated Equations	No. of Variables	Degrees of Freedom	No. of Specified Variables
Component	88	92	4	4
Temperature	107	112	5	5
Pressure	33	35	2	2
Total	228	239	11	11

9.4.2. The Plant Design Specifications.

The following design specifications and parameters are applied to have a consistent number of variables and equations.

1. Feed:

Flowrate $\times 10^{-3}$	= 2267.962	kg/hr
temperature	= 297.04	K
Concentration	= 3.5 %	

2. Brine stream:

Max. brine Temperature	= 394.905	K
Blowdown temperature	= 307.48	

Brine concentration factors;

max. VTE	= 2.	(i.e.7 %)
max. MSF	= 2.26	(i.e.7.91 %)

3. Make-Up steam:

Pressure	= 232.1	kPa
Temperature	= 398.15	K

4. Equipment design parameters and characteristics:

A. Compressor:

polytropic efficiency	= 0.83	
suction pressure	= 137.075	kPa

B. Heat Exchanges:

Heat Exchanger (unit number)	Δ Tapproach
12	4.22
13	4.34
14	4.50
15	4.61

ID = 7/8 in (=0.022225 m)

OD = 0.791 in (=0.02009 m)
Velocity = 6584 m/hr
Tube Length = 18 ft (5.4864 m)
material : 90-10 Cu-Ni

C. MSF unit:

OD = 5/8 in (= 0.015875 m)
ID = 0.014097 m
length/stage = 2.792 m
Velocity = 7 ft/sec (7680.96 m/hr)
Material : 90-10 Cu.Ni

D. Assumed Heat Losses (percentage of the heat input to the unit):

VTE = 0.1 % /unit
MSF = 0.35 % /stage
Heat exchanger = 0.02% /unit

9.4.3. The Numerical Aspects Of The Problem:

The iterative solution is started with a poor initial temperature approximations, and the convergence behaviour during the solution is observed. On one hand, the differences between the calculated and the estimated values of the MSF section dependent variables are reduced on every iteration. The error (equation 7.1) reduces almost exponentially with increasing the iteration number, see Fig.(9.12). The converged solution for this section is achieved after five iterations, and 0.71 sec. CPU time. On the other hand, the convergence of the dependent variables of the VTE section of the plant is observed to be slow. Fourteen iterations and 1.65 sec. CPU time, are required to reach the final answer. This may be due to the fluctuation of the results during the first five iterations. This is illustrated by Fig.(9.13-a,b). In both sections (i.e. MSF and VTE) the calculated heat transfer area converges because of the convergence of the other dependent variables of the section. See Table (9.13). Therefore, for this particular flowsheet the iterations are terminated as soon as the VTE dependent variables converge, equation (8.1).

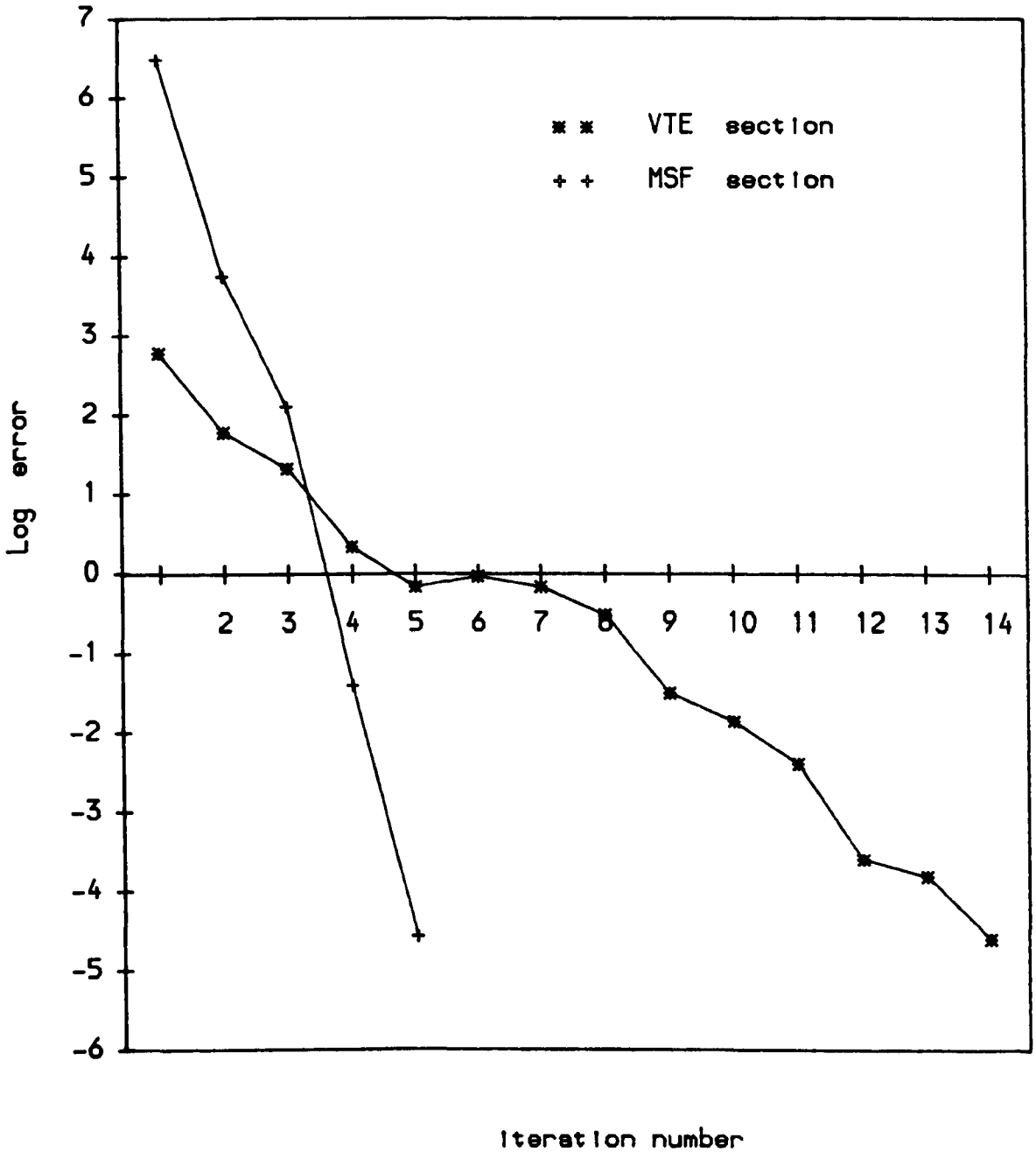

FIG. (9.12) COMPARING THE CONVERGENCE BEHAVIOUR OF THE VTE AND MSF SECTIONS OF VTE/VC/MSF PROCESS

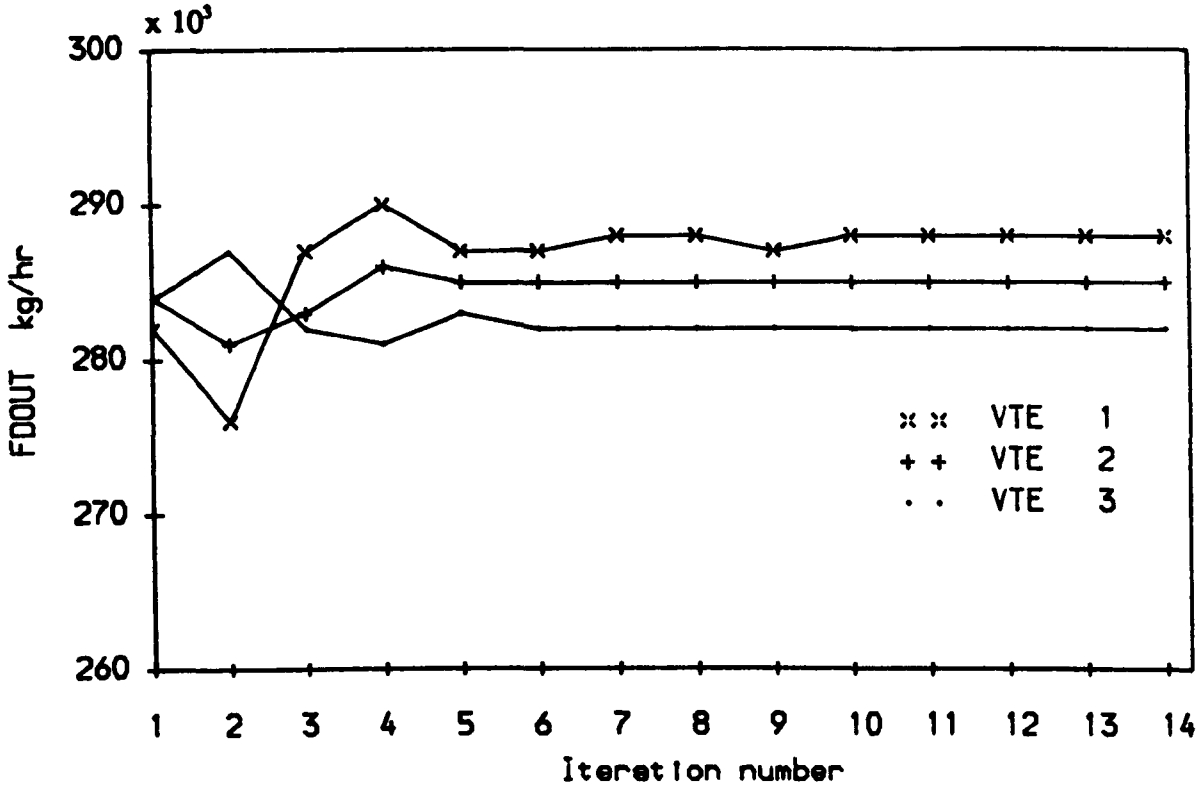

FIG. (9.13,a) CONVERGENCE OF DISTILLATE FLOWRATE OUT OF FIRST, SECOND AND THIRD EVAPORATOR

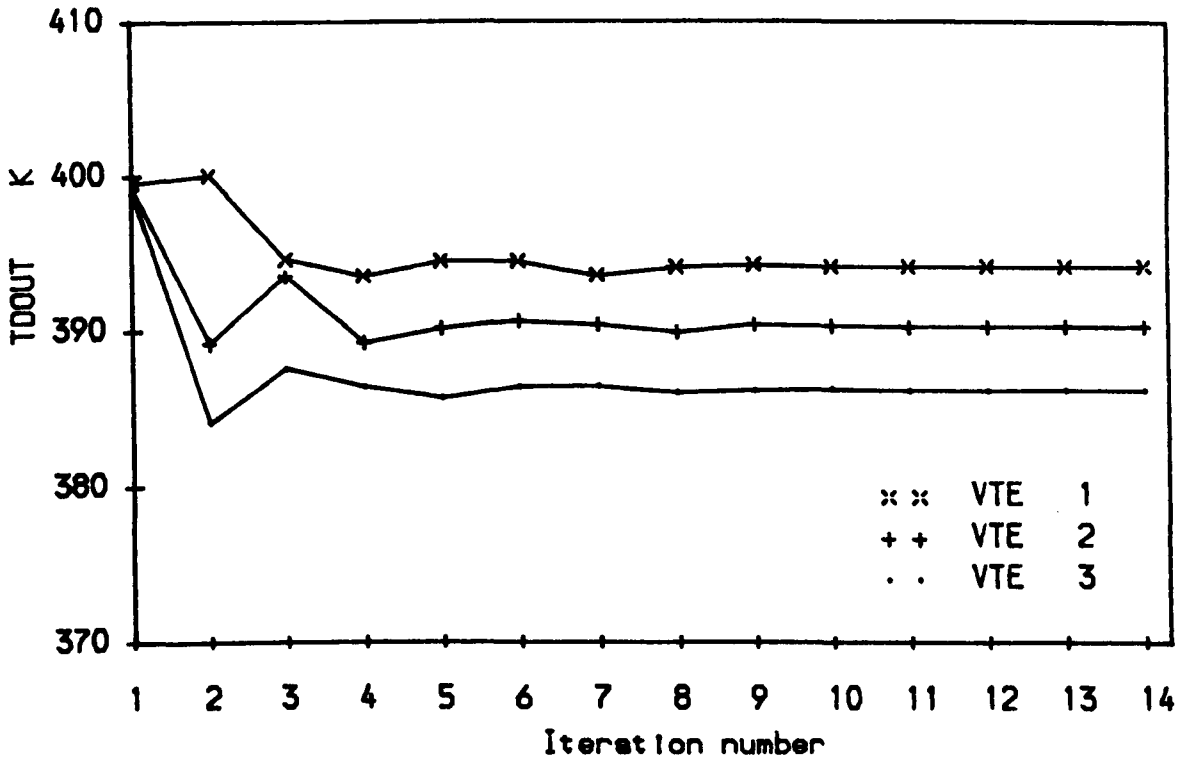

FIG. (9.13,b) CONVERGENCE OF THE DISTILLATE TEMPERATURE OUT OF FIRST, SECOND AND THIRD EVAPORATORS

Table (9.13)

Heat Transfer Area of VTE & MSF Units Convergence Behaviour

Unit Iteration	VTE	MSF Recovery	MSF Rejection
1	956.50	1998.00	736.00
2	6990.65	474.40	453.10
3	-6645.83	374.60	453.09
4	-7221.44	374.68	453.06
5	6682.86	374.67	453.06
6	6679.82	374.68	453.07
7	6838.97	374.67	453.06
8	6779.80	374.68	453.07
9	6771.06	374.67	453.06
10	6786.82	374.68	453.07
11	6783.45	374.67	453.06
12	6781.07	374.68	453.07
13	6782.77	374.67	453.06
14	6782.67	374.68	453.07

9.4.4. The Numerical Results.

The calculated variables for all the plant streams are presented in the computer print out, Appendix (G). Also, the internal stream variables of the MSF section are given in Table (9.14). The calculated heat transfer areas for VTE, heat exchangers and the power required by the compressor are provided in Table (9.15).

Table (9.14). The area of heat transfer and the internal Stream Variables of The MSF Section

St No	TCOUT [K]	TDOUT [K]	TBOUT [K]	FDOUT x10^{-3} [kg/hr]	FBOUT x10^{-3} [kg/hr]	BPR [K]	CORR [K]	TTD [K]	LMTD [K]	QLOAD x10^{-3} [kJ/hr]	AREA [m^2]	U [kJ/hr. m^2.K]
1	372.69	378.28	379.82	1140.27	1127.68	1.25	0.28	5.59	7.17	31505.75	374.68	11728.38
2	369.25	374.83	376.38	1146.77	1121.19	1.24	0.32	5.57	7.14	31268.91	374.68	11680.73
3	365.84	371.40	372.98	1153.14	1114.82	1.22	0.36	5.56	7.12	31013.98	374.68	11628.99
4	362.45	367.99	369.60	1159.38	1108.57	1.20	0.40	5.54	7.09	30741.96	374.68	11573.19
5	359.09	364.61	366.25	1165.51	1102.45	1.19	0.45	5.52	7.06	30455.21	374.68	11513.37
6	355.76	361.26	362.94	1171.50	1096.46	1.17	0.50	5.51	7.03	30156.05	374.68	11449.57
7	352.45	357.94	359.66	1177.37	1090.58	1.15	0.56	5.49	7.00	29841.57	374.68	11381.94
8	349.19	354.66	356.41	1183.12	1084.83	1.14	0.62	5.47	6.96	29515.76	374.68	11310.46
9	345.95	351.40	353.20	1188.75	1079.21	1.12	0.68	5.45	6.93	29178.79	374.68	11235.21
10	342.75	348.19	350.03	1194.26	1073.70	1.10	0.74	5.44	6.90	28832.90	374.68	11156.24
11	339.59	345.00	346.90	1199.64	1068.32	1.09	0.81	5.42	6.86	28476.83	374.68	11073.65
12	336.46	341.86	343.81	1204.90	1063.05	1.07	0.87	5.40	6.83	28112.56	374.68	10987.49
13	333.37	338.76	340.75	1210.05	1057.91	1.06	0.94	5.38	6.79	27742.65	374.68	10897.78
14	330.33	335.69	337.74	1215.08	1052.88	1.04	1.01	5.37	6.76	27365.19	374.68	10804.66
15	327.32	332.67	334.77	1220.00	1047.96	1.03	1.08	5.35	6.72	26981.34	374.68	10708.18
16	324.35	329.69	331.84	1224.80	1043.16	1.01	1.15	5.33	6.69	26593.76	374.68	10608.38
17	321.43	326.75	328.96	1229.48	1038.48	1.00	1.22	5.32	6.66	26202.16	374.68	10505.38
18	318.55	323.85	326.12	1234.06	1033.90	0.98	1.28	5.30	6.62	25805.32	374.68	10399.29
19	315.71	320.54	322.87	1239.26	1028.69	0.97	1.36	4.84	6.32	29520.13	453.07	10307.05
20	312.46	317.29	319.68	1244.33	1023.63	0.95	1.44	4.83	6.29	29016.36	453.07	10174.73
21	309.26	314.09	316.55	1249.26	1018.70	0.94	1.52	4.83	6.27	28507.61	453.07	10038.39
22	306.12	310.95	313.47	1254.06	1013.90	0.92	1.60	4.83	6.24	27995.12	453.07	9898.18
23	303.04	307.87	310.45	1258.72	1009.23	0.90	1.68	4.83	6.22	27480.22	453.07	9754.23
24	300.01	304.84	307.48	1263.26	1004.70	0.89	1.75	4.83	6.19	26962.81	453.07	9606.74

Table (9.15)
Calculated Heat Transfer Areas For VTE and Heat Exchangers

A. VTE units

Unit	$U*10^{-2}$ $kJ/m^2.hr.K$	ΔT K	Load $*10^{-9}$ kJ/hr	Area m^2
VTE1	308.18	3.25	0.678	6782.7
VTE2	301.53	2.94	0.600	6782.7
VTE3	294.54	3.01	0.600	6782.7
VTE4	287.04	3.09	0.600	6782.7

B. Heat Exchanger Units

Unit	$U*10^{-2}$	LMTD	Load$*10^{-8}$	Area
Hex 1	152.83	6.00	0.373	406.0
Hex 2	151.76	6.22	0.394	417.1
Hex 3	150.44	6.49	0.416	426.3
Hex 4	149.22	6.63	0.421	426.2

C. Compressor Unit

Volume flowrate: $339.137 * 10^3$ m^3/hr

Work : $13.6 * 10^3$ HP

9.4.5. Thermal losses effects:

In the above section, the thermal losses due to venting, heat transfer through walls of equipment, and other unaccounted for losses are considered by assuming that: 0.1 %, 0.35 %, and 0.02 % of the heat input to each VTE, MSF, and heat exchanger unit respectively are removed by the thermal losses, Hunter [1968]. Here the effect of neglecting (or eliminating) these thermal losses on the calculated results will be illustrated. Table (9.16) shows the impact of these losses on the main parameters of the plant.

As indicated in the next table, the steam economy and the capital cost of the plant may be improved by using an effective heat insulation and by elimination of heat losses through the leakage, and inefficient, or badly operated air vents. Neglecting such simple precautions to avoid

losses will obviously reduce the advantages gained by the hybrid VTE/VC/MSF system.

Table (9.16)

Effect of Thermal Losses on the Calculated Parameters

Parameter	Considering heat losses	Without heat losses
steam consump. $\times 10^{-3}$ kg/hr	27.16	19.85
MSF area (m^2)		
Recovery sect.	375.0	423.7
Rejection sect.	453.0	461.7
Hex 1 area, m^2	406.0	402.6
Hex 2 area, m^2	417.0	413.0
Hex 3 area, m^2	426.0	421.9
Hex 4 area, m^2	426.0	341.7
VTE area (m^2)	6783.0	6834.0
Compressor (BHP) $*10^{-3}$	13.6	13.9

9.5. CONCLUSION:

From the results and information presented in this chapter the following points may be concluded:

[1] The temperature difference ΔT, (and consequently compression ratio) is one of the decisive design variables. For an economic VC process ΔT should be as small as possible. It should compensate for: the temperature difference for heat transfer, various pressure drop, and the boiling point elevation.

[2] Energy economy obtained by multiple effect evaporation can often be equalized in a single effect compression evaporation system.

[3] In the particular case studied, using feed/condensate & feed/brine heat exchangers in parallel or in sequence as heat recovery units

with VC unit reduces the evaporation cost slightly. By contrast, using 3 effect evaporators as well as bleed and liquid/liquid heat exchangers configuration reduces the evaporation cost significantly.

[4] Vapour compression may be used in new plants or to improve efficiency in existing plants. Generally, this process has its economical attraction, because:

A- No or little cooling water is needed, so less pumping power and chemical treatment costs are required.

B- Its high performance ratio, since a minimum amount of energy is usually needed.

C- Small specific heat transfer area (m^2/kg), thus a small capital cost is required, and a compatible size of plant.

[5] The example problems presented in this chapter have shown the applicability of the developed program to design and simulate a hybrid distillation system. About the program and the proposed VTBVT technique, the following points may be deduced:

A- The developed package is a powerful tool for quickly evaluating a great number of possible different arrangements and/or different values of design parameters, which aims at improving the economy of existing (or being designed) plants.

B- Performing the parametric calculations using the program shows that the proposed VTBVT technique may be adopted to optimization calculations, since each step in many optimization processes is simply the redetermination of evaporation cost after a parametric change.

C- Using the developed program, dimensions with sufficient accuracy for hybrid process units (e.g. VTE/VC and/or VTE/VC/MSF) can be obtained. This enables the process to be costed, and manufactured or to confirm that the detailed dimensions of an existing plant units are adequate for a proposed new duty.

D- The program has proved to have excellent convergence characteristics for solving complex systems of inter-linked different evaporation devices.

CHAPTER 10

CONCLUSIONS AND FUTURE WORK

Arid and many non-arid areas are facing water shortage problems. Desalting of seawater is one of the main techniques to overcome these problems. The distillation process is one of the most practical and economical technique for desalting seawater.

There is a wide range of types and configurations for distillation process. Better understanding of the process performance and the interaction of various operating and design variables can be achieved by performing flowsheeting calculations for the process. A specialized flowsheeting program for performing design and simulation calculations for thermal desalination processes is developed in this work.

The sparsity and weak nonlinearities of the unit equations are among the characteristics of the distillation process mathematical models. A new numerical approach for solving these mathematical models is developed in this work. This approach takes into account the above characteristics of the distillation process mathematical models. This new approach has been referred to as: the Variable Type By Variable Type [VTBVT] approach. A full analysis of the mathematical bases of this new approach has been made in chapter 5.

The performance of the developed program using the proposed VTBVT approach for solving different distillation processes is assessed in chapters 7, 8, and 9. High reliability, fast convergence, flexibility, and generality are among the main characteristics of the package and the VTBVT approach. These points may be illustrated as follows:

- The program showed sufficient *flexibility* by solving different thermal desalination problem. Each of these problems can be solved using different combinations of specifications. In other words, the input and the problem do not have to be in a rigid form for the program. This may be illustrated by Tables (7.2), (8.10) and (9.1) for example.

  Because of this flexibility, the dependent and independent variables can be exchanged. Therefore many questions about the

operation can be answered, and different types of calculations can be performed.

- Practical flowsheeting problems may require the solution of simultaneous systems of many hundreds of equations. Using the proposed VTBVT approach, a large problem may become a number of small problems (according to the variable type), therefore, the *memory* required for the problem must be considerably reduced. Also, the computer *CPU time* is reduced because of the reduction of the mathematical operations. This fact is confirmed by the numerical results in sections 7.6.1 and 8.4.3 where the comparison of the total CPU times shows that the solution by VTBVT technique requires about one fifth and one third of that required by Newton's method (ignoring the differences in hardware) for solving FICHTNER MSF and ten MEE processes respectively.

  In brief, the computation using the developed program and the proposed technique uses reasonable amount of computer time, memory, and other resources.

- Robustness (or reliability) is the third most important property of the developed package using the proposed approach. If the iterative solution of a mathematical model using a numerical technique can be achieved from a wide range of the initial guesses, this technique is said to be "*robust*". The *robustness* of the proposed VTBVT approach is examined for different flowsheets and different types of calculations in sections 7.3.2 & 7.4.1 and Appendix {F}. These numerical results have demonstrated the robustness of the VTBVT approach.

- The developed specialized flowsheeting program has also shown its *generality* through the chapters number 7, 8, and 9 where results are discussed. These chapters show the capability of the developed program to perform design and simulation calculations for different thermal desalination process types with different configurations.

- The results *reproducibility*, and the program output *accuracy* are examined in sections 7.4.3 and 8.4.3. This is achieved by comparing the final results of the design and simulation calculations for MSF and MEE processes respectively. Also, the *validity* of the results of the same processes is examined in sections 7.6.2 and 8.4.3. This is achieved by comparing the final results of the VTBVT and Newton techniques. Furthermore, the final results of "FICHTNER" plant using The VTBVT approach and that obtained by Homig [1978],

using the stage to stage technique are compared to examine the validity of the proposed technique, see section 7.7. In all the above comparisons, the numerical results have indicated a very good agreement. This may illustrate the validity, reproducibility, and accuracy of the results.

- As illustrated in chapter 6 and Appendix (D), the data input file is easy to develop, and the output report is clearly identified, understandable , and complete. Therefore, one may summarize that the developed program is *easy to use.*
- Because of the modular structure of the program, as shown in chapter 6. New features and functions can be added and most changes can be made in the program with modest effort. So, the program is *expandable and modifiable.*

As a whole, the developed program and the proposed VTBVT technique have proved to be valid for more work. And the following idea can be implemented.

Points For Future Work.

- Corrosion problems, scale formation, and low efficiency of energy utilization are among the main practical problems in the thermal desalination processes. By adding mathematical models representing the decarbonator, the deaerator, the vacuum system, and the degassing units, to the mathematical model library developed in this work, more accurate information about the concentration of the noncondensable gases (i.e. O_2 and CO_2) can be obtained. Hence, the scale formation and the corrosion problems can be controlled, and the overall plant efficiency can be improved.
- Because of the convergence characteristics of the proposed VTBVT technique (e.g. stability, rapid convergence), "*optimization*" calculations can be added to the capability of the developed program. By these calculations the design variables can be improved during the iteration, until a further significant improvement in the objective function is considered to be unlikely.
- Manual control dominates the operation of the thermal desalination processes. Very little information has been published in the area of the computer control for these processes. Therefore, it might be worthwhile to further investigate computer control developments in these processes.

APPENDIX A

PHYSICAL & THERMODYNAMIC AND HEAT TRANSFER COEFFICIENT CORRELATIONS

A.1. Physical And Thermodynamic Correlations.

From the analysis presented in Chapter 3 it may be noted that, values of the physical and thermodynamic properties of seawater brine, pure water and steam should be calculated as a complementary part of the mathematical models. Outlined below are the relationships used to calculate these properties. Some of these relationships are specific in ft.lb.Sec. units. In this case the results are converted into SI units before returning to the calling routine.

A.1.1. Density Of Seawater:

Knowing the temperature and salt concentration of brine seawater, the density is calculated by the equation given by Homig [1978]. The equation is applicable in the temperature range of 10 to 180 C and for salinity from 0 to 160 g/kg.

$$\rho = \frac{1}{2} \times a_0 + a_1 \times Y + a_2 \times (2 \times Y^2 - 1) + a_3 \times (4 \times Y^3 - 3 \times Y) \qquad (A.1)$$

where:

$$a_0 = 2.016110 + 0.115313 \times \sigma + 0.000326 \times (2 \times \sigma^2 - 1)$$
$$a_1 = -0.0541 + 0.001571 \times \sigma - 0.000423 \times (2 \times \sigma^2 - 1)$$
$$a_2 = -0.006124 + 0.00174 \times \sigma - 0.000009 \times (2 \times \sigma^2 - 1)$$
$$a_3 = 0.000346 + 0.000087 \times \sigma - 0.000053 \times (2 \times \sigma^2 - 1)$$

$$Y = \frac{2\,t - 200}{160} \qquad \sigma = \frac{2\,X - 150}{150}$$

ρ : density , kg/m^3 t : temperature C

X : total salt content g/kg

The density of pure water is calculated from this equation by setting X = 0

A.1.2. Dynamic Viscosity Of Seawater:

The brine viscosity is represented as a function of temperature and salt concentration by Homig [1978], using the following correlation. The validity range of this correlation is 10 - 150 C and 0 - 130 g/kg salt concentration.

$$\mu = \mu_w \times \mu_R \qquad (A.2)$$

where:

μ_w : viscosity of pure water

μ_R : relative viscosity, (= 1. for pure water & > 1. for salt solution)

The viscosity of pure water is calculated by the following equation:

$$ln\ \mu_w = -3.79418 + \frac{604.129}{139.18 + t}$$

where:

t : temperature in C

μ_w : calculated in centipoise

$$\mu_R = 1 + a_1 \times X + a_2 \times X^2$$

where:

$$a = 1.474 \times 10^{-3} + 1.5 \times 10^{-5} \times t - 3.927 \times 10^{-8} \times t^2$$

$$a = 1.0734 \times 10^{-5} - 8.5 \times 10^{-8} \times t + 2.23 \times 10^{-10} \times t^2$$

X : salinity in g/kg

t : temperature in C

A.1.3. Boiling Point Elevation Of Seawater:

The boiling point rise (BPR) of seawater is given by Homig [1978] as a function of temperature (t) and salt concentration (X). This equation is valid for X from 20 to 160 g/kg and for t from 20 to 180 C

$$BPR = (B + C \times X) \times X \qquad (A.3)$$

where:

$$10^3 \times B = 6.71 + 6.43 \times 10^{-2} \times t + 9.74 \times 10^{-5} \times t^2$$

$$10^5 \times C = 2.38 + 9.59 \times 10^{-3} \times t + 9.42 \times 10^{-5} \times t^2$$

BPR : boiling point elevation in seawater, K

A.1.4. Specific Heat Capacity Of Seawater:

Knowing the brine concentration X in g/kg and temperature t in C, the specific heat of brine seawater is calculated using the following

equation in J/kg.K , Homing [1978].

$$Cp = A + B \times t + C \times t^2 + D \times t^3 \qquad (A.4)$$

where:

$$A = 4206.8 - 6.6197 \times X + 1.2288 \times 10^{-2} \times X^2$$

$$B = -1.1262 + 5.4178 \times 10^{-2} \times X - 2.2719 \times 10^{-4} \times X^2$$

$$C = 1.2026 \times 10^{-2} - 5.3566 \times 10^{-4} \times X + 1.8906 \times 10^{-6} \times X^2$$

$$D = 6.8774 \times 10^{-7} + 1.517 \times 10^{-6} \times X - 4.4268 \times 10^{-9} \times X^2$$

Cp : Specific heat capacity in J/kg.K

A.1.4. Specific heat enthalpy of seawater:

The specific enthalpy of seawater can be calculated by integrating the brine specific heat (Cp), equation (A.4), from the reference temperature 0 to the brine temperature t (C), Homig [1978].

$$h = h_0 + \int_0^t Cp \, dt \qquad (A.5)$$

Then,

$$h = h_0 + \left(A \times t + \frac{B}{2} \times t^2 + \frac{C}{3} \times t^3 \times \frac{D}{4} \times t^4 \right) \qquad (A.5,a)$$

where:

h : specific enthalpy, J/kg

h_0 : zero point enthalpy, J/kg

$h_0 = 9.6296 \times X - 0.4312402 \times X^2$

A.1.5. Thermal conductivity of seawater:

This equation is obtained from Homig [1978]. It is valid for the range of 10 to 150 C and 0 to 100 g/kg of salinity:

$$k = A + B \times t + C \times t^2 \qquad (A.6)$$

where:

$$A = 576.6 - 34.64 \, CA + 7.286 \times CA^2$$

$$B = 10^{-3} \times (1526 + 466.2 \times CA - 226.8 \times CA^2 + 28.67 \times CA^3)$$

$$C = -10^{-5} \times (581 + 2055 \times CA - 991.6 \times CA^2 + 146.4 \times CA^3)$$

and,

$$CA = \frac{28.17 \times X}{1000 - X}$$

: analytical concentration factor

t : temperature in C

k : thermal conductivity in , W/m.K

A.1.6. Latent Heat Of Vaporization Of Water As A Function Of The Boiling Temperature:

$$\lambda = 597.49 - 5.6624 \times 10^{-1} \times t + 1.5082 \times 10^{-4} \times t^2 - 3.2764 \times 10^{-6} \times t^3 \qquad (A.7)$$

where:

λ : latent heat of vaporization in, kcal/kg

t : temperature in, C

A.1.7. Enthalpy Of Superheated Steam as a Function Of Temperature And Pressure:

This property is expressed in a form convenient for automatic computation by Schnackel [1958] as follows:

$$H = f + 0.043557 \times \left[f_0 \times P + \frac{\beta_0}{2} \times \left(\frac{P}{T}\right)^2 \left\{ -\beta_6 + \beta_0 \times \left[\beta_2 - \beta_3 + 2\,\beta_7 \times \frac{\beta_0}{2} \times \left(\frac{P}{T}\right)^2 \right] \right\} \right] \qquad (A.8)$$

where:

$$\beta = \beta_0 \times \left[1. + \frac{\beta_0 P}{T^2} \times \left[\beta_2 - \beta_3 + \frac{\beta_0 P}{T^2} \times (\beta_4 - \beta_5 \times \beta_0 P) \right] \right]$$

$$\beta_0 = 1.89 - \beta_1$$

$$\beta_1 = \frac{2641.62}{T} \times 10^{80870/T^2}$$

$$\beta_2 = 82.546$$

$$\beta_3 = \frac{162460}{T}$$

$$\beta_4 = 0.21828 \times T$$

$$\beta_5 = \frac{126970}{T}$$

$$\beta_6 = \beta_0 \times \beta_3 - 2\, f_0 \times (\beta_2 - \beta_3)$$

$$\beta_7 = 2\, f_0 \times (\beta_4 - \beta_5) - \beta_0 \times \beta_5$$

$$f_0 = 0.89 - \beta_1 \times \left[\frac{372420}{T^2} + 2 \right]$$

$$f = 775.596 + 0.63296 \times T + 0.000162467 \times T^2 + 47.3635 \times \log_{10} T$$

and, H : specific enthalpy in Btu/lb

T : temperature in K

P : pressure in atm

Enthalpy of saturated steam can be calculated using this equation by knowing the saturation temperature, (calculated as a function of pressure using equation (A.11)), and the pressure.

A.1.8. Pressure Of Saturated Steam As A Function Of Temperature:

The dependence of the vapour pressure of saturated steam on temperature was formulated by Steltz and Silvestri [1958] as follows:

For $248 \leq T < 366$

$$\log \left(\frac{Pc}{P} \right) = \frac{\mathcal{T}}{T_k} \left[\frac{A + B\mathcal{T} + C\mathcal{T}^3 + E\mathcal{T}^4}{1 + D\mathcal{T}} \right] \qquad (A.9)$$

where:

$A = 3.2437814$ $\quad B = 5.86826 \times 10^{-3}$

$C = 1.1702379 \times 10^{-8}$ $\quad D = 2.1878462 \times 10^{-3}$

For $366 \leq T \leq 647$

$$\log \left(\frac{Pc}{P} \right) = \frac{\mathcal{T}}{T_k} \left[\frac{A + B\mathcal{T} + C\mathcal{T} + E\mathcal{T}}{1 + D\mathcal{T}} \right] \qquad (A.10)$$

where:

$A = 3.3463130$ $\quad B = 4.14113 \times 10^{-2}$ $\quad C = 7.515484 \times 10^{-9}$

$D = 1.3794481 \times 10^{-2}$ $\quad E = 6.56444 \times 10^{-11}$ $\quad P$: pressure, atm

T_k : temperature, K $\quad T$: temperature in F $\quad \mathcal{T}$: $Tc - T_k$

Pc : critical pressure $= 22.106 \times 10^3$ kPa

Tc : critical temperature $= 647.27$ K

A.1.9. Temperature Of Saturated Steam As A Function Pressure:

Temperature of saturated steam in (F) is calculated by giving the pressure in (psia) to the following equation, Steltz and Silvestri [1958].

For $0.2 \leq P < 450$

$$T = \sum a_i \times [\ln (10 \times P)]^i \qquad (A.11,a)$$

where:

$a_0 = 35.157890$ $\quad a_1 = 24.592588$

$a_2 = 2.1182069$ $\quad a_3 = -0.34144740$

$a_4 = 0.15741642$ $\quad a_5 = -0.031329585$

$a_6 = 0.0038658282$ $\quad a_7 = -0.00024901784$

$a_8 = 0.0000068401559$

For $450 \leq P \leq 3206$

$$T = \sum \beta_i \times (\ln P)^i \qquad (A.11,b)$$

where:

$\beta_0 = 11545.164$ $\quad \beta_1 = -8386.0182$

$\beta_2 = 2477.7661$ $\quad \beta_3 = -363.44271$

$\beta_4 = 26.690978$ $\quad \beta_5 = -0.48073813$

T = Temperature in F $\quad$ P = pressure in psia

A.1.10. Enthalpy Of Saturated Liquid:

Using the following polynomial developed by Steltz and Silvestri [1958], the enthalpy of saturated liquid is calculated as a function of temperature.

$$h = \sum a_i \times (T)^i \qquad (A.12)$$

For $50 \leq T < 360$

$a_0 = -3.2179105 \times 10$ $\quad a_1 = 1.0088084$

$a_2 = -1.1516996 \times 10^{-4}$ $\quad a_3 = 4.8553836 \times 10^{-7}$

$a_4 = -7.3618778 \times 10^{-10}$ $\quad a_5 = 9.6350315 \times 10^{-13}$

For $360 \geq T \leq 600$

$a_0 = -9.0411706 \times 10^{2}$ $\quad a_1 = 1.0673802 \times 10$

$a_2 = -4.2753836 \times 10^{-2}$ $\quad a_3 = 9.41244 \times 10^{-5}$

$a_4 = -1.0315357 \times 10^{-7}$ $\quad a_5 = 4.560246 \times 10^{-11}$

where: T : Temperature, F

h : Enthalpy, Btu/lb

A.1.11 Pressure Drop Due to Friction Loss

The frictional loss for a fluid flowing through a tube is calculated using the following equation, Ozisik [1985]

$$\Delta P = \mathfrak{F} \frac{L}{ID} \cdot \frac{\rho v_m^2}{2} \qquad (A.13)$$

$$\mathfrak{F} = 64/Re \qquad \text{for laminar flow } (Re \leq 2000)$$

$$\mathfrak{F} = (1.82 \text{ Log } Re - 1.64)^{-2} \qquad \text{for } Re \geq 4000$$

where:

ΔP = pressure drop

$\mathfrak{F}$ = friction factor

L = tube length

ID = tube inside diameter

v_m = mean velocity

Re = Reynolds number = $v_m \cdot ID/\nu$

ν = dynamic viscosity

A.2. Overall Heat Transfer Coefficient:

The following correlations are used to calculate the overall heat transfer coefficients for the flash evaporator and the condenser units. The overall heat transfer coefficient U is inversely proportional to the sum of the thermal resistances to heat transfer, Mcadams [1954] and Mothershed [1966].

$$U = 1 / \Sigma R$$

$$= [R_{ci} + R_{fi} + R_w + R_{fo} + R_{nc} + R_{co}]^{-1} \qquad (A.14)$$

where:

R_{ci} : Resistance to convection heat transfer between the cooling brine and the inner tube wall.

R_{fi} : Fouling or scale resistance on the brine side of the tube.

R_w : Resistance due to the tube wall.

R_{fo} : Fouling or scale resistance on the vapour side of the tube wall.

R_{nc} : Resistance due to the presence of noncondensable gases near the outside surface of the condenser tubes.

R_{co} : Resistance of convection heat transfer between the condensing steam and the outer tube wall.

[1] Tube Wall Resistance, R_w

The wall resistance is calculated using the following equation:

$$R_w = \frac{OD}{2\,k_m} \times \log_e \frac{OD}{ID} \qquad (A.14,a)$$

where: k_m : thermal conductivity of the material tube wall, (kcal / m.h.K).

[2] Inside Convection Resistance, R_{ci}

$$R_{ci} = \frac{1}{h_i} \times \left\{ \frac{OD}{ID} \right\} \qquad (A.14,b)$$

where h_i represents the heat transfer coefficient for inside flow in kcal/hr.m^2.K.. It is obtained using the following equation:

$$Nu = 0.027 \times (Re)^{0.8} \times (Pr)^{1/3} \times \left(\frac{\mu_w}{\mu_b}\right)^{0.14} \qquad (A.14,c)$$

where:

Nu : Nusselt number.

Re : Reynolds number.

Pr : Prandtl number.

μ : Absolute brine viscosity kg/hr.m, μ_w evaluated at the wall temperature, μ_b evaluated at stream bulk temperature.

Equation (A.14,c) may be written in the following form:

$$\frac{h_i \times ID}{k_b} = 0.027 \times \left[\frac{\rho \times \theta \times ID}{\mu}\right]_b^{0.8} \times \left[\frac{Cp \times \mu}{k}\right]_b^{1/3} \times \left[\frac{\mu_w}{\mu_b}\right]^{0.14} \qquad (A.14,d)$$

where:

k : Brine thermal conductivity, kcal/m.hr.K

ρ : Brine density, kg/m^3

θ : Brine flow velocity, m/hr

Cp : Brine specific heat capacity, kcal/kg.K

b : subscript, evaluated at the stream bulk temperature.

[3] Outside Convection Resistance, R_{co}

The resistance to convection heat transfer between the vapour and the outer tube wall is inversely proportional to the condensation coefficient h_o, as follows:

$$R_{co} = 1 / h_o \qquad (A.14,e)$$

h_0, is calculated using the following theoretical equation developed by Nusselt:

$$h_o = 0.725 \times CR \times \left[\frac{k_f^3 \times \rho_f^2 \times \lambda \times g}{N \times OD \times \mu_f \times \Delta t_f} \right]^{1/4} \qquad (A.14,f)$$

where:

h_o : mean condensing coefficient for N tubes in a vertical row.

CR : practical correction factor to account for experimentally observed deviation from the Nusselt equation, Dukler [1971].

k_f : thermal conductivity, kcal/m.hr.K

ρ_f : density, kg/m^3

g : acceleration of gravity, m/hr

λ : latent heat of condensation, kcal/ kg

μ_f : viscosity, kg/m.hr

OD : tube outside diameter, m

Δt_f : temperature drop across condensate film, K

The subscript "f" refers to the condensate film. All the physical properties in the above equation (A.14,f) are evaluated at the average film temperature.

The value of the correction factor CR is given by Homig [1978] as follows:

for $N \leq 10$

$$CR = 1.23795 + 0.0353608\ N - 0.00157035\ N^2 \qquad (A.14,g)$$

for $N > 10$

$$CR = 1.434523$$

Where N is the number of tubes in a vertical row of the rectangular cross section bundle of tubes, where the number of tubes in each vertical row are equal. However, for a circular tube bundle with triangular pitch, N in equation (A.14,g) is calculated by the following, Omar [1981]:

$$N = 0.481 \times n_T^{0.505} \qquad (A.14,h)$$

Where n_T is the total number of tubes. And N is defined as the flooding factor.

[4] Fouling Resistance

Because of the lack of knowledge in the area of fouling and scale buildup, the fouling resistances are usually combined in one overall fouling resistance, R_f. It includes the resistance due to possible presence of noncondensable gases (R_{cn}) and the fouling resistance on the inside (R_{fi}) and outside (R_{fo}) surfaces.

Based on the of manufacturers and users experience, different values of the fouling factor are determined and tabulated, Ozisik [1985].

A P P E N D I X B

COMPUTATIONAL PROBLEMS DUE TO PHYSICAL LIMITATIONS OF THE MEE PROCESSES

Computation of the multiple effect evaporation plants may be not converged until a certain accuracy of the specified variables is achieved. These variables are approximately related by the following expressions, Blomsted et al [1974].

$$S \propto \frac{F}{N} \cdot \left(1 - \frac{X_f}{X_N}\right) \tag{B.1}$$

$$A \propto \frac{\lambda_m \cdot F \cdot (1 - X_f/X_N) \cdot N}{U \cdot (T_s - T_{c,N})} \tag{B.2}$$

$$T_s - T_{b,N} + \Sigma\, BPR \propto \frac{\lambda_m \cdot F \cdot N}{U \cdot A} \cdot (1 - X_f/X_N) \tag{B.3}$$

where:

- N = Number of effects.
- S = Heating steam consumption.
- F = Feed flowrate.
- X_f = Mass fraction of solids in the feed stream.
- X_N = Mass fraction of solids in the blowdown stream.
- U = Average value of the overall heat transfer coefficient.
- A = Total evaporator heat transfer area.
- T_s = Heating steam temperature.
- $T_{c,N}$ = Final condenser temperature.
- λ_m = Average value of heat of vaporization.
- BPR = Boiling point rise.
- $T_{b,N}$ = Blowdown temperature.

Unrealistic results, e.g. negative areas, flowrates, or temperatures may appear during the computations because one or more of the above expressions are violated, for example:

[A] From the expression (B.3) it may be deduced that: by increasing the

number of effects (N) and/or by using a large unrealistic X_N, the sum of the boiling point rises (Σ BPR) also increases. This reduces the temperature driving force ($T_s - T_{b,N}$). Consequently, the heating steam (or vapour) flowrate is reduced. If the sum of the boiling point rises exceeds the overall temperature driving force, negative values of the heating steam and/or vapour flowrates are produced by the computation.

[B] By increasing the number of effects and/or by using a large unrealistic feed water flowrate (F), the heat supply for some of the effects may drop below the sensible heat demanded by these effects. As a result, the vapour flowrates out of these effects become negative. Similarly, negative brine flowrates may be produced by utilizing unrealistic small feed flowrate and/or a large temperature driving force, in other words, negative brine flowrate may be calculated when the system "boils dry", see Olivares [1983] for more details.

The computation failure could occur in one or more of the plant effects due to one or more of the above reasons.

APPENDIX C

UNIT OPERATIONS LINEAR MATHEMATICAL MODELS

Using the same procedure as that used in Chapter 5, the following tables of equations are obtained for various thermal desalination process modules. Each table contains three sets of equations, one for each variable type (component, temperature, and pressure).

Table (C.1), Linear Mathematical Model of an Evaporator Effect

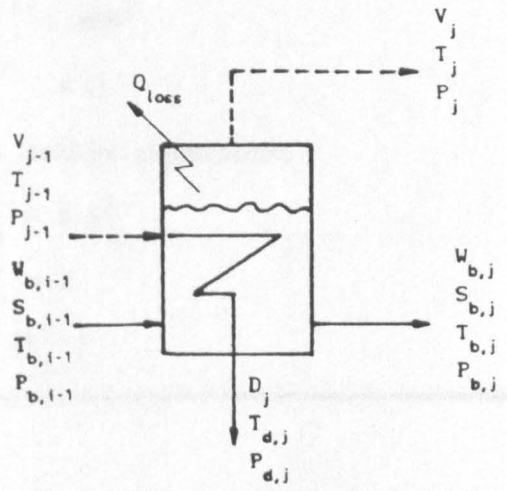

A. Component matrix equations;

$$[h_{b,j-1} - H_j]^k \cdot W_{b,j-1}^{k+1} + [H_{j-1} - h_d]^k \cdot D_j^{k+1} + [H_j - h_{b,j}]^k \cdot W_{b,j}^{k+1} = [h_{b,j} - h_{b,j-1}]^k \cdot S_{b,j-1}^k + Q_{loss}^k \quad (C.1,a)$$

$$W_{b,j-1}^{k+1} - W_{b,j}^{k+1} - V_j^{k+1} = 0 \quad (C.1,b)$$

$$S_{j-1}^{k+1} - S_j^{k+1} = 0 \quad (C.1,c)$$

$$V_{j-1}^{k+1} - D_j^{k+1} = 0 \quad (C.1,d)$$

Table (C.1), Continuation

B. Temperature matrix equations;

For simulation calculations;

$$[V_{j-1} ; b_{j-1} - UA_j]^k \cdot T_{j-1}^{k+1} - [D_j \cdot b_j]^k \cdot T_j^{k+1} + [UA_j]^k \cdot T_{b,j}^{k+1} = D_j^k \cdot a_j^k - V_{j-1}^k \cdot a_{j-1}^k \qquad (C.2,a)$$

For design calculations,*

$$[b_{j-1} \cdot V_{j-1} - \xi \cdot UA_j]^k \cdot T_{j-1}^{k+1} - [b_j \cdot D_{j-1}]^k \cdot T_j^{k+1} + \xi \cdot U^k \cdot [T_{b,j} - T_{j-1}]^k \cdot A_j^{k+1} + UA_j^k \cdot \xi \cdot T_{b,j}^{k+1} = V_{j-1}^{k+1} \cdot [a_j - a_{j-1}]^k - [T_{j-1} - T_{b,j}]^k \cdot UA^k \cdot \xi \qquad (C.2,b)$$

$$T_{b,j}^{k+1} - T_j^{k+1} = BPR^k \qquad (C.2,c)$$

$$T_{j-1}^{k+1} - T_j^{k+1} = 0 \qquad (C.2,d)$$

C. Pressure matrix equations;

$$P_{j-1}^{k+1} - P_{d,j}^{k+1} = \Delta P_j^k \qquad (C.3,a)$$

$$P_j^{k+1} - P_{b,j}^{k+1} = 0 \qquad (C.3,b)$$

$$P_j^{k+1} = f(T_j^k) \qquad (C.3,c)$$

---

* In this case the variable A_j is written as $\xi \cdot A$ to allow for variable area, where ξ is the ratio of the j^{th} stage area to the reference area, A. For the constant area solution, $\xi = 1$.

Table (C.2), Linear Mathematical Model of a Desuperheater Unit.

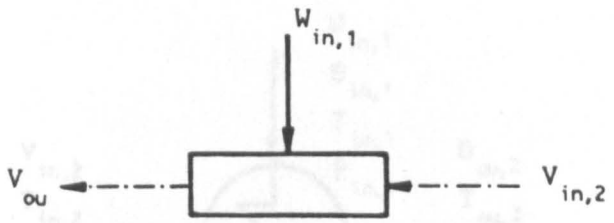

A. Component matrix equations;

$$V^{k+1}_{in,2} + W^{k+1}_{in,1} - V^{k+1}_{ou} = 0 \qquad (C.4,a)$$

$$[H]^{k}_{in,2} \cdot V^{k+1}_{in,2} + [h]^{k}_{in,1} \cdot W^{k+1}_{in,1} - [H]^{k}_{ou} \cdot V^{k+1}_{ou} = 0 \qquad (C.4,b)$$

B. Temperature matrix equations;

$$T^{k+1}_{ou} = f\,(P^{k}_{in,2}) \qquad (C.5)$$

C. Pressure matrix equations;

$$P^{k+1}_{ou} - P^{k+1}_{in,2} = 0 \qquad (C.6)$$

Table (C.3), Linear Mathematical Model of a Condenser Unit

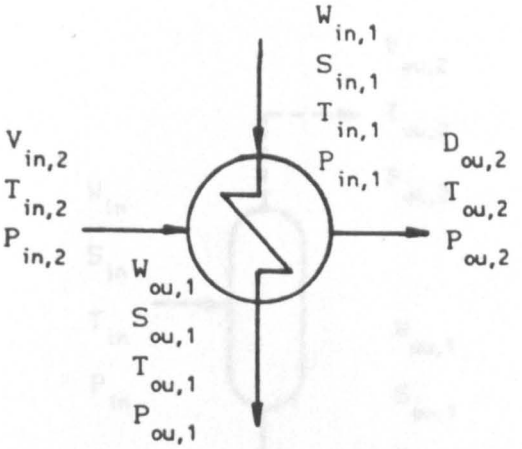

A. Component matrix equations;

$$[H_{in,2} - h_{d,ou,2}]^k \cdot V^{k+1}_{in,2} + [h_{in,1} - h_{ou,1}]^k \cdot W^{k+1}_{in,1} + [h_{in,1} - h_{ou,1}]^k \cdot S^{k+1}_{in,1} = 0 \qquad (C.7,a)$$

$$V^{k+1}_{in,2} - D^{k+1}_{ou,2} = 0 \qquad (C.7,b)$$

$$W^{k+1}_{in,1} - W^{k+1}_{ou,1} = 0 \qquad (C.7,c)$$

$$S^{k+1}_{in,1} - S^{k+1}_{ou,1} = 0 \qquad (C.7,d)$$

B. Temperature matrix equations;

$$T^{k+1}_{v,in,2} - T^{k+1}_{d,ou,2} = 0 \qquad (C.8,a)$$

For simulation calculations;

$$[1 - E]^k \cdot T^{k+1}_{in,1} + E^k \cdot T^{k+1}_{v,in,2} - T^{k+1}_{ou,1} = 0 \qquad (C.8,b)$$

where; $E = 1 - e^{-UA/[(W+S)_{in,1} \cdot Cp]_m}$

OR;

For design calculations;

$$T^{k+1}_{v,in,2} - T^{k+1}_{ou,1} = \Delta T_{approach} \qquad (C.8,c)$$

Also equation (5.12,e) can be used for design purpose .

C. Pressure matrix equations;

$$P^{k+1}_{in,1} - P^{k+1}_{ou,1} = \Delta P^k_1 \qquad (C.9,a)$$

$$P^{k+1}_{v,in,2} - P^{k+1}_{v,ou,2} = \Delta P^k_2 \qquad (C.9,b)$$

Table (C.4), Linear Mathematical Model of a Flash Unit

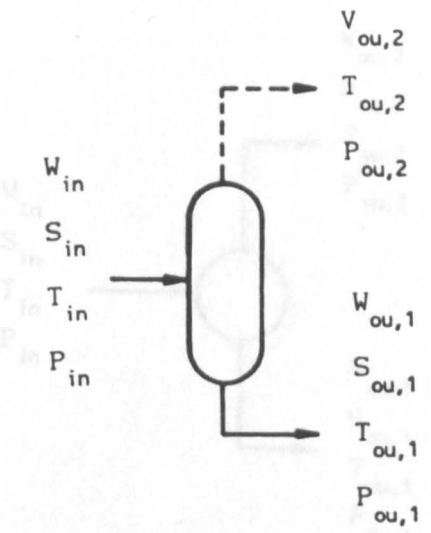

A. Component matrix equations;

$$W_{in}^{k+1} - W_{ou,1}^{k+1} - V_{ou,2}^{k+1} = 0 \qquad \text{(C.10,a)}$$

$$S_{in}^{k+1} - S_{ou,1}^{k+1} = 0 \qquad \text{(C.10,b)}$$

$$[h_{in}]^{k} \cdot W_{in}^{k+1} - [H_{ou,2}]^{k} \cdot V_{ou,2}^{k+1} - [h_{ou,1}]^{k} \cdot W_{ou,1}^{k+1} + [h_{in} - h_{ou,1}]^{k} \cdot S_{in}^{k+1} = 0 \qquad \text{(C.10,c)}$$

B. Temperature matrix equations;

$$T_{ou,1}^{k+1} - T_{ou,2}^{k+1} = 0 \qquad \text{(C.11,a)}$$

$$T_{ou,2}^{k+1} = \text{Specified constant} \qquad \text{(C.11,b)}$$

Or;

$$T_{ou,2}^{k+1} = f\,(P_{ou,2}^{k}) \qquad \text{(C.11,c)}$$

C. Pressure matrix equation;

$$P_{ou,1}^{k+1} - P_{ou,2}^{k+1} = 0 \qquad \text{(C.12)}$$

Table (C.5), Linear Mathematical Model of a Splitter Unit.

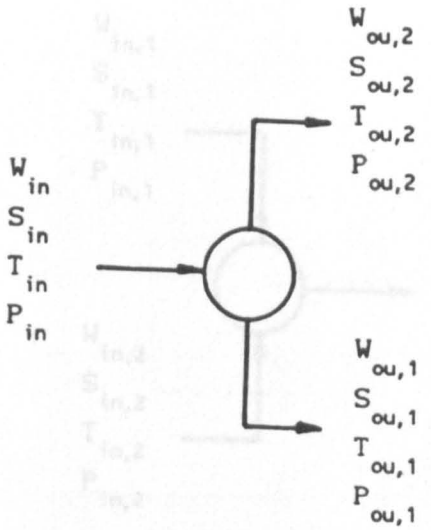

A. Component matrix equations;

$$W_{in}^{k+1} - W_{ou,1}^{k+1} - W_{ou,2}^{k+1} = 0 \qquad \text{(C.13,a)}$$

$$S_{in}^{k+1} - S_{ou,1}^{k+1} - S_{ou,2}^{k+1} = 0 \qquad \text{(C.13,b)}$$

and if $\alpha > 0$ (i. e. if α is specified)

$$W_{ou,1}^{k+1} - \alpha \cdot W_{in}^{k+1} = 0 \qquad \text{(C.13,c)}$$

$$S_{ou,1}^{k+1} - \alpha \cdot S_{ou,1}^{k+1} = 0 \qquad \text{(C.13,d)}$$

B. Temperature matrix equations;

$$T_{in}^{k+1} - T_{ou,1}^{k+1} = 0 \qquad \text{(C.14,a)}$$

$$T_{in}^{k+1} - T_{ou,2}^{k+1} = 0 \qquad \text{(C.14,b)}$$

C. Pressure matrix equations;

$$P_{in}^{k+1} - P_{ou,1}^{k+1} = 0 \qquad \text{(C.15,a)}$$

$$P_{in}^{k+1} - P_{ou,2}^{k+1} = 0 \qquad \text{(C.15,b)}$$

Table (C.6), Linear Mathematical Model of a Mixer Unit

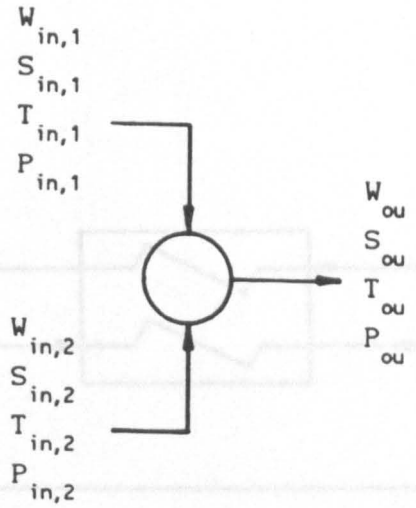

A. Component matrix equations;

$$W^{k+1}_{in,1} + W^{k+1}_{in,2} - W^{k+1}_{ou} = 0 \qquad \text{(C.16,a)}$$

$$S^{k+1}_{in,1} + S^{k+1}_{in,2} - S^{k+1}_{ou} = 0 \qquad \text{(C.16,b)}$$

B. Temperature matrix equations;

$$[(W + S) \cdot b]^{k}_{in,1} \cdot T^{k+1}_{in,1} + [(W + S) \cdot b]^{k}_{in,2} \cdot T^{k+1}_{in,2} - [(W + S) \cdot b]^{k}_{ou} \cdot T^{k+1}_{ou} = [(W + S) \cdot a]^{k}_{ou} - [(W + S) \cdot a]^{k}_{in,1} - [(W + S) \cdot a]^{k}_{in,2} \qquad \text{(C.17)}$$

C. Pressure matrix equations;

$$P^{k+1}_{in,1} - P^{k+1}_{ou} = 0 \qquad \text{(C.18,a)}$$

$$P^{k+1}_{in,2} - P^{k+1}_{ou} = 0 \qquad \text{(C.18,b)}$$

Table (C.7), Linear Mathematical Model of a Liquid/Liquid Heat Exchanger Unit.

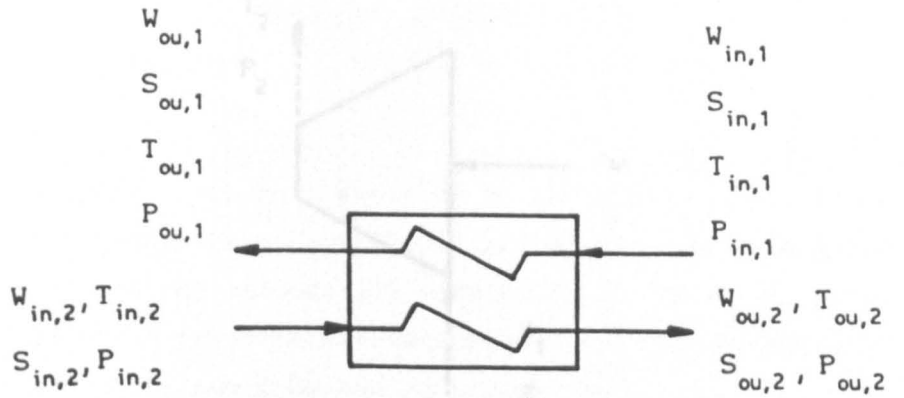

A. Component matrix equations;

$$W^{k+1}_{in,1} - W^{k+1}_{ou,1} = 0 \qquad (C.19,a)$$

$$S^{k+1}_{in,1} - S^{k+1}_{ou,1} = 0 \qquad (C.19,b)$$

$$W^{k+1}_{in,2} - W^{k+1}_{ou,2} = 0 \qquad (C.19,c)$$

$$S^{k+1}_{in,2} - S^{k+1}_{ou,2} = 0 \qquad (C.19,d)$$

B. Temperature matrix equations;

$$[F_{in,1} \cdot Cp_{m,1}]^k \cdot T^{k+1}_{in,1} - [F_{in,1} \cdot Cp_m]^k \cdot T^{k+1}_{ou,1} - [F_{in,2} \cdot Cp_{m,2}]^k \cdot T^{k+1}_{ou,2} + [F_{in,2} \cdot Cp_{m,2}]^k \cdot T^{k+1}_{in,2} = 0 \qquad (C.20,a)$$

$$T^{k+1}_{in,1} - T^{k+1}_{ou,2} - [EE]^k \cdot T^{k+1}_{ou,1} + [EE]^k \cdot T^{k+1}_{in,1} = 0 \qquad (C.20,b)$$

$$UA \cdot \left[\frac{1}{F_{in,1} \cdot Cp_{m,1}} - \frac{1}{F_{in,2} \cdot Cp_{m,2}} \right]$$

Where EE = e

Or;

$$T^{k+1}_{ou,1} - T^{k+1}_{ou,2} = \Delta T_{approach} \qquad (C.20,c)$$

C. Pressure matrix equations;

$$P^{k+1}_{in,1} - P^{k+1}_{ou,1} = \Delta P_1 \qquad (C.21,a)$$

$$P^{k+1}_{in,2} - P^{k+1}_{ou,2} = \Delta P_2 \qquad (C.21,b)$$

Table (C.8), Linear Mathematical Model of a Compressor Unit

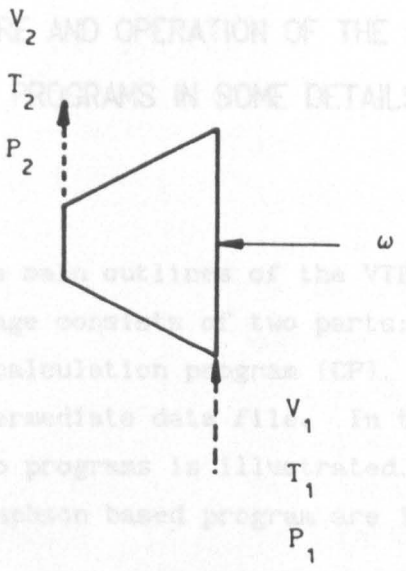

A. Component matrix equations;

$$V_1^{k+1} - V_2^{k+1} = 0 \qquad \text{(C.22)}$$

B. Temperature matrix equations;

for known ω:

$$T_2^{k+1} \times b_2^k - T_1^{k+1} \times b_1^k = [\omega/V^k] - a_2^k - a_2^k \qquad \text{(C.23,a)}$$

for unknown ω:

$$T_2^{k+1} - T_1^{k+1} \times \left\{ [P_2/P_1]^{(\gamma-1)/\gamma} \right\}^k = 0 \qquad \text{(C.23,b)}$$

C. Pressure matrix equation;

$$P_2^{k+1} - P_1^{k+1} \times \left[(T_2/T_1)^{\gamma/(\gamma-1)} \right]^k = 0 \qquad \text{(C.24)}$$

A P P E N D I X D

STRUCTURE AND OPERATION OF THE DEVELOPED PROGRAMS IN SOME DETAILS

In chapter 6 the main outlines of the VTBVT based package are emphasized. This package consists of two parts: the data structure program (DSP) and the calculation program (CP). These two parts are communicated by an intermediate data file. In this Appendix, the main points in the above two programs is illustrated. Also, the main points of the Newton Raphson based program are introduced.

D.1. THE DATA STRUCTURE PROGRAM (DSP).

D.1.1. Building The Knowledge Into The DSP.

Any flowsheet configuration may be described completely in terms of a number of units connected together by a number of streams by which the flow of information, material, and energy between the plant units is performed. So, to define a process, these two elements (i.e. streams and units) should be accurately defined.

In the DSP, the process stream is considered to be a number of vectors of properties, sufficient to define the state of the process stream. These vectors (or arrays) include flow rate, temperature, component and pressure properties separately (i.e. one array for each variable type). The logic order of these variables in its vectors is determined by pointers. So, any stream may be defined by a set of variables (or its pointers) associated with it, as well as information defining the stream such as its name and destination. With regard to the process unit, it is defined by its name, type, and the relevant data (i.e. the unit parameters).

In other words the process may be defined by a number of pointers for the stream variables, and a number of arrays for unit types, names, and parameters . These pointers and arrays are shown in Table (D.1).

Table (D.1). Arrays Created In DSP

Array	Dimension	Type	Definition
LSTFIN	3*NU	I	Flowrate pointers of the input
LSTFOU	3*NU	I	and output streams.
LSTTIN	3*NU	I	Temperature pointers of the
LSTTOU	3*NU	I	input and output streams.
LSTPIN	3*NU	I	Pressure pointers for the input
LSTPOU	3*NU	I	and the output streams.
LISTC	NC*NS	I	Component pointers of a stream.
LISTP	1*NU	I	Unit parameter pointers list.
NTYPE	1*NU	I	Unit types pointer list.
PARAM	1*NPARAM	R	Unit parameter arrays.
UNAME	1*UN	CHR	Unit name arrays.
CNAME	1*NC	CHR	Component name arrays.
SNAME	1*NSTRM	CHR	Streams name arrays.

where;

NU = Number of units. NC = Number of components.
NPARAM = Number of parameters. NSTRM = Number of streams.
I = Integer data array. R = Real data array.
CHR = Character data array.

As shown in the above table, the stream variable pointer lists into and out of a unit, consist of three columns, one column for each stream entering and leaving the unit (assuming that each unit has only up to three input and three output streams). The component pointer lists consist of two columns, one for each component (water and salt). Each of the rest of the arrays consists of one column with different lengths, such as NU, NPARAM,...etc.

D.1.2. Variable And Parameter Pointer Lists Setting Up.

As pointed out before, all the data required to completely define the problem under consideration are stored in a number of arrays. The location of a data element in a particular array may be indicated by its pointer. These pointer lists are set up by tracing the change of the stream variable values (such as temperature, flowrate, pressure, etc) across the units. If a stream variable is changed through a unit, the

pointer of this variable is increased by one for that stream out of the unit. Otherwise, the pointer of this variable for output stream is copying the previous value (i.e. the pointer value does not change). The flowrate, temperature and pressure pointer lists are set up using the same technique. Figure D.1, shows a general flowchart for setting up these pointers for inlet and outlet streams of flowsheet units. By this technique, the minimum number of non-zero and different pointer values will be stored to define the process. Consequently, a reduction in the matrix equation size will be obtained.

By coding the flowrate pointer for each stream (JOUT) out of each unit (J) in the process flowsheet as LSTFOU(JOUT,J), the pointer of each component JC in a particular stream can be created by the program and stored in an array LISTC, with two integer arguments: the first refers to the component number, and the second refers to the stream flowrate pointer as LISTC (JC,LSTFOU(JOUT,J)). This index locator specifies the position of a particular component in a particular stream with respect to the first element.

Two types of streams can be manipulated by the DSP, viz; external and internal streams. The external stream appears in the process flowsheet and has its name and destination. Internal streams may be created within the unit module to represent an internal flow, such as the flow between stages in the MSF process. The internal streams do not need to be defined by name or destination. This may make the definition of the problem much easier for the user, and the risk of making flowsheeting error may be reduced. Furthermore, this feature also allows the user to alter the number of stages in the MSF sections for further investigation without too much disturbance to the flowsheeting data and constraint specifications.

D.1.3. Specifications and Constraints.

The capability of the developed program of specifying design and operating constraints easily, may be considered one of its main features. Once the considered flowsheet streams and units are defined, and the stream variables and the modules equations are established, there will be several remaining degrees of freedom, see section 5.3. The computer program has been written in a way allowing enough flexibility in specifying these remaining degrees of freedom.

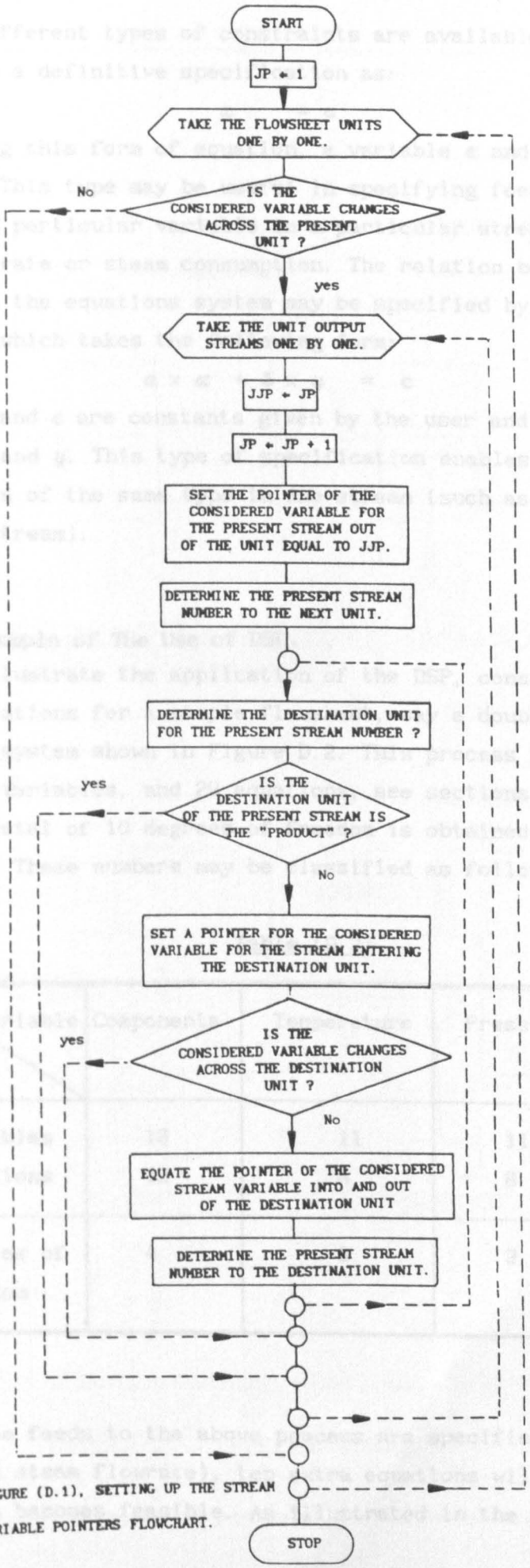

FIGURE (D.1), SETTING UP THE STREAM VARIABLE POINTERS FLOWCHART.

Two different types of constraints are available for this purpose. The first is a definitive specification as:

$$\alpha = a \qquad (D.1)$$

By generating this form of equation, a variable α and a constant a will be equated. This type may be useful in specifying feed stream variables, and fixing a particular variable in a particular stream such as the product flowrate or steam consumption. The relation between two variables in the equations system may be specified by the second type of constraints which takes the following form:

$$a \times \alpha + b \times \psi = c \qquad (D.2)$$

Where a, b, and c are constants given by the user and relating the variables α and ψ. This type of specification enables the user to relate two variables of the same type in one stream (such as the concentration ratio of a stream).

D.1.4. An Example of The Use of DSP.

To illustrate the application of the DSP, consider the steady state calculations for a simple flowsheet, say a double effect evaporation system shown in Figure D.2. This process is represented by a total of 38 variables, and 28 equations, see sections 5.3 and Appendix (C). So, a total of 10 degrees of freedom is obtained for extra constraints. These numbers may be classified as follows:

Table (D.2)

No. of \ Variable	Components	Temperature	Pressure	Total
Variables	16	11	11	38
Equations	12	8	8	28
Degrees of freedom	4	3	3	10

If the feeds to the above process are specified completely (with unknown feed steam flowrate), ten extra equations will be obtained and the solution becomes feasible. As illustrated in the previous

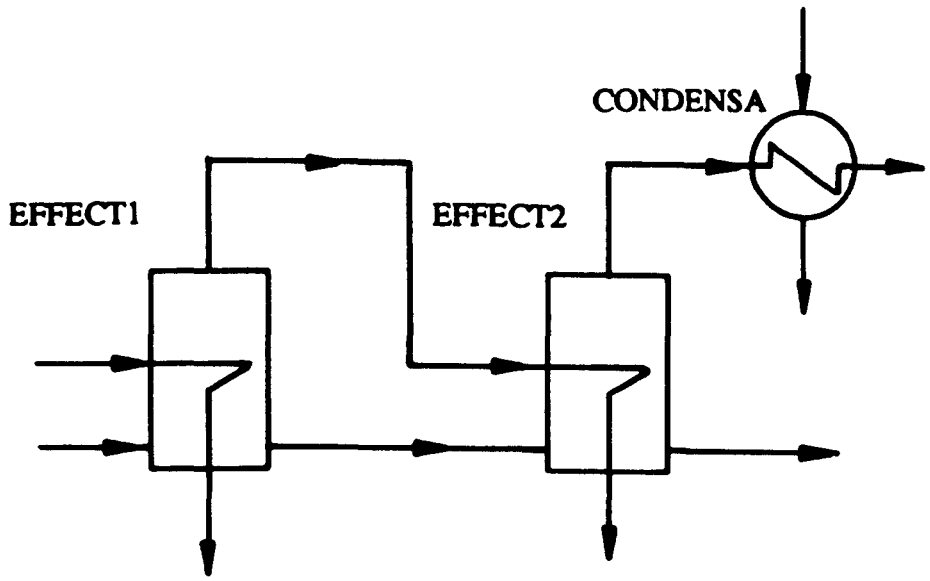

FIGURE D.2. DOUBLE EFFECT EVAPORATION SYSTEM.

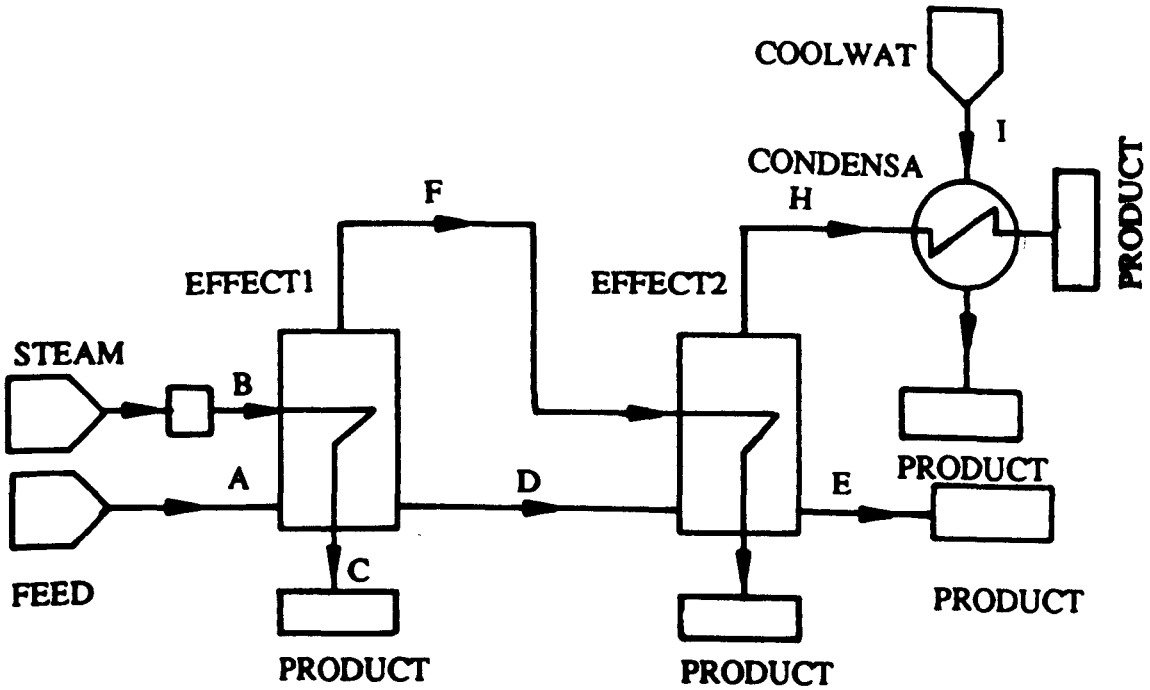

FIGURE D.3. COMPUTER MODEL CONFIGURATION FOR A DOUBLE EFFECT EVAPORATION SYSTEM.

subsection, operating and design specifications involve assigning values to particular variables associated with a unit input and output streams. For this purpose plant input and/or output streams are again treated as units which set up the suitable form of specifications, as shown in Figure D.3.

Once the computer model configuration is decided, various units and streams that occur in it must be specified. For this particular flowsheet, the full set of statements provided by the user as a data file defining the flowsheet are shown in Figure D.4.

These data are located into a number of arrays created by the program as explained before in subsection D.1.2. Figure D.5, demonstrates all these lists. The elements of these arrays can be easily accessed. This is done simply by coding the name of the array, together with an index locator specifying the position of a particular element (i.e the pointer). As shown in the figure, the created arrays include integer, real, and character variables.

Figure (D.4), Data File For The DSP

```
DOUBLE EFFECT EVAPORATION :Title
1                         :Calculation mode.
2                         :No. of components.
WATER                     :C(1)
SALT                      :C(2)
7                         :No. of units
FEED                      :Unit name
1                         :Unit type (source)
A                         :1st output stream name.
EFFECT1                   :Destination.
2                         :Stream number to the destination.
22680. 330. 150.          :F,T,P
21546. 1134.              :S(1),S(2)
STEAM                     :Unit name
1                         :Unit type
B                         :Output stream name
PSET                      :Destination
1                         :Stream number to the destination.
-1 400. -1.               :Unknown F, T, unknown P
1. 0.                     :All stream is C(1), C(2) = 0
PSET                      :Unit name
440                       :Unit type
EFFECT1                   :Destination
1                         :Which input to the destination
0.                        :Pressure value
EFFECT1                   :Unit name
400                       :Unit type
```

Figure (D.4), Continued

```
C                              :1st output stream
PRODUCT                        :Destination
D                              :2nd output stream
EFFECT2                        :Destination
2                              :Which input to the destination
F                              :3rd output stream
EFFECT2                        :Destination
1                              :Which input to the destination
150. 0.0                       :A, Q loss
EFFECT2                        :Unit name
400                            :Unit type
G                              :1st output stream
PRODUCT                        :Destination
E                              :2nd output stream
PRODUCT                        :Destination
H                              :3rd output stream
CONDENSA                       :Destination
2                              :Which input to destination
150. 0.0                       :A, Q loss
CONDENSA                       :Unit name
420                            :Unit type
PRODUCT                        :Destination of the 1st output
PRODUCT                        :Destination of the 2nd output
681271. 0.0                    :UA, Q loss
COOLWAT                        :Unit name
1                              :Unit type
I                              :Stream name
CONDENSA                       :Destination
1                              :Which input to the destination
63402. 300. 100.               :F, T, P
60321.9 3170.1                 :C(1), C(2)
```

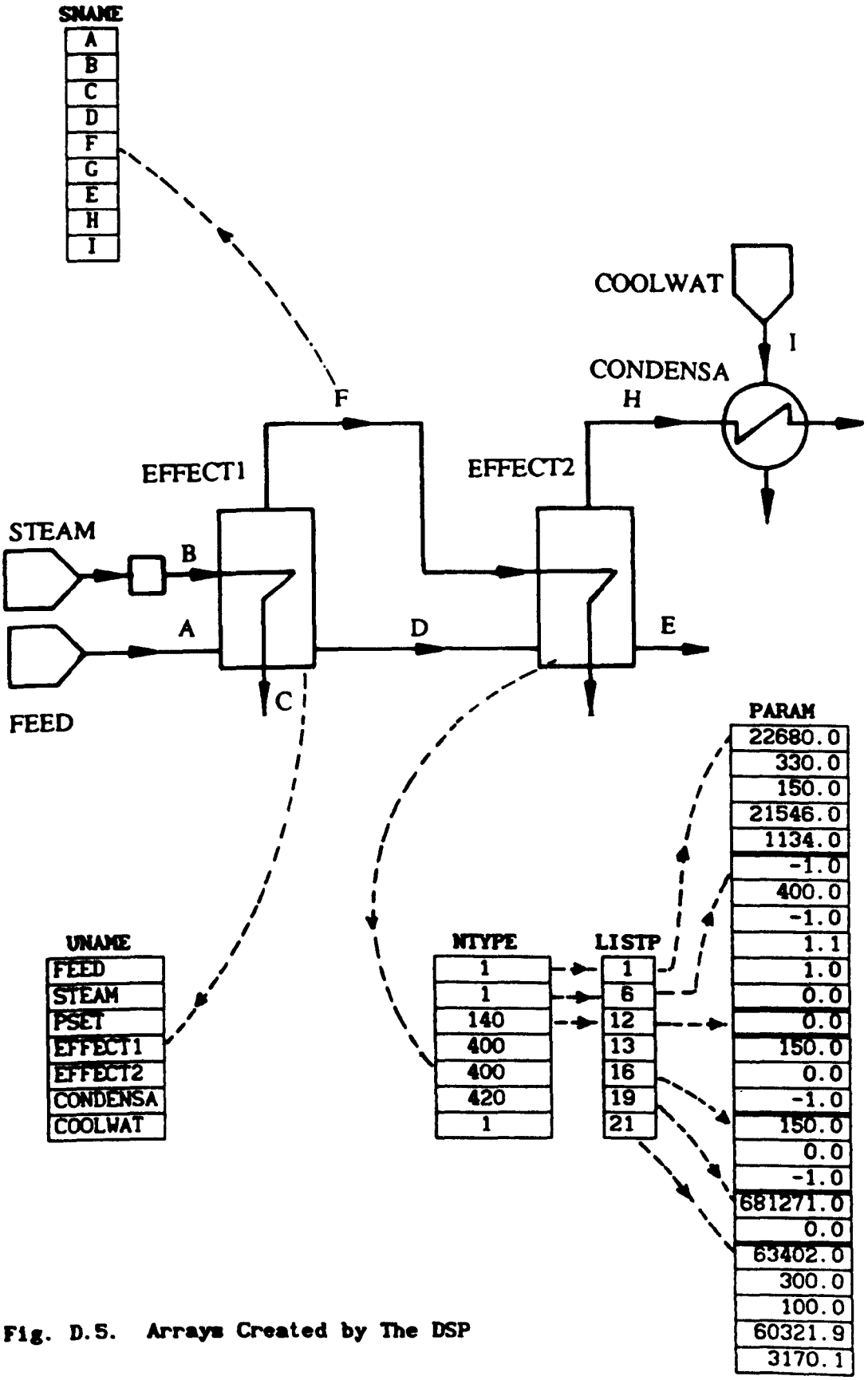

Fig. D.5. Arrays Created by The DSP

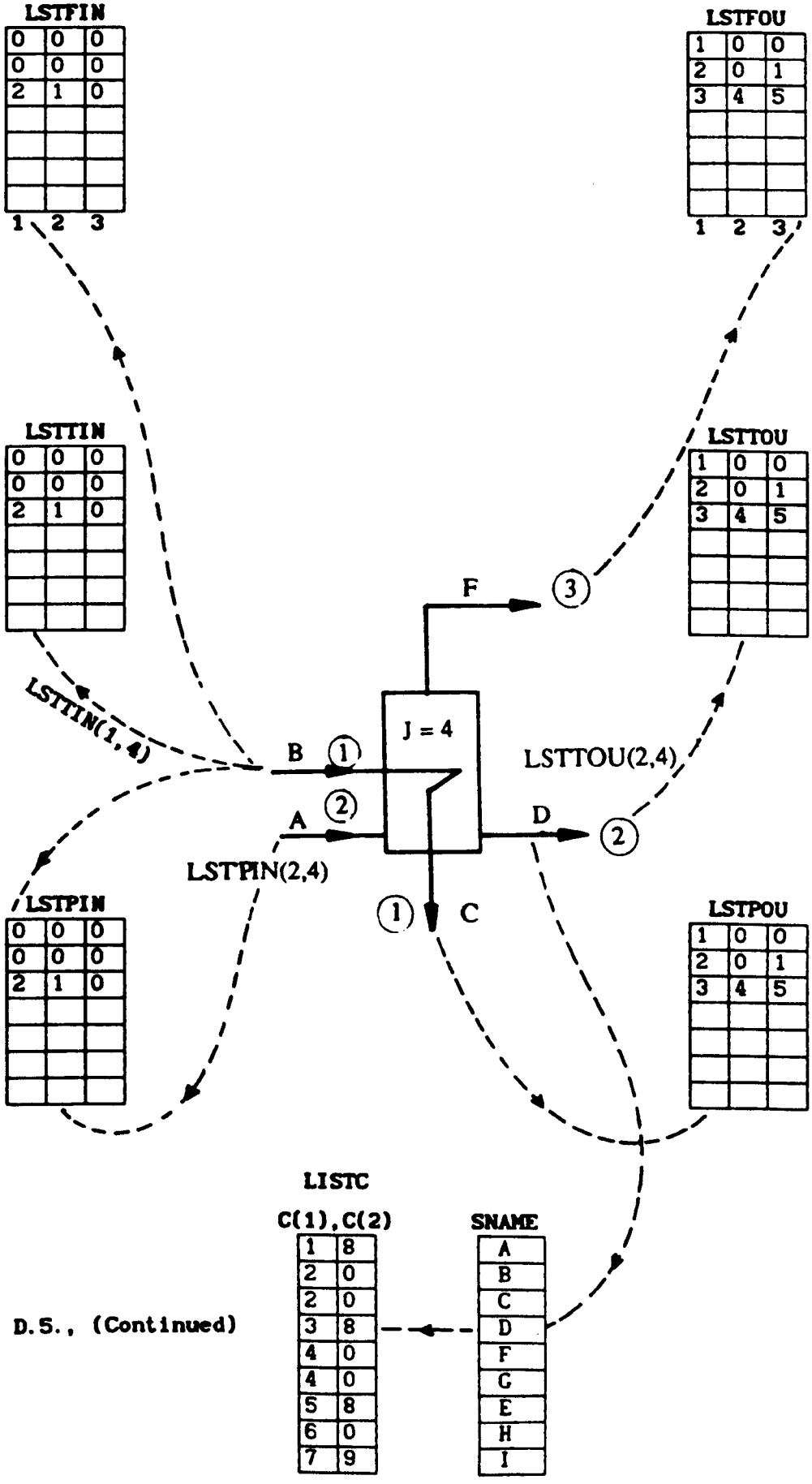

Fig. D.5., (Continued)

D.1.5. The Intermediate Data File.

The specifications and the information stored in the created arrays are then transferred as an intermediate file to the calculation program (CP). As illustrated in Figure D.6, this file comprises lists of unit names, variable pointers, unit parameters, and stream names, and also information about the number of the temperature, pressure, and component variables, as well as the calculation mode (simulation or design). From this file the following points may be noted:

[1] Each variable type set (e.g. temperature, pressure, component, ... etc.) is stored in a separate array to be manipulated easily using the VTBVT technique.

[2] The unit EFFECT1 (for example), changes the water flowrate (i.e. component No.1), of the input stream A (pointer NO. 1), by evaporating part of it. Therefore, a new pointer is created for this component in the output stream (stream D, pointer 3). However, the second component pointers for both input and output streams have the same number ,(i.e. pointer No. 8), because the salt flowrate has not been changed across the unit. Furthermore, this example shows that different streams (e.g. A & D) may pass the same flowrate of a certain component and different flowrates of the other component.

[3] By avoiding definition of identical component values, the pointer number of this variable type is reduced from sixteen as placed in table (D.2), to just nine values as recorded by the intermediate file, Figure (D.6).

[4] The calculation mode = 1 for simulation with known overall heat transfer coefficient (U).
= 2 for simulation with unknown U.
= 3 for design calculations.

```
DOUBLE EFFECT EVAPORATION
                2 <-------> No. of components
WATER ---------------------> C(1)
SALT ----------------------> C(2)
                7           No. of units
FEED                        Unit name.
                            Unit type, NTYPE(J)
                            LISTP(J)
1               1
```

Unit name (UNAME) LSTFIN (K,J) LSTTIN (K,J) LSTPIN (K,J)		input streams	LSTFOU(K,J) LSTTOU(K,J) LSTPOU(K,J)		output streams
0	0	0	1	0	0
0	0	0	1	0	0
0	0	0	1	0	0
STEAM					
1	6				
0	0	0	2	0	0
0	0	0	2	0	0
0	0	0	2	0	0
PSET					
440	12				
2	0	0	2	0	0
2	0	0	2	0	0
2	0	0	2	0	0
EFFECT1					
400	13				
2	1	0	3	4	5
2	1	0	3	4	5
2	1	0	3	4	5
EFFECT2					
400	16				
5	4	0	6	7	8
5	4	0	6	7	8
5	4	0	6	7	8
CONDENSA					
420	19				
9	8	0	9	8	0
11	8	0	9	10	0
11	8	0	9	10	0
COOLWAT					
1	21				
0	0	0	9	0	0
0	0	0	11	0	0
0	0	0	11	0	0

Figure (D.6), An intermediate Data File For The CP.

Figure (D.6), (Continued)

```
                                    No of parameters (NPARAM)
                                                  Parameter list (PARAM(J),J=1,NPARAM)
          25
 0.226800E+05  0.330000E+03  0.150000E+03  0.215460E+05
 0.113400E+04 -0.100000E+01  0.400000E+03 -0.100000E+01
 0.110000E+01  0.100000E+01  0.000000E+00  0.000000E+00
 0.150000E+03  0.000000E+00 -0.100000E+01  0.150000E+03
 0.000000E+00 -0.100000E+01  0.681271E+06  0.000000E+00
 0.634020E+05  0.300000E+03  0.100000E+03  0.603219E+05
 0.317010E+04

                                    Stream name (SNAME)
                                    No. of streams
                                          JINTF (flowrate internal variable
                                              Pointer list of component 1
                                                  Pointer list of component 2
                    9                0
A                   1                8
B                   2                0
C                   2                0
D                   3                8
F                   4                0
G                   4                0
E                   5                8
H                   6                0
I                   7                9

                   11                0      NTEM, JINTT
                   11                0      NPRES, JINTP
                    9                1      NCOMP, JINTC
                    2                       Calculation mode
```

D.2. Newton Data Structure Program (NDSP).

The previous sections are oriented towards the preparation of the proper intermediate file for the successive calculation process by the proposed VTBVT technique. In this file the elements of each variable type (e.g. temperature, component, ..) are assigned in a separate array.

However, to solve the mathematical model representing the process as one set of simultaneous equations using Newton Raphson method, the separate lists of components and temperatures in the DSP are merged into a single list in the NDSP. Apart from this point, the NDSP and the DSP both have the same configuration of structure. Also, the user data file for NDSP is the same as that used with the DSP (i.e. data file) Figure (D.4). The intermediate file produced by NDSP is shown in Figure D.7. In this file the following points may be noted;

[1] The integer number indicating the position of the first temperature element in the merged array, with respect to the first element in that array, is equal to the number of the component variables , (i.e. for this case = 10), plus 1, i.e. eleven.

[2] By avoiding the definition of the identical temperature variables of the heating and condensed vapour streams in the two effects, the pointer number of this variable type (i.e. the temperature) is reduced from 11 as recorded in Figure (D.6) to just 9 as shown in Figure (D.7).

Figure (D.7), An Intermediate File For NBCP

```
DOUBLE EFFECT EVAPORATION
         2
WATER
SALT
         7
FEED
    1          1
    0          0          0          1          0          0
    0          0          0         11          0          0
    0          0          0          1          0          0
STEAM
    1          6
    0          0          0          2          0          0
    0          0          0         12          0          0
    0          0          0          2          0          0
PSET
  440         12
    2          0          0          2          0          0
   12          0          0         12          0          0
    2          0          0          2          0          0
EFFECT1
  400         13
    2          1          0          3          4          5
   12         11          0         12         13         14
    2          1          0          3          4          5
EFFECT2
  400         17
    5          4          0          6          7          8
```

Figure (D.7), (Continued)

```
   14          13          0          14          15          16
    5           4          0           6           7           8
CONDENSA
  420          21
    9           8          0           9           8           0
   19          16          0          17          18           0
   11           8          0           9          10           0
COOLWAT
    1          23
    0           0          0           9           0           0
    0           0          0          19           0           0
    0           0          0          11           0           0
       27
  0.226800E+05  0.330000E+03  0.150000E+03  0.215460E+05
  0.113400E+04 -0.100000E+01  0.400000E+03 -0.100000E+01
  0.110000E+01  0.100000E+01  0.000000E+00  0.000000E+00
  0.150000E+03  0.000000E+00 -0.100000E+01 -0.100000E+01
  0.150000E+03  0.000000E+00 -0.100000E+01 -0.100000E+01
  0.681271E+06  0.000000E+00  0.634020E+05  0.300000E+03
  0.100000E+03  0.603219E+05  0.317010E+04
          9           0
A
          1           8
B
          2           0
C
          2           0

D
          3           8
F
          4           0
G
          4           0
E
          5           8
H
          6           0
I
          7           9
          9           0
         11           0
          9           1
          2
```

D.3. THE CALCULATION PROGRAM [CP] ORGANIZING UNITS.

D.3.1. Data Input.

Data concerning the process topology, input streams, and unit design parameters are entered by the intermediate file via the data reading subroutine, where they are verified for consistency and completeness. Knowing the number of each variable type, the program generates a number of arrays, one for each variable type (i.e COMP, FLOW, TEMP, and PRES for stream components, flowrate, temperature, and pressure consequently). Figure (D.8) shows how the temperature and component stream variables arrays (as an example) are created for the unit streams, and how the values of these variables can be retrieved.

If initial guesses for the temperature values are available the program may be supplied with them through this subroutine (i.e data input) for the solution. This is useful if a previous solution for the same or a similar plant is available, because convergence rate in this case may be improved. Otherwise, the data input reading routine will generate the required initial temperature profile to start the solution, assuming all the plant streams are salt free.

D.3.2. The Unit Modules.

In this subsection, the outline of the unit module is emphasized. A particular attention is drawn to the function, representation, and operation of this module within the calculation program (CP).

The main function of the unit module is to set up the coefficients of the equations describing its operations. Therefore, the unit module has to retrieve whatever data is necessary to form the coefficients of the linearized equations. This data may come from a previous iteration values, physical properties, and the unit parameters, via the communication region (data base section).

Each unit module has a number of equations which relate the input and output stream variables, and the unit parameters (as shown in Appendix (C)). The equation is constructed by a number of non-zero elements, where each element contains a coefficient and its associated variable. The equation is generated and set up inside the matrix, element by element, using a subroutine called ELEM. So, the topology of the matrix (the location of zero and non-zero elements) is generated at

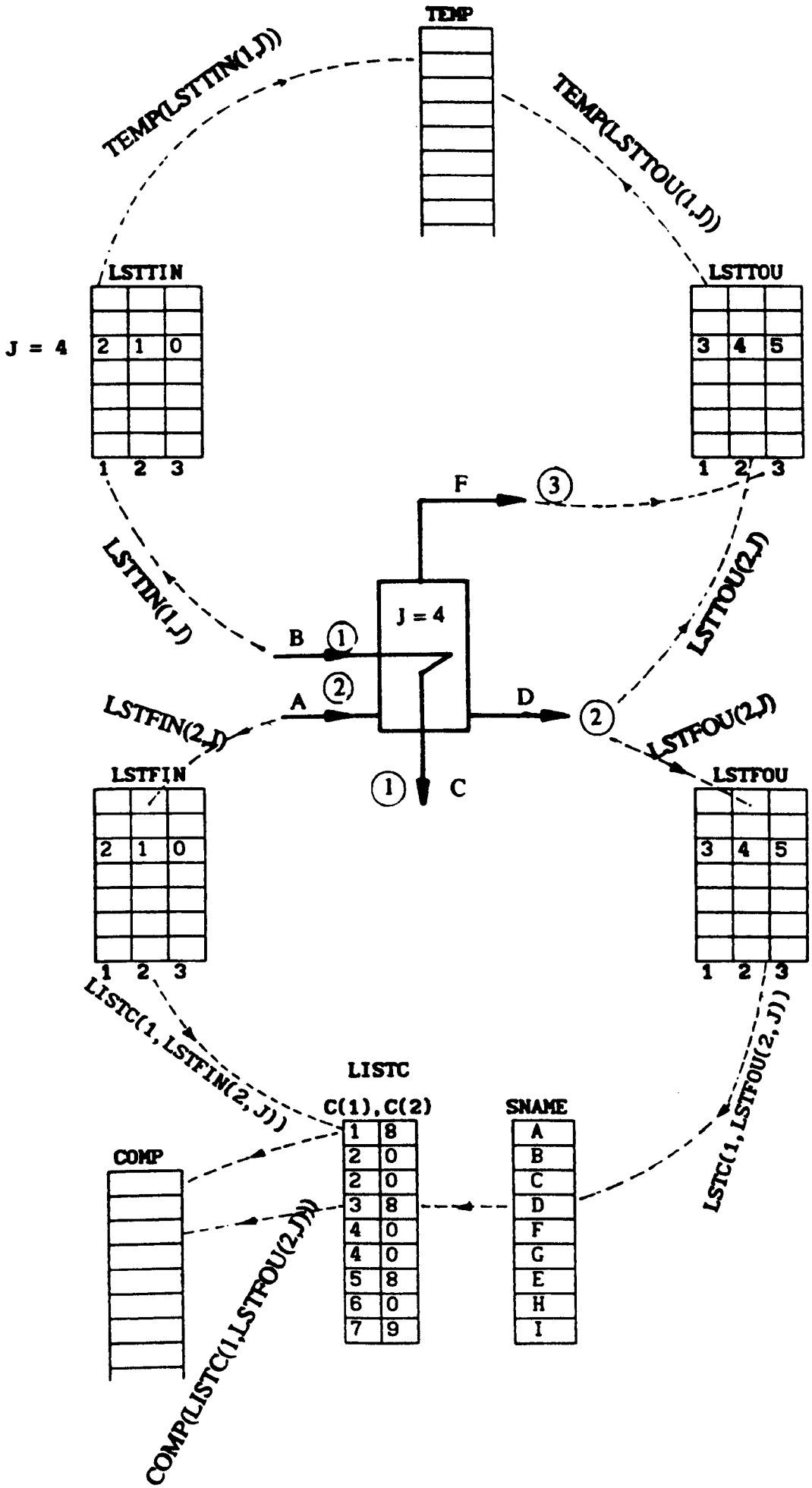

FIGURE D.8. AN EXAMPLE OF THE VARIABLE ARRAYS, {TEMP & COMP arrays}.

the same time. In writing an equation in the unit module, care is taken to structure the equations so that numerical difficulties such as dividing by zero and/or creation of redundant equations during the iteration process are avoided.

In the developed package, each unit operation is defined by three different subroutines, one for each variable type as follows:

- First, subroutines (UNC---), (the unit type number is located instead of the indicated three dashes), this type of subroutines generates the equations related to the component variables, and sets up the component matrix with the aid of the ELEM subroutine.
- Second, subroutines (UNT---), contain the equations related to the temperature variables and construct the temperature matrix.
- The third type is the subroutines (UNP---) which set up the equations relevant to the pressure variables, and build up the pressure matrix.

D.3.3. Setting Up And Solving The Sparse Matrix.

As shown in chapter 5 and Appendix {C}, the mathematical models of the considered thermal desalination processes are characterized by a significant degree of sparsity. In fact, these mathematical models can be solved by direct matrix inversion. Although this technique is easy to program, it cannot, however, exploit the mathematical model sparsity, and produce a completely full inverse matrix. For large problems, the storage is therefore extremely large and the method is very inefficient.

The alternative method to the matrix inversion is the factorization technique based on Gaussian elimination. With this technique sparsity can be exploited, and with a suitable ordering technique the number of new non-zero elements produced during factorization can be minimized. Also, with this technique the solution may be obtained with a minimum amount of storage and computation time. This is because this method only needs the non-zero elements to be stored and processed.

The non-zero elements of the original coefficient matrix are stored in a compact form. To locate each element in that form during the factorization process, accurate indexing information is required, in addition to the numerical value of the non-zero elements.

During the factorization process, new non-zero elements are generated and some of the non-zero elements may become zero. Therefore, the compacting and indexing schemes must be capable of carrying out efficiently these continuous changes.

So, the programing of the sparse matrix solver involves not only the basic aspects of factorization and numerical solution, but also the storing and identifying of the non-zero elements.

A substantial collection of routines for sparse matrix calculation is available from NAG (Numerical Algorithms Group) and IMSL (IMSL. Inc.) libraries, Rice [1985]. However, the method developed by Bending and Hutchison [1973], has been used in the developed program to solve the generated equation sets. By this routine, special ordering for the variables and equation is not required because the routine performs this by itself. Also, the ordering technique used in this routine is efficient enough to keep the generated non-zero elements to a minimum. This makes this routine much easier to use in flowsheeting calculation than many other available routines.

In this routine, the numerical values of all the non-zero elements and their locality information are stored in three arrays. These can be defined as EL (numerical value of the ELement), LR (index of Row) and LC (index of Column). So, the location of each non-zero element is simply defined by the "co-ordinates" of its position in the original coefficient matrix. This technique allows the elements of the equations to be created or reset with very little programming effort and computing time.

As the equations representing the process are generated and set up, their solution starts using the Gaussian-elimination, after re-ordering the coefficient matrix in order to achieve numerical stability, and to minimize the number of fill in. In the first pass of the solution all elements below the diagonal are eliminated, and in the stage of back substitution elements above the diagonal are eliminated to place the matrix into diagonal form. During the solution, the produced fill in elements are placed in the three arrays in the positions of elements which have already been eliminated; otherwise, they are added to the end of the three arrays.

D.3.4. Thermophysical Properties.

All the thermophysical properties are calculated in external routines. Therefore, the thermophysical models are not treated as part of the overall process matrix and are not subject to any simplification or linearization.

After a process matrix iteration, current values of temperature, pressure, and composition are provided to these routines, which in turn update the thermophysical property values required for the next matrix evaluation.

D.4. NEWTON BASED CALCULATION PROGRAM (NBCP).

Using the intermediate data file produced by NDSP explained in section D.2, the material and energy balances as well as the pressure equations are set up and solved by the NBCP. This program and the CP (illustrated in section (6.4)), have a similar construction. However, the unit module subroutines have a different function in both programs. In contrast to the CP (based on the VTBVT technique), the unit modules subroutines in this program set up the unit material and energy balance equation as one set, which is then solved using the standard second order Newton Raphson linearization technique. In this technique the linear system of equations at each iteration takes the form:

$$J(X^k) \times (X^{k+1} - X^k) = - F(X^k) \qquad (4.7)$$

Only the non-zero elements of the Jacobian matrix J(X) and F(X), are stored, and then solved using the sparse matrix routine outlined in the subsection (D.3.3).

Due to the fact that all the component and temperature variables are iterated on, they all require initialization. Newton Raphson will quickly converge from a good initial guess. The problem is to get a good initial guess. Ideally these initial guesses would be provided by the user, this is possible for relatively small problems. However, for a large flowsheet this task would be difficult. This difficulty may be overcome by using the results of the first few iterations of the VTBVT technique as good starting values for the Newton Raphson technique, this would reduce significantly the required number of iterations to the final solution.

D.5. The Result Reports.

Any program is capable of generating and printing out many numbers. However, numbers in themselves are useless unless they are adequately explained in the output. The package output is formatted for easy readability by the user. This output is written in a stream table form. This table shows the unit names, name of streams out of each unit, and stream flowrate, temperature, pressure, and composition. And also the results contains the number of iteration, the tolerance, the calculated heat transfer coefficient (if it is not given as a unit parameter), and the calculated heat transfer area for a design problem. Included with the output, are the input data upon which the results are based. Input and output tables of the VTBVT based calculation program are shown in Tables (D.3), and (D.4) respectively. Also, the results table of Newton Raphson based calculation program (NBCP), has the same layout as that in Table (D.4).

Table (D.3). Specified parameters of the flowsheet

UNIT NAME	PARAMETER	VALUE	UNITS
FEED			
	total flow rate	22680.000	kg/hr
	water flow rate	21546.000	kg/hr
	salt flow rate.	1134.000	kg/hr
	temperature....	330.000	K
	pressure.....	150.000	kPa
STEAM			
	temperature....	400.000	K
PSET			
	set pressure.....	0.000	kPa
EFFECT1			
	area of heat transfer.	150.000	m^2
	heat losses	0.000	kJ/hr
EFFECT2			
	area of heat transfer.	150.000	m^2
	heat losses	0.000	kJ/hr
CONDENSA			
	area * overall Hear transfer coefficient	681271.000	kJ/(hr.K
	pressure drop.....	0.000	kPa
COOLWATA			
	total flow rate	63402.000	kg/hr
	water flow rate	60321.898	kg/hr
	salt flow rate.	3170.100	kg/hr
	temperature....	300.000	K
	pressure.....	100.000	kPa

Table (D.4), Final Results of The CP

UNIT/STREAM	FLOW.(Kg/hr)	TEMP.(K)	PRESS.(kPa)	WATER	SALT(kg/hr)
UNIT FEED					
OUTPUT STREAM A	22680.0	330.000	150.000	21546.0	1134.000
UNIT STEAM					
OUTPUT STREAM B	10714.3	400.000	249.106	10714.3	0.000
UNIT PSET					
OUTPUT STREAM B	10714.3	400.000	249.106	10714.3	0.000
UNIT EFFECT1					
OUTPUT STREAM C	10714.3	400.000	249.106	10714.3	0.000
OUTPUT STREAM D	14557.4	389.493	168.956	13423.4	1134.000
OUTPUT STREAM F	8122.60	388.076	168.956	8122.60	0.000
UNIT EFFECT2					
OUTPUT STREAM G	8122.60	388.076	168.956	8122.60	0.000
OUTPUT STREAM E	6358.79	379.485	118.808	5224.79	1134.000
OUTPUT STREAM H	8198.61	377.860	118.808	8198.61	0.000
UNIT CONDENSA					
OUTPUT STREAM I	63492.0	372.539	100.000	60321.9	3170.100
OUTPUT STREAM H	8198.61	377.860	118.808	8198.61	0.000
UNIT COOLWATA					
OUTPUT STREAM I	63492.0	300.000	100.000	60321.9	3170.100

NO. OF ITERATIONS = 10

CPU = 0.19000 Sec.

Tolerance = 0.6732759E-05

The Calculated Overall Heat Transfer Coefficient Of Effects

EFFECT1

U = 0.148614E+05 kJ/hr.m.m.K

EFFECT2

U = 0.139874E+05 kJ/hr.m.m.K

APPENDIX E

VALIDITY OF THE PROPOSED ASSUMPTIONS FOR DEVELOPING THE VTBVT TECHNIQUE

The leading aims of this Appendix are: one: to illustrate the application of Newton Raphson technique in carrying out the performance calculations for the MEE desalination plant, figure 8.6. Two: to investigate the convergence properties of Newton's method during the iterative solution of the mathematical model, representing the process. Also, to compare these properties with the properties of the VTBVT technique (illustrated in section 8.4). Three: to examine the accuracy of the algorithm, by comparing the final results obtained by Newton and VTBVT techniques. The last two points are performed to examine the effect of the proposed assumptions (chapter 5), on the convergence properties and the results accuracy of the developed VTBVT technique.

E.1 Comparing The Convergence Properties Of Newton And VTBVT Techniques:

As pointed out in section 8.4, 161 material, energy, and heat transfer equations are needed for representing the considered MEE desalination plant. To solve those equations as one set using the traditional Newton's method (equation 4.7), 161 initial guessing values are required.

The convergence behaviour of TVOUT and FVOUT profiles are represented by Figures (E.1) and (E.2). The solution of the performance problem using NR method is nearly formed by the end of the second iteration (after 0.91 second of CPU time). To reach the final solution within the tolerance (error = 0.5×10^{-4}) four more iterations are sufficient. The total CPU time (on Amdahl 580 computer) is 2.7 seconds. After the first few iterations the convergence is rapid. This is illustrated by the numerical results tabulated in Table (E.1) and plotted in Figure (E.3), where the error reduces approximately exponentially with increasing the number of iterations.

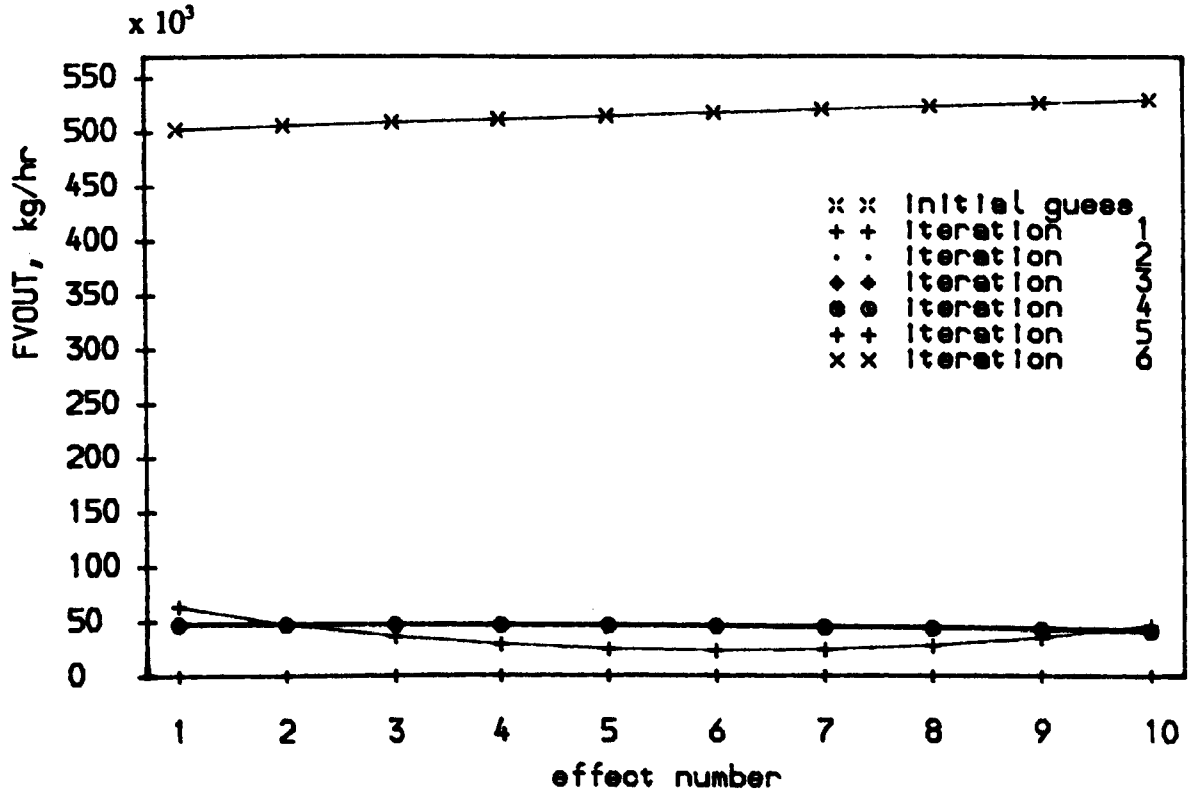

FIG. (E.2) CONVERGENCE OF THE VAPOUR FLOWRATE ALONG THE FLOWSHEET (Newton s method, case I)

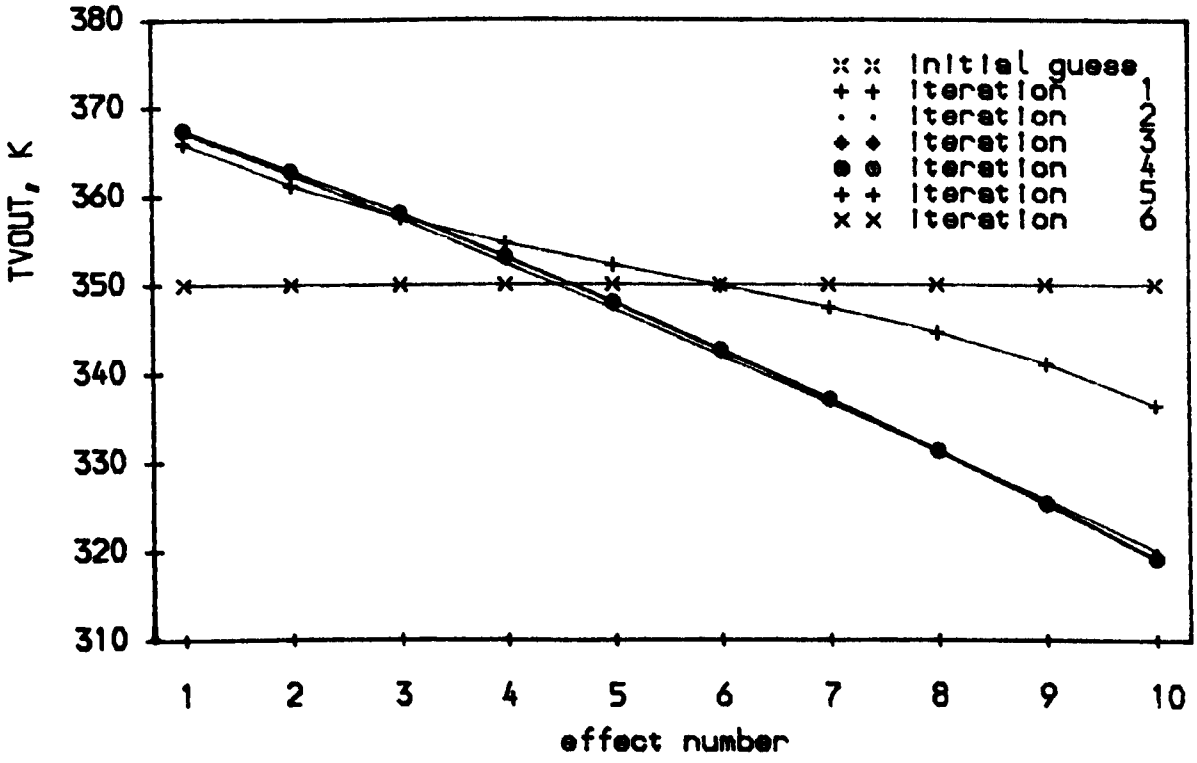

FIG. (E.1) CONVERGENCE OF THE VAPOUR TEMPERATURE ALONG THE FLOWSHEET (Newton s method, case I)

Comparing the above convergence characteristics with the VTBVT technique, presented in section 8.4, the following points can be concluded: first, as can be seen from the above results, Newton's method converges faster (6 iterations) than the VTBVT technique (14 iterations) in performing the performance calculations (case I). This may be due to the simplification (adopted in the VTBVT technique) of the Jacobian matrix by neglecting the insignificant changes of some variables during the iterations. Details of this point are presented in chapter 5. However, it should be noted that the extra number of iterations required by the VTBVT technique is, in fact, not of great practical significance, because all the iterations required by the VTBVT technique take comparatively little computation time (0.74 second). Comparison of the computational time shows that the VTBVT technique requires computational effort of less than one third of that required by Newton's method. This may be because of reducing the size of the problem by decomposing the large set of equations representing the process into smaller subsets. Therefore, the number of the mathematical operations required to achieve the solution is reduced, which consequently, leads to the reduction of the computing time. This great advantage may make the VTBVT technique much more practically attractive.

Table (E.1)

Convergence Characteristics of Newton's Method.

Iteration	Error
1	2312943.00
2	2796.906
3	36.902
4	0.240
5	0.0066
6	0.0000266

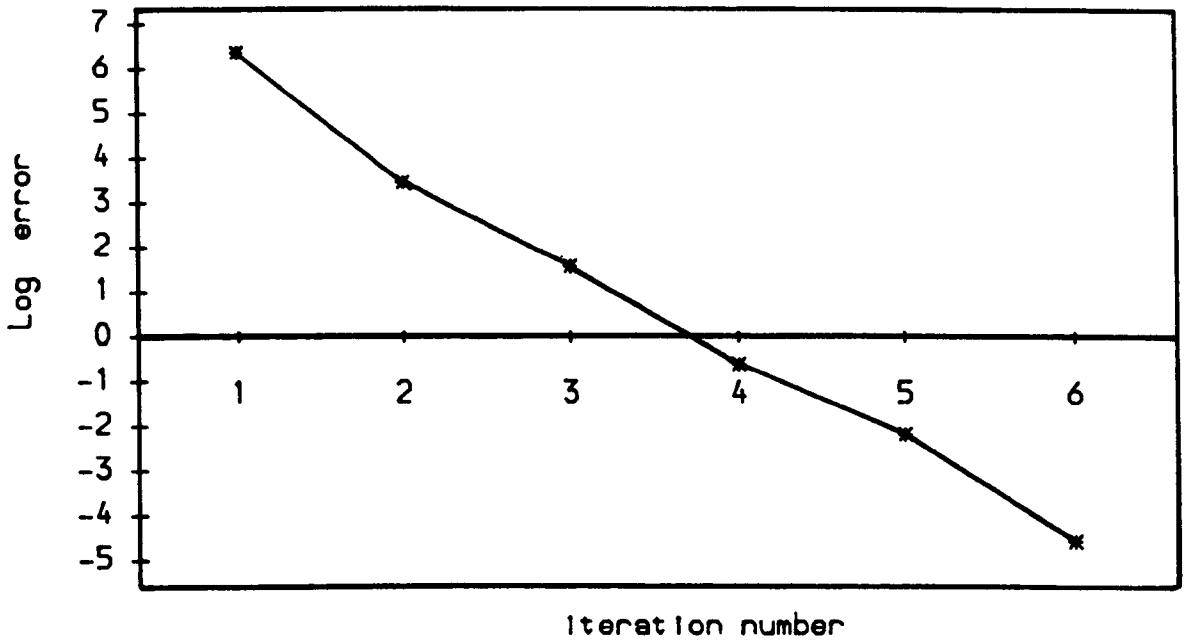

FIG. (E.3) CONVERGENCE BEHAVIOUR OF THE NEWTON RAPHSON TECHNIQUE, (performance calculation case I)

E.2. Comparing The Final Results Of Newton And VTBVT Techniques, For The Plant Performance Calculations.

The question considered in this part of the work is simple, but fundamental, namely: how do we know that the answers from the numerical computations are correct?. In fact one can never know with absolute certainty, see Rice (1983). However, in this section , the validity of the numerical results obtained by Newton and the VTBVT techniques are examined by comparing the final results of both techniques. The final results of the performance calculations (case I) for this comparison are tabulated in Tables (E.2) and (E.3). According to these tables, it could be concluded that the results obtained by the two techniques are consistent, taking into consideration the effect of the round off error and the stopping criteria (as explained in section 8.4.3) The accuracy comparison indicates that the maximum fractional error is $(8.9 \pm 5.9) \times 10^{-5}$ for TBOUT, $(1.21 \pm 0.6) \times 10^{-5}$ for TVOUT, $(8.203 \pm 0.004) \times 10^{-4}$ for FBOUT and $(1.2762 \pm 0.0482) \times 10^{-3}$ for FVOUT profiles.

Table (E.2) Comparison Between The Temperature Profiles For an MEE Plant as Calculated Using Newton And The VTBVT Technique.

EFFECT NO.	TBOUT (K)			TVOUT (K)		
	Newton	VTBVT	Error	Newton	VTBVT.	Error
1	368.060	368.062	-0.002	367.498	367.500	-0.002
2	363.473	363.474	-0.001	362.891	362.892	-0.001
3	358.720	358.720	0.000	358.117	358.116	0.001
4	353.792	353.791	0.001	353.165	353.163	0.002
5	348.679	348.677	0.002	348.025	348.022	0.003
6	343.372	343.370	0.002	342.688	342.685	0.003
7	337.865	337.862	0.003	337.148	337.144	0.004
8	332.151	332.148	0.003	331.396	331.392	0.004
9	326.224	326.222	0.002	325.428	325.424	0.004
10	320.082	320.083	-0.001	319.238	319.237	0.001

Error = Newton Results - VTBVT results.

Table (E.3) Comparison Between The Calculated Flowrate Profiles Along an MEE Plant Using the VTBVT and Newton Techniques.

EFFECT NO.	FBOUT $\times 10^{-3}$ kg/hr			FVOUT $\times 10^{-3}$ kg/hr		
	Newton	VTBVT	Error	Newton	VTBVT	Error
1	859.495	859.456	0.039	47.690	47.728	-0.038
2	812.050	811.973	0.077	47.445	47.483	-0.038
3	764.904	764.791	0.113	47.146	47.183	-0.037
4	718.141	717.992	0.149	46.763	46.799	-0.036
5	671.874	671.689	0.185	46.267	46.303	-0.036
6	626.241	626.023	0.218	45.632	45.666	-0.034
7	581.408	581.157	0.251	44.833	44.866	-0.033
8	537.561	537.278	0.283	43.847	43.879	-0.032
9	494.911	494.591	0.320	42.650	42.687	-0.037
10	453.681	453.309	0.372	41.230	41.283	-0.053

APPENDIX F

STABILITY OF THE VTBVT TECHNIQUE DURING THE SOLUTION OF AN MEE SYSTEM

In this Appendix, the stability of the VTBVT technique under a wide range of the initial guesses is examined. This is achieved by solving the performance calculation problem (case I), which is presented in sections 8.4. Starting with the following four different initial linear temperature profiles

- 300 - 0.1 * NT (where NT is the temperature variable number)
- 350 - 0.1 * NT
- 400 - 0.1 * NT (reported in section 8.4).
- 450 - 0.1 * NT

The vapour temperature TVOUT and vapour flowrate FVOUT profiles during the iterative solution for the above initial guesses are plotted in Figures (F.1), (F.2), (8.9, a,b), and (F.3) respectively. All the calculations converge to the final solution in 14 to 18 iterations.

According to the above figures, the following points can be concluded:

- The user can predict a linear temperature profile as an initial guess between 300 - 450 K (the range of the validity of the physical properties correlations used in the program).
- Also, an interesting point to note is that the convergence does not seem to depend greatly on the initial guess values.

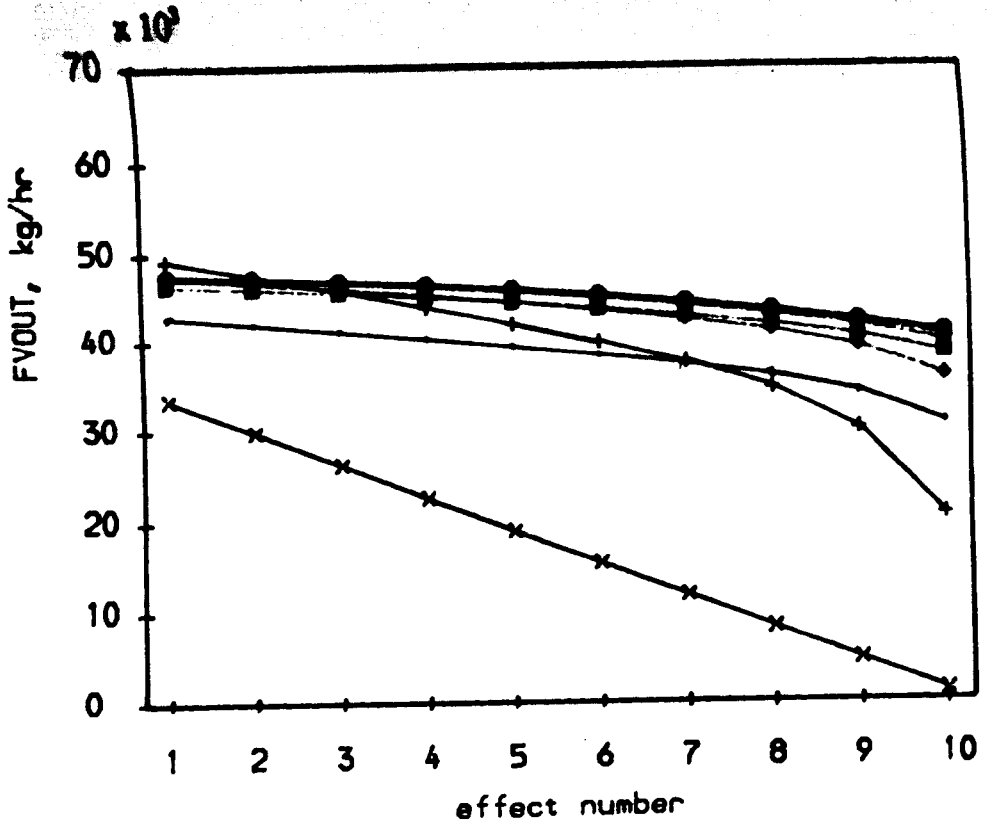

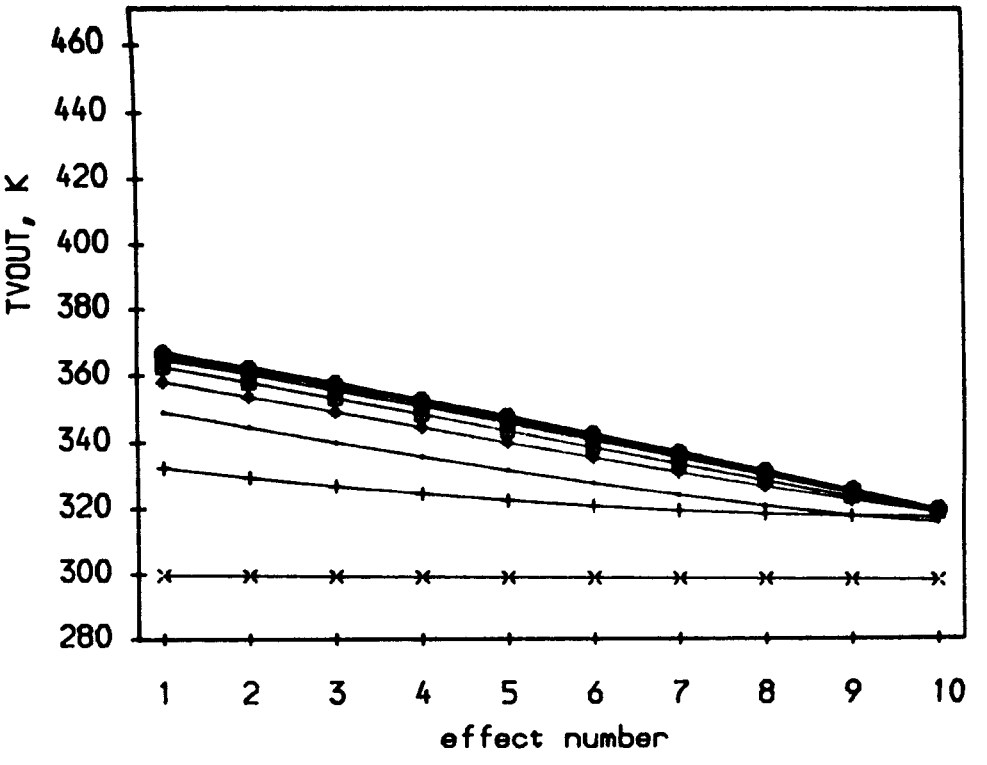

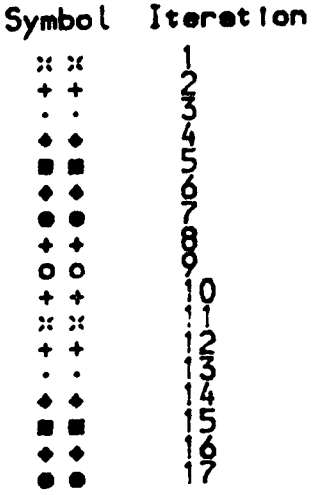

(b) FVOUT vs The Number of Effects

(a) TVOUT vs The Number of Effects

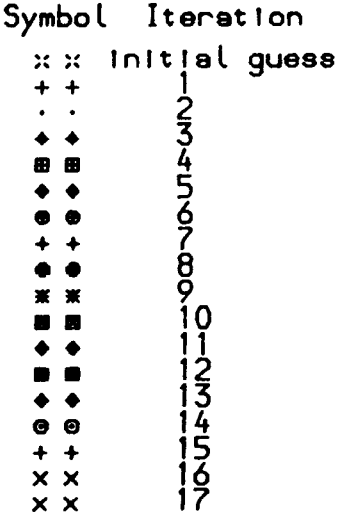

Fig. F.1. THE CONVERGENCE BEHAVIOUR OF THE VTBVT TECHNIQUE.

[Starting at; 300 - 0.1 * NT]

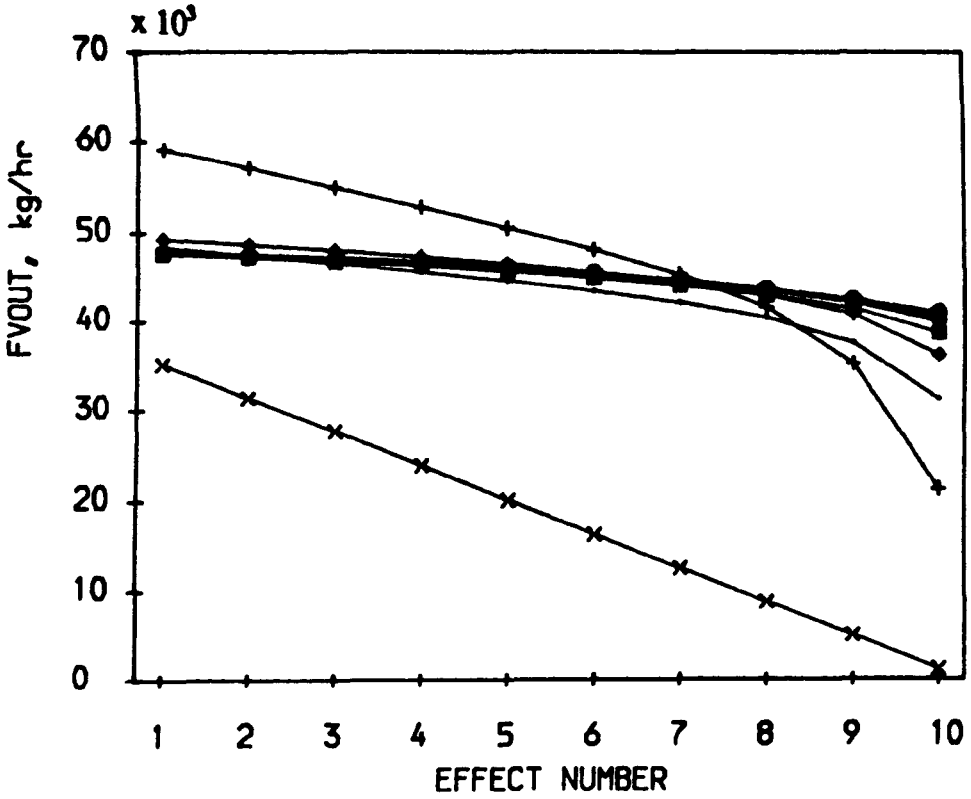

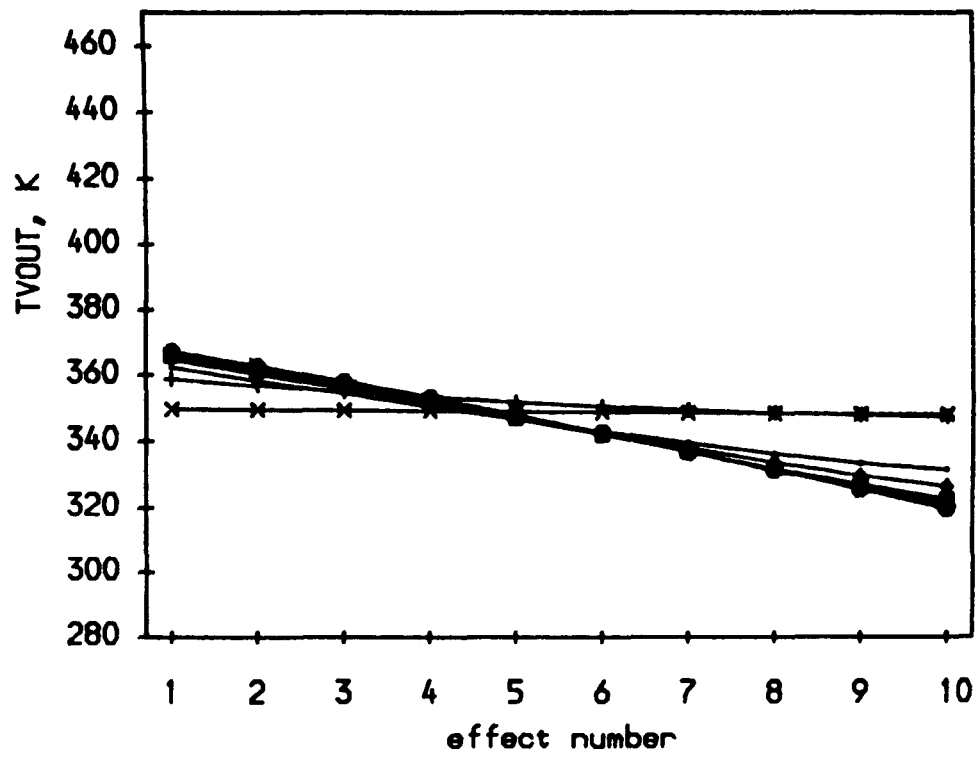

Symbol Iteration

1
2
3
4
5
6
7
8
9
10
11
12
13
14
15
16
17
18

(b) FVOUT vs The Number of Effects

(a) TVOUT vs The Number of Effects

Symbol Iteration

Initial guess
1
2
3
4
5
6
7
8
9
10
11
12
13
14
15
16
17
18

Fig. F.2. THE CONVERGENCE BEHAVIOUR OF THE VTBVT TECHNIQUE.

[Starting at; 350 - 0.1 * NT]

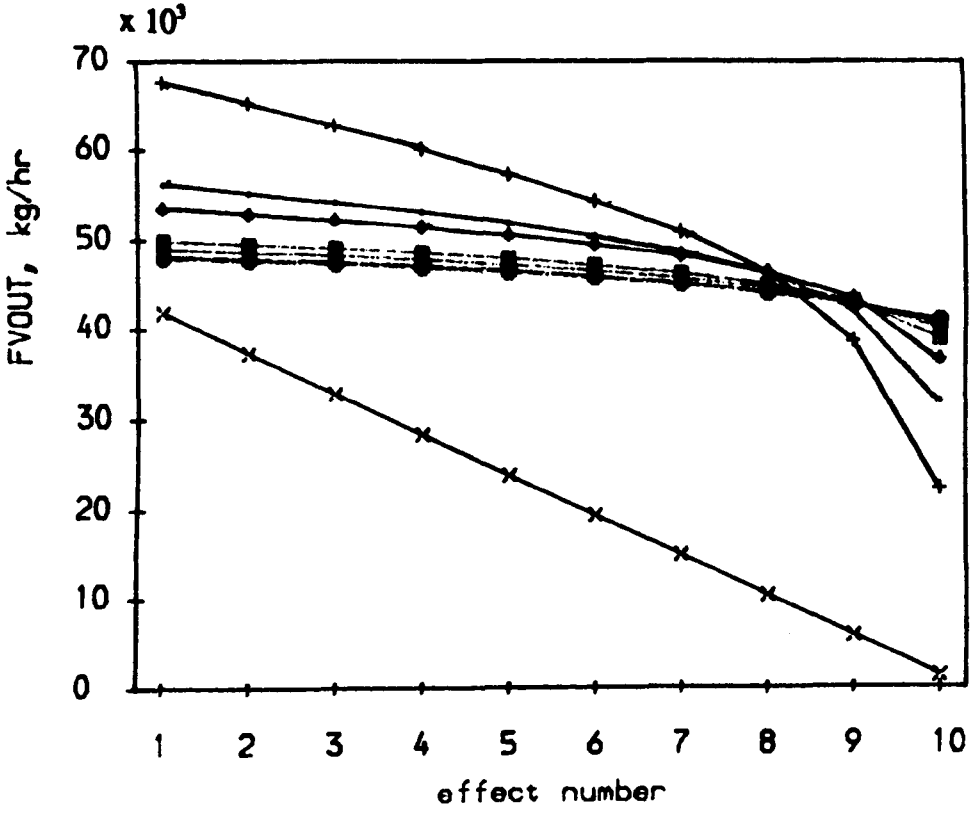

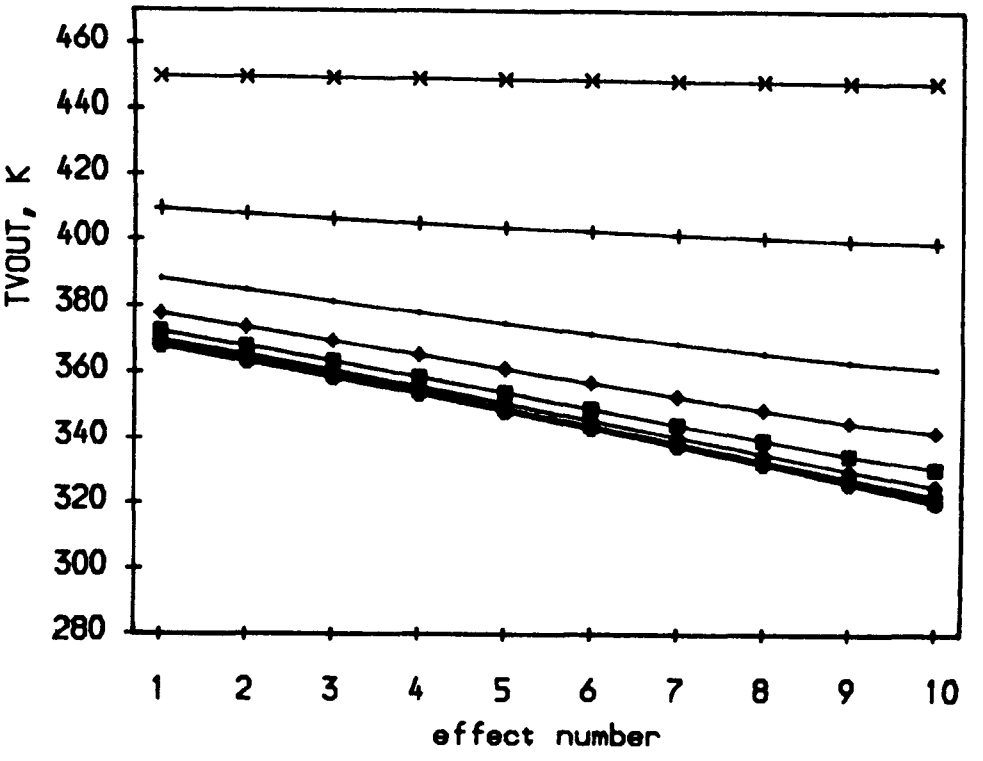

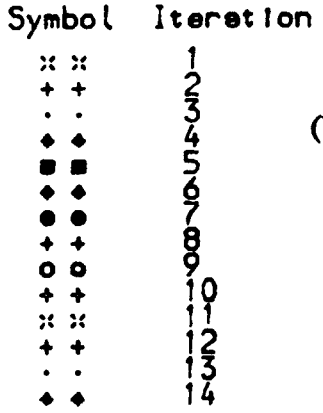

(b) FVOUT vs The Number of Effects

(a) TVOUT vs The Number of Effects

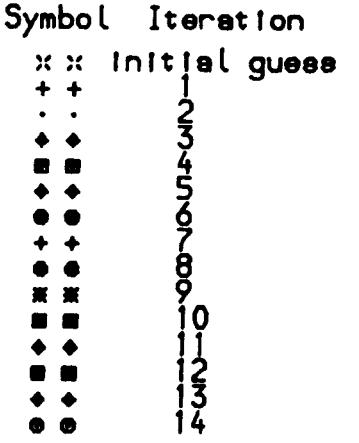

Fig. F.3. THE CONVERGENCE BEHAVIOUR OF THE VTBVT TECHNIQUE.

[Starting at; 450 - 0.1 * NT]

A P P E N D I X G

A complete output report of the design calculation for the MEE system, Figure (8.6).

UNIT/STREAM	FLOWRATE [$\times 10^{-3}$ kg/hr]	TEMP. [K]	PRESS. [kPa.]	WATER [$\times 10^{-3}$ kg/hr]	SALT
UNIT STREAM					
OUTPUT STREAM SIN	53.3716	373.150	101.350	53.3716	0.00E+00
UNIT ME1					
OUTPUT SOUT5	3.3716	373.150	101.350	53.3716	0.00E+00
OUTPUT STREAM B1	859.492	368.064	82.4967	827.741	31.7515
OUTPUT STREAM V1	47.6922	367.502	82.4967	47.6922	0.00E+00
UNIT ME2					
OUTPUT STREAM D2	40.6642	367.502	82.4967	40.6642	0.00E+00
OUTPUT STREAM B2	812.043	363.481	69.4110	780.292	31.7515
OUTPUT STREAM V2	47.4488	362.899	69.4110	47.4488	0.00E+00
UNIT ME3					
OUTPUT STREAM D3	40.5755	362.899	69.4110	40.5755	0.00E+00
OUTPUT STREAM B4	764.893	358.731	57.7244	733.141	31.7515
OUTPUT STREAM V3	47.1505	358.128	57.7244	47.1505	0.00E+00
UNIT ME4					
OUTPUT STREAM D4	40.4120	358.128	57.7244	40.4120	0.00E+00
OUTPUT STREAM B5	718.124	353.806	47.3885	686.373	31.7515
OUTPUT STREAM V4	46.7689	353.178	47.3885	46.7689	0.00E+00
UNIT ME5					
OUTPUT STREAM D5	40.1495	353.178	47.3885	40.1495	0.00E+00
OUTPUT STREAM B6	671.848	348.695	38.3508	640.097	31.7515
OUTPUT STREAM V5	46.2755	348.041	38.3508	46.2755	0.00E+00
UNIT ME6					
OUTPUT STREAM D6	39.7606	348.041	38.3508	39.7606	0.00E+00
OUTPUT STREAM B7	626.206	343.391	30.5500	594.454	31.7515
OUTPUT STREAM V6	45.6425	342.707	30.5500	45.6425	0.00E+00
UNIT ME7					
OUTPUT STREAM D7	39.2221	342.707	30.5500	39.2221	0.00E+00
OUTPUT STREAM V7	44.8456	337.168	23.9147	44.8456	0.00E+00
UNIT ME8					
OUTPUT STREAM D8	38.5095	337.168	23.9147	38.5095	0.00E+00
OUTPUT STREAM B9	537.501	332.172	18.3634	505.749	31.7515
OUTPUT STREAM V8	43.8594	331.417	18.3634	43.8594	0.00E+00
UNIT ME9					
OUTPUT STREAM D9	37.6000	331.417	18.3634	37.6000	0.00E+00
OUTPUT STREAM B10	494.837	326.247	13.8041	463.086	31.7515
OUTPUT STREAM V9	42.6636	325.450	13.8041	42.6636	0.00E+00
UNIT ME10					
OUTPUT STREAM D10	36.4741	325.450	13.8041	36.4741	0.00E+00
OUTPUT BOUT	453.597	320.106	10.1363	421.846	31.7515
OUTPUT STREAM V10	41.2399	319.261	10.1363	41.2399	0.00E+00
UNIT SP1					
OUTPUT STREAM S2	40.6642	367.502	82.4967	40.6642	0.00E+00
OUTPUT STREAM VD1	7.02802	367.502	82.4967	7.02802	0.00E+00
UNIT SP2					

OUTPUT STREAM S3	40.5755	362.899	69.4110	40.5755	0.00E+00
OUTPUT STREAM VD2	6.87334	362.899	69.4110	6.87334	0.00E+00
UNIT SP3					
OUTPUT STREAM S4	40.4120	358.128	57.7244	40.4120	0.00E+00
OUTPUT STREAM VD3	6.73845	358.128	57.7244	6.73845	0.00E+00
UNIT SP4					
OUTPUT STREAM S5	40.1495	353.178	47.3885	40.1495	0.00E+00
OUTPUT STREAM VD4	6.61947	353.178	47.3885	6.61947	0.00E+00
UNIT SP5					
OUTPUT STREAM S6	39.7606	348.041	38.3508	39.7606	0.00E+00
OUTPUT STREAM VD5	6.51490	348.041	38.3508	6.51490	0.00E+00
UNIT SP6					
OUTPUT STREAM S7	39.2221	342.707	30.5500	39.2221	0.00E+00
OUTPUT STREAM VD6	6.42047	342.707	30.5500	6.42047	0.00E+00
UNIT SP7					
OUTPUT STREAM S8	38.5095	337.168	23.9147	38.5095	0.00E+00
OUTPUT STREAM VD7	6.33610	337.168	23.9147	6.33610	0.00E+00
UNIT SP8					
OUTPUT STREAM S9	37.6000	331.417	18.3634	37.6000	0.00E+00
OUTPUT STREAM VD8	6.25939	331.417	18.3634	6.25939	0.00E+00
UNIT SP9					
OUTPUT STREAM S10	36.4741	325.450	13.8041	36.4741	0.00E+00
OUTPUT STREAM VD9	6.18945	325.450	13.8041	6.18945	0.00E+00
UNIT SP10					
OUTPUT STREAM V11	21.2443	319.261	10.1363	21.2443	0.00E+00
OUTPUT STREAM V12	19.9956	319.261	10.1363	19.9956	0.00E+00
UNIT MIX1					
OUTPUT STREAM Y3	88.2677	363.019	82.4967	88.2677	0.00E+00
UNIT MIX2					
OUTPUT STREAM Y4	135.553	358.366	69.4110	135.553	0.00E+00
UNIT MIX3					
OUTPUT STREAM Y5	182.441	353.535	57.7244	182.441	0.00E+00
UNIT MIX4					
OUTPUT STREAM Y6	228.821	348.516	47.3885	228.821	0.00E+00
UNIT MIX5					
OUTPUT STREAM Y7	274.558	343.300	38.3508	274.558	0.00E+00
UNIT MIX6					
OUTPUT STREAM Y8	319.488	337.880	30.5500	319.488	0.00E+00
UNIT MIX7					
OUTPUT STREAM Y9	363.424	332.249	23.9147	363.424	0.00E+00
UNIT MIX8					
OUTPUT STREAM Y10	406.158	326.402	18.3634	406.158	0.00E+00
UNIT MIX9					
OUTPUT STREAM D13	41.2399	319.261	10.1363	41.2399	0.00E+00
UNIT MIX10					
OUTPUT DISOU	453.587	320.333	13.8041	453.587	0.00E+00
UNIT MIX11					
OUTPUT STREAM X2	47.6922	367.502	82.4967	47.6922	0.00E+00
UNIT MIX12					
OUTPUT STREAM X3	95.1411	362.959	69.4110	95.1411	0.00E+00
UNIT MIX13					
OUTPUT STREAM X4	142.292	358.247	57.7244	142.292	0.00E+00
UNIT MIX14					
OUTPUT STREAM X5	189.060	353.357	47.3885	189.060	0.00E+00
UNIT MIX15					
OUTPUT STREAM X6	235.336	348.278	38.3508	235.336	0.00E+00
UNIT MIX16					

OUTPUT STREAM X7	280.979	343.003	30.5500	280.979	0.00E+00
UNIT MIX17					
OUTPUT STREAM X8	325.824	337.524	23.9147	325.824	0.00E+00
UNIT MIX18					
OUTPUT STREAM X9	369.684	331.833	18.3634	369.684	0.00E+00
UNIT MIX19					
OUTPUT STREAM X10	412.347	325.926	13.8041	412.347	0.00E+00
UNIT VB1					
OUTPUT STREAM BIN	907.185	364.724	100.000	875.433	31.7515
OUTPUT STREAM VD1	7.02802	367.502	82.4967	7.02802	0.00E+00
UNIT VB2					
OUTPUT STREAM BIN	907.185	360.121	100.000	875.433	31.7515
OUTPUT STREAM VD2	6.87334	362.899	69.4110	6.87334	0.00E+00
UNIT VB3					
OUTPUT STREAM BIN	907.185	355.350	100.000	875.433	31.7515
OUTPUT STREAM VD3	6.73845	358.128	57.7244	6.73845	0.00E+00
UNIT VB4					
OUTPUT STREAM BIN	907.185	350.400	100.000	875.433	31.7515
OUTPUT STREAM VD4	6.61947	353.178	47.3885	6.61947	0.00E+00
UNIT VB5					
OUTPUT STREAM BIN	907.185	345.263	100.000	875.433	31.7515
OUTPUT STREAM VD5	6.51490	348.041	38.3508	6.51490	0.00E+00
UNIT VB6					
OUTPUT STREAM BIN	907.185	339.929	100.000	875.433	31.7515
OUTPUT STREAM VD6	6.42047	342.707	30.5500	6.42047	0.00E+00
UNIT VB7					
OUTPUT STREAM BIN	907.185	334.390	100.000	875.433	31.7515
OUTPUT STREAM VD7	6.33610	337.168	23.9147	6.33610	0.00E+00
UNIT VB8					
OUTPUT STREAM BIN	907.185	328.639	100.000	875.433	31.7515
OUTPUT STREAM VD8	6.25939	331.417	18.3634	6.25939	0.00E+00
UNIT VB9					
OUTPUT STREAM BIN	907.185	322.672	100.000	875.433	31.7515
OUTPUT STREAM VD9	6.18945	325.450	13.8041	6.18945	0.00E+00
UNIT COND10					
OUTPUT STREAM BIN	907.185	316.483	100.000	875.433	31.7515
OUTPUT STREAM V11	21.2443	319.261	10.1363	21.2443	0.00E+00
UNIT COND11					
OUTPUT STREAM CF	853.862	316.483	100.000	823.977	29.8852
OUTPUT STREAM V12	19.9956	319.261	10.1363	19.9956	0.00E+00
UNIT FEED1					
OUTPUT STREAM BIN	907.185	302.500	100.000	875.433	31.7515
UNIT FEED2					
OUTPUT STREAM CF	853.862	302.500	100.000	823.977	29.8852
UNIT HEX1					
OUTPUT STREAM X2	47.6922	363.138	82.4967	47.6922	0.00E+00
OUTPUT STREAM BIN	907.185	360.360	100.000	875.433	31.7515
UNIT HEX2					
OUTPUT STREAM X3	95.1411	358.604	69.4110	95.1411	0.00E+00
OUTPUT STREAM BIN	907.185	355.826	100.000	875.433	31.7515
UNIT HEX3					
OUTPUT STREAM X4	142.292	353.891	57.7244	142.292	0.00E+00
OUTPUT STREAM BIN	907.185	351.113	100.000	875.433	31.7515
UNIT HEX4					
OUTPUT STREAM X5	189.060	348.990	47.3885	189.060	0.00E+00
OUTPUT STREAM BIN	907.185	346.212	100.000	875.433	31.7515
UNIT HEX5					

OUTPUT STREAM X6	235.336	343.893	38.3508	235.336	0.00E+00
OUTPUT STREAM BIN	907.185	341.115	100.000	875.433	31.7515
UNIT HEX6					
OUTPUT STREAM X7	280.979	338.593	30.5500	280.979	0.00E+00
OUTPUT STREAM BIN	907.185	335.814	100.000	875.433	31.7515
UNIT HEX7					
OUTPUT STREAM X8	325.824	333.081	23.9147	325.824	0.00E+00
OUTPUT STREAM BIN	907.185	330.303	100.000	875.433	31.7515
UNIT HEX8					
OUTPUT STREAM X9	369.684	327.354	18.3634	369.684	0.00E+00
OUTPUT STREAM BIN	907.185	324.576	100.000	875.433	31.7515
UNIT HEX9					
OUTPUT STREAM X10	412.347	321.405	13.8041	412.347	0.00E+00
OUTPUT STREAM BIN	907.185	318.627	100.000	875.433	31.7515
UNIT TB					
OUTPUT STREAM V10	41.2399	319.261	10.1363	41.2399	0.00E+00
UNIT TS					
OUTPUT STREAM V10	41.2399	319.261	10.1363	41.2399	0.00E+00
UNIT CSET					
OUTPUT STREAM BOU	453.597	320.106	10.1363	421.846	31.7515
UNIT VAL1					
OUTPUT STREAM D3	40.5755	362.899	82.4967	40.5755	0.00E+00
UNIT VAL2					
OUTPUT STREAM D4	40.4120	358.128	69.4110	40.4120	0.00E+00
UNIT VAL3					
OUTPUT STREAM D5	40.1495	353.178	57.7244	40.1495	0.00E+00
UNIT VAL4					
OUTPUT STREAM D6	39.7606	348.041	47.3885	39.7606	0.00E+00
UNIT VAL5					
OUTPUT STREAM D7	39.2221	342.707	38.3508	39.2221	0.00E+00
UNIT VAL6					
OUTPUT STREAM D8	38.5095	337.168	30.5500	38.5095	0.00E+00
UNIT VAL7					
OUTPUT STREAM D9	37.6000	331.417	23.9147	37.6000	0.00E+00
UNIT VAL8					
OUTPUT STREAM D10	36.4741	325.450	18.3634	36.4741	0.00E+00
UNIT VAL9					
OUTPUT STREAM V11	21.2443	319.261	10.1363	21.2443	0.00E+00
UNIT VAL10					
OUTPUT STREAM D13	41.2399	319.261	13.8041	41.2399	0.00E+00
UNIT VAL11					
OUTPUT STREAM D2	40.6642	367.502	82.4967	40.6642	0.00E+00
UNIT VAL12					
OUTPUT STREAM Y3	88.2677	363.019	69.4110	88.2677	0.00E+00
UNIT VAL13					
OUTPUT STREAM Y4	135.553	358.366	57.7244	135.553	0.00E+00
UNIT VAL14					
OUTPUT STREAM Y5	182.441	353.535	47.3885	182.441	0.00E+00
UNIT VAL15					
OUTPUT STREAM Y6	228.821	348.516	38.3508	228.821	0.00E+00
UNIT VAL16					
OUTPUT STREAM Y7	274.558	343.300	30.5500	274.558	0.00E+00
UNIT VAL17					
OUTPUT STREAM Y8	319.488	337.880	23.9147	319.488	0.00E+00
UNIT VAL18					
OUTPUT STREAM Y9	363.424	332.249	18.3634	363.424	0.00E+00
UNIT VAL19					
OUTPUT STREAM Y10	406.158	326.402	13.8041	406.158	0.00E+00

```
ITERATION     8
CPU =         0.52  SEC.
Tolerance =  0.4045E-04
The Calculated Overall Heat Transfer Coefficient Of Effects
ME1
U = 0.131226E+05  kJ/hr.m.m.K
ME2
U = 0.127282E+05  kJ/hr.m.m.K
ME3
U = 0.123194E+05  kJ/hr.m.m.K
ME4
U = 0.118953E+05  kJ/hr.m.m.K
ME5
U = 0.114550E+05  kJ/hr.m.m.K
ME6
U = 0.109979E+05  kJ/hr.m.m.K
ME7
U = 0.105233E+05  kJ/hr.m.m.K
ME8
U = 0.100305E+05  kJ/hr.m.m.K
ME9
U = 0.951918E+04  kJ/hr.m.m.K
ME10
U = 0.898887E+04  kJ/hr.m.m.K
```

A P P E N D I X H

The output report of the design calculation for the combined VTE/VC/MSF process, Figure (9.11).

UNIT/STREAM	FLOWRATE $\times 10^{-3}$ kg/hr	TEMP. K	PRESS. kPa.	WATER [$\times 10^{-3}$ kg/hr]	SALT kg/hr
UNIT STEAM					
OUTPUT STREAM S	27.1625	398.150	232.100	27..625	0.00E+00
UNIT VTE1					
OUTPUT STREAM D1	309.922	398.150	230.456	309.922	0.00E+00
OUTPUT STREAM B1	1980.41	394.905	211.092	1901.03	79.3787
OUTPUT STREAM V1	287.549	394.185	205.086	287.549	0.00E+00
UNIT VTE2					
OUTPUT STREAM D12	272.835	394.061	205.086	272.835	0.00E+00
OUTPUT STREAM B2	1695.25	391.126	187.146	1615.87	79.3787
OUTPUT STREAM V6	285.162	390.288	181.139	285.162	0.00E+00
UNIT VTE3					
OUTPUT STREAM D16	271.614	390.225	181.139	271.614	0.00E+00
OUTPUT STREAM B3	1413.04	387.219	164.594	1333.66	79.3787
OUTPUT STREAM V11	282.211	386.210	158.587	282.211	0.00E+00
UNIT VTE4					
OUTPUT STREAM D21	270.110	386.204	158.587	270.110	0.00E+00
OUTPUT STREAM B4	1133.99	383.121	143.081	1054.61	79.3787
OUTPUT STREAM V15	279.044	381.850	137.075	279.044	0.00E+00
UNIT SP4					
OUTPUT STREAM V3	16.9031	394.185	205.086	16.9031	0.00E+00
OUTPUT STREAM V2	270.645	394.185	205.086	270.645	0.00E+00
UNIT SP5					
OUTPUT STREAM V8	17.7133	390.288	181.139	17.7133	0.00E+00
OUTPUT STREAM V7	267.448	390.288	181.139	267.448	0.00E+00
UNIT SP6					
OUTPUT STREAM V13	18.5625	386.210	158.587	18.5625	0.00E+00
OUTPUT STREAM V12	263.648	386.210	158.587	263.648	0.00E+00
UNIT SP7					
OUTPUT STREAM V16	18.7610	381.850	137.075	18.7610	0.00E+00
OUTPUT STREAM V17	260.283	381.850	137.075	260.283	0.00E+00
UNIT MX2					
OUTPUT STREAM V22	309.922	398.150	230.456	309.922	0.00E+00
UNIT COMP					
OUTPUT STREAM V20	269.349	444.535	230.456	269.349	0.00E+00
UNIT HEX1					
OUTPUT STREAM C3	2267.96	389.965	93.1398	2188.58	79.3787
OUTPUT STREAM V3	16.9031	394.185	205.086	16.9031	0.00E+00
UNIT HEX2					
OUTPUT STREAM C3	2267.96	385.948	109.395	2188.58	79.3787
OUTPUT STREAM V8	17.7133	390.288	181.139	17.7133	0.00E+00
UNIT HEX3					
OUTPUT STREAM C3	2267.96	381.710	125.650	2188.58	79.3787

OUTPUT STREAM V13	18.5625	386.210	158.587	18.5625	0.00E+00
UNIT HEX4					
OUTPUT STREAM C3	2267.96	377.240	141.905	2188.58	79.3787
OUTPUT STREAM V16	18.7610	381.850	137.075	18.7610	0.00E+00
UNIT MX3					
OUTPUT STREAM D11	284.062	394.061	205.086	284.062	0.00E+00
UNIT MX4					
OUTPUT STREAM D13	556.897	394.061	205.086	556.897	0.00E+00
UNIT FT2					
OUTPUT STREAM D14	552.732	390.162	181.139	552.732	0.00E+00
OUTPUT STREAM V9	4.16535	390.162	181.139	4.16535	0.00E+00
UNIT MX5					
OUTPUT STREAM D17	570.445	390.225	181.139	570.445	0.00E+00
UNIT MX6					
OUTPUT STREAM D18	842.059	390.225	181.139	842.059	0.00E+00
UNIT FT3					
OUTPUT STREAM D19	835.598	386.198	158.587	835.598	0.00E+00
OUTPUT STREAM V18	6.46117	386.198	158.587	6.46117	0.00E+00
UNIT MX7					
OUTPUT STREAM D22	854.160	386.204	158.587	854.160	0.00E+00
UNIT MX8					
OUTPUT STREAM D23	1124.27	386.204	158.587	1124.27	0.00E+00
UNIT FT4					
OUTPUT STREAM D24	1115.20	381.943	137.075	1115.20	0.00E+00
OUTPUT STREAM V19	9.06563	381.943	137.075	9.06563	0.00E+00
UNIT MX9					
OUTPUT STREAM D26	1133.97	381.897	137.075	1133.97	0.00E+00
UNIT CS1					
OUTPUT STREAM B4	1133.99	383.121	143.081	1054.61	79.3787
UNIT FEED					
OUTPUT STREAM C1	2267.96	297.040	100.000	2188.58	79.3787
UNIT SP2					
OUTPUT STREAM D5	40.5736	398.150	230.456	40.5736	0.00E+00
OUTPUT STREAM D4	269.349	398.150	230.456	269.349	0.00E+00
UNIT SP3					
OUTPUT STREAM D7	13.4112	398.150	230.456	13.4112	0.00E+00
OUTPUT STREAM S	27.1625	398.150	230.456	27.1625	0.00E+00
UNIT DSUB					
OUTPUT STREAM V21	282.760	398.150	230.456	282.760	0.00E+00
UNIT REC					
OUTPUT STREAM C3	2267.96	372.692	158.161	2188.58	79.3787
OUTPUT STREAM D27	1234.06	323.850	12.7612	1234.06	0.00E+00
OUTPUT STREAM B5	1033.90	326.118	14.2606	954.520	79.3787
UNIT REJ					
OUTPUT STREAM C2	2267.96	315.706	98.7544	2188.58	79.3787
OUTPUT STREAM D28	1263.26	304.839	4.66806	1263.26	0.00E+00
OUTPUT STREAM B6	1004.70	307.480	5.41363	925.320	79.3787
UNIT TS3					
OUTPUT STREAM B6	1004.70	307.480	5.41363	925.320	79.3787
UNIT TS2					
OUTPUT STREAM C2	2267.96	315.706	98.7544	2188.58	79.3787
UNIT VL1					
OUTPUT STREAM D9	267.159	393.938	205.086	267.159	0.00E+00
UNIT FT1					
OUTPUT STREAM D9	267.159	393.938	205.086	267.159	0.00E+00
OUTPUT STREAM V4	2.18986	393.938	205.086	2.18986	0.00E+00
UNIT VL2					

OUTPUT STREAM D12	272.835	394.061	205.086	272.835	0.00E+00
UNIT VL3					
OUTPUT STREAM D16	271.614	390.225	181.139	271.614	0.00E+00
UNIT VL4					
OUTPUT STREAM D21	270.110	386.204	158.587	270.110	0.00E+00
UNIT VL5					
OUTPUT STREAM D14	552.732	390.162	181.139	552.732	0.00E+00
UNIT VL6					
OUTPUT STREAM D19	835.598	386.198	158.587	835.598	0.00E+00
UNIT VL7					
OUTPUT STREAM D24	1115.20	381.943	137.075	1115.20	0.00E+00
UNIT VL8					
OUTPUT STREAM S	27.1625	398.150	230.456	27.1625	0.00E+00
UNIT VL9					
OUTPUT STREAM D7	13.4112	398.150	230.456	13.4112	0.00E+00
UNIT PUMP1					
OUTPUT STREAM C1	2267.96	297.040	773.700	2188.58	79.3787
UNIT MX10					
OUTPUT STREAM V5	272.835	394.061	205.086	272.835	0.00E+00
UNIT MX11					
OUTPUT STREAM V10	271.614	390.225	181.139	271.614	0.00E+00
UNIT MX12					
OUTPUT STREAM V14	270.110	386.204	158.587	270.110	0.00E+00
UNIT MX13					
OUTPUT STREAM V20	269.349	381.897	137.075	269.349	0.00E+00
UNIT PUMP4					
OUTPUT STREAM C2	2267.96	315.706	4563.75	2188.58	79.3787

ITERATION 14

CPU = 1.65 SEC.
Tolerance = 0.3162836E-04
The Calculated Overall Heat Transfer Coefficient Of Effects
VTE1
U= 0.308182E+05 kJ/hr.m.m.K
VTE2
U= 0.301533E+05 kJ/hr.m.m.K
VTE3
U= 0.294535E+05 kJ/hr.m.m.K
VTE4
U= 0.287043E+05 kJ/hr.m.m.K

NOMENCLATURE

Letter Symbols

A	Area of heat transfer
A	A coefficient matrix
a	A particular constant for different streams (equation 5.11,d)
B	Brine mass flowrate.
B	A vector of constants.
b	A particular constant for different streams (equation 5.11,d)
C	Brine recycle concentration ratio.
Cp	Heat capacity.
CR	Particular Correction factor, equation (A.14,g)
D	Condensate flowrate, plant production.
E	Evaporation.
E	Correction matrix for material balance error (equation 4.18)
F	Liquid mass flowrate.
F	A vector of linear and nonlinear functions.
$\mathcal{F}$	Friction factor.
g	Acceleration of gravity.
H	Vapour (or steam) enthalpy & total pumping head.
H	Correction matrix for energy balance error(equation 4.24)
H	Superheated steam (vapour) enthalpy.
h	Liquid specific enthalpy.
J(X)	Matrix of partial derivatives (Jacobian matrix).
L	Tube length.
M	Makeup flowrate.
M	Occurrence matrix.
m	an element in the occurrence matrix.
N	Flooding factor & total number of stages (or effects).
NT	Temperature variable number.
Q	Heat flowrate & volume Flowrate.
P	Pressure.
R	Resistance & brine recirculation flowrate.
S	Salt flowrate & steam flowrate.
T	Temperature, K.
t	Temperature, C.

U	Overall heat transfer coefficient.
V	Vapour (or steam) flowrate.
θ	Velocity.
W	Water flowrate
ω	Work
X	Salt concentration.
$\underline{X}$	A vector of variables.

Subscripts;

aux.	Auxiliary amount.
b	Brine into and out of a unit & blowdown.
c	Cooling brine & compressor & cost.
d	Condensate from a unit.
e	Energy.
eff	Effect.
f	Fouling & film of condensate & feed.
h	Heater.
i	Present stage number & row in a matrix.
in	Input stream.
j	Present effect number & column in a matrix.
m	Mean & material & make-up.
max	Maximum value.
N	Unit number N of the plant.
ou	Output stream.
rej	Rejection section.
rec	Recovery section.
s	Steam & stage.
t	Temperature.
w	Tube wall thickness.
1	Suction of the compressor unit.
2	Delivery of the compressor unit.

Superscripts;

k	The previous iteration number.
k+1	Current iteration number.

Greek letters;

α	Splitting ratio.

γ	Polytropic index.
Δ	Difference between two values.
Δt	Temperature drop, stage temperature decrement.
ε	Predescribed tolerance.
ξ	Ratio of area of the j^{th} effect to the reference area.
η	Thermal efficiency.
λ	Latent heat of vaporization.
μ	Absolute viscosity.
ν	Dynamic viscosity
ρ	Density.

Abbreviations;

BHP	Brake horse power.
BPR	Boiling point rise.
FBOUT	Brine flowrate out of a unit.
FDOUT	Distillate flowrate out of a unit.
FF	Flooding factor.
FVOUT	Vapour flowrate out of each effect.
ID	Tube inside diameter.
NEA	Non equilibrium allowance.
Nu	Nusselt number.
OD	Tube outside diameter.
ppm	Particle per million.
Pr	Prandtl number.
TBOUT	Temperature of the brine out of a stage.
TCOUT	Cooling water temperature out of a unit.
TDOUT	Distillate water temperature out of a unit.
TVOUT	Vapour temperature out of each effect.

REFERENCES

Aly, G., "Computer Simulations of Multiple Effect FFE-VC systems for Water Desalination", Desalination, 45, 119-131, 1983.

Amundson, N.R. and Pontinen, A.J., "Multicomponent Distillation Calculations on a Large Digital Computer", Industrial and Engineering Chemistry, 50(5), May 1958.

Andrew, S.M., "Computer Flowsheeting Using Network 67 : an Example", Trans. Instn Chem. Engrs., 46, 123, 1968.

Arad, N., P. Glueckstern and Y. Kantor, "Enhancement of Product Water output Rate by Design Modifications of Existing Multistage Flash Evaporator Plants", Fourth International Symposium on Fresh Water From The Sea, 1, 135-142, 1973.

Ayangbile, W.O., E.O.Okeke, and G.S.G. Beveridge,"Generalised Steady-State Cascade Simulation Algorithm in Multiple-Effect Evaporation", Computers &Chemical Engineering, 8 (3/4), 235-242, 1984.

Azbel, D., "Heat Transfer Applications in Process Engineering", Noyes Publications, N.Jersey, 1984.

Barba, D., G. Liuzzd and G. Tagliaferri,"Mathematical Model For Multi flash Desalting Plant Control", 4th International Symposium on Fresh Water Form the Sea, 1, 153-168, 1973.

Bending, M.J. and H.P. Hutchison, "The Calculation of Steady State Incompressible Flow in Large Networks of Pipes", Chem. Eng. Science, 1857-1864, 1973.

Berger, F. and F.A. Perris, "FLOWPACK II - a New Generation of Systems for Steady State Process Flowsheeting", 12th Symposium on Computer Applications in Chemical Engineering, CACE '79,

Montreux, Switzerland, 1979.

Bolmstedt, U. and C. Gudmundson, "Improved Methods For Design and Evaporation Calculations of Multiple Effect Evaporation Plants", Svensk Papperstidning, 1, 27, 1974.

Browell, R.W. and J.H. Burris, "ORFIG-MSF : a FORTRAN Code for Operational Studies of Fixed Geometry Multistage", ORNL/MT - 3275, 1971.

Broyden, C.G., "A Class of Methods For Solving Nonlinear Simultaneous Equations", Math. Comp. 19, 577, 1965.

Buros, O.K., "The U.S.A.I.D. Desalination Manual", CH2M Hill International Corp., Gainesville, Fl. (Aug. 1980).

Chang, H.Y. and I.E. Over, "Selected Numerical Methods and Computer Programs for Chemical Engineers", Sterling Swift, Manchaca, Tex., 1981.

Chauvel, A., Leprince, P., Barthel, Y. and Raimbault, C., "Manual of Economic Analysis of Chemical Processes", McGraw Hill, N.Y., 1981

Chen, H.S. and M.A. Stadtherr, "A Simultaneous Modular Approach to Process Flowsheeting and Optimization, Part I: Theory and Implementation", AIChE J., 31(11), 1985.

CHESS, "Chemical Engineering Simulation System", System Guide, Houston, Texas, Technical Publishing Company, 1968.

Dodge, B.F. and A.M. Eshaya, "Thermodynamic of Some Desalting Processes", Advan. Chem. Ser., No. 27, 1960.

D'orival, M., "Water Desalting and Nuclear Energy", Karl Thiemig Pulp., Munich, 1967.

Dukler, A.E., L.C. Elliott and A.L. Parber, "Distillation Plant Data Book", Huston Research Inc. for OSW, Houston, Texas, 1971.

Easterday, R.J., "FLASH : an IBM-7000 Code For Computing MSF Plant Design For the Desalination of Sea Water", ORNL/TM - 1244, 1965.

Easterday, R.J., W.L. Griffith, R.M. Keller and R.B. Winsbro, "a Comparison of Alternative Computer Code for the Design of Saline Water Conversion Plants Utilizing the Single-effect Multi-stage Flash Evaporation Process", ORNL/TM - 1321, 1966.

El-Sayed, Y.M. and Silver, R.S., "Fundamentals of Distillation" in Principles of Desalination, Ed. by Spiegler, K.S. and Laird, A.D.K., Academic Press, New York, 1980.

Elsayed, M.M., "Rational Bases for Designing Vapour Compression Water Desalination Systems", Desalination, 58, 213-225, 1986.

Flower, J.R., V. Karanovic, "Simulation of Alternative Flowsheets For Treatment of Solvay Process Distillate Effluent", Inst. Chem. Eng. Annual Research Meeting, April, 1982.

Flower, J.R. and M.E. Whithead, "Computer Aided Design : a Survey of Flowsheeting Programs, Part I", The Chemical Engineering, 272, 208, 1973.

Flower, J.R. and Nafey, A.S.M., "The Design and Simulation of seawater Desalination Plants", I. Chem. E. Annual Research Meeting, 1986.

Fort, W.G.S., "MSF-21 :a FORTRAN Code for the Plant Calculation or Optimization of Multistage Flash (MSF) Desalination Plant", ORNL/TM - 3535, Part V, 1972.

Fort, W.G.S. and J.V. Wilson, "VTE-21 : a FORTRAN Code for the Rapid Calculation or Optimization of Vertical Tube Evaporator (VTE) Desalination Plants", ORNL/TM 3535, Part VI, 1976.

Friday, J.R. and B.D. Smith, "An Analysis of the Equilibrium Stage Separations Problem - Formulation and Convergence", AIChE J., 10, 698, 1964.

Gaunt, R.E., "Experience in Multi-stage Flash Process", First International Symposium on Water Desalination, Washington, (October 1965).

Genthner, K. and M. El-allawy, "Assessment of MSF Evaporator Design With Reduced Cooling Water Requirements", Desalination, 31, 57-68, 1979.

Glueck, A.R. and R.W. Bradshaw, "A mathematical Model For a Multistage Flash Distillation Plant", 3rd International Symposium on Fresh Water from the Sea, Vol. 1, 95-108, 1970.

Glueckstern, P., J.V. Wilson and S.A. Reed, "Modifications of ORNL's Computer Programs MSF-21 and VTE-21 For the Evaluation and Rapid Optimization of Multistage Flash and Vertical Tube Evaporations", ORNL/MT - 5230, 1976.

Gorczynski, E.W., "Quasilnear Reactor Models", Ph.D. Thesis, Dept of Chemical Engineering, University of Cambridge, 1977.

Griffith, W.L. and R.M. Keller, "SALINE : a FORTRAN Computer Program For the Process Design of Saline Water Conversion Plant Using the Multi Stage Flash Evaporation Process", ORNL/TM - 1299, 1965.

Guimaraes, J.C.,"Modeling, Simulation, And Control of Energy - Intensive Processes in The Pulp Industry", Ph.D. Thesis, University of Idaho, Moscow, Idaho, 1980.

Guneratne, D.C., "Distillation Desalination Plants Simplified Mathematical Models", AEEW - R 860, (May 1973).

Guthrie, K.M.,"Capital Cost Engineering", Chemical Engineering, March 24, 1969.

Hammond, R.P., Off. Saline Water Res. Develop. Progr. Rept. No. 391, 1968.

Hapke, J. and B. Uckermann, "Combined MSF/VTE Modules for Hybrid Thermal Seawater Desalination Plants", Desalination, 39, 373, 1981.

Hayakawa, k, H. Satori, and K. Konish, "Process Simulation on a Multi-Stage Flash Distillation Plant", 4th International Symposium on Fresh Water from the Sea, 1, 303-312, 1973.

Helal, A.M., "Mathematical Modeling and Simulation of Multistage Flash (MSF) Desalination Plants", Ph.D. Thesis, University of Leeds, 1985.

Helal, A.M., M.S. Medani, M.A. Soliman, and J.R. Flower, "A Tridiagonal Matrix Model For Multistage Flash DEsalination Plants", Comp. & Chem. Eng., 10, (4), 327-347, 1986.

Hilton, C.M., "Numerical Studies in Engineering Based Chemical Process Flowsheeting", Ph. D. Thesis, University of Illinois, 1982.

Hirth, L.J. and G.R. Sampat, "Computer Program for Multiple-Effect Evaporation With Auxiliary Heat Recovery Features", Chem. Eng. Prog. Symp. Series No. 113, Vol. 67, 1971.

Hitchcock, A.J., J.E.C. Mills, B. Stuart, and F.C. Wood, "Experience With Computer Programs For the Multiple Distillation of Sea Water", I.Chem.E. Symposium Series, No. 23, (1967: London).

Hlavacek, V. and P.V. Rompay,"Simulation of Countercurrent Separation Processes Via Global Approach", Computers & Chemical Engineering, 9 (4), 343-350, 1985.

Holland, C.D.,"Fundamentals and Modeling of Separation Processes", Prentice-Hall, Englewood Cliffs, N.J., 1975.

Homig, H.E., "Sea Water and Sea Water Distillation", Fichtner Handbook, Vulkan Verlay, Essen, 1978.

Howe, E. D., "Fundamentals of Water Desalination", Marcel Dekker, N.Y., 1974.

Huang, C.J., H.M. Lee, and A.E. Dukler, "Mathematical Model And Computer Program for Simulation and Optimum Design of Vertical Tube Evaporation Plants for Saline Water Conversion" Desalination, 6, 25-56, 1969.

Hughes, C.H. and D.K. Emmermann, "VTE/VC for Seawater", Chemical Engineering Progress, 72-73, (July 1981).

Hunter, J.A., Sieder, E.M., and Senatore, S.J., "Design and Economic Study of a Gas Turbine Powered Vapour Compression Plant for Evaporation of Seawater", OSW, Research and Development Progress Report No. 377, 1968.

Jernqvist, A., G. Olgard and B. Hedstrom, "a Digital Computer Program for Multiple Effect Evaporation", Svensk Papperstidning, 15, 477, 1966.

Ketchum, R.G., "A Combined Relaxation Newton like Method as a Global Approach to the Computation of the Thermal Processes", Chem. Eng. Sci., 31, 277 ,1979.

King, C.J., "Separation Processes", 2nd Ed., McGraw-Hill, New York, 1980.

Koko, F.W. and D.D. Joye, "Design Calculations for Multiple-Effect Evaporators. 2. Comparison of Linear and Nonlinear Methods", Ind. Eng. Chem. Res. 26, 104-107, 1987.

Kubicek, M., V. Hlavacek, and F. Prochaska, "Global Modular Newton-Raphson Technique For Simulation of an Interconnected Plant Applied to complex Rectification Columns", Chem. Engng. Sci., 31, 277, 1976.

Kurby, H.J., H.H. Erdmann, and K.H. Simmrock, "Reducing Energy Consumption of Multiple Effect Evaporators by Optimum Design", Chem. Proc. Anal. Des. Using Computer, 1982.

Lambert, R.N. and D.D. Joye, "Design Calculations for Multiple-Effect Evaporators. 1. Linear Method", Ind. Eng. Chem. Res., 26, 100-104, 1987.

Ledet, W.P. and D.M. Himmelblau, "Decomposition Procedures for the Solving of Large Scale Systems", Adv. Chem. Engng, 8, 185, 1970.

Lin, T.D. and R.S.H. Mah, "A Sparse Computation System for Process Design And Simulation: I. Data Structures and Processing

Techniques", AIChE J., 24, 830 ,1978.

Lior, N., "Equations Used to Calculate Non-Equilibrium in Open Channel Flash Evaporators", ASME paper 84-WA/Sol-34.

Locke, M.H., "A CAD Tool Which Accommodates an Evolutionary Strategy in Engineering Design Calculations", Ph. D. Thesis, Carnegie Mellon University, 1982.

Lucia, A. and S. Macchietto, "New Approach to Approximation of Quantities Involving Physical Properties Derivatives in Equation Oriented Process Design", AIChE J., 29, 705, 1983.

Mah , R.S.H., "Structural Decomposition in Chemical Engineering Computation", 72nd AIChE Nat. Meeting, St. Louis (May 21-26, 1972).

McAdams, W. H., "Heat Transmission", 3rd.ed., McGraw Hill, N.Y., 1954.

Medani, M.S., M.A. Soliman, A.M. Helal and J.R. Flower, "Computer Simulation of Desalination Plants in Saudi Arabia", 7th International Symposium on Fresh Water From the Sea, 1, 85-98, 1980.

Minton, P.E., "Handbook of Evaporation Technology", Noyse Publications, N. Jersey, 1986.

Motard, R.L., M. Shacham, and E.M. Rosen., "Steady State Chemical Process Simulation", AIChE J., 21, 417-436, 1975.

Mothershed, C.T., "ORSEF : a FORTRAN Code For the Calculation of Multistage Flash Evaporation Desalination Plant Design", ORNL/TM - 1542, 1966.

Naphtali, L.M. and D.P. Sandholm, "Multicomponent Separation Calculations by Linearization", AIChE J, 17, 1971.

National Water Supply, "Desalting Plants Inventory Report No.7", Improvement Association, (May 1981).

Newkirk, R.W. and M.E. Marwede, Off. Saline Water Res. Develop. Progr. Report No. 691, 1969.

Ojima, M., M. Ayai, and M. Tsujita, "A Study of Desalination by 100 T/D Vertical Multi-Effect Evaporator", 4th int. symp. on fresh water from the sea, 1, 429-437, 1973.

Olivares, E.T., "Simulation Models of Thermal Desalination Plants Using Multistage Multi flash Evaporation", M.Sc. dissertation, Chem. Eng. Dept., Leeds Univ., 1983.

Omar, A. M., "Simulation of Multi-Stage Flash (MSF) Desalination Plants", M.Sc. Thesis, University of Petroleum and Minerals, Dhahran, Saudi-Arabia, September, 1981.

Omar, A.M."Simulation of MSF Desalination Plants", Desalination, 45, 65-76, 1983.

Ortega, J.M. and W.C. Rheinboldt, "Iterative Solution of Nonlinear Equations in Several Variables", Academic Press, N.Y., 1970.

Ozisik, M.N., "Heat Transfer- Basic Approach", McGraw-Hill, N.Y., 1985.

Perkins, J.D., "Efficient Solution of Design Problems Using a Sequential Modular Flowsheeting Program", 12th Symposium on Computer Applications in Chemical Engineering, CACE 79, Montreux, 1979.

Perry, J.H. and C.H. Chilton, "Chemical Engineers' Handbook", McGraw-Hill, New York, 1973.

Porteous, A., "Saline Water Distillation Process", Longman, London, 1975.

Radovic, L.R, Tasic, A.Z, Grozdanic, D.K, Djordjevic, B.D. and Valent, V.J., "Computer Design And Analysis of Operation of a Multiple-Effect Evaporator System in The Sugar Industry", Ind. Eng. Chem. Process Des. Dev., 18, (2), 1979.

Rautenbach, R. and H.G. Buchel, "Modular Program For Design and Simulation of Desalination Plants", 7th International Symposium on Fresh Water From the Sea, 1, 153-161, 1980.

Rice, J.R.,"Numerical Methods, Software, and Analysis", McGraw Hill, New York, 1983.

Rose, L.M., "The Application of Mathematical Modeling to Process Development and Design", Applied Science Publishers, 1974.

Rudd, D.F,. and C.C. Watson, "Strategy of Process Engineering", Wiley, N.Y., 1968.

Sargent, R.W.H.,"Advances In Modelling And Analysis of Chemical Process Systems", Computers & Chemical Engineering, 7 (4), 219-237, 1983.

Sargent, R.W.H., "a Review of Methods For Solving Non-linear Algebraic Equations, in Foundations of Computer Aided Chemical Process Design, Eds, R.S.H. Mah and W.D. Seider, 1, Engineering Foundation, N.Y., 1980.

Sargent, R.W.H., "The Decomposition of Procedures and Algebraic Equations (Edited by G.A. Waston). Numerical Analysis Proceedings, Biennial Conference, Dundee 1977, Lecture Note in Mathematics 630, pp. 158-178, Speringer-Verlag, Berlin, 1978.

Schalien, R.V., L. Vihma and P. Saarela, "Studies on the Evaporation of Spent Liquors From Pulping Processes, III a Simulation Model of Multiple-effect Evaporator System For Digital Computers", Kemian Teollisuus, 1, 1970.

Schnackel, H.C., "Formulations for the Thermodynamic Properties of Steam and Water", ASME Transactions, J. Heat Transfer, 80, 959-66, 1958.

Schubert, L.K., "Modification of a quasi- Newton Method for Nonlinear Equations With a Sparse Jacobian", Math. Comp. 25, 27, 1970.

Schweitzer, O.R., "Reverse Synthesis Simplifies Problem Solving", Chemical Engineering, 19, (June, 1978).

Senatore, S.J. and E.N. Sieder, "Conceptual Design Studies of a Dual Purpose and a Vapour Compression Water only 750 MGD Plant", International Atomic Energy Agency, Paper No. SM-113/33, 1969.

Shacham, M., S. Macchietto, L.F. Stutzman and P. Babcock, "Equation

Oriented Approach to Process Flowsheeting", Comput. chem. Eng., 6, 79, 1982.

Shacham, M., "Decomposition of Systems of Nonlinear Algebraic Equations", AIChE J., 30, 92, 1984.

Sherwood, T.K., "A Course In Process Design", The M.I.T. Press, Cambridge, Massuchusetts, 1963.

Shewchuk, C.F., "MASSBAL: A Flowsheeting Program for The Pulp and Paper Industry", in Computer-Aided Process Plant Design, Leesely, M.E. (editor), Gulf Publishing Company, 1982.

Silver, R.S., "Review of Distillation Processes for Fresh Water from the Sea", 1st European Symposium on Fresh Water From the Sea, Athens, 1962.

Simpson, H.C., "National Engineering Laboratory Report No. 329, (London:Ministry of Technology), pp. 20, 1967.

Soliman, M.A., "A Mathematical Model for Multi-Stage Flash Desalination Plants", J. Eng. Sci. Univ. Riyadh, 7, No. 2, pp. 143-150, 1981.

Spiegler, K.S. and A.D. Laird, "Principles of Desalination", Part A, 2nd Ed., Academic Press, N.Y., 1980.

Stadtherr, M.A. and C.M. Hilton, "Development of a New Equation Based Process Flowsheeting System: Numerical Studies", AIChE Symposium Series, 78 (214), 12-28, 1982.

Standiford, F. C., "Evaporation is a Unit Operation", Chem. Eng., 70, 185, (Dec. 9, 1963).

Steinbruchel, A.B. and R.D. Rhinesmith, "Design of Distilling Plants" in Principles of Desalination, Ed. by Spiegler, K.S. and Laird, A.D.K., Academic Press, New York, 1980.

Steltz, W.G. and G.J. Silverstri, "The Formulation of Steam Properties for Digital Computer Application", ASME Transactions, J. of Heat Transfer, 80, 967, 1958.

Stewart, G. and G.S.G. Beveridge, "Steady State Cascade Simulation in

Multiple Effect Evaporation", Computers and Chemical Engineering, 1, 95-108, 1977.

Tierney, J.W. and J.A. Bruno, "Equilibrium Stage Calculations", AIChE J., 13, 556, 1967.

Tleimat, B.W., "Novel Approach to Distillation by Vapour Compression Distillation", Printed paper 69-WA/PID -1, A.S.M.E., (Nov. 1969).

Van Winkle, R., "Investigation of the need for Variable Orifices in Multistage Flash Evaporators", ORNL-TM - 2746, 1970.

Waite, S.J., "EVAP: A Simulation and Design Program for Multiple-Effect Evaporators", in Computer-Aided process Plant Design, Leesely, M.E. (editor), Gulf Publishing Company, 1982.

Wang, J.C. and G.E. Henke, "Tridiagonal Matrix for Distillation", Hydrocarbon Process, 45, 155, 1966.

Westerberg, A.W., H.P. Hutchison, R.L. Motard, and P. Winter, "Process Flowsheeting", Cambridge University Press, 1979.

Wood, F.C. and R. Herbert, "The Characteristics of Dual Process Desalination Plant Combing vapour Compression and Multi-stage Flash Evaporators", Proc. Symp. Nucl. Desalination, Madrid, 1968.